Computer-aided design and synthesis of novel anti-DENV nucleoside analogues

A thesis submitted in accordance with the conditions governing candidates for the degree of

Philosophiae Doctor in Cardiff University

by

Cecilia Maria Cima

January 2017

School of Pharmacy and Pharmaceutical Sciences

Cardiff University

To mum and dad

A mamma e papà

This work was supported by the Henson Research Foundation and by the Life Science Research Network Wales, an initiative funded through the Welsh Government's Ser Cymru program.

SUMMARY

Dengue virus (DENV) is one of the most important human pathogens among the genus *flavivirus*, with 3.9 billion people at risk of infection through mosquitoes, such as the widely spread 'Asian tiger' mosquitoes, and the four serotypes of DENV are endemic in over 100 countries in tropical and subtropical regions. Clinical manifestations of infection with DENV range from flu-like symptoms to the life-threatening dengue haemorrhagic fever. The dramatic increase in the incidence of the DENV infection, the rapid spread of DENV to new areas and the recent re-emergence of another member of the genus *flavivirus*, Zika virus (ZIKV), have highlighted the urgent need for specific antiviral therapies against infections with DENV and related viruses, which are not currently available. DENV RNA-dependent RNA polymerase (RdRp), the enzyme responsible for the synthesis of the viral genome, is one of the most attractive targets for the development of direct acting antiviral agents but its molecular mechanisms are poorly understood. Thefore, the aims of this PhD project were i) to build a model of the *de novo* initiation complex of DENV RdRp, of which there is currently no crystal structure available, ii) *in silico* design and synthesis of novel nucleoside and nucleotide analogues as potential inhibitors of DENV replication, iii) and finally to investigate the mechanism of the RNA synthesis by DENV RdRp.

Molecular modelling techniques allowed for the creation of a model of the *de novo* initiation complex. The application of *in silico* drug design approaches resulted in the identification of three families of promising adenosine analogues: ribose-modified, nucleobase-modified and acyclic adenosine analogues. Strategies for the preparation of these nucleosides were investigated and ten adenosine analogues and eight nucleotide prodrugs, which are phosphoramidate ProTides, of specific nucleosides were synthesised and sent for biological evaluation *in vitro*. Innovative microwave irradiation conditions for the preparation of phosphoramidate ProTides were developed and successfully applied to synthesised nucleoside analogues. Finally, the application of molecular dynamics simulation methods on different complexes of DENV RdRp provided insights on the conformational changes of DENV RdRp during the synthesis of the viral genome. These results contributed to the understanding of DENV RdRp activity and will aid the design of inhibitors of the viral replication.

TABLES OF CONTENTS

ABBREVIATIONS

GENERAL ABBREVIATIONS

% v/v	% volume/volume (volume concentration)
2D	Two-dimensional
3D	Three-dimensional
3dGMP	3'-Deoxyguanosine monophosphate
ADA	Adenosine deaminase
ADE	Antibody dependent enhancement
ADME	Absorption distribution metabolism and excretion
ANP	Acyclic nucleoside phosphonate
aq.	Aqueous
ATP	Adenosine triphosphate
AZT	Azidothymidine
BHK-21	Baby hamster kidney cells
BLA	Biologics license application
C	Capsid protein
CC_{50}	Half maximal citotoxicity concentration
COSY	Correlation spectroscopy
CPE	Cytopathic effect
CRDS	Curdlan sulfate
CS	Cyclisation sequence
Da	Dalton
DAA	Direct-acting antiviral
DENV	Dengue virus
DF	Dengue fever
DHF	Dengue haemorrhagic fever
DHODH	dihydroorotate dehydrogenase
DNA	Desoxyribonucleic acid
dsRNA	Double stranded RNA
DSS	Dengue shock syndrome
E	Envelope protein
EC_{50}	Half maximal effective concentration
ER	Endoplasmic reticulum
Fc	Crystallisable fragment
FcR	Crystallisable fragment receptor
FDA	Food and Drug Administration
FE	Fast eluting
GTP	Guanosine triphosphate
HCV	Hepatitis C virus
Hint	Histidine triad nucleotide-binding protein
HIV	Human immunodeficiency virus
HPLC	High-performance liquid

	chromatography
HRMS	High resolution mass spectrometry
HSQC	Heteronuclear single-quantum correlation spectroscopy
HSV	Herpes simplex virus
HTS	High-throughput screening
Huh7	Human hepatoma cells
i + 1 site	catalytic site
i site	initiation site
IgG	Immunoglobulin G
IL	Interleukin
IMPDH	Inosine monophosphate dehydrogenase
INF-γ	Interferon-γ
JEV	Japanese encephalitis virus
kb	Kilobase
LAV	Live attenuated vaccine
LBDD	Ligand-based drug design
LC	Liquid chromatography
M	Membrane protein
MD	Molecular dynamics
MHC	Major histocompatibility complex
mRNA	Messenger RNA
MS	Mass spectrometry
MTase	Methyltransferase
MW	Molecular weight
MWI	Microwave irradiation
NI	Nucleoside inhibitors
NITD	Novartis Institute for Tropical Diseases
NLS	Nuclear-localisation sequence
NME	New molecular entity
NMR	Nuclear magnetic resonance
NNI	Non-nucleoside inhibitor
NOAEL	No-observable-adverse-effect level
NOE	Nuclear Overhauser effect
NOESY	Nuclear Overhauser effect spectroscopy
NS	Non-structural protein
NSAID	Non-steroidal anti-inflammatory drug
NTP	Nucleotide triphosphate
ORF	Open reading frame
PBMC	Primary human peripheral blood mononuclear cells
PI	Protease inhibitor
PIV	Purified inactivated virus
PLANTS	Protein-Ligand ANT System
PNP	Purine nucleoside phosphorylase
prM	Pre-membrane protein
QSAR	Quantitative structure-activity relationship
RBV	Ribavirin
RdRp	RNA-dependent RNA polymerase
RMSD	Root-mean-square deviation

RNA	Ribonucleic acid
rt	Room temperature
SAH	*S*-adenosyl homocysteine
SAM	*S*-adenosyl methionine
SAR	Structure-activity relationship
SBDD	Structure-based drug design
SE	Slow eluting
SLA	Stem-loop A
SPC	Simple point charge
ssRNA	Single stranded RNA
TBEV	Tick-borne encephalitis virus
TGN	Trans-Golgi network
TLC	Thin layer chromatography
TNF-α	Tumor necrosis factor α
UAR	Upstream of AUG region
US	United States
UTR	Untranslated region
UV	Ultraviolet
VS	Virtual screening
VZV	Varicella zoster virus
WHO	World Health Organization
WNV	West Nile virus
YFV	Yellow fever virus
ZIKV	Zika virus

AMINO ACID ABBREVIATIONS

Ala	A	Alanine	Leu	L	Leucine
Asn	N	Asparagine	Lys	K	Lysine
Asp	D	Aspartic acid	Met	M	Methionine
Arg	R	Arginine	Phe	F	Phenylalanine
Cys	C	Cysteine	Pro	P	Proline
Glu	E	Glutamic acid	Ser	S	Serine
Gln	Q	Glutamine	Thr	T	Threonine
Gly	G	Glycine	Trp	W	Tryptophan
His	H	Histidine	Tyr	Y	Tyrosine
Ile	I	Isoleucine	Val	V	Valine

1 INTRODUCTION

1.1 DENGUE VIRUS

1.1.1 GENUS *FLAVIVIRUS*

Dengue virus (DENV) is a small, enveloped virus belonging to the family *Flaviviridae*, genus *flavivirus*. The family comprises three genera: *flavivirus*, *pestivirus* and *hepacivirus*.[1] More than 70 viruses belong to the genus *flavivirus* that have originated from a common ancestor.[2] The majority of flaviviruses are arboviruses (arthropod-borne viruses) as their transmission between vertebrate hosts occurs by arthropod vectors (mosquitoes or ticks).[1]

Most flaviviruses are not relevant from a medical point of view. In fact, many flaviviruses circulate between birds and small mammals, which are their natural hosts. Humans may become infected when in close proximity with the cycle and infection may remain asymptomatic or cause mild febrile syndromes. In such cases, a low level of viraemia is often induced in humans and does not enable further transmission of the infection.[1] However, a small group of flaviviruses including DENV[1, 3], yellow fever virus (YFV), Japanese encephalitis virus (JEV), West Nile virus (WNV)[1] and the recently emerged Zika virus (ZIKV),[4, 5, 6] represent important exceptions. Besides non-human primates and some other animals, humans represent the natural hosts of these viruses and infection may lead to a variety of diseases.

Being responsible for 390 million infections every year, DENV is one of the most significant human pathogens. Infection with any of the four existing DENV serotypes can be associated with a wide spectrum of clinical features, from a non-specific viral fever, referred to as dengue fever (DF), to a life-threatening condition, known as dengue haemorrhagic fever (DHF)[1, 3] (see section 1.1.3 for a description of the clinical manifestations of the infection).

ZIKV has recently become a threat to human health in a global context.[4, 5, 6] The current outbreak in the Americas and the Caribbean has caused over 2 million infections in over 30 countries since 2015.[6] Due to the potential spread to temperature climate aereas and to the association of ZIKV infection with severe neurological complications and foetal malformations, ZIKV was declared a Public Health Emergency of International Concern in February 2016.[7]

To date, there is no specific treatment for any flavivirus infection and vaccines are available only for a limited number of viruses, such as YFV and JEV.[8] Recently, one DENV vaccine has been licensed for use in endemic countries.[9] However, the vaccination only provides partial protection against the four serotypes of DENV and will only be beneficial for a restricted population (refer to

section 1.1.6).[10, 11] Therefore, the development of new agents against flaviviral infections remains of high priority.

1.1.2 EPIDEMIOLOGY

Today DENV is the most widely distributed mosquito-borne human pathogen, being endemic in over 100 countries throughout South East Asia, the Western Pacific, the Americas and Africa[12] (Figure 1).

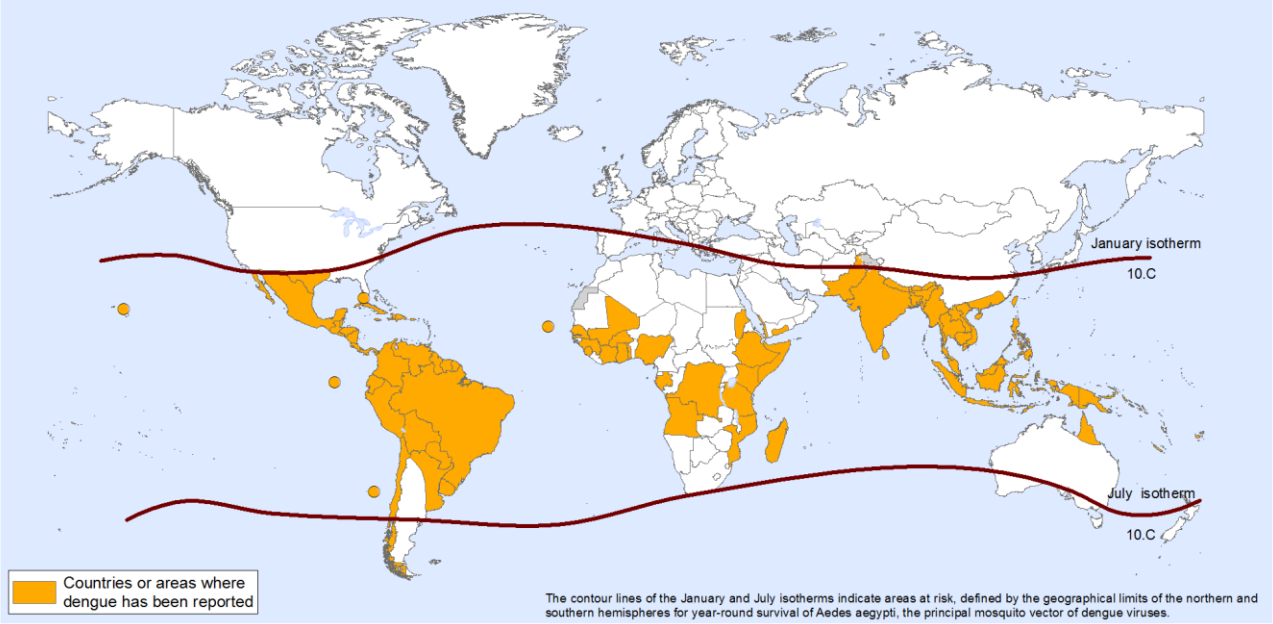

Figure 1. Geographical distribution of dengue-endemic areas in 2013. Lines of the January isotherm and July isotherm define areas of year-round survival of *Aedes Aegypti* mosquitoes. Figure reproduced under permission by WHO.[13]

DENV has been circulating since antiquity (10 000 years) and the earliest description of a syndrome compatible with DF has been found in a Chinese medical encyclopaedia dating back to the Chin Dynasty (265 – 420 A.D.). First epidemics occurred in the 17th century in the West Indies and Central America.The first accurate clinical description of dengue fever was by Benjamin Rush, regarding the epidemic that occurred in Philadelphia in 1780.[1, 14, 15]

Expansion of DENV has been linked to the spreading of its primary mosquito vector, *Aedes aegypti*. Since World War II, rapid urbanisation and increased transportation and human travel allowed for a worldwide resurgence of the mosquito and for the following spread of dengue.[14, 15]

In the 1950s and 1980s the first epidemics of DHF were observed in South East Asia and the Americas, respectively.[14, 15] Today, DHF represents a leading cause of paediatric morbidity and mortality in many countries of the Asian region.[14]

Recently, a dramatic rise in the number of dengue cases has been reported worldwide, with an estimated 30-fold increase of reported DENV infections in the last few decades.[3, 16] The World Health Organization (WHO) estimated that the incidence falls in the range of 50 million to 100 million and around 40% of the World's population is at risk of infection, accounting for 2.5 billion people.[3, 12, 17] The worldwide estimated cases of DHF are 500 000 per year, resulting in over 20 000 deaths.[18] However, the true burden caused by DENV is likely to be even higher: recent estimates reported that up to 3.9 billion people may be at risk of infection in 128 countries[19] and the real incidence may be more than three times the estimate of the WHO, with 390 million cases annually.[20]

Factors involved in the continuous increase in the incidence of DENV infections include the intensification of the disease in endemic areas and the geographical expansion of DENV to previously unaffected areas. Many countries in South East Asia and Western Pacific, which were hypoendemic (circulation of only one serotype) until ten years ago, are now hyperendemic (circulation of numerous serotypes) with epidemics occurring regularly every 3 to 5 years.[14, 15] Hyperendemicity occurs in the majority of countries in the Americas too, although DENV transmission was efficiently controlled in the region by the middle of the 20th century.[1, 14, 15] In Africa the number of cases is likely to be underestimated due to the fact that dengue is not officially reported to the WHO and to the common misdiagnosis of dengue infections as malaria, a disease that is significantly spread throughout the region.[19] Dengue epidemics caused by all four serotypes occur frequently in the African region, however severe manifestations are observed in sporadic cases.[14, 15]

Dengue infection of international travellers to dengue-endemic countries (imported cases) occurs frequently.[21] The virus represents the leading cause of febrile illnesses in returned travellers from every region except Sub-Saharan Africa and Central America, being confirmed or suspected more frequently than malaria.[21, 22] Although severe dengue manifestations are rare in travellers,[21] the incidence of infections in international travellers is relevant as it contributes to the significant spread of DENV to new areas. Indeed, the threat of dengue epidemics is now real in Europe and in the US.[12, 15, 23, 24] Intercontinental trade of used car tires containing eggs of *Aedes albopictus* caused the establishment of this mosquito, a secondary vector of DENV, in Europe by the 20th

century.[1, 14, 24] Imported cases in travellers are frequent and local transmission, made possible by the presence of the mosquito, has been observed in France and Croatia in 2010.[3] Moreover, an important outbreak occurred in the Madeira Islands of Portugal in 2012 and resulted in over 2 000 local cases and several imported cases in other European countries.[3] Similarly, both imported and locally acquired cases have been reported with increasing frequency in the US, especially in Florida, Texas, Puerto Rico and Hawaii.[3, 23, 24]

1.1.3 CLINICAL FEATURES

There are four different serotypes of DENV, named DENV-1, DENV-2, DENV-3 and DENV-4.[14] In the enzootic, or sylvatic, transmission cycle, DENV circulates between non-human primates and mosquito vectors in Asian and African rain forests and rarely infect humans in small rural centres (rural transmission cycle).[14] The urban transmission cycle of DENV is the most important one from a public health point of view. The vectors involved are the *Aedes aegypti* mosquito and the *Aedes albopictus* mosquito, which is commonly known as 'Asian tiger' mosquito. The *Aedes aegypti* mosquito is the primary vector and is highly domesticated: adult female mosquitoes feed on humans (anthrophilic), rest indoors and breeds in collections of water in and around homes, for instance storage jars, containers, flower vases etc.[14]

After biting an infected person in the viremic phase of the illness, a period that may vary from 2 to 10 days, the mosquito becomes infected and, following an incubation period in the vector of 8 to 12 days, is capable of transmitting the virus by feeding or just probing on another person. Infection in humans may become apparent after a variable incubation period (from 3 to 14 days), and clinical manifestations vary in severity.[1, 14, 25] As mentioned before, two distinctive illnesses, DF and DHF, are caused by DENV infection.

1.1.3.1 Dengue fever

In young children the manifestation of dengue infection is often a febrile illness, which can not be differentiated from other viral diseases.[1, 14] In older children and adults DF is characterised by a classical fever-arthralgia-rash syndrome with a sudden onset of high fever and various symptoms, including headache, weakness, skin rash, and muscles and joints pain, the latter of which might be severe (bacause of this common symptom, dengue fever is also known as 'breakbone fever').[14] DF is generally self-limiting; although it resolves in few days (the fever may last from 2 to 7 days),

many adult patients experience a prolonged phase of convalescence associated with weakness and depression, which may last for weeks after the acute phase of the illness.[1, 14] Haemorrhagic manifestations are common and include skin haemorrhages, gum and nose bleeding as well as gastrointestinal haemorrhages. Other frequently occurring features are low blood platelet and leukocyte counts and high blood transaminase levels.[1, 14] Given the non-specificity of symptoms, only laboratory tests by virus isolation or antibody detection can confirm DENV infection.[1]

1.1.3.2 Dengue haemorrhagic fever

DHF or severe dengue occurs primarily in young children under the age of 15 years, but cases are observed also in the adult population.[1, 14] The onset of DHF does not allow to distinguish this life-threatening disease from either DF or other febrile illnesses, being characterised by an abrupt onset of fever. This initial febrile phase usually lasts for 2 to 7 days and is accompanied by non-specific symptoms.[1, 14] The critical stage in DHF is the defervescence, when initial fever subsides, on day 3 to 7 of illness. The characteristic manifestation is plasma leakage from the blood vessels into the interstitial space due to increased vascular permeability, which may be very severe. Patients also present reduced platelet and leukocyte counts and clotting abnormalities. Haemorrhagic manifestations are mild and usually include scattered petechiae, whereas bleeding and gastrointestinal haemorrhages occur less commonly.[1, 14] Four grades of DHF (I – IV) of increasing severity have been classified by the WHO.[14, 25] The symptoms described above corresponds to the mildest form, DHF-I, which differs from DHF-II by the absence of bleeding. In contrast, in DHF-II additional gum, nose and gastrointestinal bleeding is present. DHF-III is characterised by circulatory collapse and hypovolemic shock due to plasma leakage (rather than blood loss). In DHF-IV the patient is moribund due to severe plasma leakage and undetectable pressure. Grades III and IV are also referred to as dengue shock syndrome (DSS) and are life-threatening conditions: if untreated, DSS causes death of the patient in shock within 8 to 24 hours. Appropriate fluid replacement therapy usually allows for rapid recovery, which is followed by a short period of convalescence (2 to 3 days) for patients with any grade of DHF.[1, 14, 25]

1.1.4 CLINICAL MANAGEMENT

No antiviral agents are available against DENV infection, therefore treatment is symptomatic according to clinical manifestations. Most cases present a self-limiting illness and do not need hospitalisation. The patient should drink and avoid aspirin, because of its anti-platelet effect, as well as other non-steroidal anti-inflammatory agents (NSAIDs), which may worsen gastrointestinal bleeding. Paracetamol may be administered to provide symptomatic relief.[1] Patients with DF or mild DHF (grades I and II) may recover spontaneously and do not require intravenous administration of fluids, whereas patients with DSS (DHF-III and DHF-IV) need hospital admission to ensure an accurate management of the illness.[1, 26] Intravenous administration of electrolyte and colloid solutions is essential to stabilise the plasma volume and restore blood pressure, but requires careful regulation to avoid fluid overload once fluids will be reabsorbed.[1, 12, 26]

1.1.5 PATHOGENESIS OF DHF

Increased risk for DHF appears to be associated with secondary dengue infection (infection with a heterologous virus serotype following a primary infection) and with particularly virulent viral strains.[1, 8, 25, 27, 28] Therefore, both a host immunologic factor and a viral factor may be involved in the pathogenesis of DHF.[1, 8, 25] However, the lack of a suitable animal model for DENV presents an obstacle in the study of DHF pathogenesis, which still remains largely unclear.[25]

An increased likelihood for patients, especially children, for developing DHF has been shown in epidemiological studies for those who are experiencing secondary infections with DENV.[27] After infection with one serotype the patient develops life-long immunity for the specific serotype thanks to virus-specific memory T-lymphocytes. Prior circulating antibodies derived from a primary infection, as well as acquired maternal IgG, although responsible for immunity for the specific serotype, are a risk factor for DHF. The so called ‘antibody-dependent enhancement (ADE) of infection’ theory has been proposed to explain the pathogenesis of DHF (figure 2).[25, 28]

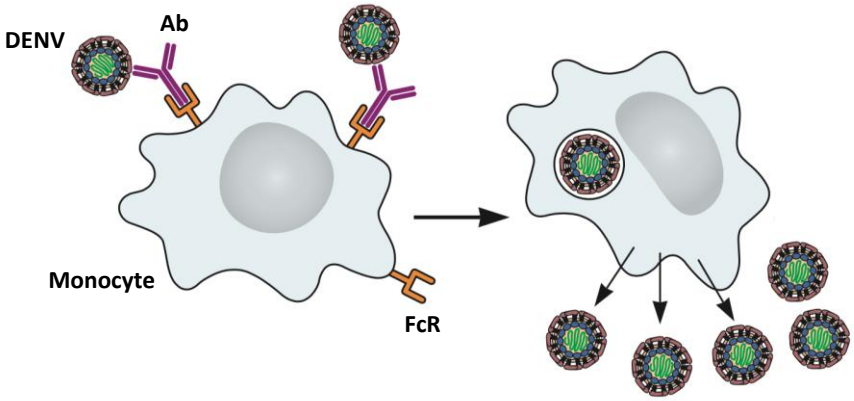

Figure 2. 'Antibody-dependent enhancement' of DENV infection. DENV: dengue virus; Ab: cross-reactive antibodies; FcR: Crystallisable fragment receptor. Figure adapted from Virology Blog by V. Racaniello under the license Creative Commons BY 3.0.[29]

Antibodies to the first virus serotype are not able to neutralise the heterologous virus serotype, but are cross-reactive. The resulting complexes bind immunoglobulin crystallisable fragment receptors (FcRs) expressed on the cell surface of leucocytes, especially monocytes. The formation of these non-neutralising antibody-virus complexes facilitates the entry of the new virus into monocytes and leads to an increased intracellular viral replication, and thus viraemia, which appears to be directly correlated to the increased severity of illness.[28] Infected cells expose viral antigens (major histocompatibility complex, MHC), leading to the stimulation of T-lymphocytes and the production of cytokines, in particular interferon-γ (INF-γ). The increased level of cytokines results in the activation of other macrophages that will upregulate the expression of FcRs and MHC on their cell-surface, making them more susceptible to viral infection and thus initiating a chain reaction. The higher levels of cytokines produced by macrophages, lymphocytes and endothelial cells might also have a direct effect in the severity of the disease, as they might result in increased capillary permeability and thus facilitate the potentially fatal plasma leakage associated with DHF.[1, 25]

Additionally, the combination of specific serotypes may be correlated to the severity of the developed illness: indeed, primary infections with DENV-1 or DENV-3 followed by a secondary infection with DENV-2 appear to be the most pathogenic sequences of infections.[30]

Despite many cases of dengue haemorrhagic fever occurring in patients experiencing a secondary infection, the illness is also reported in infants during primary infection with DENV.[31, 32] This

observation suggests the involvement of alternative or contributing factors playing a role in the pathogenesis of DHF. Like other animal viruses, DENV exists in different virus strains, which are genetic variants of the same serotype.[1, 14, 30] Some virus strains present a mostly sylvatic transmission cycle, hence they only infect humans sporadically.[1, 14, 30] Other virus strains in their urban transmission cycle infect humans and cause a mild syndrome, whereas other genetically different viruses are characterised by higher virulence.[30] Infections with a virulent viral strain of DENV may be associated with an increased virus replication and thus an increased severity of the clinical manifestation.[30]

1.1.6 PREVENTION

To date, a specific anti-DENV therapy is not available. Until the recent approval of the dengue vaccine by Sanofi Pasteur (CYD-TDV, DengVaxia®),[33] dengue prevention and control relied exclusively on vector control methods. The WHO presented many strategies for reducing *Aedes* mosquitoes populations, mainly by limiting the breeding of *Aedes* mosquitoes in urban areas and by the use of insecticides and larvicides.[12] However, effective preventative programs have proven not to be sustainable in dengue-endemic areas as a long-term approach and both health education as well as community participation would be essential for effective and long-lasting mosquito control.[1, 3] Simple preventative measures, such as the use of insect repellents and mosquito nets, should be adopted by travellers to tropical areas, especially during the rainy season, to decrease exposure to mosquito bites, and thus reduce the risk of infection and limit DENV geographical expansion.[1, 21]

The approval of DengVaxia in 2015 is the result of a challenging development process that lasted 20 years. The difficulties associated with the development of a dengue vaccine were mainly due to the presence of four dengue serotypes.[34, 10] Infection with one serotype allows for the development of a life-long immunity to the specific serotype involved in the primary infection. A cross-protective immunity against the other serotypes is observed over a short period of time following convalescence.[34, 10] However, on the long term the pre-existence of antibodies against one serotype increases the risk of severe dengue during a secondary infection.[25, 28] Therefore, the administration of a non-tetravalent vaccine may actually predispose for severe dengue, rather than eliciting protection.[8, 16] In order to be safe, a dengue vaccine therefore needs to be capable of inducing a balanced protective immunity against all four virus serotypes. Furthermore, the ideal

dengue vaccine should be safe and effective for use in both children and adults.[8, 16] Moreover, the cost should be affordable to most people living in dengue-endemic areas, which include many developing or poor countries.[8, 16]

CYD-TDV by Sanofi Pasteur is an attenuated chimeric vaccine, constructed by replacement of pre-membrane (prM) and envelope (E) genes from each DENV serotypes into the licensed yellow fever virus vaccine (YFV-17D) backbone. The four distinct recombinant viruses are combined in the final formulation.[34, 10] Previous evaluations (preclinical, clinical Phase I and Phase II trials) demonstrated CYT-TDV to be safe and immunogenic, capable of inducing neutralising antibodies against each of the four serotypes, following a three-dose schedule over a 12-month period.[35] Nevertheless, the induction of broadly neutralising antibodies did not correlate with protection against dengue in humans, demonstrating that more reliable markers of immunity to evaluate dengue vaccine candidates are required.[8, 16] In fact, CYD-TDV was found to be ineffective against DENV-2 in a Phase IIb efficacy study in Thailand[35] and this result was confirmed in two clinical Phase III trials, which involved larger populations.[36, 37] Although the overall vaccine efficacy was 56.5% and 60.8% in these large-scale Phase III studies conducted in Asia and in Latin America respectively, the vaccine failed to elicit a high level of protection against DENV-2 (efficacy against DENV-2 was 35.0% and 42.3% in the two Phase III studies).[36, 37] However, a significant reduction of the risk of hospitalisation due to DHF was observed (88.5% and 80.3%, respectively) among participants over nine years of age.[36, 37] CYT-TDV was partially effective against DENV serotypes and the response to vaccination was variable depending on the age as well as on the previous exposure to DENV of the participants. In fact, vaccine efficacy was higher in DENV seropositive individuals among all ages, suggesting that the vaccine may be beneficial in endemic countries where most of the people have already encountered the virus.[10, 11, 38, 39] Given the complex efficacy profile of the dengue vaccine by Sanofi Pasteur, the level of dengue burden and the population target of vaccination need to be carefully considered before introducing DengVaxia® (CYT-TDV) in a national immunisation programme.[10, 11] Follow-up studies will be of crucial importance to monitor the long-term effects of the vaccination in endemic countries, including the occurrence of severe dengue as well as the duration of the protection,[10] as the immunity seems to wane in few years.[40]

Besides CYD-TDV, several other dengue vaccine candidates have been developed, including classical live attenuated vaccines (LAV), chimeric attenuated vaccines, recombinant live attenuated

vaccines, purified inactivated viruses (PIV), protein subunit vaccines and DNA vaccines.[8, 16, 34, 41, 42, 43] Vaccines in tetravalent formulation that entered clinical trials are summarised in table 1.

Table 1. Tetravalent DENV vaccine candidates in clinical trials.

Developer	Type	Method	Clinical trial	Status
MU[a], Sanofi Pasteur	classical LAV	sequential passages through cell cultures	Phase II	discontinued
WRAIR[b], GlaxoSmithKline	classical LAV	sequential passages through cell cultures	Phase II	discontinued
Sanofi Pasteur	chimeric attenuated vaccine	prM/E proteins in Yellow Fever 17D vaccine backbone	Phase III completed	marketed as DengVaxia®
CDC[c], Takeda	chimeric attenuated vaccine	prM/E proteins in attenuated DENV-2 strain backbone	Phase III	ongoing
NIAID[d], NIH[e]	chimeric attenuated vaccine	prM/E protein in viral strains attenuated by nucleotide deletion at 3'-untranslated region (UTR)	Phase III	ongoing
WRAIR[b], GlaxoSmithKline	PIV	non-replicating viruses in the presence of adjuvants	Phase I	ongoing
WRAIR[b]	combination of PIV and classical LAV	synergy between two previously developed vaccines	Phase I	ongoing
NMRC[f]	DNA vaccine	plasmid encoding prM/E genes from each DENV serotypes	Phase I	ongoing
Merck	subunit protein vaccine	truncated E proteins from each serotype	Phase I	ongoing

[a]Mahidol University, Thailand. [b]Walter Reed Army Institute of Research, USA. [c]Center for Disease Control (Inviragen, USA and Takeda, Japan). [d]National Institute of Allergy and Infectious Disease, USA. [e]National Institute of Health, Laboratory of Infectious Diseases, USA. [f]Naval Medical Research Centre, USA.

1.1.7 REPLICATION CYCLE

Flaviviruses are small enveloped viruses, spherical in shape with a diameter of approximately 50 nm. The viral genome is a single-stranded, positive-sense RNA, approximately 11 kb in length. The nucleocapsid is enveloped by an inner lipid bilayer, which is acquired from host cells, and an outer glycoprotein shell.[44] Figure 3 illustrates the replication cycle of DENV in the host cell from the entry of the viral particle to the exocytosis of mature virions.[45]

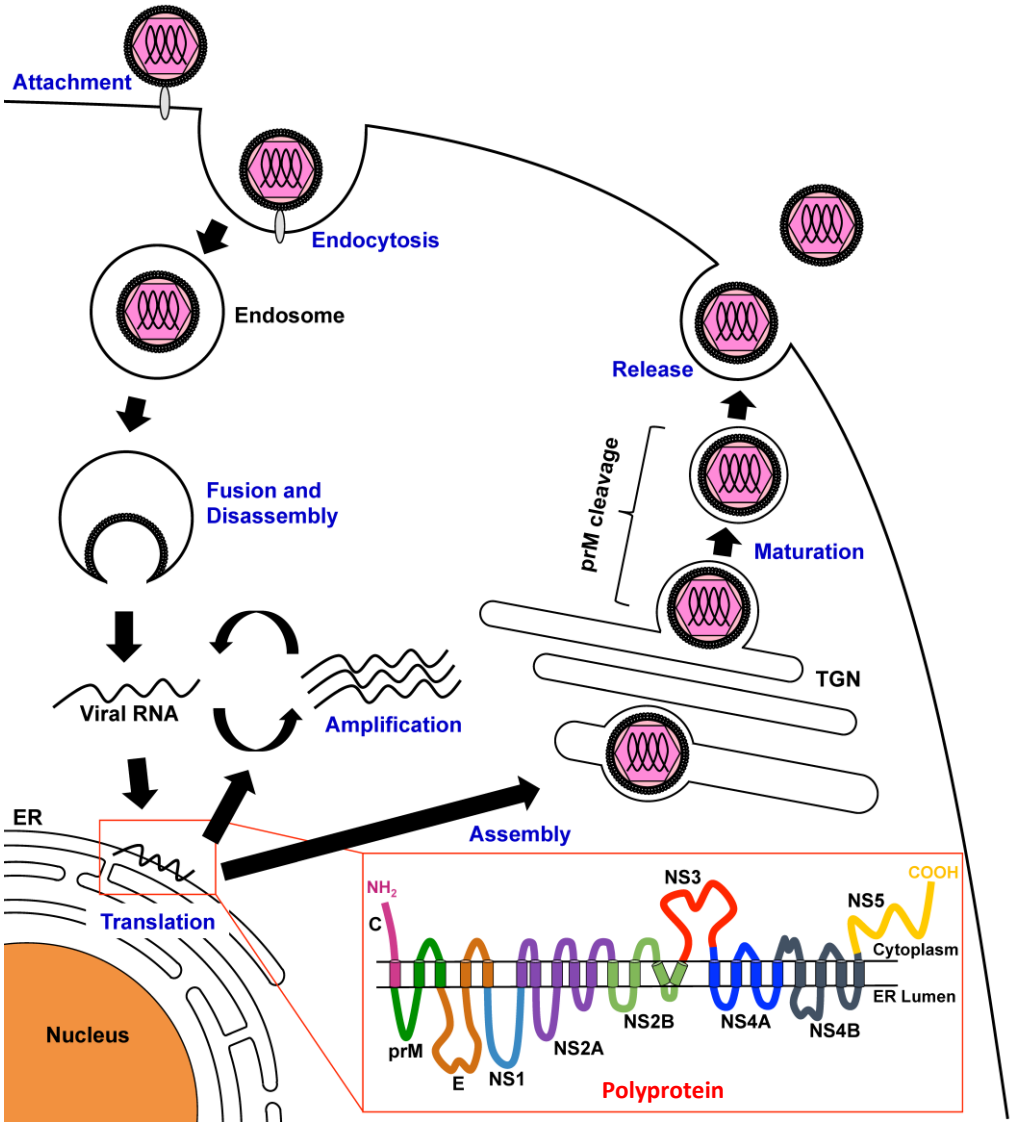

Figure 3. DENV replication cycle. The red frame shows the putative organisation of the viral polyprotein through the ER membrane. ER: endoplasmic reticulum; TGN: trans-Golgi network; C: capsid; prM: pre-membrane; NS1 to 5: non-structural proteins 1 to 5. Figure adapted from Kato *et al.* under the license Creative Commons BY 4.0.[45]

The interaction between the virus particle and multiple receptors on the surface of host cells is responsible for the internalisation of the virus via clathrin-mediated endocytosis.[46] Lowering of the pH inside the endosome causes an irreversible conformation change in the E protein, from dimer to trimer, that facilitates the fusion of the viral and endosomal membranes. The nucleocapsid is released into the cytoplasm and disassembles. The viral genome is then translated into a single polyprotein that undergoes post-translational cleavage by host and viral proteases, thus generating the viral proteins. The synthesis of this polyprotein is induced by the viral genome itself, which acts as mRNA, and occurs at the membrane of the endoplasmic reticulum (ER). In the early phase of the infection, the synthesis of new antiviral genomes (amplification) occurs in the cytoplasm whereas, at a later stage of the infection, this process is translocated to a structure referred to as replication complex (RC).[44, 45] The RC consists of viral genomes and membranous organelles derived from the ER and the trans-Golgi network (TGN), whose formation is induced by DENV infection.[44, 45, 46] The viral RNA presents a single open reading frame (ORF) between two highly structured and conserved 3' and 5' untranslated regions (UTRs). The ORF of the viral genome codes for the aforementioned polyprotein, which includes ten viral proteins required for the viral life cycle: three structural proteins and seven non-structural proteins (Figure 4).[34, 46]

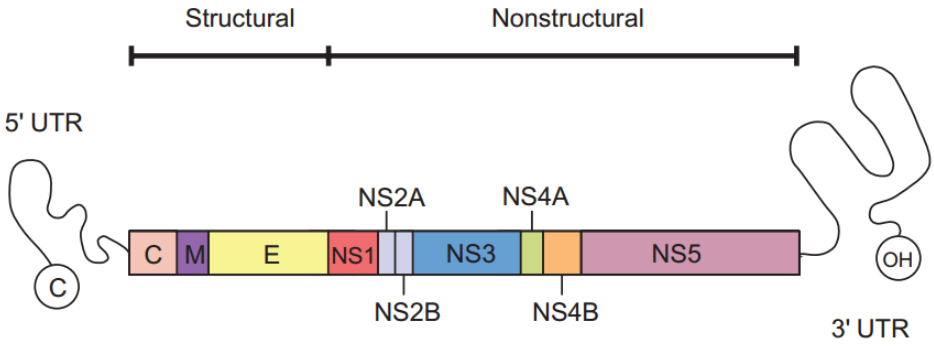

Figure 4. DENV genome codes for ten viral proteins. C: capside; M: membrane precursor or prM; E: envelope; NS1 to 5: non-structural proteins 1 to 5; UTR: untranslated region. Figure reproduced from Simmons *et al.* under the license Creative Commons BY-NC 3.0.[34]

The structural proteins capsid (C), E and prM form the virion. The non-structural proteins are NS1, NS2A and NS2B, NS3, NS4A and NS4B, NS5 and are involved in RNA genome replication, virion assembly as well as evasion of the host immune response.[46] The non-structural protein 5 (NS5) comprises a RNA-dependent RNA polymerase (RdRp) responsible for the synthesis of the viral

genome. RdRp synthesises a negative-sense intermediate RNA strand, which is the template for the synthesis of double stranded RNA (dsRNA). Capping of the 5' end of the positive-sense RNA genome is catalysed by the viral methyltransferase (MTase) domain located at the N-terminus of NS5. The processed dsRNA is unwound by non-structural protein 3 (NS3), which contains a RNA helicase at its C-terminal. The viral genome is encapsulated by the C protein in the cytoplasm to form the nucleocapsid that acquires the viral envelope by budding through the ER membrane containing the E and prM proteins. The immature viral particles traffic through the TGN. The extracellular release of the virion occurs via exocytosis after accumulation in intracytoplasmic vesicles, where the prM protein undergoes cleavage by an host protease (furin) into the membrane (M) protein in the late stage of maturation of the virion into an infectious virus.[25, 46, 47, 48]

1.1.8 DRUG DEVELOPMENT

As previously described in this thesis, hospital admission of DENV-infected patients is required for the clinical management of the potentially fatal DHF. This is the major cause of the huge economic burden posed by DENV infections in dengue endemic countries, many of which are resource-poor.[49] Vector control has proved itself not to be an efficient strategy for prevention of the disease in these countries and vaccination with the recently licensed dengue vaccine by Sanofi Pasteur does not provide complete protection against all four serotypes of DENV (see section 1.1.6 for further details). Furthermore, a dengue vaccine will not reach the majority of the population that is at risk of infection, because of limited vaccine production capability and transport as well as high cost of the new vaccine.[49] A safe and effective antiviral drug for the treatment of DENV infection, which as of yet is not available, would be highly beneficial not only for DENV-infected patients but also to reduce the expenditures that are due to DENV infections in endemic countries. Even if a true tetravalent dengue vaccine will be available, an antiviral agent would still be needed in countries with a low vaccination or for parts of the population who cannot receive the vaccine for safety reasons (e.g. young children, pregnant women). In addition, the administration of an anti-DENV drug would rapidly reduce viraemia in DENV-infected patients, thus decreasing the risk of progression of the disease to severe manifestations as well as preventing spread of the virus to others through mosquitoes.[50] For these reasons, an anti-DENV therapy is an urgent unmet

medical need. Large efforts have thus been undertaken in this field and are described in this section.

The development of an anti-DENV drug can be based on two general strategies: the inhibition of viral targets by direct-acting antiviral (DAA) agents and the inhibition of host targets that are either essential for viral replication or involved in the development of severe clinical manifestations.[48, 50] The viral target-based approach has been successfully applied to the development of DAA agents effective against other viruses, such as human immunodeficiency virus (HIV) and hepatitis viruses.[51, 52, 53] Advanced studies have been undertaken on hepatitis C virus (HCV) in the past[52] and the similarity of DENV to HCV, viruses belonging to the same family of *Flaviviridae*, make it plausible to repurpose anti-HCV drugs or drug candidates for DENV.[34, 50]

1.1.8.1 Host target-based approach

Despite the advantage of a high barrier for the emergence of resistance, the host target-based approach is challenging as it lacks selectivity, and thus is often associated with toxicity.[48, 50] However, it has been proven to be a valid antiviral approach as exemplified by the marketed anti-HIV drug, Maraviroc (**1**, figure 5), an inhibitor of a host co-receptor for virus entry.[54]

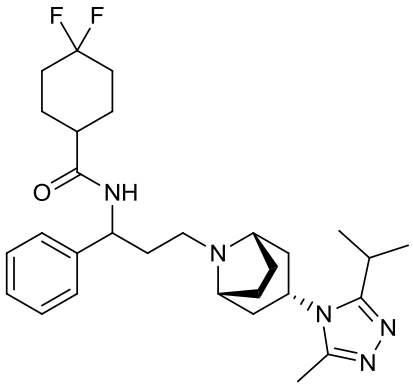

1

Figure 5. Structure of the anti-HIV drug Maraviroc (**1**).

In the case of DENV, multiple receptors on different cell types mediate viral entry and this represents an important obstacle for the identification of host target antagonists as inhibitors of the viral entry.[48, 50] In addition to proteins, lipids are also involved in different stages of the DENV replication cycle.[55] As inhibitors of cholesterol biosynthesis, statins were evaluated for their

potential antiviral activity *in vitro* and were found to exert an effect on both the viral entry as well as the maturation and release of viral particles.[56] However, clinical trials demonstrated that the administration of Lovastatin (**2**, figure 6) was not beneficial in dengue patients.[57]

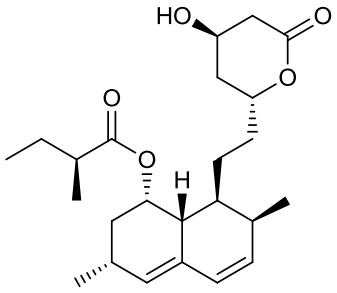

2

Figure 6. Structure of Lovastatin (**2**).

The inhibition of human enzymatic activities, which are essential for viral replication, seems to be a more promising approach for the identification of broadly active anti-DENV agents. Besides virus-encoded proteins, the DENV replication cycle requires host proteases and glucosidases. Host signal peptidases are responsible for the cleavage of a number of junctions in the single polyprotein derived from the translation of the viral genome, while furin activity is essential in the late maturation of virions as this host protease cleaves the prM protein into the mature membrane (M) protein.[48] However, inhibition of host proteases is likely to be associated with severe side effects.[48] Host glucosidases that are located in the ER lumen are essential for the correct folding and the glycosylation of both structural and non-structural viral proteins. The host α-glucosidase inhibitor Celgosivir (**3**, figure 7) was safe and well tolerated in a Phase Ib trial[58] and will be further evaluated for its efficacy in dengue patients.[59, 55]

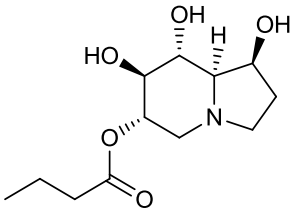

3

Figure 7. Structure of the anti-DENV drug candidate Celgosivir (**3**).

Cellular purine[60] and pyrimidine[50] biosynthetic pathways represent potential host targets for developing broadly active antiviral agents. The nucleoside analogue 1-β-D-ribofuranosyl-3-ethynyl-[1,2,4]triazole (ETAR, **4**, figure 8), which is structurally related to the anti-HCV drug ribavirin (RBV), was found to inhibit the replication of all four serotypes of DENV *in vitro* and is a promising drug candidate for the treatment of flaviviral infections.[60] The fact that the antiviral activity was suppressed by supplementary guanosine suggests that ETAR inhibits the host enzyme inosine monophosphate dehydrogenase (IMPDH), resulting in the depletion of guanosine triphosphate (GTP).[60]

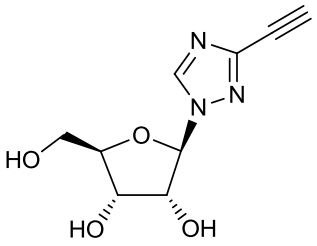

4

Figure 8. Structure of the IMPDH inhibitor ETAR (**4**).

Similarly, inhibitors of the dihydroorotate dehydrogenase (DHODH), a host enzyme involved in *de novo* pyrimidine biosynthesis, were active against a variety of virus families *in vitro*.[50] Figure 9 shows the structure of NITD982 (**5**) as an example of this class of compounds. However, no efficacy was observed *in vivo* suggesting that inhibiting DHODH actually may not represent an effective antiviral strategy.[50]

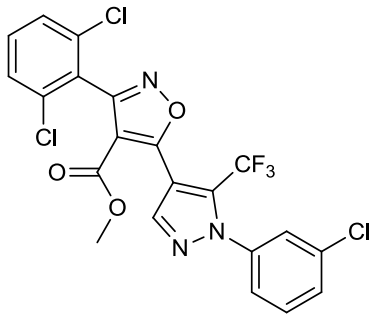

5

Figure 9. Structure of the DHODH inhibitor NITD982 (**5**).

Finally, targeting the pathological pathway that leads to plasma leakage and other DHF symptoms is an alternative strategy.[50, 61] In particular, the modulation of the cytokine response against DENV may prevent the progression to severe dengue.[56] The anti-inflammatory agents prednisolone (**6**, figure 10) and chloroquine (**7**, figure 10) were evaluated in clinical trials.[62, 63] The latter also acts by interfering with both early and late phases of the viral replication cycle.[56, 64] Although both agents were safe, no beneficial effects were observed in dengue patients,[62, 63] suggesting that the approach remains of poor feasibility due to the incomplete understanding of the illness.[50, 61]

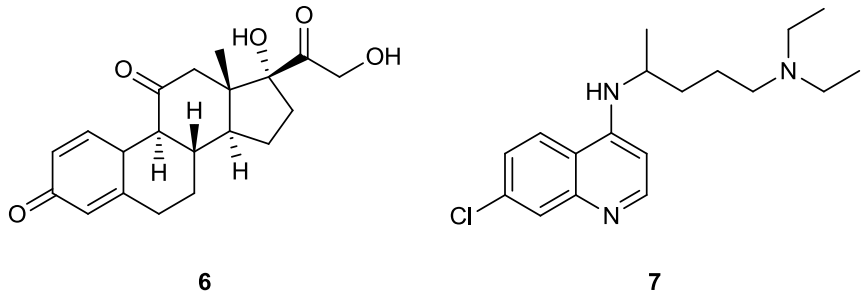

6 **7**

Figure 10. Structures of the anti-inflammatory agents prednisolone (**6**) and chloroquine (**7**).

1.1.8.2 Viral target-based approach

Antiviral agents have been directed to target both structural and non-structural viral proteins, principally the E, NS3 and NS5 proteins, in order to inhibit viral entry into cells and replication, respectively.[50, 65]

The E protein is the largest structural protein (500 amino acids) and is embedded in the lipid membrane of the virus. The role of the E protein in the attachment to the host cell surface and the fusion to the endosomial membrane allows for the design of viral entry inhibitors based on targeting this viral protein. Indeed, targeting viral entry is a known strategy for antiviral therapeutics as, in a similar way, HIV-gp41, which is a subunit of HIV envelope protein, is inhibited by Enfuvirtide, an approved anti-HIV drug that acts by blocking the fusion of viral and host cell membranes.[50] DENV E protein consists of three domains (I, II and III). A hydrophobic pocket interacting with the detergent molecule β-*N*-octylglucoside has been identified between domains I and II. Both small-molecules occupying this pocket, such as compound **8** in figure 11, or peptides interacting with the E protein inhibit the conformational changes (from dimer to trimer) of this structural protein, which are essential for the fusion of viral and host membrane.[66, 67]

Furthermore, the polysaccharide curdlan sulfate (CRDS, **9**, figure 11), was also reported to inhibit the E protein of all four DENV serotypes *in vitro* by binding in a newly discovered pocket at the interface between domains I and II.[65, 68] Recently developed strategies involve the use of monoclonal antibodies directed against epitopes within the E protein, either to prevent host cell binding or to block the rearrangement of the viral protein required for the fusion step.[65, 69]

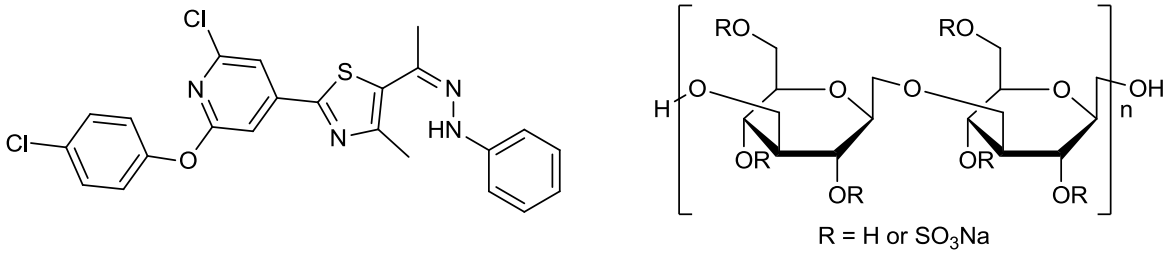

8 **9**

Figure 11. Structures of a small molecule inhibitor targeting the β-*N*-octylglucoside pocket (**8**) and the polysaccharide curdlan sulfate (**9**).

The DENV C protein is a highly basic protein that interacts with the viral RNA genome to form the nucleocapsid, and is involved in both the uncoating and assembly of the virions. In the cytoplasm, C proteins are arranged in concave-shaped homodimers that are attached to ER membranes at the 'top', whereas the RNA is believed to bind the 'floor' of this concave structure.[70, 71] ST-148 (**10**, figure 12) has been recently reported as a potent DENV replication inhibitor both *in vitro* and *in vivo*,[70, 71] through stabilisation of capsid self-interaction and formation of rigid oligomers, altering both release of viral genome from nucleocapsids and late-stage assembly of viral particles.[71]

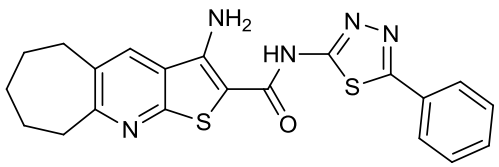

10

Figure 12. Structure of the C inhibitor ST-148 (**10**).

Among the ten non-structural proteins encoded by the viral genome, only NS3 and NS5 are known enzymes. Although activities of the other non-structural proteins remain to be clearly understood, they appear to be essential for RNA replication. In particular, NS2A, NS2B, NS4A and NS4B are transmembrane proteins involved in the formation of the viral replication complex and represent valid antiviral targets.[48, 65]

The DENV protease consists of the N-terminal domain of NS3 (170 amino acids) and an approximately 40 amino acid region of NS2B.[48] The enzyme is a serine protease containing the catalytic triad of His51, Asp75 and Ser135.[48] As already mentioned, the translation product of the viral genome is a long polyprotein that needs to be cleaved into the individual proteins. The viral protease NS2B-NS3 is responsible for the cleavage of specific junctions (precisely, between C-prM, NS2A-NS2B, NS2B-NS3, NS3-NS4A, NS4A-2K peptide and NS4B-NS5), whereas host proteases (signal proteases) cleave the other sites of this polyprotein.[61] The NS2B-NS3 activity is essential for viral replication, therefore the enzyme represents a valid antiviral target.[48, 65] Protease inhibitors (PIs) have also been successfully developed for the treatment of other antiviral infections, in particular there are ten HIV-1 PIs and two HCV PIs (telaprevir and boceprevir) currently in clinical use.[50, 53] However, treatment with PIs is generally associated with the rapid emergence of drug-resistant viral strains, hence PIs need to be administered in combination with other antiviral agents, especially for long-term therapy (both HIV-1 and HCV cause chronic diseases).[50] Furthermore, telaprevir and boceprevir do not exhibit a pan-genotypic effect, being active only against HCV genotype-1.[50] Although dengue is an acute illness, the identification of NS2B-NS3 inhibitors effective against all four DENV serotypes might be a significant challenge and combination with another DAA agent would be required.[50] To date, there are no PIs against DENV which have advanced to preclinical trials. The main challenge in the development of PIs is related to the properties of the active site of NS2B-NS3, which is relatively flat and negatively charged. The positively charged scaffold required to interact with the active site would cause poor permeability through membranes and antiviral activity would be compromised by pharmacokinetic aspects.[48, 50, 65] However, the design of peptidomimetics as well as the identification of small-molecule inhibitors through high-throughput screening (HTS) of libraries[48, 50, 65] remain valid approaches for developing potential DENV PIs. Recent *in silico* design efforts enabled the identification of effective and more membrane permeable peptidomimetics (figure 13) that represent a promising starting point for further development.[72]

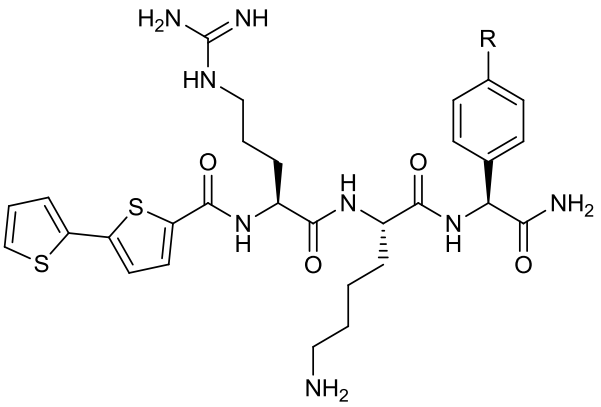

Figure 13. General structure of peptidomimetics inhibitors of the NS2B-NS3 protease.

A further antiviral target is the DENV RNA helicase, which is located at the C-terminus of NS3 (approximately 440 amino acids).[50] The main role of the RNA helicase is to unwind the dsRNA, separating the positive sense single stranded RNA (ssRNA) that constitutes the viral genome, from the negative sense RNA template. Although helicases share high structural similarity, the presence of an additional domain in the viral helicase compared to host ones may allow for developing selective inhibitors. Additionally, an adenosine triphosphate (ATP)-binding site is present in the NS3 domain and is endowed with both ATP-hydrolysis and nucleotide triphosphatase activities.[48, 73] Unfortunately, the DENV helicase domain does not show any significant pocket and the ATP-binding pocket is shallow and polar, and thus challenging to target with a small-molecule inhibitor.[48] As of yet, there are no marketed helicase inhibitors for the treatment of HCV infections and only few compounds are undergoing studies as potential DENV helicase inhibitors, including ivermectin (**11**, figure 14) and ST-610 (**12**, figure 14).[50] Recently, the inhibition of the ATP-hydrolysis was demonstrated to be sufficient to confer antiviral activity.[73] This discovery may facilitate future advances towards novel DENV NS3 inhibitors.[65]

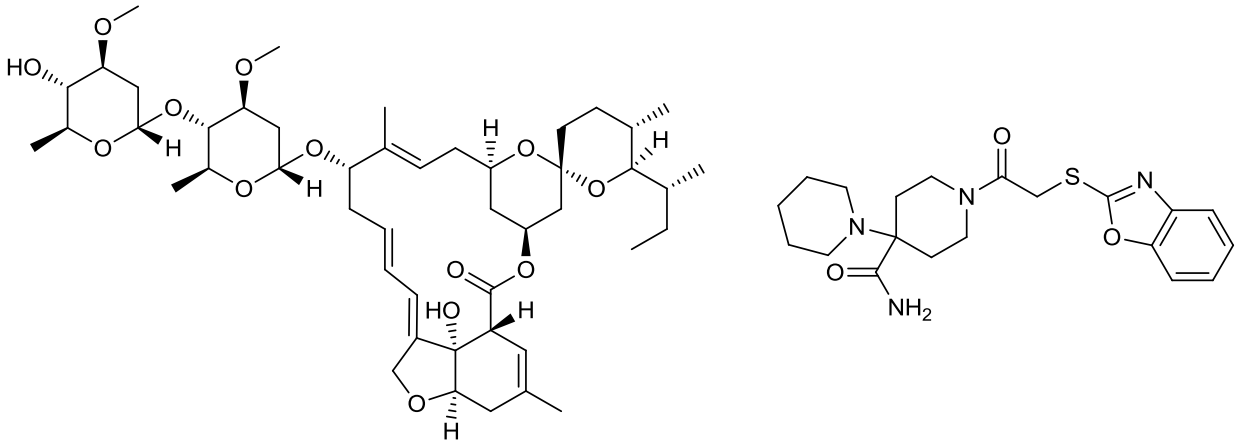

11 **12**

Figure 14. Structures of the DENV helicase inhibitors ivermectin (**11**) and ST-610 (**12**).

NS5 is the largest DENV protein, being approximately 900 amino acids long with a mass of 104 kDa. NS5 contains a methyltransferase (MTase) at its N-terminus (approximately 270 amino acids) and an RdRp at its C-terminus (approximately 600 amino acids).[74] DENV MTase has a dual activity as it catalyses both the methylation of the *N*-7 position of guanine at the 5'-end of the RNA genome and the methylation of the hydroxyl group at the 2'-position of the first adenosine nucleotide, and thus is involved in the viral RNA capping synthesis.[65, 75] *S*-adenosyl methionine (SAM) is the methyl donor for both methylation reactions with *S*-adenosyl homocysteine (SAH) being generated as a by-product.[61] The two distinct reactions occur in one single active site and are sequential. Therefore, repositioning of the RNA substrate is required after the first methylation of the *N*-7 position of guanine to allow the second methylation at the 2'-OH of the ribose of the internal adenosine.[75, 76] The *N*-7 methylated cap then binds to DENV MTase in a second pocket, referred to as the GTP pocket, so that the second methylation reaction can occur.[75, 76] Although the activity of the MTase is essential for viral replication and the enzyme constitutes a valid antiviral target, the highly conserved domain of the enzyme makes it challenging to design selective viral MTase inhibitors that do not interfere with the activity of host MTases.[65] Nevertheless, the SAM-binding site as well as the GTP pocket have been investigated as potential targets for drug development. Indeed, both SAM analogues interacting with the active site, such as compound **13** in figure 15, and molecules binding to the GTP pocket, including BG-323 (**14**, figure 15), have been identified, proving the druggability of the viral MTase.[50, 65, 76]

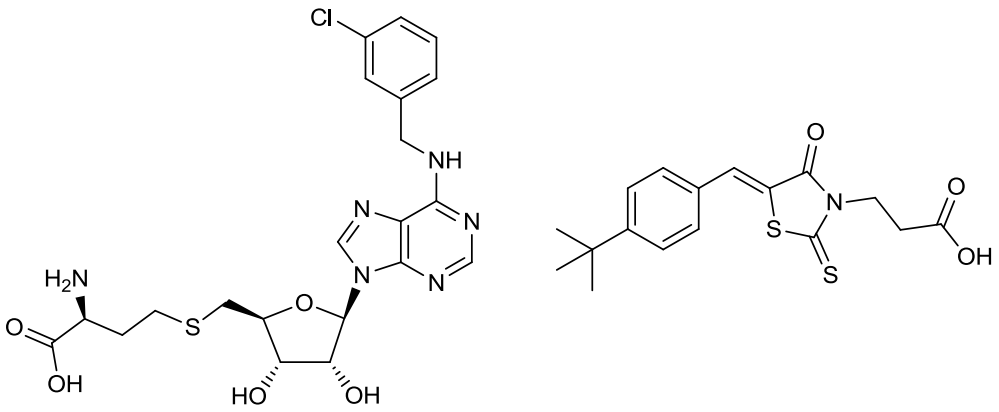

13 **14**

Figure 15. Structures of DENV MTase inhibitors targeting the active site (**13**) and the GTP pocket (**14**).

The RdRp domain of DENV NS5 is likely to be the most attractive target for the development of specific antiviral agents. Firstly, NS5 is the most conserved protein among the four serotypes of DENV, which share a minimum of 67% identity of their respective amino acid sequences,[74] as well as other RNA viruses of the *Flaviviridae* family. Secondly, the activity of the polymerase is essential for viral RNA synthesis, and therefore for viral replication.[48, 65] Finally, host cells lack RdRp activity, leading to fewer inhibiting effect on host enzymes.[48, 65] Structural and functional properties of DENV RdRp will be described in section 1.2.1. Inhibition of the viral polymerase can be achieved by two different classes of compounds: nucleoside inhibitors (NIs) and non-nucleoside inhibitors (NNIs). NNIs are small molecules that act as non-competitive inhibitors by interacting with the polymerase in allosteric sites. Commonly, NNIs stabilise an inactive conformation of the enzyme or interfere with the conformational changes required for RNA synthesis.[48, 50] The first allosteric inhibitors of DENV RdRp were *N*-sulfonylanthranilic acid derivatives, such as NITD2 (**15**, figure 16), possibly acting by sterically blocking the tunnel for the access of the RNA template to the polymerase active site. However, development of these compounds did not advance due to their poor pharmacokinetic properties.[77] Recently, a number of DENV RdRp inhibitors targeting allosteric pockets have been identified by *in silico* drug design methods.[78, 79, 80] Specific NNIs are described in paragraph 2.1.3.4 of this work.

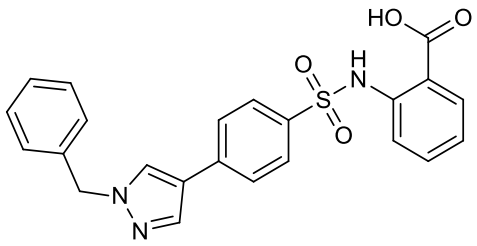

15

Figure 16. Structure of the DENV RdRp allosteric inhibitor NITD2 (**15**).

The main drawbacks of NNIs are associated with the fact that allosteric sites are generally less conserved than the active site of the polymerase. Drug-resistant virus strains may circulate and rapidly emerge upon treatment with a NNI, hence combination with a second antiviral agent may be required. For the same reason, NNIs might not be active against all four DENV serotypes.[48, 50]

A novel strategy for the inhibition of DENV replication is the disruption of the interaction of DENV RdRp with its partner proteins, such as the viral protein NS3 and the cellular α,β_1-importins.[76] The structural elements involved in the NS5-NS3 as well as the NS5-importin interactions have been identified in the DENV RdRp crystal structure, as described in detail in section 1.2.1. Although an exact role remains to be clarified, the binding of NS5 with its partner proteins appears to be crucial for viral replication.[50] The anti-helminthic drug ivermectin (**11**), previously identified as inhibitor of both the DENV helicase and protease,[50] was recently reported to disrupt the interaction between NS5 and the α,β_1-importins.[76] *N*-4-hydroxyphenyl retinamide (4-HPR), also called fenretinide (**16**, figure 17), inhibits DENV replication *in vitro* and *in vivo* and acts by blocking the NS5-importins interaction.[76]

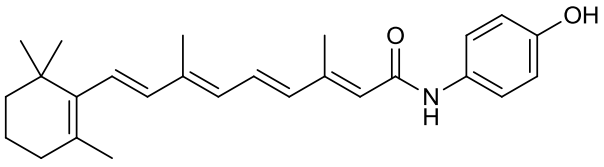

16

Figure 17. Structure of 4-HPR (**16**).

NIs, in their triphosphate active form, are competitive inhibitors and act by incorporation into the nascent RNA strand. Being directed to the highly conserved active site of the viral polymerase, NIs

overcome the disadvantages of NNIs such as the emergence of resistance and the lack of activity against all four serotypes of DENV.[48, 50, 65] On the other hand, drawbacks of this class of DAAs include complexity of prediction of the structure-activity relationship (SAR) and *in vivo* toxicity, which is often not observed in previous *in vitro* studies (see section 1.2.2 for further details).[48, 50, 65] In this respect, the adenosine analogue NITD008 (**17**, figure 18) is a noteworthy example. NITD008, a potent inhibitor of DENV RdRp *in vitro* and *in vivo*, did not show any cytotoxicity in over 100 biochemical assays; however, its further development as an anti-DENV agent had to be terminated due to severe side-effects observed in animals.[81, 82] The cytidine analogue prodrug balapiravir (**18**, figure 18), which was originally evaluated for the treatment of HCV infections, was repurposed as an anti-DENV candidate.[50, 56, 65] Although a potent inhibiting effect was observed *in vitro*,[50, 56, 65] balapiravir was found not to be beneficial in a clinical Phase II trial.[83] Nevertheless, the fact that balapiravir is the only DAA that reached clinical trials in humans so far demonstrates the high potential of NIs as anti-DENV agents.[65]

Properties of NIs and anti-DENV NIs will be further described in paragraph 1.2.2.2.

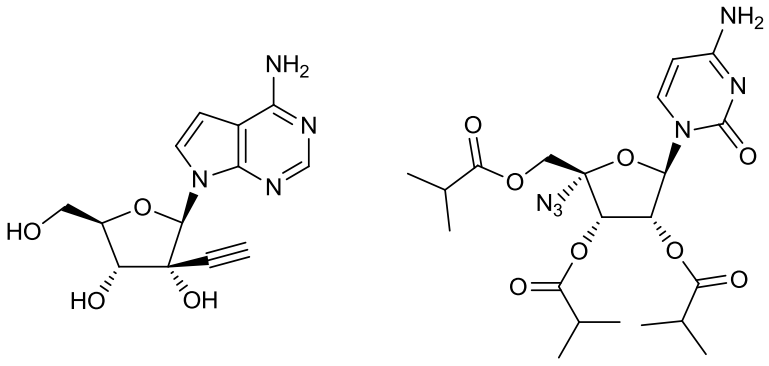

17 **18**

Figure 18. Structures of NITD008 (**17**) and balapiravir (**18**).

Extensive efforts were undertaken to develop an anti-DENV therapy, as exemplified in this section. To date, a restricted number of drugs, including two non-specific drugs, one host-targeting antiviral agent and one DAA, have reached clinical evaluation, none of which showed encouraging results.[55, 56, 58, 62, 63, 64, 83] An effective agent for the treatment of DENV infection remains an urgent unmet medical need.

1.2 DENV POLYMERASE AS A DRUG TARGET

1.2.1 DENV POLYMERASE

DENV polymerase is a RdRp, capable of *de novo* RNA synthesis, hence in the absence of a peptide or RNA primer. DENV polymerase synthesises a transient dsRNA intermediate, composed of viral positive and negative sense RNA strands. The negative sense RNA acts as a template for the synthesis of the new positive sense RNA, which displaces the old one in the dsRNA.[84] The dsRNA is then unwound and the positive sense ssRNA, which is the viral genome, is available for translation to the viral polyprotein, synthesis of complementary negative sense RNA strands or assembly of viral particles.

Complementary sequences are present at the 5' and 3'-ends of the viral genome, named cyclisation sequences (CS) and 'upstream of AUG regions' (UAR). The interactions between these regions (long-range RNA-RNA interactions) cause the viral RNA to circularise (figure 19).[84, 85, 86]

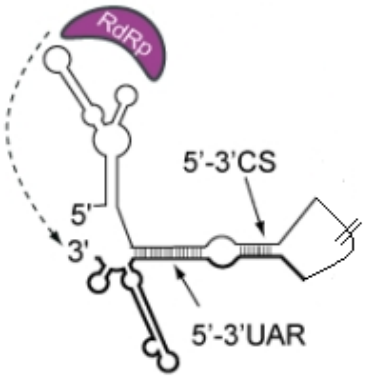

Figure 19. Schematic representation of circular DENV genome. 5'-3'CS and 5'-3'UAR are long-range RNA-RNA interactions causing genome cyclisation. DENV RdRP recognises the 5'-end and initiates RNA synthesis at the 3'-end of the negative sense ssRNA. CS: cyclisation sequence; UAR: upstream of AUG regions. RdRp: RNA-dependent RNA polymerase. Figure adapted from Gebhard *et al.* under the license Creative Commons BY-NC-SA 3.0.[86]

Cyclisation of the viral genome represents a crucial feature for the *de novo* synthesis of the negative sense RNA strand, as DENV RdRp specifically recognises a promoter element, called stem-loop A (SLA), at the 5'-end before starting the *de novo* RNA synthesis from the 3'-end of the ssRNA template.[84, 85, 86] In contrast, the presence of the 3'-end of the negative sense RNA template in

the dsRNA replicative intermediate seems to be sufficient for the synthesis of the complementary positive sense ssRNA. This may be explained by the fact that in the dsRNA replicative intermediate the SLA at the 5'-end of the old positive positive sense RNA is positioned near the 3'-end of the negative sense RNA template, and thus it may promote binding to the RdRp domain.[84, 85, 86] However, the exact mechanism of the *de novo* initiation of RNA synthesis by *flavivirus* polymerases is not yet fully understood.

The DENV RdRp domain is located at the C-terminus of NS5 and consists of around 600 amino acids.[74, 84] Three crystal structures of the *apo* DENV RdRp have been reported (Protein Data Bank codes 2J7U, 4HHJ and 4C11).[74, 87, 88] Additionally, the full length DENV NS5 structure as well as the NS5 dimer structure have been solved very recently (Protein Data Bank codes 4V0R and 5CCV).[89, 90] In the available crystal structures, DENV RdRp is in the 'closed' conformation characteristic of primer-independent viral polymerases and shows a right-handed architecture consisting of three subdomains, fingers, palm and thumb (figure 20).

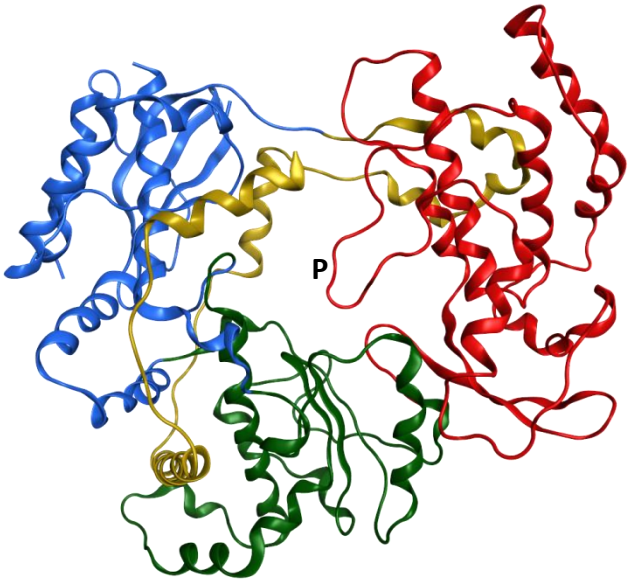

Figure 20. View of the DENV RdRp (Protein Data Bank code 4HHJ).[52] The protein is displayed as ribbon and colours distinguish domains as follows: fingers in blue, palm in green and thumb in red; the two NLSs are shown in yellow. RdRp: RNA-dependent RNA polymerase; NLS: nuclear-localisation sequence; **P**: priming loop.

Although this overall structure is typical of known viral RNA polymerases, the additional presence of two nuclear-localisation sequences (NLS) at the N-terminal region (residues 320-368 and 369-389) is a peculiarity of DENV RdRp compared to other flaviviral RdRp and is thought to influence the structural properties of the protein.[74] Interestingly, one of the two NLSs (residues 320-368) also interacts with the C-terminal domain of NS3, suggesting that the enzymes may modulate their respective activities.[74] Furthermore, the NLSs interact with the intracellular transport proteins importin-α and importin-β, allowing the DENV RdRp to enter the nucleus. However, the exact function of the localization of the polymerase in the nucleus remains yet to be clarified.[61, 74] The palm is the most conserved subdomain and contains the Gly-Asp-Asp catalytic active site (residues 662-664). Asp553 is also involved in the mechanism of formation of the phosphodiester bond: it deprotonates the 3'-hydroxyl group of the nucleotide, generating the anion that attacks the α-phosphate of the incoming nucleotide triphosphate (NTP).[84] The coordination of two Mg^{2+} ions by Asp533 via a molecule of water and by Asp664 in the active site is essential for the activity of the polymerase.[74] Although the exact role of the divalent cations remains uncertain, they may be important to position the incoming nucleotide.[61] The active site is encircled by several loops, named fingertips, that contribute to shaping the tunnel for the access of the ssRNA template from the top of the RdRp to the active site and keeping the protein in a 'closed' conformation, which is required in the initiation phase of the *de novo* RNA synthesis.[44] The fingertips region, which is at the top of the protein, constitutes a link between the fingers and the thumb and is characterised by a high degree of flexibility. An additional loop, the so-called priming loop (figure 20, **P**), contributes to maintaining the RdRp in the 'closed' conformation which is observed in the crystal structures. The priming loop **P** (residues 782-809) belongs to the thumb subdomain and projects towards the active site, which it partially occludes.[74] This loop, which is not present in primer-dependent polymerases, is equivalent to the beta-loop observed in HCV RdRp[91] and is believed to be essential for *de novo* RNA synthesis and is thought to provide the platform that stabilises the initiation complex required for *de novo* RNA synthesis.[61] An aromatic amino acid of the priming loop **P** needs to stack against the nucleobase of the incoming NTP during the initiation phase. A conserved residue of tyrosine is thought to act as key priming residue in other primer-independent polymerases (Tyr448 in HCV NS5B)[84] whereas a tryptophan or an histidine may have this role in *flavivirus* polymerases (Trp795, His798 in DENV RdRp).[77, 84, 92] A second narrow tunnel through the centre of DENV RdRp, which is almost perpendicular to the tunnel of the ssRNA template,

allows the NTPs to access the catalytic site from the back of the polymerase, whereas the front of this tunnel is partially obstructed by the priming loop.[61]

DENV RdRp hosts two zinc-binding sites in the fingers and thumb subdomains. The first Zn^{2+} ion, coordinated by Cys446, Cys449, His441 and Glu437, is also observed in the WNV RdRp crystal structure, whereas the second Zn^{2+} ion represents a peculiarity of DENV RdRp.[74, 84, 93] The binding site of this additional cation consists of His712, His714, Cys728 and Cys847 and is in close position to the expected binding site of the incoming NTP, in a hinge between the thumb and the palm.[74, 84, 93]

A concave surface is observed at the base of the fingers subdomain, close to the N-terminal region of the protein. It was suggested that this surface may accommodate the MTase domain of NS5.[74] However, a flexible linker was identified between the RdRp and MTase domains in the DENV RdRp crystal structure by Lim *et al*.,[88] and in the full length DENV NS5 crystal structure by Zhao *et al*.[89] and the NS5 dimer by Klema *et al*.[90] This inter-domain linker can adopt different conformations and thus allows the two globular domains to adopt various orientations and modulate their respective enzymatic activities.[88, 89, 90]

De novo RNA synthesis involves the initial condensation of two nucleotides having complementary nucleobases to the two 3'-terminal nucleobases of the RNA template.[44, 74] As mentioned above, a 'closed' conformation of the RdRp is required for stabilising the complex in the initiation phase and for catalysing the formation of the phosphodiester bond between the first two nucleotides.[44] As previously mentioned, the priming loop **P** is believed to represent the structural element that provides the initiation platform, however also the fingers subdomain may be involved in the network of interactions that stabilises the initiation complex.[84, 87] It has been hypothesised that the crystal structures of *flavivirus* polymerases capture the enzymes in a pre-initiation conformation.[84] Upon initiation of the RNA synthesis, concerted conformational changes of the fingers may occur and bring these loops in contact with the first NTPs in an initiation-competent 'closed' conformation.[74, 84]

After the dinucleotide stage of the synthesis of the RNA, the polymerase needs to undergo drastic conformational changes to an 'open' structure that allows for the elongation of the RNA growing strand and egress of the dsRNA from the front of the enzyme.[44, 74] As the priming loop **P** partially occludes the path of the dsRNA, it is thought to be the main site of conformational changes during the activity of the enzyme. A rotation of the thumb outwards may also occur during the activity of DENV RdRp, leading to a more open conformation. The Zn^{2+} ion located in the thumb subdomain

may play a role in the regulation of this rotation, and therefore in the transition from initiation to elongation.[84, 93] Details on the conformation of RdRp during the elongation phase are unknown, as a crystal structure of the *flavivirus* polymerase in complex with the newly synthesised dsRNA is not yet available.

1.2.2 NUCLEOSIDE INHIBITORS

DENV RdRp has an essential role in viral replication and may represent the ideal target for developing DAAs. As previously mentioned, two main strategies can be pursued for inhibiting the synthesis of viral RNA by the polymerase, using NNIs or NIs.[48, 50] Nucleoside analogues, which make up the most abundant class of marketed antiviral agents,[48, 50, 94] are prodrugs that become active upon intracellular conversion to their corresponding triphosphates by host cell kinases. The triphosphate form then targets the active site of the polymerase and acts as a competitive inhibitor by mimicking the natural NTP substrate of the enzyme. Finally, the triphosphate derivative is incorporated into the nascent RNA, either causing chain termination or inducing mutations in the new viral genome. NIs offer important advantages over other classes of antiviral drugs. Firstly, since NIs interact with the highly conserved active site of the polymerase, NIs have a higher barrier for the emergence of resistance compared to other DAAs.[48, 50, 65] Secondly, NIs are likely to be effective against a variety of related viruses, including the four serotypes of DENV, other flaviviruses and HCV, given the structural similarity of their polymerases.[48, 50, 65]

On the other hand, the development of NIs is often challenging. Phosphorylation of the nucleoside analogue to mono-, di- and finally triphosphate are catalysed by host kinases. Therefore, the nucleoside analogue needs to be recognised by – and act as substrate of – cellular kinases, whereas the triphosphate derivate must selectively inhibit the viral polymerase. Moreover, as the antiviral activity of a potential NI is the result of several events, including cellular uptake via nucleoside transporters and intracellular activation by host kinases, the prediction of SAR of this class of compounds is often not a suitable approach for identifying potent compounds.[48, 50, 65] Another major challenge associated with NIs is their unpredictable toxicity *in vivo*. Toxicity due to inhibition of the mitochondrial polymerase γ in host cells has been observed as a common side effect, especially with deoxy-nucleoside analogues used in long-term treatment.[48] Although mitochondrial toxicity might not be a significant issue in the case of anti-DENV NIs, which are

typically ribose nucleosides administered for less than a week,[50] extensive *in vivo* studies need to be carried out to evaluate these kind of toxicities, which are often not observed *in vitro*.[48, 50] Furthermore, nucleoside analogues are polar compounds, and thus have poor membrane permeability which results in poor cellular uptake by passive diffusion and bioavailability *in vivo*.[48, 50, 65] Finally, nucleoside analogues and their mono- and diphosphate derivatives are poor substrates of cellular kinases, resulting in an inefficient metabolism to the bioactive triphosphate. The first phosphorylation often represents the rate limiting step in the activation process and might compromise the antiviral activity of NIs.[48, 50, 95]

1.2.2.1 Nucleoside and nucleotide prodrugs

As described above, poor cellular permeation and limited phosphorylation are issues commonly encountered with nucleoside analogues. Poor cellular permeation could be overcome by a nucleoside prodrug approach. This method consists of the conjugation of a cleavable moiety, such as an ester, to the nucleoside in order to increase lipophilicity and improve pharmacokinetic properties of compounds.[48, 50, 96] However, nucleoside prodrugs may be poor substrates for metabolic enzymes, thus resulting in poor activation.[96] Furthermore, this prodrug strategy does not overcome the issue of an inefficient conversion of the nucleoside analogue to its monophosphate form.

The nucleotide prodrug technology therefore aims at bypassing limiting first phosphorylation step by delivering the nucleotide monophosphate directly into cells. The nucleotide monophosphate itself is not a suitable candidate drug as the presence of negative charges at physiological pH make it unstable in biological media as well as highly hydrophilic and thus unable to diffuse across the cellular membrane.[95] However, the charges of the phosphate moiety can be masked by additional hydrophobic groups at the phosphorus centre.[48, 50, 95] The resulting nucleotide prodrug is a neutral molecule, which is characterised by increased lipophilicity compared to the parent nucleoside, and reaches the intracellular compartment by passive diffusion through the membrane. The nucleotide monophosphate is released following hydrolytic or enzymatic metabolism and trapped inside the cell due to the unprotected charges. Further phosphorylation steps of the mono- and diphosphate derivatives generate the biologically active NTP.[95] The application of the nucleotide prodrug approach improves pharmacokinetic properties and boosts biological activity of the parent nucleoside.[95]

Table 2. Summary of nucleotide monophosphate prodrug approaches.

Prodrug approach	**Classes**	**General structure**
Phosphotriester	Bis(pivaloyloxymethyl) (POM)	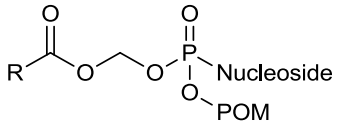
	Bis(*S*-acylthioethyl) (SATE) Bis(dithiodiethyl) (DTE)	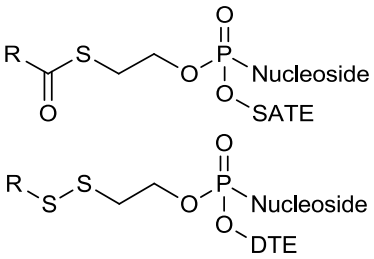
	HepDirect	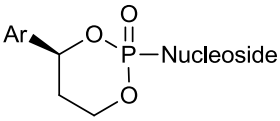
	CycloSal	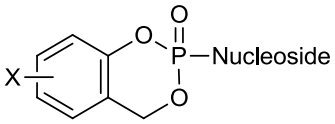
Phosphoramidate	ProTide (aryloxyphosphoramidate)	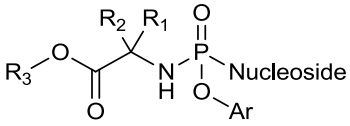
	Phosphoramidate monoester	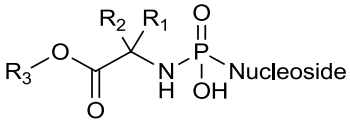
	Cyclic phosphoramidate	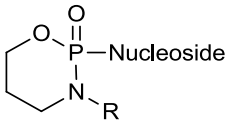
Phosphorodiamidate	Phosphorodiamidate	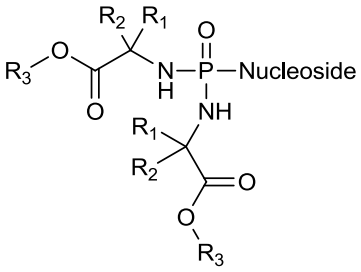
3’,5’-Cyclic prodrug	3’-5’-Cyclic triester and ProTide	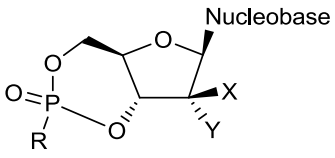

Several methodologies have been developed to mask the hydrophilic phosphate with neutral lipophilic moieties and are summarised in table 2.[95, 97, 98] In this work the phosphoramidate ProTide approach will be described.

The ProTide strategy was invented by McGuigan *et al*. and applied for the first time to the anti-HIV nucleoside analogue azidothymidine (AZT).[99] In these compounds, which are named ProTides, the negatively charged phosphate is masked by an amino acid alkyl or aryl ester and a second aryl moiety attached to the phosphorus centre (aryloxyphosphoramidate, figure 21). A ProTide presents three sites of possible modification: the aryl moiety, the amino acid and the ester. However, L-alanine is the most commonly used amino acid as it demonstrated a good biological profile,[100] whereas different combinations of the other two structural elements are generally explored in a series of ProTides to study the antiviral effect. A possible limitation of the phosphoramidate ProTide approach is the chirality of the phosphorus centre. ProTides are obtained as diastereoisomeric mixture (in approximately a 1:1 ratio) and separation of the two species, which are generally associated with different activity profiles, can be difficult.

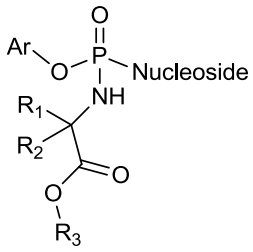

Figure 21. General structure of ProTides.

The putative activation pathway of ProTides involves two enzymatic steps (scheme 1).[101] The first step is the hydrolysis of the amino acid ester moiety catalysed by an esterase or carboxypeptidase type enzyme. The nucleophilic carboxylate derivative undergoes spontaneous cyclisation, with the displacement of the aryl moiety and subsequent water-mediated opening of the unstable ring. The nucleotide monophosphate is released following hydrolysis of the N-P bond catalysed by a phosphoramidase type enzyme (hystidine triad nucleotide-binding protein, Hint).[101]

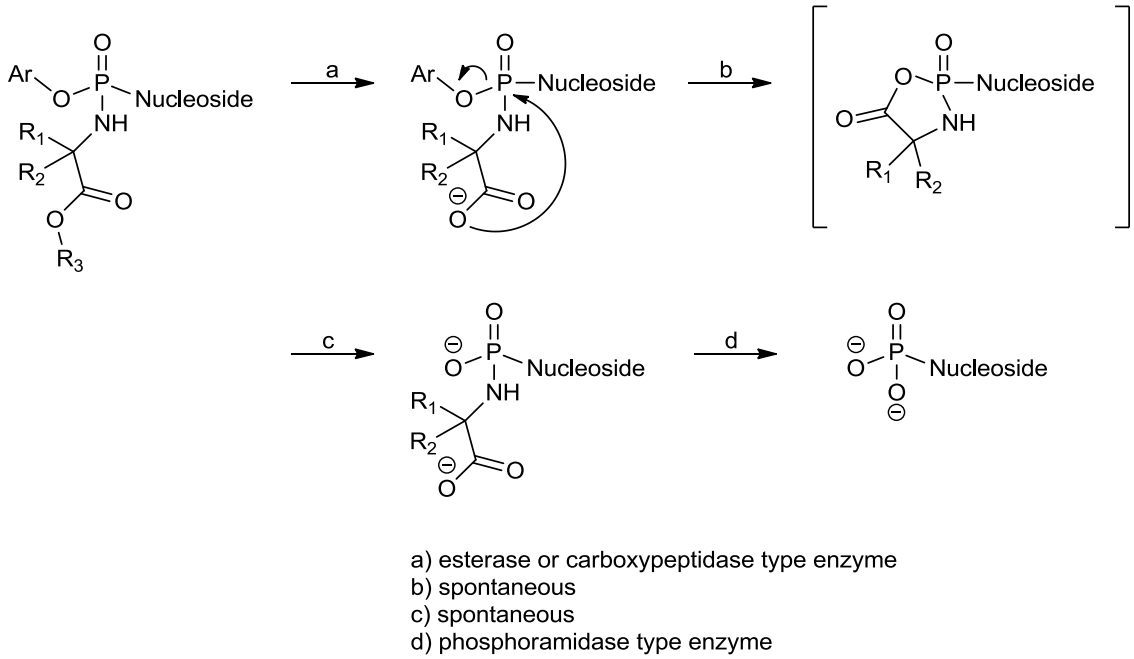

Scheme 1. Putative bioactivation pathway of a ProTide.[101]

According to the proposed mechanism of bioactivation, both the initial ester hydrolysis and the amino acid cleavage need to be possible in order to deliver the nucleotide monophosphate intracellularly, and thus to observe biological activity. The requirement of two cellular enzymes may therefore represent a limitation of the ProTide approach. For example, the application of the phosphoramidate strategy to the broadly active antiviral agent RBV generated only poorly active ProTides (figure 22), suggesting poor metabolism of the prodrug to the active monophosphate form. Indeed, enzymatic assays and molecular modelling studies suggested that the intermediate metabolites of the RBV ProTides are not substrates of the human Hint enzyme.[102]

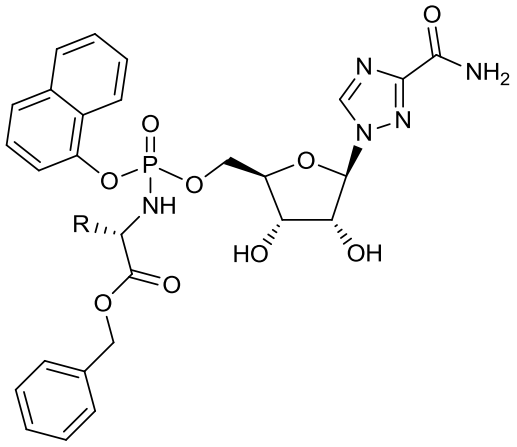

Figure 22. General structure of ribavirin ProTides.

Similarly, the application of the ProTide approach to the 7-deaza analogue of 2'-*C*-methyl-6-*O*-methylguanosine (figure 23), which is inactive against HCV due to poor cellular uptake and limited phosphorylation, failed to greatly restore the antiviral activity.[103] In contrast, the L-alanine neopentyl phosphoramidate ProTide of its 7-aza analogue (INX-08189 or BMS-986094, **19**, figure 23) progressed to clinical trials as an anti-HCV agent.[104]

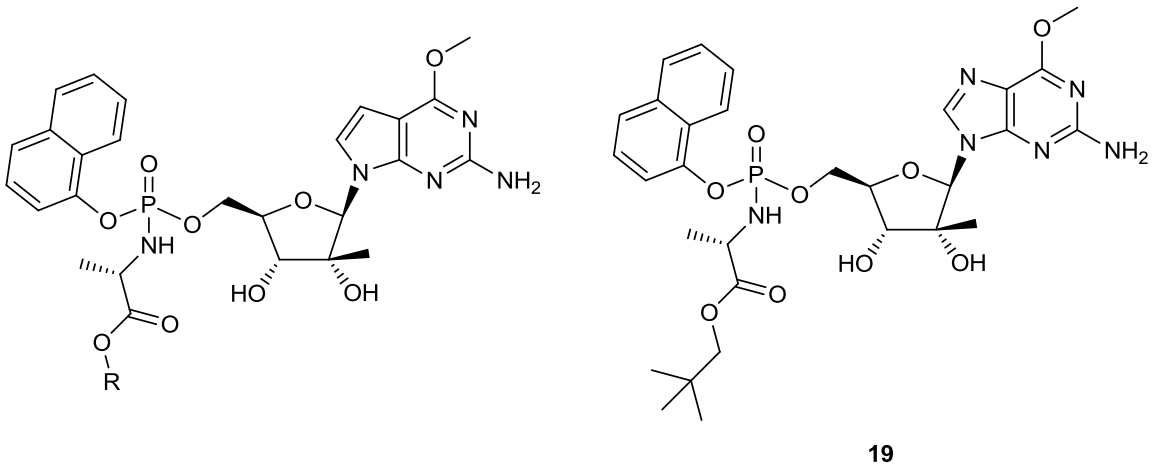

19

Figure 23. General structure of the 7-deaza-2'-*C*-methyl-6-*O*-methylguanosine ProTides compared to INX-08189 (**19**).

Despite these specific difficulties associated with the phosphoramidate ProTide approach, this nucleotide prodrug strategy was applied to various anticancer and antiviral nucleoside analogues.[99, 100, 104, 105, 106, 107, 108] A remarkable example is the L-alanine benzyl phosphoramidate

of the anticancer drug Gemcitabine (NUC-1031, **20**, figure 24), which was recently reported to bypass the resistance mechanisms that often limit the clinical use of the parent nucleoside.[106] NUC-1031 is currently in a clinical Phase III trial.[106]

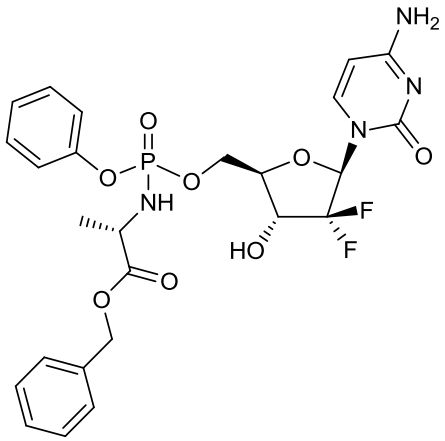

20

Figure 24. Structure of the Gemcitabine ProTide NUC-1031 (**20**).

Finally, the phosphoramidate ProTide technique has been clinically validated by the approval of two antiviral drugs. In fact, the single diastereoisomer of the L-alanine isopropyl phosphoramidate of 2'-deoxy-2'-α-fluoro-2'-β-*C*-methyluridine, Sofosbuvir (PSI-7977, **21**, figure 25) and of the acyclic phosphonate Tenofovir, Tenofovir alafenamide (GS-7340, **22**, figure 25), are now in clinical use for the treatment of HCV and HIV infections respectively.[107, 108]

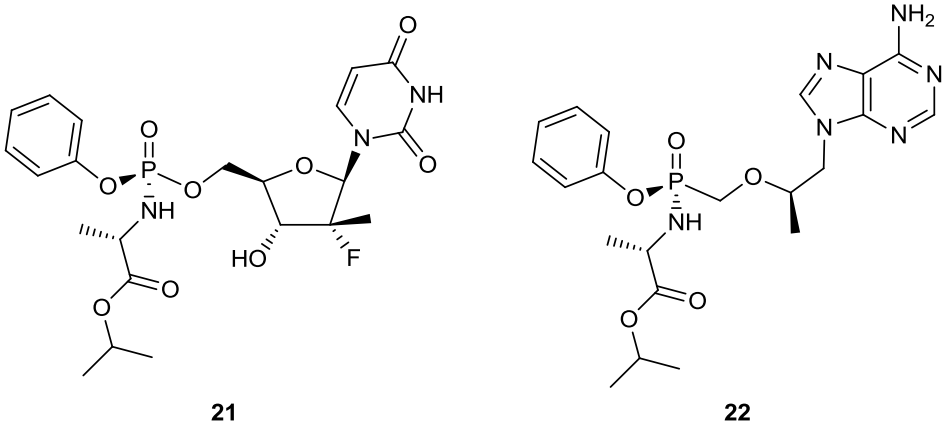

21 **22**

Figure 25. Structures of Sofosbuvir (PSI-7977, **21**) and Tenofovir alafenamide (GS-7340, **22**).

1.2.2.2 Anti-DENV NIs

Despite the difficulties linked to their development, NIs remains the most promising class of DAAs.[94] Cross-reactivity of NIs against HCV and DENV has been observed and repurposing has proved to be a valid strategy. 7-Deaza-2'-*C*-methyladenosine (**23**, figure 26), a potent inhibitor of HCV replication, was found to be broadly active against several members of the family *Flaviviridae*, including DENV (EC_{50} 15 μM).[109] Compared to the natural nucleoside, the inhibitor presents two modifications: i) the introduction of a 2'-*C*-methyl group (possibly able to sterically prevent the binding of the next incoming nucleotide), and ii) the carbon substitution of the *N*-7 position of the purine base, which increased the potency of the compound and significantly improved its pharmacokinetic properties. Indeed, the deamination by adenosine deaminase (ADA) to an inactive inosine derivative and the cleavage of the nucleoside by purine nucleoside phosphorylase (PNP) were found to be greatly reduced.[110, 111] Similarly, balapiravir (**18**, figure 26), a tri-isobutyrate ester prodrug of 4'-azidocytidine (R1479) originally developed as a potential anti-HCV agent, showed anti-DENV activity *in vitro*[50] and was evaluated in a clinical Phase II trial.[83] Unexpectedly, treatment of DENV-infected patients with balapiravir failed to produce any significant improvement of symptoms and clinical evaluation of this cytidine analogue was terminated due to lack of potency.[83]

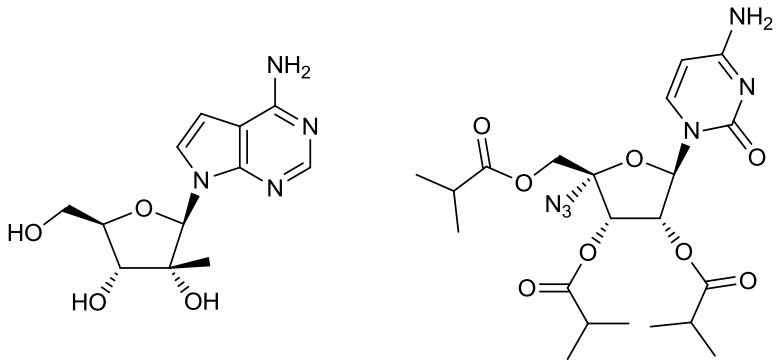

23 **18**

Figure 26. Structures of 7-deaza-2'-*C*-methyladenosine (**23**) and balapiravir (**18**).

A novel class of 2'-*C*-acetylene substituted adenosine analogues was identified by Novartis Institute for Tropical Diseases (NITD) as potent inhibitors of DENV replication both *in vitro* and *in vivo*.[81, 82, 112] NITD008 (**17**, figure 27) is the 7-deaza modification of adenosine combined with the

introduction of an acetylene at the 2'-position of the ribose moiety. NITD008 potently inhibited all the four DENV serotypes on different cell lines with submicromolar EC_{50}, as well as other members of the family *Flaviviridae*, including HCV, and was not cytotoxic *in vitro* at concentrations of up to 50 µM.[81] *In vivo* efficacy was examined in a dengue animal model: both multiple-dose treatment[81] and single-dose treatment[82] of DENV-infected mice with NITD008 suppressed peak viraemia and reduced cytokine elevation. Furthermore, the compound completely protected mice from death in a dengue mouse lethal model.[81, 82] Similarly, NITD449 (**24**, figure 27), the 7-carbamoyl derivative of NITD008, showed an EC_{50} < 1 µM for all four DENV serotypes and related viruses (YFV, WNV, HCV) and was not cytotoxic *in vitro* at concentrations of up to 12.5 µM.[112] However, a prodrug approach was required in order to overcome the low level of bioavailability of NITD449 when orally dosed in animals and thus to evaluate the efficacy of the compound *in vivo*. The addition of isobutyric acid via cleavable ester linkage at the 3' and 5'-*O*-positions of NITD449 led to the prodrug NITD203 (**25**, figure 27), which exhibited improved pharmacokinetic properties.[112] Furthermore, NITD203 was rapidly converted to the active compound, was not cytotoxic *in vitro* at concentrations of up to 25 µM and selectively inhibited viruses within the family *Flaviviridae* at submicromolar levels of EC_{50}.[112] *In vivo* efficacy was demonstrated for NITD203 in a dengue viraemia mouse model.[112] Although none of the adenosine analogues showed cytotoxicity in over 100 biochemical assays, NITD008 and NITD203 did not reach a satisfactory no-observable-adverse-effect level (NOAEL) in 2-week *in vivo* toxicity studies.[81, 112] The causes of this unexpected toxicity are currently under investigation.[112]

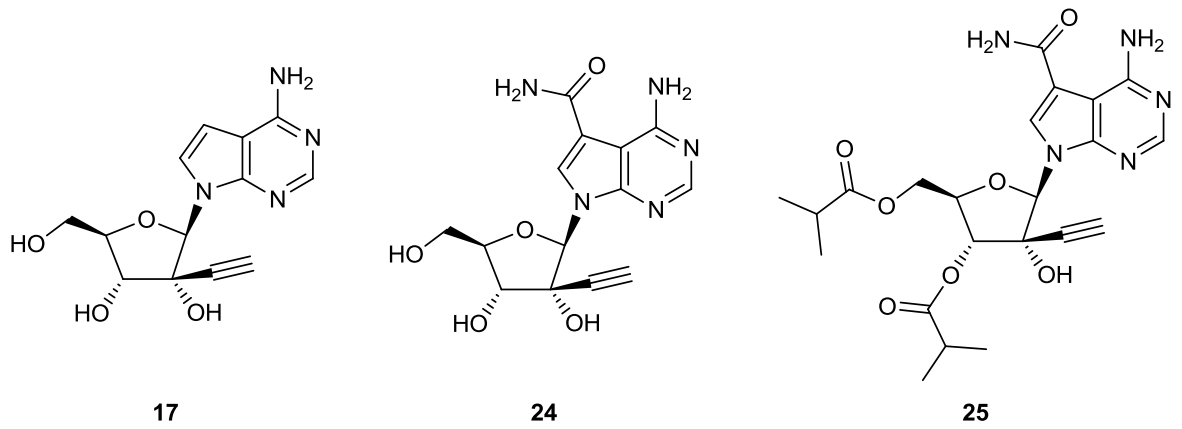

17 **24** **25**

Figure 27. Structure of the 2'-*C*-acetylene 7-deazaadenosine analogues NITD008 (**17**), NITD449 (**24**) and NITD203 (**25**).

Recently, a number of nucleoside analogues have been reported to inhibit the DENV RdRp activity *in vitro*.[113, 114, 115, 116, 117] The majority of the NIs against DENV are purine derivatives. The introduction of a carbon group at the 4'-position combined with various 7-deaza modifications of adenosine generated a small series of compounds (figure 28) with micromolar activity *in vitro* (EC_{50} from 5.55 to 10.06 μM).[113]

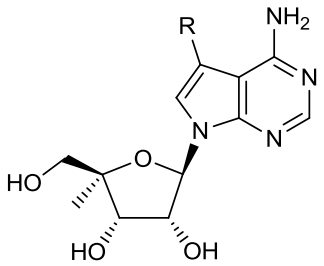

Figure 28. General structure of the anti-DENV 4'-*C*-methyl-7-deazaadenosine analogues.

A novel class of 2-amino-2'-*C*-methyladenosine analogues (figure 29) showed an EC_{50} in the range from 5.0 to 9.5 μM.[114] All the nucleosides share a 2,6-diaminopurine heterobase, which is further modified at the *N*-6 position or 8-position, and the 2'-*C*-methyl moiety in the ribose. The main element of novelty in this family is represented by the presence of an additional substituent at the 1'-anomeric position of the ribose.

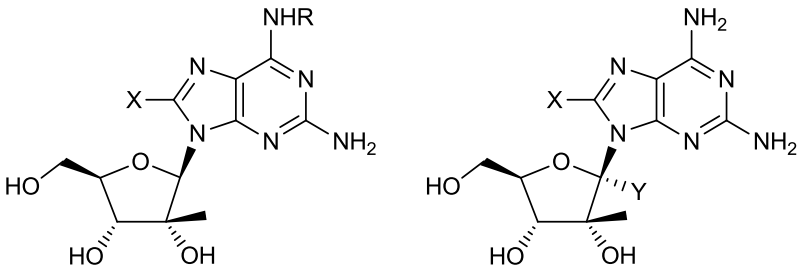

Figure 29. General structures of the anti-DENV 2,6-diaminopurine nucleosides.

Tichý *et al*. focused on base-modified nucleosides and identified a novel class of benzo-fused 7-deazaadenosine analogues (figure 30) as anti-DENV agents (EC_{50} from 14.8 to 39.6 μM).[115] Additionally, the replacement of the 4-amino group with 5-membered hetaryl cycles, such as furyl and thienyl, yielded derivatives with submicromolar activity against DENV *in vitro* (figure 30).[116]

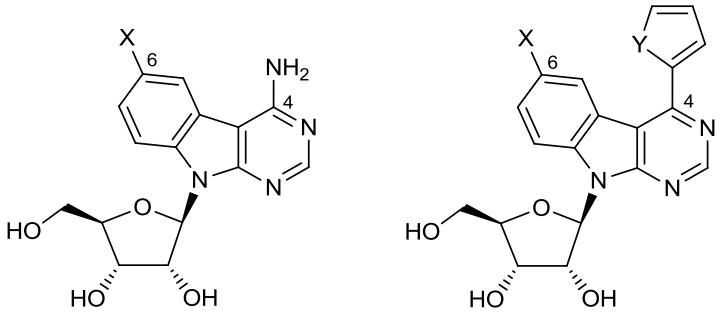

Figure 30. General structures of the anti-DENV benzo-fused derivatives of 7-deazaadenosine.

Finally, the first example of an anti-DENV phosphoramidate ProTide was reported by Yeo *et al.* in 2015.[117] In fact, the previously mentioned anti-HCV agent INX-08189 (**19**) inhibited DENV replication *in vitro*, suggesting that the application of the nucleotide prodrug approach may be useful for the development of a highly needed treatment of DENV infection.

Collectively, these results exemplify the challenges associated with the development of safe and effective NIs, especially in the context of providing safe and effective anti-DENV therapeutics. Nevertheless, the nucleoside and nucleotide-based approaches are a promising strategy for inhibiting DENV replication and are going to be explored in this work.

1.3 MOLECULAR MODELLING

1.3.1 THE DRUG DISCOVERY PROCESS

A drug discovery programme is initiated due to an unmet medical need, in order to find a therapy for an untreated disease or to improve the existing treatment for a disease.[118] The starting point is the identification of a suitable drug target, often a protein such as an enzyme, a receptor, an ion channel or a transporter, but also a nucleic acid or a gene.[118, 119, 120] The ideal target macromolecule is closely linked to the illness, and should be safe and 'druggable', so that its function may be modulated by a drug molecule.[118] The properties of the drug target may differ depending on the disease that need to be addressed.[119] For instance, a total inhibition of an antimicrobial drug target is generally desired to induce death of a pathogen or to stop its replication in the human body. In this case, the target needs to be essential for survival of the target organism and selectively present in the pathogen, besides being 'druggable'.[119] As the nature of the target may vary, also the drug may be a small molecule or a larger biological therapeutic, like a peptide or an oligonucleotide.[118]

The following phase of the drug discovery process is hit identification and lead optimisation. The hit is a biologically active 'drug-like' molecule, typically showing an activity in the range 100 nM to 5 µM.[118] Hit molecules can be identified in different ways, using HTS, virtual screening (VS) or other rational drug design methods. Generally whole series of hits are selected for progression towards the next step in the drug discovery process. In the field of small molecule drug discovery, a hit is usually a simple and low-weighted chemical entity.[118] This is of crucial importance because further optimisation of hit molecules usually involves an increase in molecular weight of the resulting drug candidate. In fact, several chemical analogues of the hit series need to be synthesised and evaluated for biological activity against the target, in the attempt to produce more potent and selective compounds as well as improve suboptimal pharmacokinetic properties (hit-to-lead phase). In this early stage of the drug discovery process, physicochemical properties, such as solubility and permeability through membranes, as well as *in vitro* absorption, distribution, metabolism and excretion (ADME) properties are being considered.[118] The most promising compound is being selected as lead compound, is further optimised by chemical modifications, and finally may progress to preclinical evaluation. Testing using *in vivo* models is useful to assess toxicology and ADME profiles, so as to verify whether the compound is safe and thus can advance to clinical evaluation and to estimate its initial dose in humans.[118] The three Phases of clinical

trials provide data on the safety and the efficacy of the drug candidate in larger and larger samples of the human population (table 3).[121] Eventually, if Phase I to III are completed successfully, the drug is approved for commercialisation and enters a fourth Phase, in which the effect of the new therapeutic is monitored continuously during its clinical use.[121]

Table 3. Phases of clinical trials.

Clinical trials	**Population**	**Aims**
Phase I	healthy volunteers	to evaluate safety, tolerability at ascending dose regimens, pharmacokinetic properties
Phase II	hundreds of patients	to evaluate efficacy compared to placebo or gold standard therapy in the market (when available)
Phase III	thousands of patients	to strengthen statistics and confirm previous findings
Phase IV (post approval)	World's population	to monitor the drug after reaching the market (pharmacovigilance)

The drug discovery process is long (between 12 and 15 years from the initial idea to the launch of the new medicine in the market) and expensive, with a cost of over £1 billion for a new drug.[118, 122] Besides being time-consuming and costly, the process is characterised by a high risk of failure.[118, 122, 123] Clinical trials of drug candidates may be terminated unsuccesfully due to the lack of clinical efficacy or to toxicity issues in humans.[118, 122, 123] It was estimated that only one in ten drug candidates that advances to human evaluation is actually approved for commercialisation, meaning that the rate of failure once clinical trials are reached is as high as 90%.[118, 122]

In the last 60 years, pharmaceutical progress has importantly contributed to extending life expectancy. From 1950 to 2014, 1 405 new therapeutics were approved for commercialisation, of which 1 249 are new molecular entities (NMEs), that refer to small molecule drugs, and 156 are new biologics license applications (BLAs).[122, 124] Despite a temporary rise in the number of Food and Drug Administration (FDA)-approvals between 1995 and 1999 and also an extraordinary peak of productivity in 2014,[124] the trend of new drug output remains linear, with companies delivering new therapeutics at a constant rate (24 new drugs per year on average).[122] However, the expenditure of production has seen an exponential increase, raising concerns about the sustainability of the pharmaceutical industries.[122]

1.3.2 MOLECULAR MODELLING APPROACHES

Given the challenges associated with the development of novel drugs and the previously described 'pharmaceutical crisis', there is a need for innovative techniques to reduce the time and costs as well as increase the success rate of the drug discovery process. Being based on computational technology, molecular modelling represents one of the possible answers to these issues. Being a rational method for drug design, it finds its antithesis in the experimental method, which is based on the discovery of new hits by chance, using HTS and combinatorial chemistry.[125, 119]

In the field of the molecular modelling, computational techniques are applied to explain chemical systems in terms of mathematical models.[126] The model is indeed a simplified description of a complex system, such as the interactions of a target with its ligand, in mathematical terms. Computational calculations can be performed on the mathematical model and enable the prediction and the understanding of properties of the modelled system, starting from known properties at the atomic scale.[126] Molecular modelling may be involved at different stages of the drug discovery process, especially in the key steps of identification of hit series and optimisation of lead compounds.[127, 128] In order to elicit its biological effect, the drug molecule needs to interact with a specific target. This recognition of the drug and its target relies on the high level of complementarity between the ligand and a pocket in the target macromolecule, which are often mediated by the formation of hydrogen bonds and hydrophobic interactions.[127] Molecular modelling techniques allow for the prediction of these interactions, which is fundamental for any *in silico* drug design approach. The required time and costs for these computational techniques are radically reduced compared to the chemical synthesis and biological evaluation of large series of chemical compounds. In addition to pharmacodynamic properties, the behaviour of the drug in the human body from its administration to its excretion (ADME and toxicology profile) is essential for the biological activity of a drug. Computational techniques can be applied in this field as well, thus selecting and then optimising compounds, in a quick, safe, and cost-effective way.[127, 128]

For these reasons, molecular modelling techniques have become of increasing importance in drug discovery over the past two decades.[119, 128, 129] The increasing computational power and calculation capacity further encourage the application of fast and inexpensive molecular modelling methods.[119, 125] Finally, the accuracy of mathematical models describing chemical systems is also improving allowing for the simulation of more complex molecular environments as well as for more precise and reliable results.[128]

In silico approaches in drug discovery may be broadly classified in structure-based and ligand-based drug design, depending on the availability of the three-dimensional (3D) information of the macromolecular target. Structure-based approaches rely on the 3D structure of the target to optimise the binding of the drug to the target, whereas ligand-based approaches are preferable when a series of active compounds are available and can furnish information about the binding mode in the absence of the 3D structure.[127, 128]

1.3.2.1 Structure-based drug design

Structure-based drug design (SBDD) methodologies exploit the known 3D structure of the target, which is obtained experimentally or constructed using molecular modelling methods, to identify novel drugs and enhance their activity.[127, 128] The application of SBDD has seen a constant rise, thanks to the availability of a rapidly increasing number of proteins with a known 3D structure.[119, 120, 128] Indeed, the sequencing of the human genome combined with advances in the methodologies for structure determination, such as X-ray crystallography and nuclear magnetic resonance (NMR) experiments, provides new potential drug targets at an accelerated rate, and thus new opportunities for the application of structure-based computational methods.[119, 128]

Once the target with a known 3D structure has been chosen, the initial step of any SBDD study is the identification of a potential binding site for small molecules, a pocket, in the macromolecular target.[119] A variety of methodologies can be adopted, such as the modification of the structure of an initial ligand to maximise complementary interactions, the screening of a database of compounds *in silico*, or the *de novo* generation of potential hit molecules by positioning small fragments in the binding site and linking them together.[119, 127]

Molecular docking is a widely used structure-based technique that consists of the prediction of the geometry of the ligand-target complex or, in other words, the binding mode of a small molecule in the designated pocket of the protein.[127, 128] The process applies search algorithms, known as docking algorithms, to define the ligand pose, which is the conformation and orientation of the small molecule within the binding site.[129] Conformations of the ligand are taken into account in the docking process to have sufficient accuracy of the results.[128, 129] Conformational changes of the target protein, loop fluctuation and movement of protein domains notably influence ligand binding. However, such a protein flexibility is normally not considered because flexible docking requires computationally expensive calculations.[125] In addition to docking algorithms, scoring functions are used to evaluate the interactions established in the ligand-target complex and,

ultimately, to predict binding affinity of the molecule on the basis of shape and electrostatic complementarities.[129] Scoring functions allow for ranking the docked conformations that were generated for each molecule. However, they are only approximate and a good score is not always indicative of high binding affinity.[119, 129] As a consequence, visual evaluation of the generated poses using computer graphics software is generally fundamental for the final selection of the best molecules.[119, 129]

The docking process is the basis of both VS and *de novo* design.[119, 130] VS consists of the search for compounds having suitable geometry and electronic features to fit the specific binding site, using docking algorithms.[128, 130] Such an *in silico* screening is fast and allows for the screening of large virtual libraries in a short time.[128]

The *de novo* generation method aims at the design of new molecules which are not present in the literature or compound databases.[119] It involves the docking of small fragments into the binding site of the target, followed by the assembly of the positioned fragment into a larger molecule.[119, 127, 128] The fact that small fragments are capable of fully exploring the binding site represents an advantage of this methodology. On the other hand, the designed molecules are often very complex and their syntheses difficult to accomplish, which again limits the application of this procedure.[119, 128]

Molecular dynamics (MD) simulation is a powerful structure-based technique, that aims at predicting the behaviour of a molecular system over time.[128, 131] The MD simulation is the generation of successive configurations of the system, in small time steps, and consists of the analysis of the trajectory of each atom of the molecular system through the simultaneous solution of the Newton's second law of motion (equation 1).[131, 132]

$$F_i = m_i * a_i = m_i * \frac{\partial v_i}{\partial t} = m_i * \frac{\partial^2 x_i}{\partial t^2}$$

Equation 1. Newton's second law of motion.[132] *F* = force, *m* = particle mass, *a* = acceleration, *v* = velocity, *t* = time, *x* = distance along one coordinate and *i* = 1 to *N*.

The motion analysis is complemented by the calculation of energies, forces and potentials on atoms using mathematical functions named force fields.[131] The application of MD simulation techniques is particularly useful to evaluate the binding interactions in non-static ligand-target complexes, thus accounting for induced conformations, the stability of such complexes as well as

the conformational changes of macromolecules over time.[128] These investigations provide insights into processes that may be difficult to study empirically and that are often fundamental for *in silico* drug design studies.

1.3.2.2 Ligand-based drug design

Ligand-based drug design (LBDD) approaches are generally applied when the 3D information on the target is not available or, frequently, they are used in combination to structure-based techniques. LBDD methods rely on the chemical structure of drug-like molecules and on their empirical activity data.[127]

One of the most significant LBDD method is based on the prediction of quantitative structure-activity relationships (QSAR). The QSAR model is a mathematical function that correlates biological data available for a set of molecules to structure-derived properties that, importantly, are expressed in terms of numbers.[127, 128] These properties are known as molecular descriptors. They are deduced from the molecular formula, the two-dimensional (2D) or 3D chemical structures and may vary significantly. Some examples are molecular weight, partition coefficient, number of rotatable bonds, number of double bonds, volume and surface-related numerical properties.[127] The aims of QSAR predictions are to identify features that are important for activity and give indications on how to modify molecular descriptors to enhance their biological profile.[127]

Molecular descriptors are of crucial importance also in the case of similarity search. The rationale behind this approach is that molecules binding to the same pocket of a target will show a certain degree of similarity.[128] Therefore, molecular databases can be screened *in silico* to search for molecules similar to a lead compound. The measurement of the degree of similarity (similarity coefficient) is achieved starting from the molecular descriptors, according to different mathematical methods.[127]

Finally, in the pharmacophore search, a third LBDD technique, the *in silico* screening of molecular databases is performed on the basis of the presence and the relative positions of key chemical features of the ligand.[127] A pharmacophore is a set of chemical features (hydrogen bond donor and acceptor, hydrophobic and aromatic groups, anion and cation) that are essential for the interaction of the ligand with the target, often in a conformation-dependent spatial relationship (3D pharmacophore). The chemical features of molecules in databases are compared to the pharmacophore to identify potential ligands.[127]

1.4 AIMS AND OBJECTIVES

The four serotypes of DENV represent a major health burden in the tropical and subtropical areas and are rapidly spreading to new countries. Half of the world population, accounting for approximately 3.9 billion people, is at risk of infection with DENV, raising considerable concern within the scientific community. The development of a vaccine has proven to be very challenging and the recently licensed dengue vaccine by Sanofi Pasteur provides limited benifits. To date, treatment of DENV infection is only symptomatic and unable to prevent the progression of the disease to life-threatening conditions. In consequence, the development of specific antiviral drugs which are effective against all four serotypes of DENV is of great importance.

The overarching aim of this PhD project was the preparation of novel nucleoside and nucleotide analogues as potential anti-DENV agents aimed to inhibit the viral RdRp. To achieve this, the specific aims were as follows.

- To create a model representative of the *de novo* initiation complex of DENV RdRp for the application of computer-aided drug design approaches. Although crystal structures of DENV RdRp have been solved, structural information on DENV RdRp in complex with the RNA template and the priming NTPs (*de novo* initiation complex) is currently not available. The construction of a model would provide a useful tool for the application of SBDD techniques.

- To design families of nucleoside analogues using molecular modelling techniques, in particular by predicting the binding affinity of ribose-modified and heterobase-modified nucleosides for the active site of the DENV RdRp model, and by identifying novel acyclic scaffolds replacing the ribose moiety of the nucleosides.

- To acquire knowledge on the mechanism of the RNA synthesis by the DENV RdRp through molecular modelling techniques, in particular by the application of MD simulation methods on representative complexes of the DENV RdRp in the different phases of RNA synthesis.

- To synthesise nucleoside analogues and phosphoramidate ProTide derivatives. The ProTide nucleotide prodrug strategy is applied to overcome common issues of nucleosides, such as poor cell permeation, susceptibility to metabolic degradation, poor phosphorylation to active species and toxicity. An optimisation of the procedure for the synthesis of

phosphoramidate ProTides would ease the preparation of analogues within this class of biologically relevant compounds and is therefore investigated in this work.

1.5 REFERENCES

[1] T. Solomon, M. Mallewa. Dengue and other emerging flaviviruses. *J. Infect.*, 42: 104-115, 2001.

[2] G. Kuno, G.-J. J. Chng, K. R. Tsuchiya, N. Karabatsos, C. B. Cropp. Phylogeny of the genus flavivirus. *J. Virol.*, 72(1): 73-83, 1998.

[3] World Health Organisation. Dengue and severe dengue. Fact sheet, updated July 2016. http://www.who.int/mediacentre/factsheets/fs117/en/, accessed January 2017.

[4] World Health Organisation. Zika virus. Fact sheet, updated September 2016. http://www.who.int/mediacentre/factsheets/zika/en, accessed January 2017.

[5] K. B. Anderson, S. J. Thomas, T. P. Endy. The emergence of Zika virus: a narrative review. *Ann. Intern. Med.*, 165(3): 175-183, 2016.

[6] S. C. Weaver, F. Costa, M. A. Garcia-Blanco, A. I. Ko, G. S. Ribeiro, G. Saade, P.-Y. Shi, N. Vasilakis. Zika virus: history, emergence, biology, and prospects for control. *Antiviral Res.*, 130: 69-80, 2016.

[7] World Health Organisation. WHO statement on the first meeting of the International Health Regulations (2005) (IHR 2005) Emergency Committee on Zika virus and observed increase in neurological disorders and neonatal malformations. WHO statement, 1st February 2016. http://www.who.int/mediacentre/news/statements/2016/1st-emergency-committee-zika/en/, accessed January 2017.

[8] T. Ishikawa, A. Yamanaka, E. Konishi. A review of successful flavivirus vaccines and the problem with those flaviviruses for which vaccines are not yet available. *Vaccine*, 32(12): 1326-1337, 2014.

[9] Sanofi Pasteur. First dengue vaccine approved in more than 10 countries. 4th October 2016. http://www.sanofipasteur.com/en/articles/first_dengue_vaccine_approved_in_more_than_10_countries.aspx, accessed January 2017.

[10] World Health Organisation. Dengue vaccine: WHO position paper – July 2016. Weekly epidemiological record, 30: 349-364, 2016.

[11] N. M. Ferguson, I. Rodríguez-Barraquer, I. Dorigatti, L. Mier-y-Teran-Romero, D. J. Laydon, D. A. T. Cummings. Benefits and risks of the Sanofi-Pasteur dengue vaccine: modelling optimal deployment. *Science*, 353(6303): 1033-1036, 2016.

[12] World Health Organisation. Dengue: guidelines for diagnosis, treatment, prevention and control. New edition, 2009.

[13] Reprinted from World Health Organisation. Dengue, countries or areas at risk, 2013. http://gamapserver.who.int/mapLibrary/Files/Maps/Global_DengueTransmission_ITHRiskMap.png?ua=1, accessed January 2017. Copyright (2014).

[14] D. J. Gubler. Dengue and dengue haemorrhagic fever. *Clin. Microbiol. Rev.*, 11(3): 480-496, 1998.

[15] N. E. A. Murray, M. B. Quam, A. Wilder-Smith. Epidemiology of dengue: past, present and future prospects. *Clin. Epidemiol.*, 5: 299-309, 2013.

[16] S. Murrell, S.C. Wu, M. Butler. Review of Dengue virus and the development of a vaccine, *Biotech. Adv.*, 29:239-247, 2011.

[17] J. D. Stanaway, D. S. Shepard, E. A. Undurraga, Y. A. Halasa, L. E. Coffeng. O. J. Brady, S. I. Hay, N. Bedi, I. M. Bensenor, C. A. Castañeda-Orjuela, T.-W. Chuang, K. B. Gibney, Z. A. Memish, A. Rafay, K. N. Ukwaja, N. Yonemoto, C. J. L. Murray. The global burden of dengue: an analysis from the global burden of disease study 2013. *Lancet Infect. Dis.*, 16: 712-723, 2016.

[18] D. J. Gubler. The global emergence/resurgence of arboviral diseases as public health problems. *Arch. Med. Res.*, 33(4): 330-342, 2002.

[19] O. J. Brady, P. W. Gething, S. Bhatt, J. P. Messina, J. S. Brownstein, A. G. Hoen, C. L. Moyes, A. W. Farlow, T. W. Scott, S. I. Hay. Refining the global spatial limits of dengue virus transmission by evidence-based consensus. *PLoS Negl. Trop. Dis.*, 6(8): e1760, 2012.

[20] Bhatt S. et al. The global distribution and burden of dengue. *Nature*, 496: 504-507, 2013.

[21] I. Ratnam, K. Leder, J. Black, J. Torresi. Dengue fever and international travel. *J. Travel Med.*, 20(6): 384-393, 2013.

[22] D. O. Freedman, L. H. Weld, P. E. Kozarsky, T. Fisk, R. Robins, F. von Sonnenburg, J. S. Keystone, P. Pandey, M. S. Cetron, GeoSentinel Surveillance Network. Spectrum of disease and relation to place of exposure among ill returned travellers. *N. Engl. J. Med.*, 354(2): 119-130, 2006.

[23] G. L. C. Ferreira. Global dengue epidemiology trends. *Rev. Inst. Trop. Sao Paulo*, 54(Suppl. 18): S5-S6, October 2012.

[24] D. Morens, A. S. Fauci. Dengue and hemorrhagic fever: a potential threat to public health in the United States. *JAMA*, 299: 214-216, 2008.

[25] W. J. H. McBride, H. Bielefeldt-Ohmann. Dengue viral infections; pathogenesis and epidemiology. *Microb. Infect.*, 2: 1041-1050, 2000.

[26] B. H. Halstead. Dengue. *Lancet*, 370: 1644-1652, 2007.

[27] S. B. Halstead. Pathogenesis of dengue: challenges to molecular biology. *Science*, 239: 476-481, 1988.

[28] S. B. Halstead, E. J. O'Roulke. Antibody-enhanced dengue virus infection in primate lymphocytes. *Nature*, 265: 739-741, 1977.

[29] V. Racaniello. Antibodies aid dengue and Zika virus infection. Virology Blog. http://www.virology.ws/2016/07/28/antibodies-aid-dengue-and-zika-virus-infection/, accessed January 2017.

[30] N. Sangkawibha, S. Rojanasuphot, S. Ahandrik, S. Virlyapongse, S. Jatanasen, V. Salitul, B. Phanthumachinda, S. B. Halstead. Risk factors in dengue shock syndrome: a prospective epidemiologic study in Rayong, Thailand. I. The 1980 outbreak. *Am. J. Epidemiol.*, 120(5): 653-669, 1984.

[31] R. M. Scott, S. Simmannitya, W. H. Bancroft, P. Mansuwan. Shock syndrome in primary dengue infections. *Am. J. Trop. Med. Hyg.*, 25: 866-874, 1976.

[32] W. J. S. Barnes, L. Rosen. Fatal hemorrhagic disease and shock associated with primary dengue infection on a Pacific island. *Am. J. Trop. Med. Hyg.*, 23: 495-506, 1974.

[33] Sanofi Pasteur. DengVaxia®, world's first dengue vaccine, approved in Mexico. 9th December 2015. http://www.sanofipasteur.com/en/articles/dengvaxia-world-s-first-dengue-vaccine-approved-in-mexico.aspx, accessed December 2015.

[34] M. Simmons, N. Teneza-Mora, R. Putnak. Advances in the development of vaccines for dengue fever. *Vaccine: development and therapy*, 2: 1-14, 2012.

[35] A. Sabchareon, D. Wallace, C. Sirivichayakul, K. Limkittikul, P. Chanthavanich, S. Suvannadabba, V. Jiwariyavej, W. Dulyachai, K. Pengsaa, T. A. Wartel, A. Moureau, M. Saville, A. Bouckenooghe, S. Viviani, N. G. Tornieporth, J. Lang. Protective efficacy of the recombinant, live-attenuated, CYD tetravalent dengue vaccine in Thai school children: a randomised, controlled phase 2b trial. *Lancet*, 380: 1559-1567, 2012.

[36] M. R. Capeding, N. H. Tran, S. R. S. Hadinegoro, H. I. H. J. M. Ismail, T. Chotpitayasunondh, M. N. Chua, C. Q. Luong, K. Rusmil, D. N. Wirawan, R. Nallusamy, P. Pitisuttithum, U. Thisyakorn, I.-K. Yoon, D. van der Vliet, E. Langevin, T. Laot, Y. Hutagalung, C. Frago, M. Boaz, T. A. Wartel, N. G. Tornieporth, M. Saville, A. Bouckenooghe, CYD14 Study Group. Clinical efficacy and safety of a novel tetravalent dengue vaccine in healthy children in Asia: a phase 3, randomised, observer-masked, placebo-controlled trial. *The Lancet*, 384(9951): 1358-1365, 2014.

[37] Sanofi Pasteur. Sanofi Pasteur's dengue vaccine candidate successfully completes final landmark Phase III clinical efficacy study in Latin America. Press release, 3rd September 2014. http://www.sanofipasteur.com/en/articles/sanofi-pasteur-s-dengue-vaccine-candidate-successfully-completes-final-landmark-phase-3-clinical-efficacy-study-in-latin-america.aspx, accessed August 2015.

[38] T. Pang, D. G. Y. Thiam, T. Tantawichien, Z. Ismail, S. Yoksan. Dengue vaccine – time to act now. *The Lancet*, 385: 1725-1726, 2015.

[39] I. Rodriguez-Barraquer, L. Mier-y-Teran-Romero, N. Ferguson, D. S. Burke, D. A. T. Cummings. Differential efficacy of dengue vaccine by immune status. *The Lancet*, 385: 1726, 2015.

[40] S.Velumani, Y. X. Toh, S. Balasingam, S. Archuleta, Y. S. Leo, V. C. Gan, T. L. Thein, A. Wilder-Smith, K. Fink. Low antibody titers 5 years after vaccination with the CYD-TDV dengue vaccine in both pre-immune and naïve vaccines. *Hum. Vaccin. Immunother.*, 12(5): 1265-1273, 2016.

[41] L. M. Schwartz, M. E. Halloran, A. P. Durbin, I. M. Longini Jr. The dengue vaccine pipeline: implications for the future of dengue control. *Vaccine*, 33: 3293-3298, 2015.

[42] K. S. Vannice, A. Durbin, J. Hombach. Status of vaccine research and development of vaccines for dengue. *Vaccine*, 34: 2934-2938, 2016.

[43] Y. Liu, J. Liu, G. Cheng. Vaccines and immunization strategies for dengue prevention. *Emerg Microbes Infect.*, 5(7):e77, 2016.

[44] C. Caillet-Saguy, S. P. Lim, P.-Y. Shi, J. Lescar, S. Bressanelli. Polymerases of hepatitis C viruses and flaviviruses: structural and mechanistic insights and drug development. *Antiviral Res.*, 105: 8-16, 2014.

[45] F. Kato, T. Hishiki. Dengue virus reporter replicon is a valuable tool for antiviral drug discovery and analysis of virus replication mechanisms. *Viruses*, 8(5): 122, 2016.

[46] H. M. Van der Shaar, M. J. Rust, C. Chen, H. van der Ende-Metselaar, J. Wilschut, X. Zhuang, J. M. Smit. Dissecting the cell entry pathway of dengue virus by single-particle tracking in living cells. *PLoS Pathog.*, 4(12): e1000244, 2008.

[47] V. Sreenivasulu Reddy, R. Bagyalakshmi, T. Sandhyarani, E. Arthi. Dengue virus infection – current overview and vaccine update. *JCTMB*, 1(3): P19-P25, 2013.

[48] C. G. Noble, Y.-L. Chen, H. Dong, F. Gu, S. P. Lim, W. Schul, Q.-Y. Wang, P.-Y. Shi. Strategies for development of dengue virus inhibitors. *Antiviral Res.*, 85: 450-462, 2010.

[49] G. Dow, E. Mora. The maximum potential market for dengue drugs V 1.0. Antiviral Res., 96: 203-212, 2012.

[50] S. P. Lim, Q.-Y. Wang, C. G. Noble, Y.-L. Chen, H. Dong, B. Zou, F. Yokokawa, S. Nilar, P. Smith, D. Beer, J. Lescar, P.-Y. Shi. Ten years of dengue drug discovery: progress and prospects. *Antiviral Res.*, 100: 500-519, 2013.

[51] C. Flexner. HIV drug development: the next 25 years. *Nat. Rev. Drug Discov.*, 6: 956-966, 2007.

[52] R. Bartenschlager, V. Lohmann, F. Penin. The molecular and structural basis of advanced antiviral therapy for hepatitis C virus infection. *Nat. Rev. Microbiol.*, 11: 482-496, 2013.

[53] E. De Clercq. Three decades of antiviral drugs. *Nat. Rev. Drug Discov.*, 6: 941, 2007.

[54] S. S. Lieberman-Blum, H. B. Fung, J. C. Bandres. Maraviroc: A CCR5-receptor antagonist for the treatment of HIV-1 infection. *Clin. Ther.*, 30(7): 1228-1250, 2008.

[55] V. A. Villareal, M. A. Rodgers, D. A. Costello, P. L. Yang. Targeting host lipid synthesis and metabolism to inhibit dengue and hepatitis C viruses. *Antiviral Res.*, 124: 110-121, 2015.

[56] S. J. F. Kaptein, J. Neyts. Towards antiviral therapy for treating dengue virus infections. *Curr. Opin. Pharmacol.*, 30: 1-7, 2016.

[57] J. Whitehorn, C. V. Nguyen, L. P. Khanh, D. T. Kien, N. T. Quyen, N. T. Tran, N. T. Hang, N.T. Truong, L. T. Hue, N. T. Cam Huong, V. T. Nhon, T. Van Tram, J. Farrar, M. Wolbers, C. P. Simmons, B. Wills. Lovastatin for the treatment of adult patients with dengue: a randomized, double-blind, placebo-controlled trial. *Clin. Infect. Dis.*, 62: 468-476, 2016.

[58] J. G. Low, C. Sung, L. Wijaya, Y. Wei, A. P. S. Rathore, S. Watanabe, B. H. Tan, L. Toh, L. T. Chua, Y. Hou, A. Chow, S. Howe, W. K. Chan, K. H. Tan, J. S. Chung, B. P. Cherng, D. C. Lye, P. A. Tambayah, L. C. Ng, J. Connolly, M. L. Hibberd, Y. S. Leo, Y. B. Cheung, E. E. Ooi, S. G. Vasudevan. Efficacy and safety of celgosivir in patients with dengue fever (CELADEN): a phase 1b, randomised, double-blind, placebo-controlled, proof-of-concept trial. *Lancet Infect. Dis.*, 14(8): 706-715, 2014.

[59] C. Sung, Y. Wei, S. Watanabe, H. S. Lee, Y. M. Khoo, L. Fan, A. P. S. Rathore, K. W.-K. Chan, M. M. Choy, U. S. Kamaraj, O. M. Sessions, P. Aw, P. F. de Sessions, B. Lee, J. E. Connolly, M. L. Hibberd, D. Vijaykrishna, L. Wijaya, E. E. Ooi, J. G.-H. Low, S. G. Vasuvan. Extended evaluation of virological, immunological and pharmacokinetic endpoints of CELADEN: a randomized, placebo-controlled tral of celgosivir in dengue fever patients. *PLoS Negl. Trop. Dis.*, 10(8): e0004851, 2016.

[60] M. McDowell, S. R. Gonzales, S. C. Kumarapperuma, M. Jeselnik, J. B. Arterburn, K. A. Hanley. A novel nucleoside analog, 1-β-D-ribofuranosyl-3-ethynyl-[1,2,4]triazole (ETAR), exhibits efficacy against a broad range of flaviviruses *in vitro*. *Antiviral Res.*, 87: 78-80, 2010.

[61] C. G. Noble, P.-Y. Shi. Structural biology of dengue virus enzymes: towards rational design of therapeutics. *Antiviral Res.*, 96: 115-126, 2012.

[62] V. Tricou, N. N. Minh, T. P. Van, S. J. Lee, J. Farrar, B. Wills, H. T. Tran, C. P. Simmons. A randomized controlled trial of chloroquine for the treatment of dengue in Vietnamese adults. *PLoS Negl. Trop. Dis.*, 4(8):e785, 2010.

[63] D. T. Tam, T. V. Ngoc, N. T. Tien, N. T. Kieu, T. T. Thuy, L. T. Thanh, C. T. Tam, N. T. Truong, N. T. Dung, P. T. Qui, T. T. Hien, J. J. Farrar, C. P. Simmons, M. Wolbers, B. A. Wills. Effects of short-course oral corticosteroid therapy in early dengue infection in Vietnamese patients: a randomized, placebo-controlled trial. *Clin. Infect. Dis.*, 55(9): 1216-1224, 2012.

[64] H. Beesetti, N. Khanna, S. Swaminathan. Investigational drugs in early development for treating dengue infection. *Expert Opin. Investig. Drugs*., 25(9): 1059-1069, 2016.

[65] W. Mei Kok. New developments in flavivirus drug discovery. *Exp. Opin. Drug Discov.*, 11(5): 433-445, 2016.

[66] T. Kampmann, R. Yennamalli, P. Campbell, M. J. Stoermer, D. P. Fairlie, B. Kobe, P. R. Young. *In silico* screening of small molecule libraries using the dengue virus envelope E protein has identified compounds with antiviral activity against multiple flaviviruses. *Antiviral Res.*, 84(3):234-241, 2009.

[67] M. A. Alhoot, A. K. Rathinam, S. M. Wang, R. Manikam, S. D. Sekaran. Inhibition of dengue virus entry into target cells using synthetic antiviral peptides. *Int J Med Sci*, 10(6):719-729, 2013.

[68] K. Ichiyama, S. B. Gopala Reddy, L. F. Zhang, W. X. Chin, T. Muschin, L. Heinig, Y. Suzuki, H. Nanjundappa, Y. Yoshinaka, A. Ryo, N. Nomura, E. E. Ooi, S. G. Vasudevan, Takashi Yoshida, Naoki Yamamoto. Sulfated polysaccharide, curdlan sulfate, efficiently prevents entry/fusion and restricts antibody-dependent enhancement of dengue virus infection *in vitro*: a possible candidate for clinical application. *PloS Negl. Trop. Dis.*, 7(4): e2188. 2013.

[69] G. Fibriansah, S.-M. Lok. The development of therapeutic antibodies against dengue virus. *Antiviral Res.*, 128: 7-19, 2016.

[70] C. M. Byrd, D. Dai, D. W. Grosenbach, A. Berhanu, K. F. Jones, K. B. Cardwell, C. Schneider, K. A. Wineinger, J. M. Page, C. Harver, E. Stavale, S. Tyavanagimatt, M. A. Stone, R. Bartenschlager, P. Scaturro, D. E. Hruby, R. Jordan. A novel inhibitor of dengue virus replication that targets the capsid protein. *Antimicrob. Agents Chemother.*, 57(1): 15-25, 2013.

[71] P. Scaturro, I. M. L. Trist, D. Paul, A. Kumar, E. G. Acosta, C. M. Byrd, R. Jordan, A. Brancale, R. Bartenschlager. Characterization of the mode-of-action of a potent dengue virus capsid inhibitor. *J. Virol.*, 88(19): 11540-11555, 2014.

[72] M. A. Behnam, D. Graf, R. Bartenschlager, D. P. Zlotos, C. D. Klein. Discovery of nanomolar dengue and West Nile virus protease inhibitors containing a 4-benzyloxyphenylglycine residue. *J. Med. Chem.*, 58(23): 9354-9370, 2015.

[73] N. L. Sweeney, A. M. Hanson, S. Mukherjee, J. Ndjomou, B. J. Geiss, J. J. Steel, K. J. Frankowski, K. Li, F. J. Schoenen, D. N. Frick. Benzothiazole and pyrrolone flavivirus inhibitors targeting the viral helicase. *ACS Infect. Dis.*, 1(3):140-148, 2015.

[74] T. L. Yap, T. Xu, Y.-L. Chen, H. Malet, M.-P. Egloff, B. Canard, S. G. Vasudevan, J. Lescar. Crystal structure of the dengue virus RNA-dependent RNA polymerase catalytic domain at 1.85-angstrom resolution. *J. Virol.*, 81(9): 4753-4765, 2007.

[75] H. Dong, D. C. Chang, M. H. C. Hua, S. P. Lim, Y. H. Chionh, F. Hia, Y. H. Lee, P. Kukkaro, S.-M. Lok, P. C. Dedon, P.-Y. Shi. 2'-*O* methylation of internal adenosine by flavivirus NS5 methyltransferase. *PLoS Pathog.*, 8(4): e1002642, 2012.

[76] S. P. Lim, C. G. Noble, P.-Y. Shi. The dengue virus NS5 protein as a target for drug discovery. *Antiviral Res.*, 119: 57-67, 2015.

[77] P. Niyomrattanakit, Y.-L. Chen, H. Dong, Z. Yin, M. Qing., J. F. Glickman, K. Lin, D. Mueller, H. Voshol, J. Y. H. Lim, S. Nilar, T. H. Keller, P.-Y. Shi. Inhibition of dengue virus polymerase by blocking of the RNA tunnel. *J. Virol.*, 84(11): 5678-5686, 2010.

[78] S. Anusuya, D. Velmurugan, M. M. Gromiha. Identification of dengue viral RNA-dependent RNA polymerase inhibitor using computational fragment-based approaches and molecular dynamics study. *J. Biomol. Struct. Dyn.*, 34(7): 1512-1532, 2016.

[79] F. Yokokawa, S. Nilar, C. G. Noble, S. P. Lim, R. Rao, S. Tania, G. Wang, G. Lee, J. Hunziker, R. Karuna, U. Manjunatha, P.-Y. Shi, P. W. Smith. Discovery of potent non-nucleoside inhibitors of dengue viral RNA-dependent RNA polymerase from a fragment hit using structure-based drug design. *J Med Chem.*, 59(8): 3935-3952, 2016.

[80] D. Tarantino, R. Cannalire, E. Mastrangelo, R. Croci, G. Querat, M. L. Barreca, M. Bolognesi, G. Manfroni, V. Cecchetti, M. Milani. Targeting flavivirus RNA dependent RNA polymerase through a pyridobenzothiazole inhibitor. *Antiviral Res*., 134: 226-235, 2016.

[81] Z. Yin, Y.-L. Chen, W. Schul, Q.-Y. wang, F. Gu, J. Duraiswamy, R.R. Kondreddi, P. Niyomrattanakit, S. B. Lakshminarayana, A. Goh, H. Y. Xu, W. Liu, B. Liu, J. Y. H. Lim, C. Y. Ng, M. Qing, C. C. Lim, A. Yip, G. Wang, W. L. Chan, H. P. Tan, K. Lin, B. Zhang, G. Zou, K. A. Bernard, C. Garrett, K. Beltz, M. Dong, M. Weaver, H. He, A. Pichota, V. Dartois, T. H. Keller, P.-Y. Shi. An adenosine nucleoside inhibitor of dengue virus. *Proc. Natl. Acad. Sci.*, 106(48): 20435-20439, 2009.

[82] Y.-L. Chen, Z. Yin, J. Duraiswamy, W. Schul, C. C. Lim, H. Y. Xu, M. Qing, A. Yip, G. Wang, W. L. Chan, H. P. Tan, M. Lo, S. Liung, R. R. Kondreddi, R. Rao, H. Gu, H. He, T. H. Keller, P.-Y. Shi. Inhibition of dengue virus RNA synthesis by an adenosine nucleoside. *Antimicrob. Agents Chemother.*, 54(7): 2932-2939, 2010.

[83] N. M. Nguyen, C. N. Tran, L.K. Phung, K. T. Duong, A. Huynh Hle, J. Farrar, Q. T. Nguyen, H. T. Tran, C. V. Nguyen, L. Merson, L. T. Hoang, M. L. Hibberd, P. P. Aw, A. Wilm, N. Nagarajan, D. T. Nguyen, M. P. Pham, T. T. Nguyen, H. Javanbakht, K. Klumpp, J. Hammond, R. Petric, M. Wolbers, C. T. Nguyen, C. P. Simmons. A randomized, double-blind placebo controlled trial of balapiravir, a polymerase inhibitor, in adult dengue patients. *J. Infect. Dis.*, 207: 1442-1450, 2013.

[84] H. Malet, N. Massé, B. Selisko, J.-L. Romette, K. Alvarez, J. C. Guillemot, H. Tolou, T. L. Yap, S. Vasudevan, J. Lescar, B. Canard. The flavivirus polymerase as a target for drug discovery. *Antiviral Res.*, 80: 23-35, 2008.

[85] S. L. Alcaraz-Estrada, M. Yocupicio-Monroy, R. M. del Angel. Insights into dengue virus genome replication. *Future Virol.*, 5(5): 575-592, 2010.

[86] L. G. Gebhard, C. V. Filomatori, A. V. Gamarnik. Functional RNA elements in the dengue virus genome. *Viruses*, 3: 1739-1756, 2011.

[87] C. G. Noble, S. P. Lim, y.-L- Chen, C. W. Liew, L. Yap, J. Lescar, P.-Y. Shi. Conformational flexibility of the dengue virus RNA-dependent RNA polymerase revealed by a complex with an inhibitor. *J. Virol.*, 87(9): 5291-5295, 2013.

[88] S. P. Lim, J. H. Koh, C. C. Seh, C. W. Liew, A. D. Davidson, L. S. Chua, R. Chandrasekaran, T. C. Cornvik, P.-Y. Shi, J. Lescar. A crystal structure of the dengue virus NS5 polymerase delineates inter-domain amino acids that enhance its thermostability and *de novo* initiation activities. *J. Biol. Chem.*, 288: 31105-31114, 2013.

[89] Y. Zhao, T. S. Soh, J. Zheng, K. W. K. Chan, W. W. Phoo, C. C. Lee, M. Y. F. Tay, K. Swaminathan, T. C. Cornvik, S. P. Lim, P.-Y. Shi, J. Lescar, S. G. vasudevan, D. Luo. A crystal structure of the dengue virus NS5 protein reveals a novel inter-domain interface essential for protein flexibility and virus replication. *PLoS Pathog.*, 11(3): e1004682, 2015.

[90] V. J. Klema, M. Ye, A. Hindupur, T. Teramoto, K. Gottipati, R. Padmanabhan, K. H. Choi. Dengue virus non structural protein 5 (NS5) assembles into a dimer with a unique methyltransferase and polymerase interface. *PLoS Pathog.*, 12(2): e1005451, 2016.

[91] R. T. Mosley, T. E. Edwards, E. Murakami, A. M. Lam, R. L. Grice, J. Du, M. J. Sofia, P. H. Furman, M. J. Otto. Structure of hepatitis C virus polymerase in complex with primer-template RNA. *J. Virol.*, 86(12): 6503-6511, 2012.

[92] B. Selisko, S. Potisopon, R. Agred, S. Priet, I. Varlet, Y. Thillier, C. Sallamand, F. Debart, J.-j. Vasseur, B. Canard. Molecular basis for nucleotide conservation at the ends of the Dengue virus genome. *PLoS Phatog.*, 8(9): e1002912, 2012.

[93] J. Lescar, B. Canard. RNA-dependent RNA polymerases from flaviviruses and *Picornaviridae*. *Curr. Opin. Struct. Biol.*, 19: 759-767, 2009.

[94] L. P. Jordheim, D. Durantel, F. Zoulim, C. Dumontet. Advances in the development of nucleoside and nucleotide analogues for cancer and viral diseases. *Nat. Rev. Drug Disc.*, 12: 447-464, 2013.

[95] U. Pradere, E. C. Garnier-Amblard, S. J. Coats, F. Amblards, R. F. Schinazi. Synthesis of nucleoside phosphate and phosphonate prodrugs. *Chem. Rev.*, 114: 9154-9218, 2014.

[96] F. Li, H. Maag, T. Alfredson. Prodrugs of nucleoside analogues for improved oral absorption and tissue targeting. *J. Pharm. Sci.*, 97(3): 1109-1133, 2008.

[97] M. Meppen, B. Pacini, R. Bazzo, U. Koch, J. F. Leone, K. A. Koeplinger, M. Rowley, S. Altamura, A. Di Marco, F. Fiore, C. Giuliano, O. Gonzalez-Paz, R. Laufer, V. Pucci, F. Narjes, C. Gardelli. Cyclic phosphoramidates as prodrugs of 2'-*C*-methylcytidine. *Eur. J. Med. Chem.*, 44: 3765-3770, 2009.

[98] T. H. M. Jonckers, A. Tahri, L. Vijgen, J. M. Berke, S. Lachau-Durand, B. Stoops, J. Snoeys, L. Leclercq, L. Tambuyzer, T. Lin, K. Simmen, P. Raboisson. Discovery of 1-((2*R*,4a*R*,6*R*,7*R*,7a*R*)-2-isopropoxy-2-oxidodihydro-4*H*,6*H*-spiro[furo[3,2-*d*][1,3,2]dioxaphosphinine-7,2'-oxetan]-6-yl)pyrimidine-2,4(1*H*,3*H*)-dione (JNJ-54257099), a 3'-5'-cyclic phosphate ester prodrug pf 2'-deoxy-2'-spirooxetane uridine triphosphate useful for HCV inhibition. *J. Med. Chem.*, 59(12): 5790-5798, 2016.

[99] C. McGuigan, R. N. Pathirana, N. Mahmood, G. K. Devine, A. J. Hay. Aryl phosphate derivatives of AZT retain activity against HIV1 in cell lines, which are resistant to the action of AZT. *Antiviral Res.*, 17: 311-321, 1992.

[100] C. McGuigan, H.-W. Tsang, D. Cahard, K. Turner, S. Velazquez, A. Salgado, L. Bidois, L. Naesens, E. De Clercq, J. Balzarini. Phosphoramidate derivatives of d4T as inhibitors of HIV: the effect of the amino acid variation. *Antiviral Res.*, 35: 195-204, 1997.

[101] D. Saboulard, L. Naesens, D. Cahard, A. Salgado, R. N. Pathirana, S. Velazquez, C. McGuigan, E. De Clercq, J. Balzarini. Characterization of the activation pathway of phosphoramidate triester prodrugs of stavudine and zidovudine. *Mol. Pharmacol.*, 56: 693-704, 1999.

[102] M. Derudas, A. Brancale, L. Naesens, J. Neyts, J. Balzarini, C. McGuigan. Application of the phosphoramidate ProTide approach to the antiviral drug ribavirin. *Bioorg. Med. Chem.*, 18: 2748-2755, 2010.

[103] C. Bourdin, C. McGuigan, A. Brancale, S. Chamberlain, J. Vernachio, J. Hutchins, E. Gorovits, A. Kolykhalov, J. Muhammad, J. Patti, G. Henson, B. Bleiman, K. D. Bryant, B. Ganguly, D. Hunley, A. Obikhod, C. R. Walters, J. Wang, C. V. S. Ramamurty, S. K. Battina, C. S. Rao. Synthesis and evaluation against hepatitis C virus of 7-deaza analogues of 2'-*C*-methyl-6-*O*-methyl guanosine nucleoside and L-Alanine ester phosphoramidates. *Bioorg. Med. Chem. Lett.*, 19(15): 4316-4320, 2009.

[104] J. H. Vernachio, B. Bleiman, K. D. Bryant, S. Chamberlain, D. Hunley, J. Hutchins, B. Ames, E. Gorovits, B. Ganguly, A. Hall, A. Kolykhalov, Y. Liu, J. Muhammad, N. Raja, C. R. Walters, J. Wang, K. Williams, J. M. Patti, G. Henson, K. Madela, M. Aljarah, A. Gilles, C. McGuigan. INX-08189, a phosphoramidate prodrug of 6-*O*-methyl-2'-*C*-methyl guanosine, is a potent inhibitor of hepatitis C virus replication with excellent pharmacokinetic and pharmacodynamic properties. *Antimicrob. Agents. Chemother.*, 55(5): 1843-1851, 2011.

[105] M. Derudas, D. Carta, A. Brancale, C. Vanpouille, A. Lisco, L. Margolis, J. Balzarini, C. McGuigan. The application of phosphoramidate ProTide technology to acyclovir confers anti-HIV inhibition. *J. Med. Chem.*, 52: 5520-5530, 2009.

[106] M. Slusarczyk, M. H. Lopez, J. Balzarini, M. Mason, W. G. Jiang, S. Blagden, E. Thompson, E. Ghazaly, C. McGuigan. Application of ProTide technology to Gemcitabine: a successful approach to overcome the key cancer resistance mechanisms leads to a new agent (NUC-1031) in clinical development. *J. Med. Chem.*, 57: 1531-1542, 2014.

[107] M. J. Sofia, D. Bao, W. Chang, J. Du, D. Nagarathnam, S. rachakonda, P. G. Reddy, B. S. Ross, P. Wang, H.-R. Zhang, S. Bansal, C. Espiritu, M. Keilman, A. M. Lam, H. M. M. Steuer, C. Niu, M. J. Otto, P. A. Furman. Discovery of a β-D-2'-deoxy-2'-α-fluoro-2'-β-*C*-methyluridine nucleotide prodrug (PSI-7977) for the treatment of hepatitis C virus. *J. Med. Chem.*, 53: 7202-7218, 2010.

[108] A. S. Ray, M. W. Fordyce, J. M. Hitchcock. Tenofovir alafenamide: a novel prodrug of tenofovir for the treatment of Human Immunodeficiency virus. *Antiviral Res.*, 125, 63-70, 2016.

[109] D. B. Olsen, A. B. Eldrup, L. Bartholomew, B. Bhat, M. R. Bosserman, A. Ceccacci, L. F. Colwell, J. F. Fay, O. A. Flores, K. L. Getty, J. A. Grobler, R. L. LaFemina, E. J. Markel, G. Migliaccio, M. Prhavc, M. W. Stahlhut, J. E. Tomassini, M. MacCoss, D. J. Hazuda, S. S. Carroll. A 7-deaza-adenosine analog is a potent and selective inhibitor of hepatitis C virus replication with excellent pharmacokinetic properties. *Antimicr. Agents Chemother.*, 48(10): 3944-3953, 2004.

[110] A. B. Eldrup, C. R. Allerson, C. F. Bennett, S. Bera, B. Bhat, N. Bhat, M. R. Bosserman, J. Brooks, C. Burlein, S. S. Carroll, P. D. Cook, K. L. Getty, M. MacCross, D. R. McMasters, D. B. Olsen, T. P. Prakash, M. Prhavc, Q. Song, J. E. Tommassini, J. Xia. Structure-activity relationship of purine ribonucleosides for inhibition of hepatitis C virus RNA-dependent RNA polymerase. *J. Med. Chem.*, 47: 2283-2295, 2004.

[111] A. B. Eldrup, M. Prhavc, J. Brooks, B. Bhat, T. P. Prakash, Q. Song, S. Bera, N. Bhat, P. Dande, P. D. Cook, C. F. Bennett, S. S. Carroll, R. G. Ball, M. Bosserman, C. Burlein, L. F. Colwell, J. F. Fay, O. A. Flores, K. Getty, R. L. LaFemina, J. Leone, M. MacCoss, D. R. McMasters, J. E. Tommassini, D. Von Langen, B. Wolanski, D. B. Olsen. Structure-activity relationship of heterobase-modified 2'-C-methyl rinonucleosides as inhibitors of hepatitis C virus RNA replication. *J. Med. Chem.*, 47: 5284-5297, 2004.

[112] Y.-L. Chen, Z. Yin, S. B. Lakshminarayana, M. Qing, W. Schul, J. Duraiswamy, R. R. Kondreddi, A. Goh, H. Y. Xu, A. Yip, B. Liu, M. Weaver, V. Dartois, T. H. Keller, P.-Y. Shi. Inhibition of dengue virus by an ester prodrug of an adenosine analog. *Antimicrob. Agents Chemother.*, 54(8): 3255-3261, 2010.

[113] P. Nauš, O. Caletková, P. Perlíková, L. Poštová Slavětínská, E.Tloušťová, J. Hodek, J. Weber, P. Džubák, M. Hajdúch, M. Hocek. Synthesis and biological profiling of 6- or 7-(het)aryl-7-deazapurine 4'-*C*-methylribonucleosides. *Bioorg. Med. Chem.*, 23: 7422-7438, 2015.

[114] L. Bassit, P. Chatterjee, B. Kim, S. J. Coats, R. F. Schinazi. 2,6-Diaminopurine nucleosides are a novel class of anti-DENV inhibitors. *First International Symposium of Human Vector-Borne Diseases HVBD DART*. December 12-13, 2013.

[115] M. Tichý, R. Pohl, E. Tloust'ová, J. Weber, G. Bahador, Y.-J. Lee, M. Hocek. Synthesis and biological activity of benzo-fused 7-deazaadenosine analogues. 5- and 6-substituted 4-amino- or 4-alkylpyrimido[4,5-*b*]indole ribonucleosides. *Bioorg. Med. Chem.*, 21: 5362-5372, 2013.

[116] M. Tichý, R. Pohl, H. Y. Xu, Y.-L. Chen, F. Yokokawa, P.-Y. Shi, M. Hocek. Synthesis and antiviral activity of 4,6-disubstituted pyrimido[4,5-*b*]indole ribonucleosides. *Bioorg. Med. Chem.*, 20: 6123-6133, 2012.

[117] K. L. Yeo,Y.-L. Chen, H. Y. Xu, H. Dong, Q.-Y. Wang, F. Yokokawa, P.-Y. Shi. Synergistic suppression of dengue virus replication using a combination of nucleoside analogs and nucleoside synthesis inhibitors. *Antimicrob. Agents. Chemother.*, 59(4): 2086-2093, 2015.

[118] J. P. Hughes, S. Rees, S. B. Kalindjian, K. L. Philpott. Principles of early drug discovery. *Br. J. Pharmacol.*, 162: 1239-1249, 2011.

[119] A. C. Anderson. The process of structure-based drug design. *Chem. Biol.*, 10: 787-797, 2003.

[120] S. G. Dahl, I. Sylte. Molecular modelling of drug targets: the past, the present and the future. *Basic. Clin. Pharmacol. Toxicol.*, 96: 151-155, 2005.

[121] U.S. Food and Drug Administration. The FDA's drug review process: ensuring drugs are safe and effective. Updated November 2014.
http://www.fda.gov/drugs/resourcesforyou/consumers/ucm143534.htm, accessed August 2015.

[122] B. Munos. Lessons from 60 years of pharmaceutical innovation. Nat. Rev. Drug. Discov., 8: 959-968, 2009.

[123] R. G. Frank. new estimates of drug development costs. *J. Health Econ.*, 22: 325-330, 2003.

[124] A. Mullard. 2014 FDA drug approvals. *Nat. Rev. Drug Discov.*, 14: 77-81, 2015.

[125] P. J. Gane, p. M. Dean. Recent advances in structure-based rational drug design. *Curr. Opin. Struct. Biol.*, 10: 401-404, 2000.

[126] A. R. Leach. Useful concepts in molecular modelling. Molecular modelling – Principles and applications. *Pearson Education Limited, Harlow*, 2nd edition: 1-25, 2001.

[127] A. R. Leach. The use of molecular modelling and chemoinformatics to discover and design new molecules. Molecular modelling – Principles and applications. *Pearson Education Limited, Harlow*, 2nd edition: 640-726, 2001.

[128] N. Zonta, A. Coluccia, A. Brancale. Advanced *in silico* approaches in antiviral research. *Antiviral Chem. Chemother.*, 20: 147-151, 2010.

[129] D. B. Kitchen, H. Decornez, J. R. Furr, J. Bajorath. Docking and scoring for drug discovery: methods and applications. Nat. Rev. Drug Discov., 3: 935-949, 2004.

[130] R. D. Taylor, P. J. Jawsbury, J. W. Essex. A review of protein-ligand docking methods. *J. Comput. Aided Mol. Des.*, 16: 151-166, 2002.

[131] A. R. Leach. Molecular dynamics simulation methods. Molecular modelling – Principles and applications. *Pearson Education Limited, Harlow*, 2nd edition: 353-409, 2001.

[132] M. J. Abraham, D. van der Spoel, E. Lindahl, B. Hess, and the GROMACS development team. *GROMACS User Manual version 5.0.6*, www.gromacs.org, 2015.

2 RESULTS AND DISCUSSION

2.1 MOLECULAR MODELLING STUDIES ON DENV RdRp

2.1.1 DENV RdRp *DE NOVO* INITIATION COMPLEX

Several crystal structures of DENV RdRp have been reported and show the polymerase domain in a 'closed' conformation representative of a pre-initiation state.[1, 2, 3, 4] However, the crystal structure of DENV RdRp binding the nucleic acid has not been solved. A complete *de novo* initiation complex (ternary complex) of DENV RdRp would show the enzyme bound to an ssRNA template and priming nucleotides complementary to the 3'-end of the template, as well as to two Mg^{2+} ions in the active site.

In the model of the *de novo* initiation complex proposed by Yap *et al*. in 2007 (figure 31),[1] a GTP-binding site has been identified in the polymerase crystal structure and provides the priming (or *de novo* initiation) platform.[1, 5] A high concentration of GTP is required for initiating the RNA synthesis with the *de novo* mechanism, regardless of the exact nucleotide sequence at the 3'-end of the RNA template.[1, 5] As described in section 1.2.1, the nucleobase of the priming nucleotide (GTP) stacks against an aromatic residue of the priming loop (Trp795 in this model)[1] in the initiation site (*i* site). This interaction positions the priming nucleotide in a way that it can form base pairing Watson Crick hydrogen bonds with the nucleotide at the 3'-end of the RNA template. The triphosphate moiety of the GTP is coordinated by Ser710, Arg729 and Arg737 which are strictly conserved and in vicinity to the priming loop.[1]

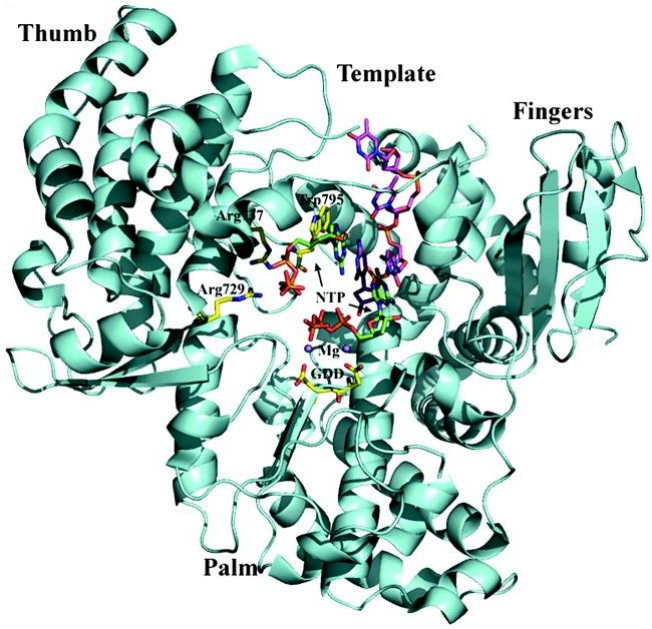

Figure 31. The DENV RdRp *de novo* initiation complex model proposed by Yap *et al*.[1] Nucleotides are shown as green sticks and indicated by arrows. The priming GTP in the initiation (*i*) site stacks against Trp795, shown as sticks in yellow. GTP: guanosine triphosphate; NTP: nucleotide triphosphate. Figure reproduced under permission by the American Society for Microbiology.

A second model of the DENV RdRp *de novo* initiation complex, proposed by Selisko *et al*. in 2012 (figure 32),[6] describes a similar binding site for the priming NTP. The coordination of the triphosphate moiety of the priming nucleotide (ATP in this model) by Ser710, Arg729 and Arg737 in the *i* site was confirmed. The 3'-hydroxyl group of the ATP is positioned close to the α-phosphate of the incoming nucleotide (GTP) which occupies the catalytic site (*i* + 1). However, the nucleobase of the priming ATP stacks against a residue of histidine (His798) of the priming loop, rather than Trp795.[6]

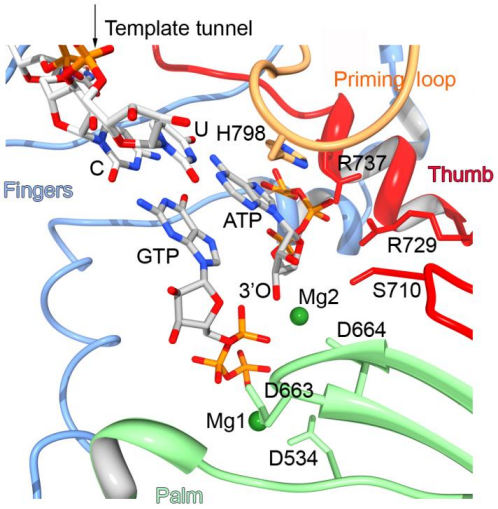

Figure 32. The DENV RdRp *de novo* initiation complex model proposed by Selisko *et al*.[6] Nucleotides are shown as sticks in light grey. The priming ATP in the initiation (*i*) site stacks against His798 (shown as sticks in orange), and the second NTP is coordinated to the Mg^{2+} ions (Mg1 and Mg2, displayed as green spheres) in the catalytic (*i* + 1) site. ATP: adenosine triphosphate; GTP: guanosine triphosphate; NTP: nucleotide triphosphate. Figure reproduced from Selisko *et al*. under the Creative Commons Attribution license.[6]

In conclusion, both models of the DENV RdRp *de novo* initiation complex highlight the key role of the priming loop in initiating the RNA synthesis. However, the crystal structure of the DENV RdRp ternary complex is still missing and would provide a precise characterisation of the residues responsible for the interaction with the dinucleotide in the priming (*i*) and catalytic (*i* + 1) sites.[5, 6]

2.1.1.1 Construction of DENV RdRp *de novo* initiation complex model

The availability of a model of the DENV RdRp *de novo* initiation complex would represent an essential tool for the design of novel nucleoside analogues. The procedure used in this work for the construction of the model of DENV polymerase binding the ssRNA template and the priming nucleotides was reported by Migliaccio *et al*.[7] for generating a model of HCV polymerase bound to the inhibitor 2'-*C*-methyladenosine triphosphate. The templates used by the authors[7] were the HCV NS5B crystal structure (Protein Data Bank code 1GX6) and the initiation complex crystal structure reported for the bacteriophage ϕ6 RdRp (Protein Data Bank code 1HI0). Similarly, the model for the DENV RdRp *de novo* initiation complex was built from the DENV polymerase crystal structure (Protein Data Bank code 4HHJ)[2] and the crystal structure of the HCV polymerase in

complex with a short dsRNA, published by Mosley *et al*. in 2012 (figure 33, Protein Data Bank code 4E78).[8]

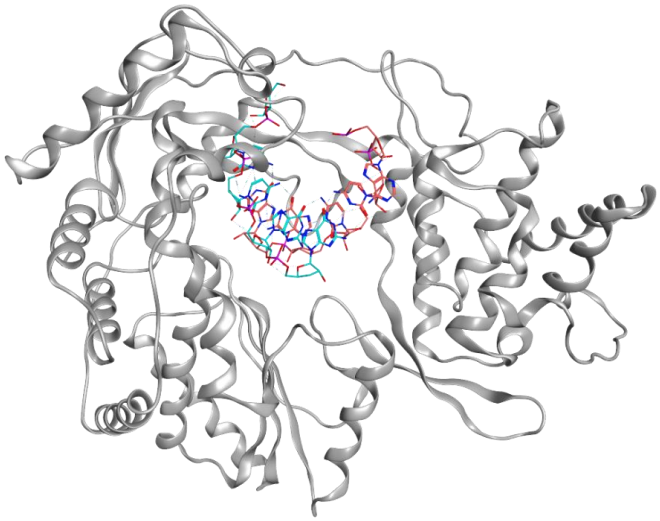

Figure 33. Crystal structure of the HCV NS5B ternary complex (Protein Data Bank code 4E78).[8] The back view of the polymerase shows the double stranded RNA, displayed as sticks (nascent RNA in light blue, template RNA in pink). HCV NS5B. Hepatitis C virus non-structural protein 5B.

Because of the structural similarity between the two polymerases, it was possible to use the available crystal structure for the HCV NS5B complex[8] as a template for the construction of the model of the ternary complex of DENV polymerase. The DENV polymerase crystal structure was superposed on the HCV ternary complex crystal structure[8] and the nucleic acid from the latter was imported into the active site of DENV polymerase. The growing strand was shortened to a dinucleotide, made of guanosine monophosphate (GMP) and 3'-deoxyguanosine monophosphate (3dGMP), in order to fit the smaller pocket of DENV polymerase, which is partially occluded by the priming loop. The dinucleotide was then divided into the priming nucleotide (GMP) in the *i* site and the second nucleotide (3dGMP) in the *i* + 1 site that was then converted to its triphosphate form in order to mimic the incoming NTP, the substrate of the polymerase for the formation of the first phosphodiester bond. As the used crystal structure of DENV polymerase[2] lacks the two cations required for the coordination of the triphosphate moiety of the incoming NTP, two magnesium ions were added to the active site and manually positioned in coordination with the three aspartate residue (Asp533, Asp663 and Asp664) identified by the crystallography data reported by *Yap et al*.[1] In order to use this model for the design of adenosine-based nucleoside

analogues, 3dGTP was converted to ATP and, as a consequence, the complementary cytidine in the template was converted to uridine to maintain the base-pairing hydrogen bonds (figure 34). The interactions between the 2' and the 3'-hydroxyl groups and Asp538 as well as the base pairing interactions were enforced by high strength constraints. Finally, the model was refined through iterative cycles of energy minimisation.

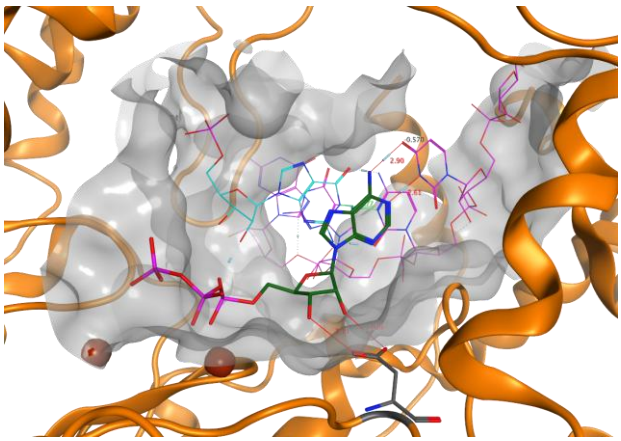

Figure 34. View of the priming (*i*) site and the active (*i* + 1) site of the DENV RdRp *de novo* initiation complex model. The priming nucleotide (GTP) and the RNA template are shown as sticks in light blue and pink, respectively; the incoming nucleotide (ATP) is shown in thick sticks and coloured in dark green; Asp538 is displayed as thick sticks in grey and the Mg^{2+} ions as red spheres. DENV RdRp: Dengue virus RNA-dependent RNA polymerase. GTP: guanosine triphosphate; ATP: adenosine triphosphate.

2.1.1.2 Validation of the model

The novel model was validated by docking studies of the phosphorylated forms of adenosine analogues that have been reported to be inhibitors of DENV polymerase. The molecules were 2'-*C*-methyl-7-deazaadenosine,[9] the 2'-*C*-acetylene analogues series reported by Novartis Institute for Tropical Diseases,[10, 11, 12] 2-amino-2'-*C*-methyladenosine[13] and the novel series of benzo-fused 7-deazaadenosine analogues reported by Tichý *et al*.[14, 15] These DENV RdRp inhibitors are described in paragraph 1.2.2.2 and the molecules submitted to the docking process are summarised in table 20 in the APPENDIX.

The docking results were evaluated based on the geometry of the complex whereas the ranking according to score values was not taken into account as the electrostatic interactions between the negatively charged phosphate moiety and the Mg^{2+} ions are dominant and render the scoring

functions unreliable.[16, 17] To overcome this issue, the best scoring poses generated by the docking algorithm were visually inspected to verify the presence of key geometrical features: the alignment of the adenosine analogue to the structure of the natural substrate (ATP), the presence of base pairing interactions with the complementary nucleotide in the RNA template, the coordination of the 2' and the 3'-hydroxyl groups of the ribose to Asp538 and, finally, the positioning of the phosphate or triphosphate moiety in relation to the Mg^{2+} ions. Figure 35 shows the docking pose of the monophosphorylated compounds NITD008 and NITD449 superposed on ATP, and exemplifies the general binding mode of an adenosine analogue in the active site of the DENV RdRp *de novo* initiation model.

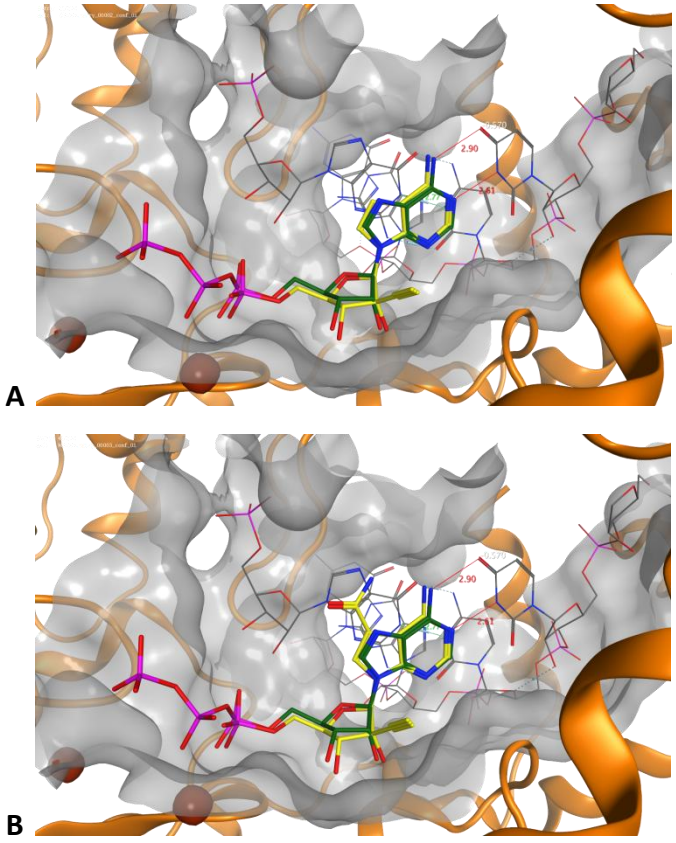

Figure 35. Docking poses of 2'-*C*-ethynyl-7-deazaadenosine (NITD008, **A**) and the 7-carbamoyl derivative (NITD449, **B**) in the monophosphate form. The docked molecules and the natural substrate ATP are shown as sticks, in yellow and dark green respectively. ATP: adenosine triphosphate.

Overall, the phosphorylated adenosine analogues in both their monophosphate and triphosphate forms gave excellent docking results, confirming the reliability of the model.

Additionally, in order to check the stability of the molecular system, the model was submitted to an MD simulation,[18] after modelling two loops (spanning residues from 406 to 420 and from 457 to 469) that were missing in the original DENV RdRp crystal structure (Protein Data Bank code 4HHJ).[2]

The MD simulation was analysed by observing the behaviour of the protein and the Mg^{2+} ions over the time of the simulation. During the performed MD simulation, the overall structure did not undergo major structural changes. In particular, the Mg^{2+} ions maintained the coordination with the aspartate residues as well as with the triphosphate moiety of the incoming NTP. In addition, the interactions between the 2' and 3'-hydroxyl groups of the ribose and Asp538 were not affected. Therefore, these results demonstrated the stability of the molecular system.

2.1.2 *IN SILICO* DESIGN OF NOVEL ADENOSINE ANALOGUES

Docking of the phosphorylated form of adenosine analogues known to have anti-DENV activity was performed using the developed model of the DENV RdRp *de novo* initiation complex (see paragraph 2.1.1.2 for details) and gave excellent results, confirming that the model is reliable and may be used for the design of novel adenosine analogues *in silico*. Docking of families of adenosine analogues was performed in order to predict their binding affinity in the active site of DENV RdRp, and therefore their potential role as DENV inhibitors. Additionally, adenosine analogues in which the five-membered ring of the ribose moiety is replaced by a linear scaffold were selected after screening a database of molecular linkers and docked into the active site of the DENV RdRp model.

2.1.2.1 Docking studies

In order to identify the most promising modifications in the structure of ATP, the natural substrate of the polymerase, families of ribose-modified and purine-modified adenosine nucleoside analogues were submitted to docking studies using the model of the DENV RdRp *de novo* initiation complex.

As previously described for the docking of known DENV RdRp inhibitors (paragraph 2.1.1.2), the geometry of the complex observed in the docking poses, rather than the associated scoring, was considered to evaluate docking results. Following visual inspection of the best docked conformations for each molecule, their binding mode was evaluated on the basis of the presence of key geometrical features, which were i) the alignment of the adenosine analogue to the reference structure of ATP; ii) the presence of base pairing interactions with the complementary nucleotide in the RNA template; iii) the interaction of the 2' and 3'-hydroxyl groups of the ribose to Asp538 and iv) the coordination of the phosphate or triphosphate moiety to the Mg^{2+} ions. A good binding mode was assigned to the molecule when at least one docked conformation characterised by the presence of all listed geometrical features (i to iv) could be identified. A distorted conformation of the ribose ring compared to the reference structure of the natural substrate may compromise the exact alignment to ATP (feature i); however the binding mode may still be considered good if the other listed criteria (ii to iv) were fulfilled. Finally, when a major distortion of the overall conformation compared to the reference structure of ATP (feature i) was observed or the essential interactions with the template, the protein residues or the Mg^{2+} ions in

the active site (features ii to iv) were not present, a poor binding mode was assigned to the molecule.

2.1.2.1.1 Ribose-modified 7-substituted 7-deazaadenosine analogues

Based on the chemical structures of the known adenosine analogues showing anti-DENV activity (2'-*C*-methyl-7-deazaadenosine[9] and the 2'-*C*-acetylene derivatives series reported by NITD [10, 11, 12]), modifications at the 7-deaza position in the purine base and the 2'-position in the ribose moiety were considered in the first family of compounds.

The introduction of either methyl or ethynyl groups in the 2'-position was well tolerated by the active site of the DENV RdRp model in various 7-substituted 7-deazaadenosine analogues. Explored substituents at the 7-deaza position were halogens, carbamoyl, cyano and acetylene groups as well as the five-membered rings oxadiazole and pyrazole due to the presence of these moieties in the structures of various known anti-HCV or anti-DENV agents (summarised in table 4).

1'-*C*-Substitution is a structural feature which was recently reported in a novel class of anti-DENV nucleoside analogues.[13] In order to explore the effect of this novel modification on the binding affinity, the substitution with either methyl or ethynyl groups was moved to the anomeric position of the 7-deazaadenosine analogues within the family. Good docking results were obtained for all docked molecules (table 4).

Table 4. Docking results for various 7-substituted 2'-*C*-methyl or 2'-*C*-acetylene 7-deazaadenosine analogues and corresponding 1'-*C*-substituted derivatives.

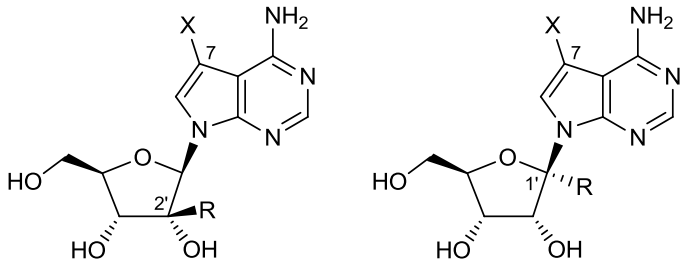

R = CH_3 or CCH

X	**2'-position**	**1'-position**
proton	good binding	good binding
fluoro	good binding	good binding
chloro	good binding	good binding
bromo	good binding	good binding
iodo	good binding	good binding
carbamoyl	good binding	good binding
cyano	good binding	good binding
acetylene	good binding	good binding
oxadiazole	good binding	good binding
pyrazole	good binding	good binding

Given the promising docking results of 1'-*C*-methyl and 1'-*C*-ethynyl modified 7-deazaadenosine analogues, the effect of the nature of the substituent at the anomeric position on the binding affinity was further investigated. Docking studies were performed with various 1'-substituted 7-deazaadenosine derivatives, as summarised in table 5.

Small, especially linear groups pointing inwards such as the cyano and acetylene moieties, gave good docking results (figure 36, **A**). The larger groups *n*-propyl and *i*-propyl were tolerated, however a distortion of the ribose moiety compared to the binding mode of ATP was required to fit the active site. In contrast, the anomeric substitution with a primary amine or a carbamoyl moiety was not accepted by the polymerase, as the base pairing interactions between the 7-deazaadenine and the complementary base in the RNA template were lost (figure 36, **B**).

Table 5. Docking results for various 1'-*C*-substituted 7-deazaadenosine analogues.

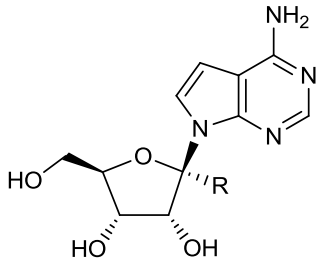

R	**1'-position**
methyl	good binding
ethyl	good binding
vinyl	good binding
cyano	good binding
aminomethyl	poor binding
carbamoyl	poor binding
ethynyl	good binding
methylethynyl	good binding
chloroethynyl	good binding
n-propyl	good binding*
i-propyl	good binding*
hydroxymethyl	good binding

*A distortion of the ribose moiety was observed.

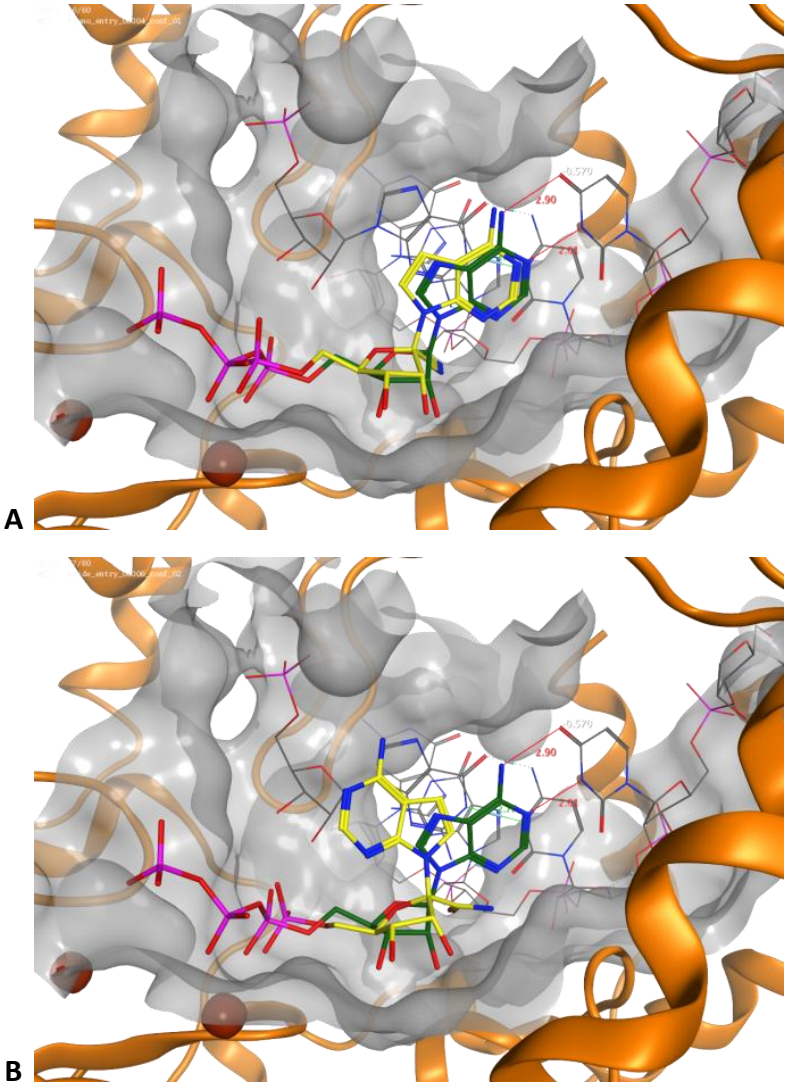

Figure 36. Docking poses of 1'-*C*-cyano-7-deazaadenosine (**A**) and the 1'-*C*-carbamoyl analogue (**B**) in the monophosphate form. The docked molecules and the natural substrate ATP are shown as sticks, in yellow and dark green respectively. The good binding mode of the former is compared to the poor one of the latter, in which the position of the nucleobase is twisted and the base pairing is lost. ATP: adenosine triphosphate.

Finally, the binding affinity of a family of 1',2'-*C*,*C*-bis-substituted 7-deazaadenosine analogues was evaluated. The docked nucleosides bear a methyl group at the 2'-position and various substituents at the anomeric position, as summarised in table 6. Interestingly, all the molecules showed good docking results. However, only the introduction of small and linear substituents, such as methyl, ethyl, cyano and ethynyl groups did not cause a distortion of the ribose ring, which was in contrast with the vinyl or larger moieties. Figure 37 illustrates an example of docking pose of a 1',2'-*C*,*C*-bis-substituted 7-deazaadenosine analogue.

Table 6. Docking results for various 1'-*C*-substituted 7-deaza-2'-*C*-methyladenosine analogues.

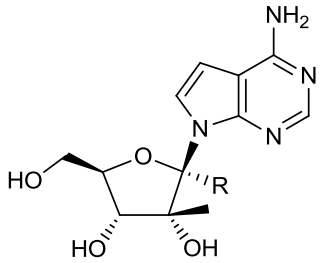

R	**1'-position**
methyl	good binding
ethyl	good binding
vinyl	good binding*
cyano	good binding
aminomethyl	good binding*
carbamoyl	good binding*
ethynyl	good binding
methylethynyl	good binding*
chloroethynyl	good binding*
n-propyl	good binding*
i-propyl	good binding*
hydroxymethyl	good binding*

*A distortion of the ribose moiety was observed.

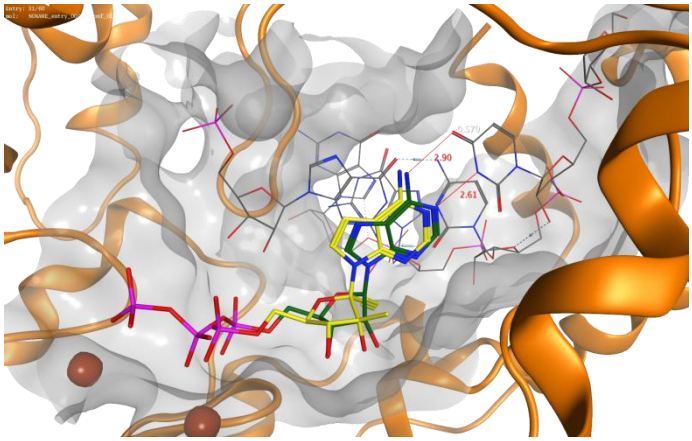

Figure 37. Docking pose of 1'-*C*-acetylene-2'-*C*-methyl-7-deazaadenosine monophosphate. The docked molecule and the natural substrate ATP are shown as sticks, in yellow and dark green respectively. ATP: adenosine triphosphate.

A small family of 2-amino-2'-*C*-methyladenosine analogues was also submitted to docking studies. The substitution of the methyl group with an ethynyl group as well as the introduction of the same carbon groups at the anomeric position produced 2-aminoadenosine analogues showing good binding modes (table 7).

Table 7. Docking results for 2-aminoadenosine analogues substituted at the 2'-position and the anomeric position.

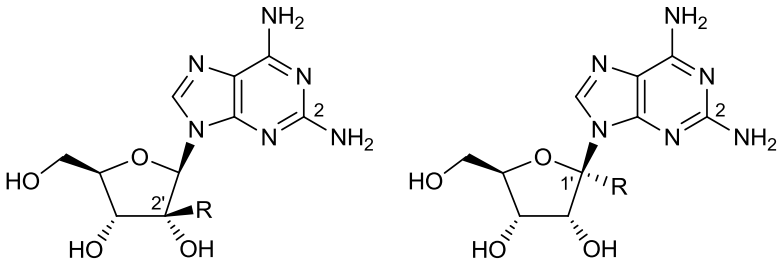

R	2'-position	1'-position
methyl	good binding	good binding
ethynyl	good binding	good binding

2.1.2.1.2 Ribose-modified benzo-fused 7-deazaadenosine analogues

The series of benzo-fused 7-deazaadenosine analogues reported to be active against DENV by Tichý *et al*.[14, 15] demonstrated that the active site of DENV RdRp is capable of accommodating nucleoside analogues which are substituted at the 7-deaza position with large groups. However, the ribose moiety in this series was unmodified. Therefore, series of ribose-modified derivatives were docked into the active site of the DENV RdRp *de novo* initiation model to investigate the effect on the binding affinity induced by the addition of carbon groups in the ribose moiety. Docking results for this family of compounds are summarised in table 8.

The introduction of either methyl or ethynyl groups at the 2'-position of the nucleoside was generally well tolerated, as exemplified in figure 38. Similar results were observed when carbon groups were introduced at the anomeric position of the tricyclic adenosine analogues. Poor docking results were obtained exclusively for those analogues in which the primary amine in 4-position was replaced by heterocyclic moieties (2-furyl, 2-thienyl or 2-benzofuryl). Whereas the ribose-unmodified analogues were reported to be active against DENV,[15] the 2'-*C*- or 1'-*C*-substitution appeared to negatively affect the binding affinity of these novel derivatives.

Table 8. Docking results for ribose-modified benzo-fused 7-deazaadenosine analogues.

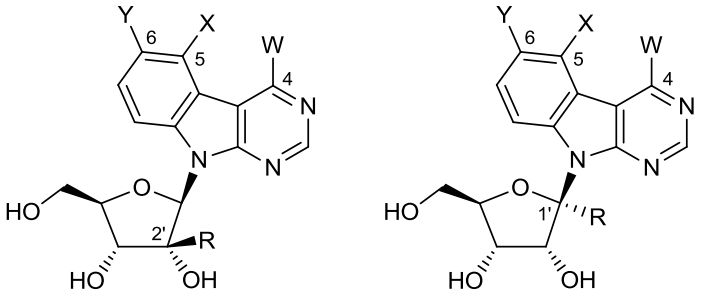

Nucleobase			**2'-position**		**1'-position**	
4-W	**5-X**	**6-Y**	**methyl**	**ethynyl**	**methyl**	**ethynyl**
amino	H	H	good binding	good binding	good binding	good binding
amino	chloro	H	good binding	good binding	good binding	good binding
amino	H	chloro	good binding	good binding	good binding	good binding
amino	*n*-butyl	H	good binding	good binding	good binding	good binding
amino	H	3-thienyl	good binding	good binding	good binding	good binding
amino	H	2-benzofuryl	good binding	good binding	good binding	good binding
2-furyl	H	chloro	good binding	good binding	poor binding	poor binding
2-thienyl	H	chloro	poor binding	poor binding	good binding	poor binding
2-benzofuryl	H	chloro	good binding	good binding	good binding	poor binding

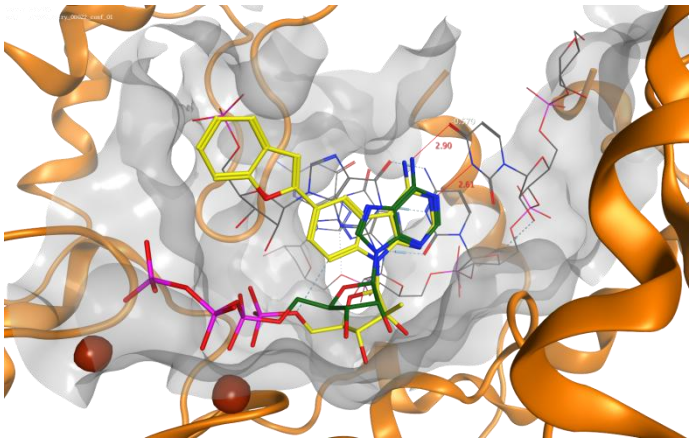

Figure 38. Docking pose of the 2'-*C*-methyl derivative of 4-amino-6-benzofuran-2-yl-9-β-D-ribofuranosyl-pyrimido[4,5-*b*]indole monophosphate. The docked molecule and the natural substrate ATP are shown as sticks, in yellow and dark green respectively. The modification at the ribose moiety is tolerated and the large substituent at the benzo-fused 7-deazaadenine fit well in the active site. ATP: adenosine triphosphate.

2.1.2.2 Design of acyclic adenosine analogues

In the model of the DENV RdRp *de novo* initiation complex, the ATP molecule is involved in key interactions in the catalytic site of the polymerase. The adenine base pairs with a complementary uracil base in the RNA template, the triphosphate moiety is coordinated by two catalytic ions of Mg^{2+} and the hydroxyl groups in 2' and 3'- positions are engaged in hydrogen bond interactions with an aspartate residue (Asp538). The ribose ring provides a linker between the triphosphate and the nucleobase moieties of the NTP and the coordination of the free hydroxyl groups contributes to holding the substrate in the active site. An acyclic inhibitor of DENV RdRp should thus be engaged in similar interactions in the active site. Therefore, the adenine needs to interact with the complementary base in the RNA template, whilst the aliphatic moiety should contain a hydroxyl group holding the triphosphate moiety at the correct distance to coordinate with the Mg^{2+} ions, and a second hydrogen bond donor to maintain the additional interaction with the aspartate residue. These essential features of the linker between the nucleobase and the phosphorylated hydroxyl group may also be found in a linear scaffold, compared to the cyclic ribose scaffolds. Replacement of the five-membered ring of the ribose moiety by a linear linker represents an attractive strategy for the *in silico* design of acyclic nucleoside analogues as potential inhibitors of DENV RdRp.

2.1.2.2.1 Scaffold replacement

In the search for acyclic adenosine analogues, the model of the DENV RdRp *de novo* initiation complex was used to screen a database of linkers that could replace the ribose ring of ATP (**26**, figure 39) in the active site of the polymerase. The five carbon atoms, the oxygen atom and the 2' and 3'-hydroxyl groups of the ribose constituted the scaffold used for the screening.

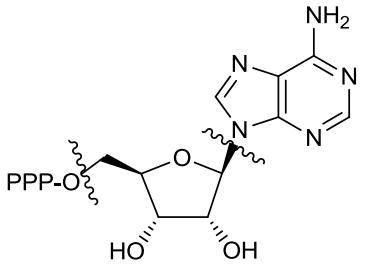

26

Figure 39. Structure of ATP (**26**) showing the scaffold for the screening of a database of linkers. PPP: triphosphate.

Linkers were selected on the basis of three additional properties: a Tanimoto index of similarity with ATP less than 0.8, a molecular weight of the resulting nucleotide triphosphate analogue lower than 525 Da (comparable to the molecular weight of ATP of 507.18 Da), and the presence of a hydrogen bond donor mimicking the 3'-hydroxyl group of the original ribose ring. The thus performed screening resulted in 83 entries, of which twelve entries corresponded to linear fragments which are shown in figure 40. The most common scaffold was a four carbon 2,3-unsaturated chain bearing different substituents on the alkene, namely hydroxymethyl and aminomethyl moieties (entries ***a*** – ***l***, figure 40).

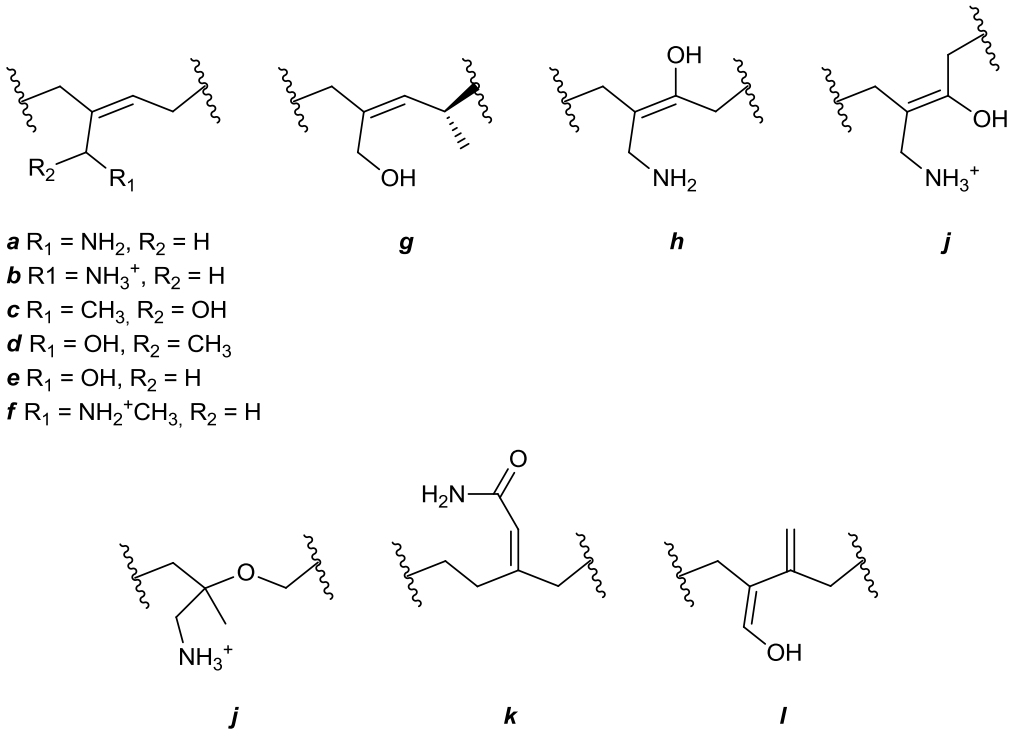

Figure 40. Linear linkers resulting from the screening of a database of linkers for the replacement of the cyclic ribose moiety of the original nucleoside.

2.1.2.2.2 Docking studies

A prediction of the binding affinity of the twelve acyclic nucleoside analogues which resulted from the scaffold replacement was obtained by docking studies using the model of the DENV RdRp *de novo* initiation complex. Docking results were evaluated based on visual inspection of the best scoring poses for each docked molecule, while ranking according to the scoring was not taken in consideration because of the aforementioned unreliability of the scoring functions in the presence

of the Mg^{2+} cations. The evaluated geometrical features were: i) the correct position of the nucleobase, interacting with the corresponding nucleotide in the RNA template; ii) the coordination of the triphosphate moiety with the Mg^{2+} ions and iii) the position of the hydrogen bond donor in coordination to Asp538. When all listed geometrical features (i to iii) could be observed in the same docked conformation, a good binding mode was assigned to the molecule. On the other hand, the binding mode was considered poor when any of the listed geometrical features were not present.

The results from the docking of the acyclic adenosine analogues, which are summarised in table 9, helped selecting the most promising linkers. The molecules containing entry ***e*** (**27**, figure 41) and entry ***g*** (**28**, figure 41) were chosen as target compounds because of their excellent docking results. Specifically, the acyclic adenosine analogue bearing the linear scaffold ***g*** was an attractive target compound due to the similarity of its binding mode in the active site of the model of DENV RdRp with the binding mode of the 1'-*C*-substituted adenosine analogues, which was previously predicted by docking studies (figure 36, **A** in paragraph 2.1.2.1.1). Furthermore, the synthetic accessibility of the linear scaffold ***e***[19] and the possibility of applying the phosphoramidate ProTide approach to synthesised nucleosides were important factors for the selection of the target acyclic adenosine analogues. The synthetic strategies towards the selected acyclic adenosine analogues will be described in section 2.2.4.

Table 9. Docking results for acyclic adenosine analogues.

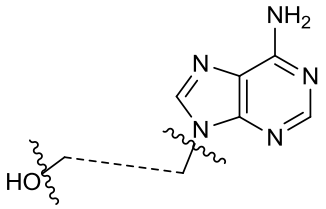

Entry	Docking result
a	poor binding
b	good binding
c	good binding
d	good binding
e	good binding
f	good binding
g	good binding
h	poor binding
i	good binding
j	good binding
k	poor binding
l	poor binding

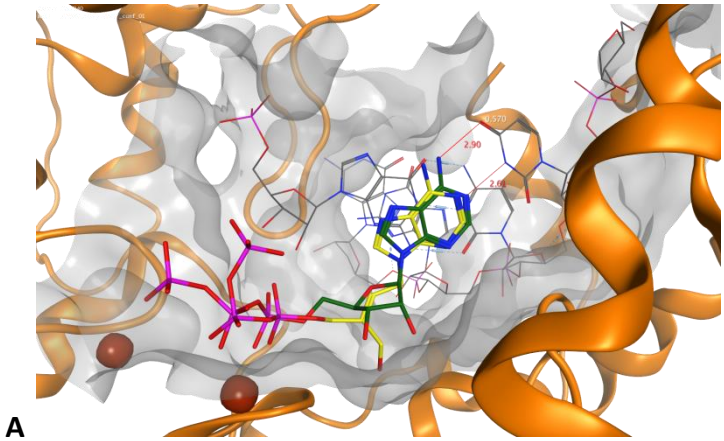

A

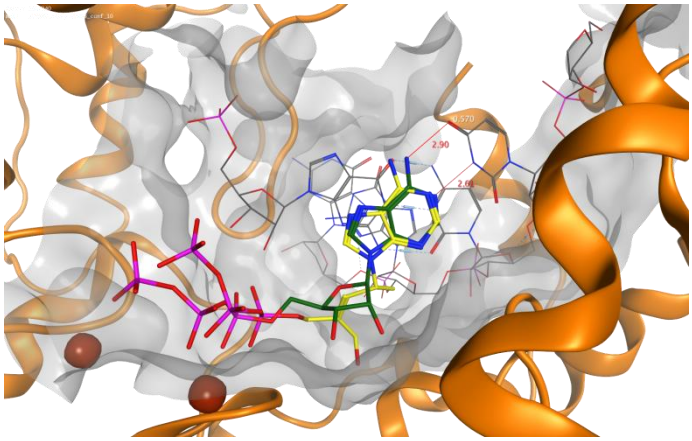

B

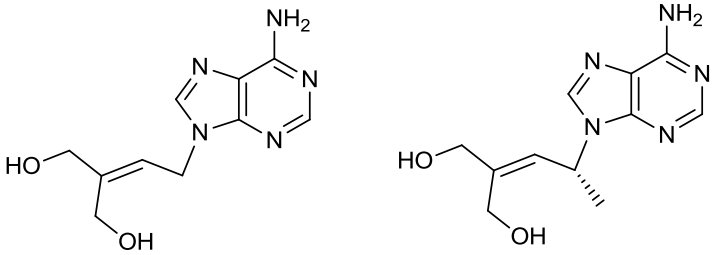

27 (*R*)-enantiomer of **28**

Figure 41. Docking poses (**A** and **B**) and chemical structures of the selected acyclic adenosine analogues **27** and (*R*)-enantiomer **28**. The docked molecules and the natural substrate ATP are shown as sticks, in yellow and dark green respectively. ATP: adenosine triphosphate.

2.1.3 MOLECULAR DYNAMICS SIMULATIONS

Crystal structures of the DENV RdRp have been reported.[1, 2, 3, 4] Several loops contribute to keeping the polymerase in a closed conformation which is required in the initiation phase of the *de novo* RNA synthesis. In particular, these are the priming loop that projects towards the active site, and other very flexible loops at the top of the polymerase that link the thumb to the fingers, which are aptly named fingertips.[1] Details on the available crystal structures of DENV RdRp are described in section 1.2.1. It is assumed that the polymerase needs to undergo drastic conformational changes to adopt an open structure and accommodate the dsRNA in the elongation phase of the RNA synthesis.[1, 5, 6] However details on this transition are unknown as the polymerase domain in complex with the template and the nascent RNA strands (ternary complex) has not yet been crystallised.

MD simulations were performed on the *apo* DENV RdRp domain and on different complexes of the polymerase bound to the nucleic acid with the aim of providing insights in the conformational changes of DENV polymerase during the synthesis of the RNA and, especially, of understanding the destiny of the priming loop in the open elongation-competent structure of the enzyme.

The MD simulations were analysed visually by observing the behaviour of the different elements in the complex (protein, nucleic acid, cations) over time. First, the complex obtained from each MD simulation was superposed to the original starting complex (before the MD simulation). This allowed to check for the stability of the position of the two Mg^{2+} ions and of the overall structure of the protein, features that are indicative of a reliable simulation. Then, the movement of flexible loops of the protein and the formation of new interactions between residues of those loops and the nucleic acid were considered. These results are described in the following paragraphs as results of the MD simulation.

2.1.3.1 Model of the complete *apo* DENV RdRp

The available crystal structures of DENV polymerase[1, 2, 3, 4] are incomplete due to the presence of highly flexible loops. Therefore, the construction of a model of the complete *apo* structure of DENV polymerase was required before building the model of the ternary complex. In the crystal structure of DENV polymerase (Protein Data Bank code 4HHJ),[2] two loops were unsolved: a first loop spanning residues from 406 to 420 (loop **L1**, 15 residues) and a second loop spanning residues from 457 to 469 (loop **L2**, 13 residues). Both missing loops were modelled based on the

amino acid sequence. Additionally, two Mg^{2+} ions, which were missing in the original crystal structure, were added in the active site in coordination with Asp533, Asp663 and Asp664. This created model was refined by performing an MD simulation.

During the MD simulation, the modelled loops (**L1** and **L2**) as well as the priming loop **P** were flexible (figure 42). The priming loop (**P**) moved further towards the still empty active site. Overall, the stability of the molecular system was confirmed by the preservation of the coordination of the cations with the three aspartate residues (figure 43).

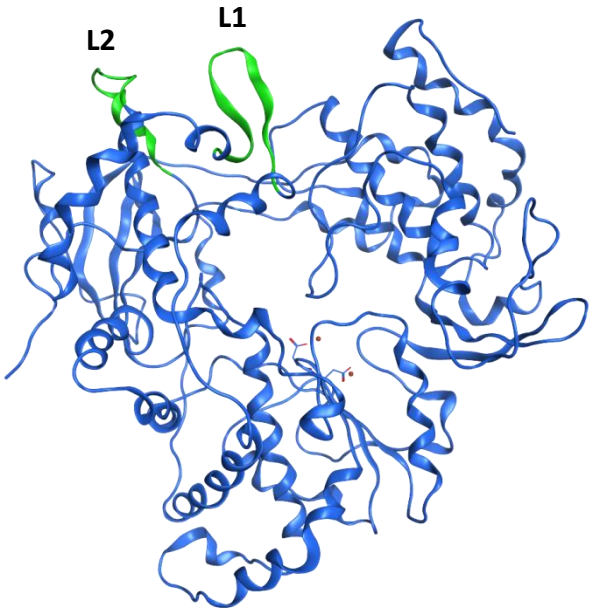

Figure 42. Front view of the model of complete *apo* DENV RdRp after the MD simulation. The modelled loops (loops **L1** and **L2**) are shown as ribbons in light green. DENV RdRp: Dengue virus RNA-dependent RNA polymerase; MD: molecular dynamics.

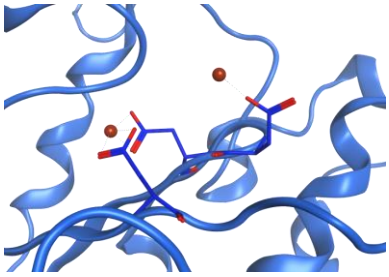

Figure 43. View of the active site of the model after the MD simulation showing the Mg^{2+} ions coordinating the side chain of three aspartate residues (533, 663, 664). The two cations are displayed as red spheres and the aspartate residues as blue sticks. DENV RdRp: Dengue virus RNA-dependent RNA polymerase; MD: molecular dynamics.

2.1.3.2 Model of the complete *de novo* initiation complex

The model of the complete *apo* structure of DENV polymerase was used for building the model of the initiation complex, in which the polymerase binds a short dsRNA and an additional ssRNA that mimics the RNA template entering the active site. As described for the construction of the first model of the DENV RdRp *de novo* initiation complex (see paragraph 2.1.1.1), the short dsRNA was imported from the available crystal structure of HCV ternary complex.[8] The priming loop **P** in the *apo* structure of DENV polymerase projects towards the centre of the enzyme, thereby partially occupying the space for the nascent dsRNA. The conformation of the priming loop was modified, by deleting the loop from residues 782 to 809 and by modelling it based on the amino acid sequence in the presence of the imported dsRNA. The nucleic acid was further modified to build an extra ssRNA representative of the RNA template that reaches the active site through the putative tunnel at the top of the polymerase.[1, 2, 6] The ssRNA corresponding to the template was copied, bound to the existing template through a phosphodiester bond and positioned as described in the literature.[1, 2, 6] The two flexible loops (loops **L1** and **L2**) were re-modelled to accommodate the ssRNA in the tunnel. An additional short loop from the thumb (spanning residues from 740 to 747, loop **L3**), which is solved in the crystal structure, also contributed to shaping the tunnel. The built initiation complex was submitted to an MD simulation.

During the MD simulation, the priming loop **P** was further pushed outwards by the nucleic acid (figure 44). The re-modelled loops **L1** and **L2** were very flexible as well and moved further outwards, thus widening the tunnel for the entering template (figure 45). During the MD simulation, the hydrogen bonds between two pairs of heterobases in the dsRNA were lost, as

shown in figure 46, as the nucleotides had the possibility to move freely in the large space that was still available at the front of the polymerase.

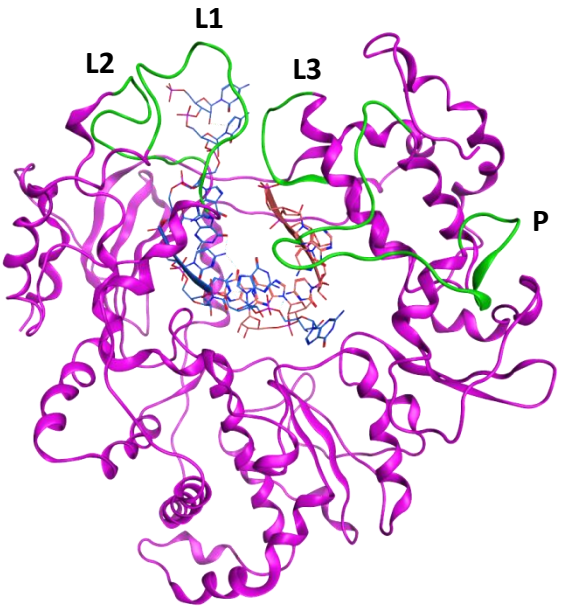

Figure 44. Front view of the DENV RdRp *de novo* initiation complex model after the MD simulation. Loops playing a crucial role in the initiation phase as specified in the text are shown as ribbons in light green. The RNA template and growing strand are displayed as ribbons and sticks and coloured in blue and in pink, respectively. DENV RdRp: Dengue virus RNA-dependent RNA polymerase; MD: molecular dynamics.

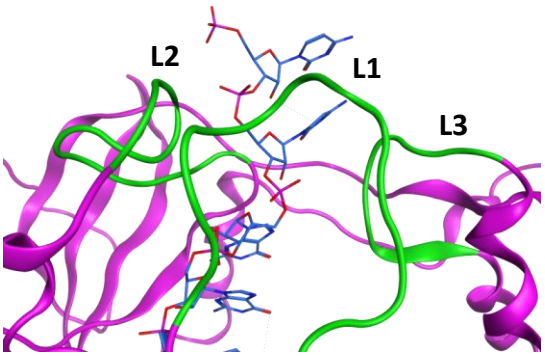

Figure 45. View of the tunnel for the RNA template after the MD simulation. Three main loops, shown as green ribbons, encircle the ssRNA, displayed as blue sticks. MD: molecular dynamics.

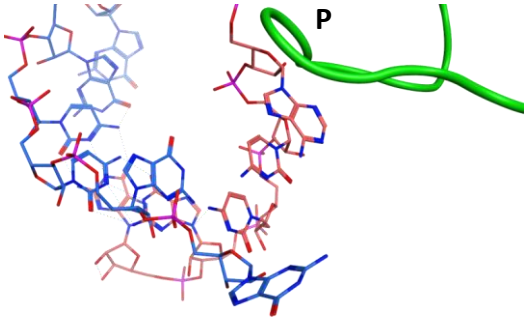

Figure 46. View of the nucleic acid from the front of the RdRp after the MD simulation. The dsRNA is distorted and some base pairing interactions are lost during the MD simulation. The priming loop **P** is shown as ribbon in green, the RNA template and growing strand as sticks in blue and in pink, respectively. RdRp: RNA-dependent RNA polymerase; MD: molecular dynamics.

2.1.3.3 Model of the elongation complex

The initiation complex which resulted from the MD simulation was used for the creation of the ternary complex representative of the elongation phase of the synthesis of the RNA, when the polymerase binds a long dsRNA and the extra ssRNA template entering the active site. The long dsRNA was built starting from the 4-nucleotide long dsRNA from the crystal structure of the HCV ternary complex.[8] A copy of this molecule was bound to the existing one following the orientation of the double helix to obtain a 8-nucleotide long dsRNA, that was imported into the active site of the initiation complex. This new long dsRNA replaced the short one of the initiation complex (figure 44) and was linked to the ssRNA via a phosphodiester bond. The priming loop **P** was partially deleted (residues from 782 to 796) and re-modelled based on the amino acid sequence to accommodate the longer nucleic acid, which extended outwards at the front of the polymerase. The resulted complex was submitted to an MD simulation.

All the base-pairing interactions were now maintained during the MD simulation and the long dsRNA moved without altering the double helix conformation (figure 47). In fact, the nucleic acid underwent a rotation that moved the growing strand upwards and in contact with the priming loop **P**, as illustrated in figure 48. In the elongation complex resulting from this last MD simulation, some residues of the priming loop **P** interacted with the growing strand: specifically, a residue of arginine (Arg792) coordinated the phosphate backbone of the growing strand, and while Trp795 did not interact directly with the nucleic acid, this residue was nevertheless in a good position for stacking against the nucleobase of the priming nucleotide (figure 49).

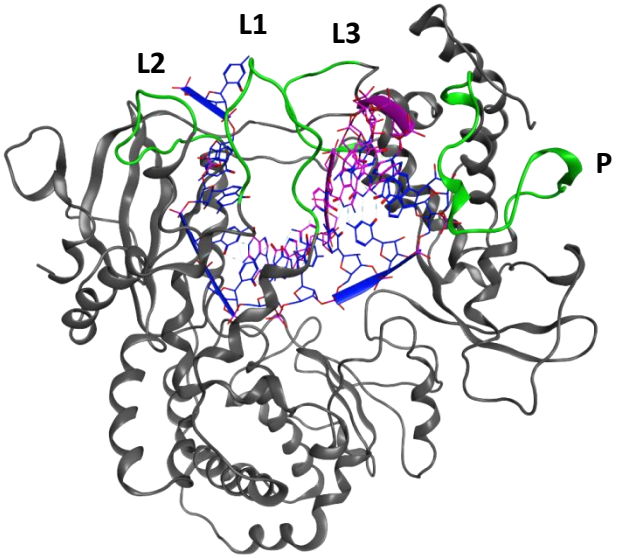

Figure 47. Front view of the DENV RdRp elongation complex model after the MD simulation. The long dsRNA passes through the protein and extends outwards at the front of the DENV RdRp. Important loops are shown as ribbons in light green. The RNA template and growing strand are displayed as ribbons and sticks and coloured in dark blue and in dark pink, respectively. DENV RdRp: Dengue virus RNA-dependent RNA polymerase; MD: molecular dynamics.

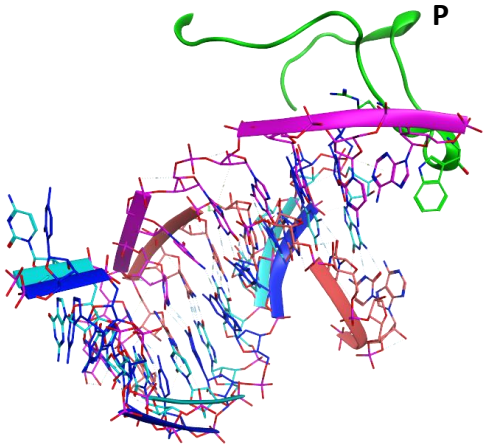

Figure 48. Rotation of the nucleic acid during the MD simulation. The RNA template and the growing strand after the MD simulation, shown in ribbons and sticks and coloured in dark blue and pink, respectively, are superposed on the double stranded RNA before the MD simulation, displayed in ribbons and sticks in light blue and light pink, respectively. The growing strand in the elongation complex (dark pink) is in contact with the priming loop **P**, shown as green ribbon. MD: molecular dynamics.

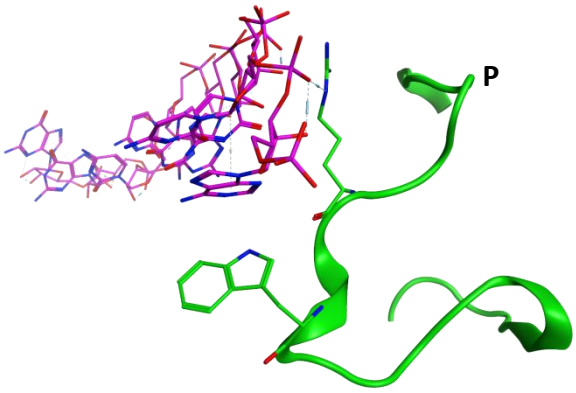

Figure 49. View of the growing strand and the priming loop **P** from the front of the RdRp. The ssRNA is shown as sticks coloured in dark pink. The priming loop **P** is displayed as green ribbon with residues of Arg792 and Trp795 as green sticks. RdRp: RNA-dependent RNA polymerase.

2.1.3.4 Concluding remarks

The set of MD simulations suggested that the conformational changes of specific loops of the DENV RdRp, especially the loop spanning residues from 406 to 420 (loop **L1**), and the priming loop **P**, play a crucial role in the activity of the polymerase.

Figure 50 highlights the function of loop **L1**, showing the models of the DENV RdRp in the three phases of the replication of the RNA: pre-initiation (*apo* structure), initiation and elongation. In the *apo* structure, loop **L1** hindered the top of the protein (**A**), then progressively moved outwards in the initiation complex (**B**) and the elongation complex (**C**), shaping the tunnel for the RNA template entering the active site from the top of the polymerase.

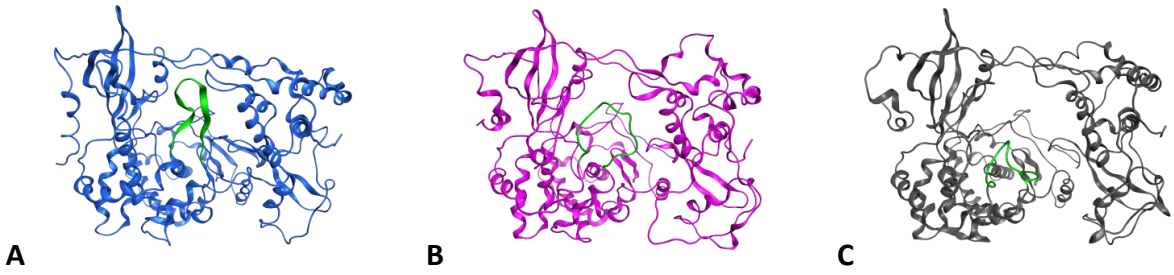

Figure 50. Top view of the models of the DENV RdRp in the pre-initiation (**A**), initiation (**B**) and elongation (**C**) phase of the RNA synthesis. Loop **L1** is shown as green ribbon. DENV RdRp: Dengue virus RNA-dependent RNA polymerase.

The key role of loop **L1** in the transition to the elongation phase of the RNA synthesis was confirmed by the crystal structure of DENV polymerase in complex with the allosteric inhibitor NITD107 (**29**, figure 52), as reported by Noble *et al*. (Protein Data Bank code 3VWS).[2] A dimer of the inhibitor is positioned in the centre of the polymerase (figure 51) and interacts with residues of loop **L1** (Phe412 and Thr413, figure 52). When the crystal structure was superposed to the model of the DENV *de novo* initiation complex, the overall structures of the proteins were in alignment whereas the crystallised loop **L1** was blocked in a folded conformation pointing inwards. According to the authors,[2] NITD107 may act by preventing the conformational changes of the loop, thus blocking the tunnel of the RNA template. The results of the MD simulations performed in this work are in agreement with the suggested function of the loop.

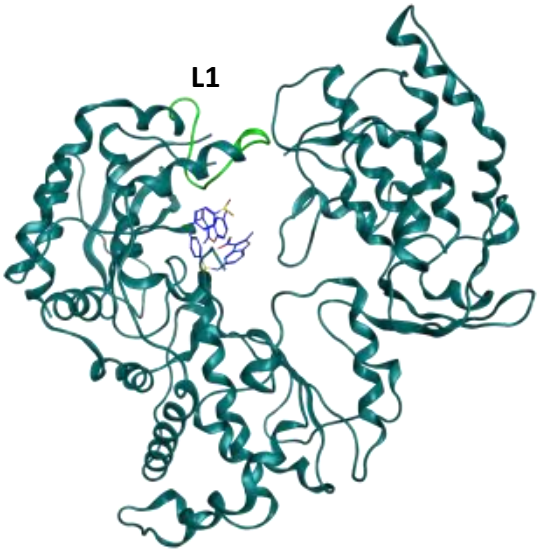

Figure 51. Front view of the crystal structure of the DENV RdRp binding the allosteric inhibitor **29** (dimer). NITD107 is displayed as sticks in blue and loop **L1** as ribbon in light green (Protein Data Bank code 3VWS).[2] DENV RdRp: Dengue virus RNA-dependent RNA polymerase.

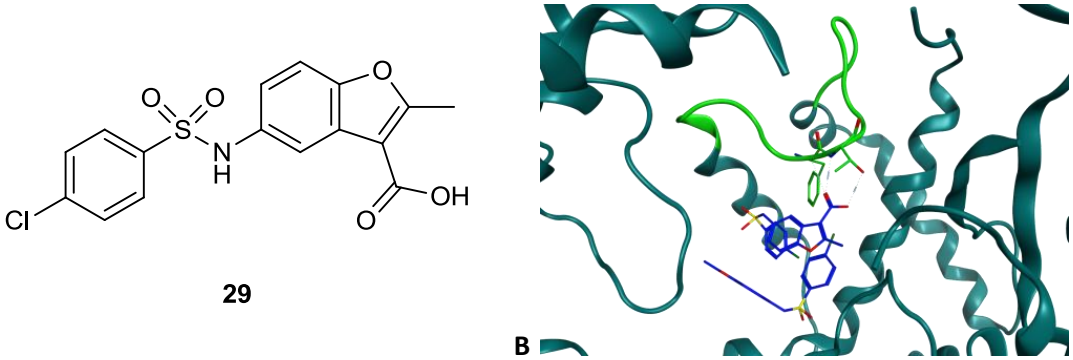

Figure 52. Chemical structure of the allosteric inhibitor **29** reported by NITD (**A**) and view of the dimer of compound **29** from the back of the RdRp (**B**). Compound **29** is shown as sticks in blue and loop **L1** as ribbon in light green, with the residues involved in the interaction (Phe412 and Thr413) with the inhibitor displayed as green sticks (Protein Data Bank code 3VWS).[2] RdRp: RNA-dependent RNA polymerase.

MD simulation studies also suggested that the flexibility of the priming loop **P** is important for the activity of the polymerase as well. Figure 53 shows the models of the DENV RdRp in the different phases of the RNA synthesis. The priming loop **P** moved from its initial position pointing inwards in the *apo* DENV RdRp (**A**) to an open conformation as the polymerase initiates the RNA synthesis (**B**) and elongates the dsRNA (**C**), allowing for its egress from the front of the polymerase. Additionally, the interaction between the priming loop **P** and the growing strand observed in this study confirmed the role of Arg792 and Trp795 of providing the priming platform for the initiating NTP, as it was previously suggested by various authors.[1, 20]

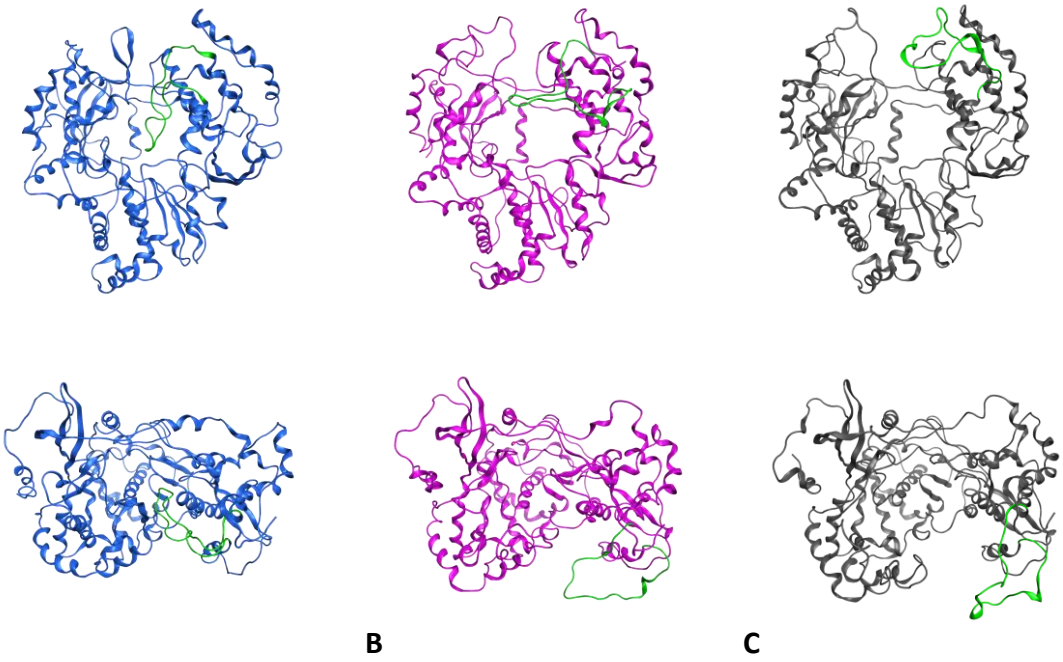

Figure 53. Front view and top view of the models of the DENV RdRp in the pre-initiation (**A**), initiation (**B**) and elongation (**C**) phase of the RNA synthesis. The priming loop **P** is shown as green ribbon. DENV RdRp: Dengue virus RNA-dependent RNA polymerase.

The results of the set of MD simulations provided useful information on the conformation of the DENV RdRp during the elongation phase of the synthesis of the RNA and may have important implications in the design of novel inhibitors of the viral polymerase. Similarly to NITD107, which targets the loop shaping the tunnel for the RNA template (loop **L1**), a potential allosteric inhibitor could interact with key residues of the priming loop, such as Arg792 and Trp795, and may act by blocking the conformational changes of the priming loop **P**, whose flexibility is essential for the viral replication.

At the time of this studies, no allosteric inhibitors targeting the priming loop **P** of the DENV RdRp were reported. Very recently, two indipendent studies resulted in the identification of novel NNIs of DENV RdRp interacting with residues of the priming loop **P**. The lead compound **30** shown in figure 54 was selected by Tarantino *et al.*[21] The crystal structure of DENV RdRp in complex with the allosteric inhibitor revealed that the molecule interacts with residues of loop **L1**, as it was previously observed for compound **29**. Additionally, unlike any other known NNIs, compound **30** further extends towards the priming loop **P**, with an aromatic ring stacking against Trp795 (figure 54, **B**, Protein Data Bank code 5IQ6).[21]

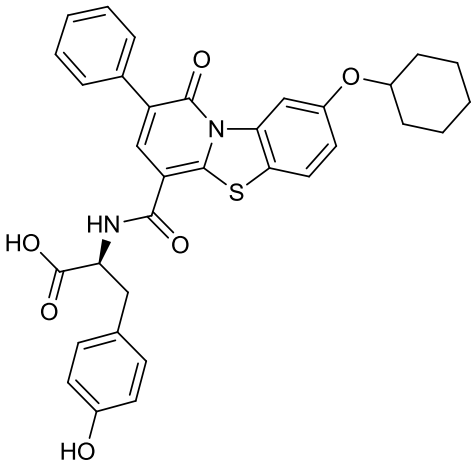

A 30

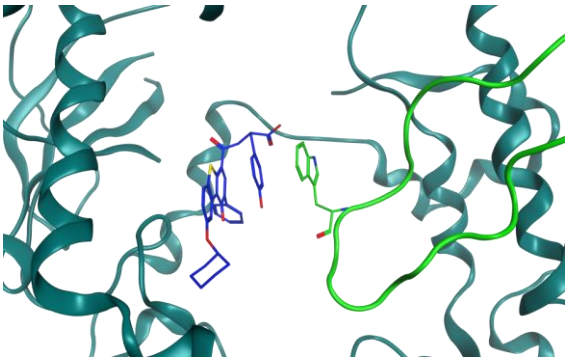

B

Figure 54. Chemical structure of the allosteric inhibitor **30** reported by Tarantino *et al.* (**A**) and view of the molecule from the front of the RdRp (**B**).[21] Compound **30** is displayed as sticks in blue and the priming loop **P** as ribbon in light green (Protein Data Bank code 5IQ6).[21]

RdRp: RNA-dependent RNA polymerase.

A second allosteric inhibitor (**31**, figure 55) was designed by Yokokawa *et al.*[22] and occupies a pocket between the priming loop **P** and the thumb subdomain, as observed in the crystal structure of the DENV RdRp in complex with the molecule. In particular, compound **31** establishes a hydrogen bond interaction with the backbone of Trp795 (figure 55, **B**, Protein Data Bank code 5I3P).[23]

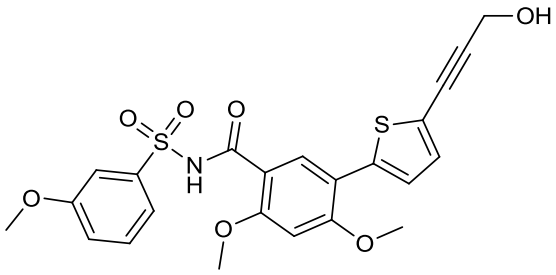

A 31

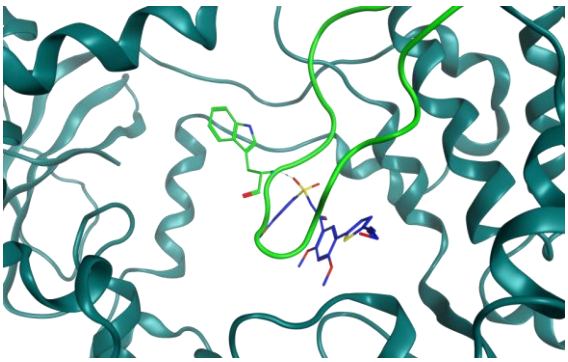

B

Figure 55. Chemical structure of the allosteric inhibitor **31** reported by Yokokawa *et al.* (**A**)[22] and view of the molecule from the front of the RdRp (**B**).[23] Compound **31** is displayed as sticks in blue and the priming loop **P** as ribbon in light green (Protein Data Bank code 5I3P).[23]

RdRp: RNA-dependent RNA polymerase.

As highlighted by the MD simulation studies which were described in this section, Trp795 in the priming loop **P** is a key residue for the recognition of the initiating NTP. The recently reported crystal structures showed two different allosteric inhibitors interacting with the priming loop **P**, specifically with Trp795, and confirmed the essential role of the priming loop **P** in the activity of the polymerase.[21, 22] The NNIs adopted a different orientation in respect of the priming loop **P**, suggesting that two nearby pockets may be exploited for the inhibition of the DENV RdRp. Nevertheless, both allosteric inhibitors identified by Tarantino *et al.*[21] and Yokokawa *et al.*[22] may act by stabilising the DENV RdRp in a 'closed' conformation, thus preventing the conformational changes required for the synthesis of the viral genome.

In conclusion, the priming loop **P** was demonstrated to play an essential role in the viral replication. Therefore, targeting Trp795, Arg792 or other residues of the priming loop **P** may represent a novel strategy for the development of an effective agent against DENV.

2.2 SYNTHESIS OF NUCLEOSIDE AND NUCLEOTIDE ANALOGUES

The following sections describe the synthesis of ribose-modified and nucleobase-modified nucleoside analogues as potential anti-DENV agents and the application of the phosphoramidate ProTide technology.

Nucleosides investigated in this work are adenine-based, as the majority of known DENV RdRp inhibitors.[9, 10, 11, 12, 13, 14, 15] The most promising structurally modified analogues were identified by performing molecular modelling studies (see section 2.1.2 for details). Specifically, three families of adenosine analogues were selected: i) ribose-modified, ii) benzo-fused 7-deaza, and iii) acyclic adenosine analogues, and are illustrated in figure 56.

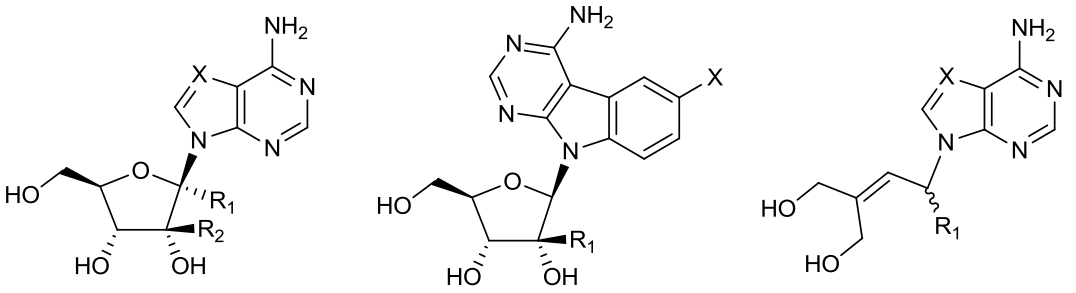

Figure 56. General structures of the families of adenosine analogues whose syntheses were investigated in this work.

In this work, the general strategy for the synthesis of nucleosides was a convergent method that offered the advantage of affording a variety of nucleosides by combining modified glycosylating agents, or linear aliphatic moieties in the case of acyclic adenosine analogues, to different nucleobases.

As described in paragraph 1.2.2.1, the phosphoramidate ProTide approach represents a convenient method for delivering the nucleotide monophosphate intracellularly as it bypasses the rate limiting first phosphorylation step.[24, 25, 26]

To date, only one nucleotide prodrug has been described in the literature as an anti-DENV agent.[27] Therefore, the field is still largely unexplored. In order to investigate the effect of the monophosphate prodrug on the antiviral activity and on the toxicity, often a major limitation associated with nucleoside inhibitors, of the parent nucleosides, the ProTide technique was applied to the commercially available reference compound 2'-*C*-methyladenosine and to the synthesised nucleosides.

The 5'-*O*-phosphoramidate derivatives are conventionally prepared by phosphorochloridate chemistry, according to procedures adapted from Van Boom *et al*.[28] and Uchiyama *et al*.[29] and optimised by the McGuigan research group.[30] The synthesis involves the coupling reaction between the parent nucleoside and an aryl amino acid phosphorochloridate, in the presence of a base (scheme 2).[30] The aryl amino acid phosphorochloridate is synthesised by reaction of an amino acid ester salt with an aryl phosphorodichloridate in the presence of Et_3N.[30]

Two different strategies for the synthesis of ProTides were developed.[30] In the first method, *t*BuMgCl is used as a base in the coupling reaction to remove the proton from the 5'-hydroxyl group. The method is generally associated with relatively good yields and prevents the reaction to occur at the heterocyclic amine;[30] however, it lacks selectivity towards primary hydroxyl groups in the nucleoside. As a consequence, the reaction of the phosphorochloridate with the nucleoside may afford the desired 5'-*O*-phosphoramidate together with the 3'-*O*-phosphoramidate and the bis-3',5'-*O*,*O*-phosphoramidates, depending on the nature of the nucleoside and the number of reagent equivalents used for the preparation.[30] In the second method, *N*-methylimidazole is used in place of the Grignard reagent *t*BuMgCl. This approach allows for the selective reaction of the phosphorochloridate at the 5'-hydroxyl group of the nucleoside. Therefore it is commonly applied in the case of parent nucleosides having two or more hydroxyl groups, and avoids additional steps of selective protection of reactive functionalities and their deprotection.[30]

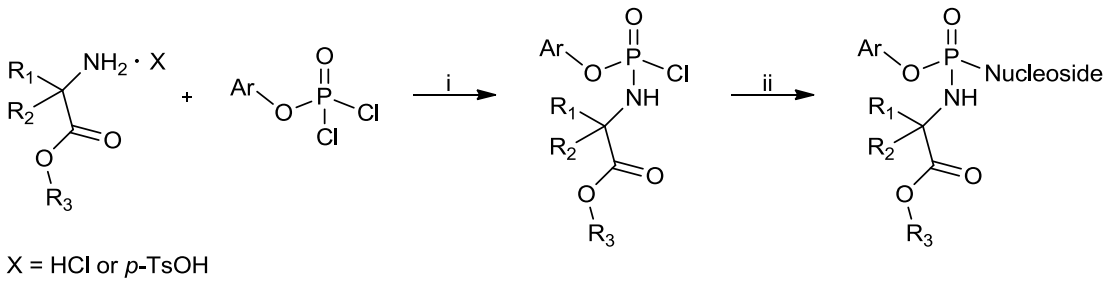

Scheme 2. Conventional synthesis of ProTides.[30] *Reagents and conditions:* i) Et_3N, DCM, -78 °C to rt, 2-4h; ii) Nucleoside, *t*BuMgCl or NMI, THF, rt, 16-20h.

Recently, a modified method was reported which is based on the use of the Grignard reagent *t*BuMgCl and alternative phosphoramidating reagents, such as pentafluorophenolate or *p*-nitrophenolate derivatives (scheme 3).

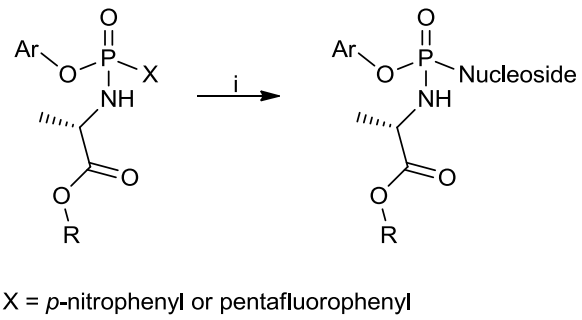

X = *p*-nitrophenyl or pentafluorophenyl

Scheme 3. Alternative synthesis of ProTides.[31] *Reagents and conditions:* i) Nucleoside, *t*BuMgCl, THF, rt, 18h.

The substitution of the chlorine with these different leaving groups in the reagents increases their stability compared to the conventionally employed phosphorochloridate, while maintaining sufficient reactivity in the coupling reaction with the nucleoside.[31] The ease of preparation and stability of the *p*-nitrophenolate reagents made this optimised method the first choice for the synthesis of specific ProTides of nucleoside analogues in this work.

Regardless of the specific method employed for the preparation of ProTides, the final compounds are obtained as mixtures of two diastereoisomers, due to the chiral centre at the phosphorus.[30] The phosphoramidate ProTides prepared in this work were evaluated for their antiviral activity as diastereoisomeric mixtures.

2.2.1 SYNTHESIS OF PHOSPHORAMIDATING REAGENTS

Various aryl phosphorodichloridate and amino acid ester salts can be synthesised and coupled in combinations, to obtain a series of different phosphoramidates of the parent nucleoside. In this work, the phosphorochloridates **35** and **36** were prepared from commercially available starting materials, phenyl phosphorodichloridate **34** and the corresponding L-alanine benzyl and isopropyl ester salts **32** and **33**, respectively (scheme 4). The mixture was treated with Et_3N in DCM under anhydrous conditions at low temperature (-78 °C).[30, 32] After 1 hour, the mixture was allowed to reach room temperature and allowed to react until full conversion. The disappearance of the phosphorodichloridate **34** was monitored by ^{31}P NMR (a singlet at δ 3.99 ppm). The phosphorochloridate **35** was quickly purified by column chromatography whereas the isopropyl analogue **36** could be isolated by trituration in anhydrous Et_2O. Both phosphorochloridates were obtained as mixtures of diastereoisomers in an even ratio, as confirmed by the presence of two peaks in the ^{31}P NMR.

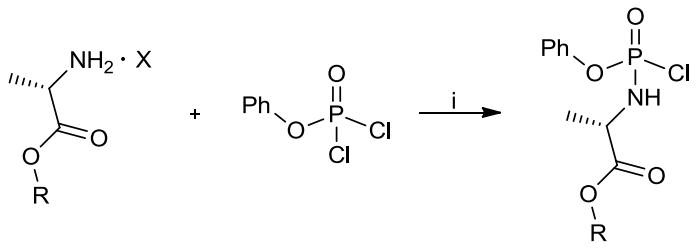

32 X = *p*-TsOH and R = Bn
33 X = HCl and R = *i*Pr

34

35 R = Bn
36 R = *i*Pr

Scheme 4. Synthesis of the phosphorochloridates **35** and **36**. *Reagents and conditions:* i) Et_3N, DCM, -78 °C to rt, 3h (**35**, 94% yield; **36**, 95% yield).

Additionally, the *p*-nitrophenolate phosphoramidating reagents were employed in this work as alternative to the conventionally used phosphorochloridates. The benzyl and isopropyl derivatives **37** and **38** were synthesised from the previously prepared phosphorochloridates **35** and **36**, respectively, by treatment with 4-nitrophenol and Et_3N in DCM under anhydrous conditions at -78 °C (scheme 5).

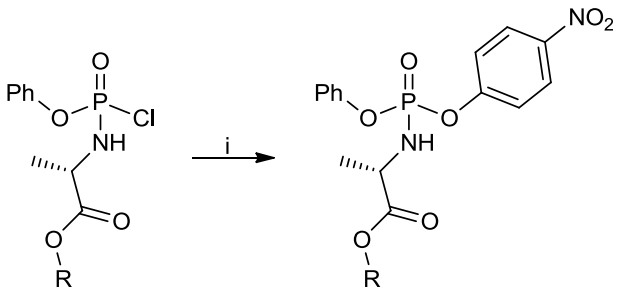

35 R = Bn
36 R = *i*Pr

37 R = Bn
38 R = *i*Pr

Scheme 5. Synthesis of the *p*-nitrophenolate phosporamidating reagents **37** and **38** from the phosphorochloridates **35** and **36**. *Reagents and conditions:* i) 4-nitrophenol, Et_3N, DCM, -78 °C to -40 °C, 2h (**37**, 73% yield; **38**, 63% yield).

A second method for the synthesis of the *p*-nitrophenolate reagents **37** and **38** employs commercially available starting materials (scheme 6).[31] Treatment of 4-nitrophenyldichloro phosphate **39** with phenol in the presence of Et_3N in DCM under anhydrous conditions at -78 °C, followed by the addition of the chosen L-Alanine ester salt **32** or **33**, afforded the desired phosphoramidating reagents in excellent yields. Compounds **37** and **38** were purified by column chromatography and isolated from undesired side-products of the reaction. Indeed, the bis-phenolate and bis-L-Alanine ester *p*-nitrophenolate phosphates were obtained in 2-3% yield and 2% yield, respectively.

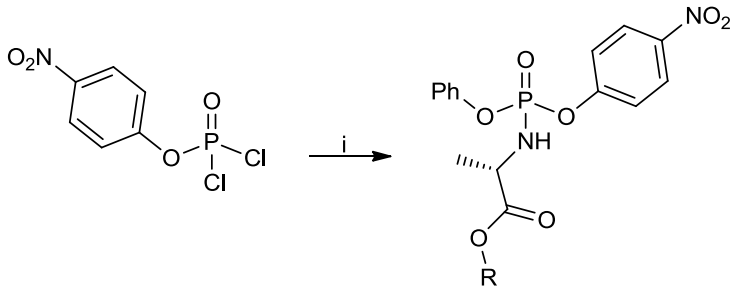

39

37 R = Bn
38 R = *i*Pr

Scheme 6. Synthesis of the *p*-nitrophenolate phosporamidating reagents **37** and **38** from commercially available starting materials. *Reagents and conditions:* i) phenol, Et_3N, DCM, -78 °C, 1h, then **32** or **33**, Et_3N, DCM, -50 °C to 0 °C, 3h (**37**, 90% yield; **38**, 86% yield).

For the synthesis of ProTides from the prepared phosphoramidating reagents, refer to the sections describing the synthesis of the relative parent nucleoside (2.2.2, 2.2.3 and 2.2.4).

2.2.2 SYNTHESIS OF RIBOSE-MODIFIED ADENOSINE ANALOGUES

This family of nucleosides included ribose-modified adenosine and 7-deazaadenosine analogues. The modification of the ribose ring was the introduction of a carbon group, such as the methyl group, at the 2'-position or at the anomeric position. The 2'-*C*-substitution is a common structural feature among antiviral agents[9, 33] and some 2'-*C*-methyl and 2'-*C*-acetylene modified adenosine analogues have been reported for their anti-DENV activity.[9, 10, 11, 12] In contrast, examples of 1'-*C*-substituted nucleoside analogues are scarce in the literature as the introduction of a carbon substitutent at the anomeric position is synthetically challenging.[34, 35, 36, 37, 38] Nevertheless, this modification characterises a novel class of 2-aminoadenosine analogues showing anti-DENV activity *in vitro.*[13] Refer to paragraph 1.2.2.2 and table 20 in the APPENDIX for details on the biological properties of these compounds.

In this work, the ribose-modification was combined with the replacement of the *N*-7 with a methine group (7-deaza modification) at the level of the nucleobase. The binding affinity of the nucleosides within the family was predicted using molecular docking methodologies, as described in paragraph 2.1.2.1. Figure 57 shows the structure of the ribose-modified adenosine analogues **40** and **41**, whose synthesis is described in this section.

Finally, the phosphoramidate ProTide approach was applied to explore the possibility of enhancing the anti-DENV activity as well as decreasing the toxicity of nucleoside analogues.

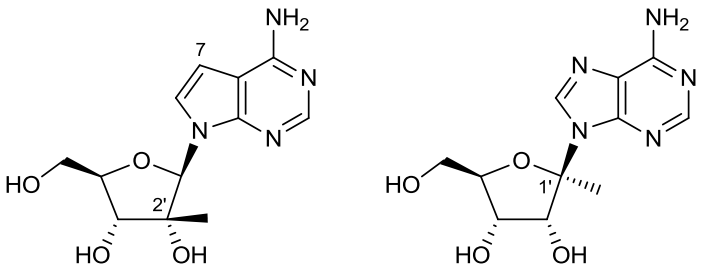

40 **41**

Figure 57. Structures of **40** and **41** as examples of ribose-modified nucleosides.

2.2.2.1 Synthesis of 2'-*C*-modified 7-deazaadenosine analogues

For the synthesis of 2'-*C*-modified nucleosides, both linear[39] and convergent[40, 41, 42] approaches have been reported. As already mentioned, the convergent method was adopted in this work as it is more flexible and allows for the introduction of the carbon substituent in a stereoselective

fashion, driven by the configuration of other functionalities in the ribose ring. An appropriate glycosylating agent is prepared first and can be coupled to different synthesised or commercially available heterobases, such as 6-chloropurine and 6-chloro-7-deazapurine.

In order to introduce a carbon group by treatment with an organolithium reagent or an organomagnesium reagent, a ketone group in the 2-position of the sugar intermediate needs to be present. Furthermore, the addition reaction should give the 2-β-*C*-substituted ribose as the exclusive or major product. The stereochemistry of other substituents in the glycosylating agent plays a crucial role in the stereoselectivity of the addition, in particular the presence of a methoxy group in the 1-α-position allows for the stereoselective addition of the alkyl group in the 2-β-position.[40, 41] The keto-compound 3,5-*O*-(tetraisopropyldisiloxane-1,3-diyl)-1-*O*-methyl-α-D-ribofuran-2-ulose **45** was identified as a potential sugar intermediate. The attempted synthetic route is shown in scheme 7.

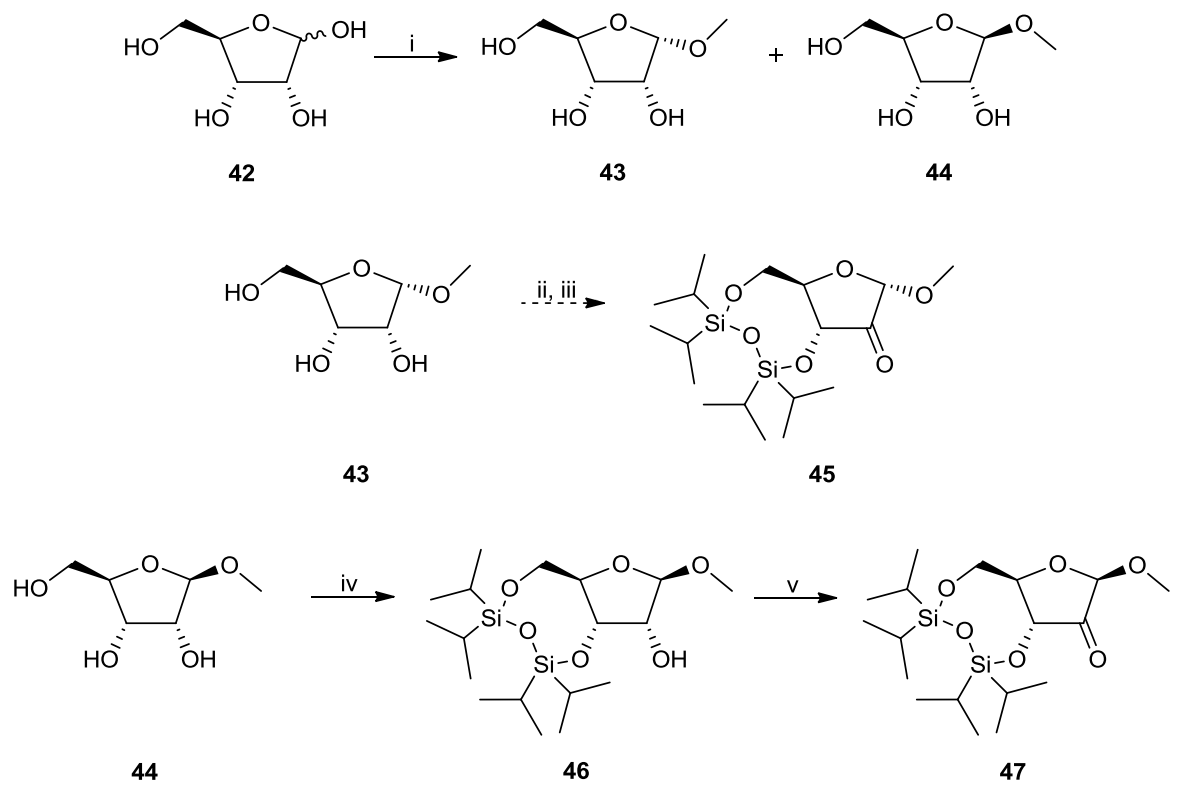

Scheme 7. Synthetic route towards keto-sugar intermediates (**45** and **47**). *Reagents and conditions:* i) H_2SO_4, CH_3OH, rt, 24h (α-anomer **43**, 10% yield and β-anomer **44**, 64% yield); ii) $TIPDSCl_2$, pyridine; iii) oxidation; iv) $TIPDSCl_2$, pyridine, 0 °C to rt, 1h (**46**, 67% yield); v) oxidation (see text for details).

Treatment of the inexpensive starting material D-ribose **42** with methanol in the presence of concentrated sulfuric acid[43] afforded 1-*O*-methyl-D-ribofuranose as a separable anomeric mixture with excellent yield. The configuration of the anomeric position was confirmed by comparison of experimental NMR spectroscopy data to the literature:[44] in the ^{1}H NMR spectra, the anomeric proton appears as a singlet at δ 4.63 ppm in the β-anomer **44** and as a doublet at δ 4.71 ppm with a coupling constant of 2.2 Hz in the α-anomer **43**; also in the ^{13}C NMR spectra the signals of the anomeric carbon differ substantially (δ 108.0 ppm for the β-anomer **44**, δ 104.8 ppm for the α-anomer **43**). However, the desired α-anomer **43** was only a minor product (ratio α:β was 1:6.5) and could not be separated from unreacted starting material. As compound **43** could not be isolated, the feasibility of the following steps were verified using the purified β-anomer **44** (scheme 7). Before performing the oxidation of the 2-hydroxyl group to the ketone, it is necessary to protect the 3 and 5-hydroxyl groups using a protecting group that would be stable in the presence of Grignard reagents. 1,1,3,3-Tetraisopropyldisiloxane seemed an advantageous protecting group as it allowed for the selective protection of 3 and 5-positions of the 1-*O*-substituted ribose, whereas the 2-hydroxyl group remained available for the following oxidation. Compound **44** was treated with 1,3-dichloro-1,1,3,3-tetraisopropyldisiloxane in anhydrous pyridine for 4 hours at room temperature.[45] Protected product **46** was obtained in moderate yield (30%) after purification by column chromatography. When the reaction time was prolonged to 16 hours,[46] several side-products were obtained and **46** could not be isolated after column chromatography. Finally, treatment with the disiloxane reagent over 1 hour at room temperature[44] provided **46** in good yield (67%) and the formation of side-products was not observed.

The oxidation of the secondary alcohol of the TIPDS-protected sugar **46** was attempted using pyridinium chlorochromate (PCC, Corey-Suggs reagent).[47] Scheme 8 shows the mechanism of oxidation. The reaction occurs via an intermediate chromate ester that undergoes elimination to afford the carbon-oxygen double bond. Compound **46** was treated with PCC in DCM at room temperature for 24 hours. In a second attempt, the reaction with PCC was carried out in refluxing DCM for 16 hours. Reactions were monitored by mass spectrometry, however no conversion of the 2-hydroxyl group was observed.

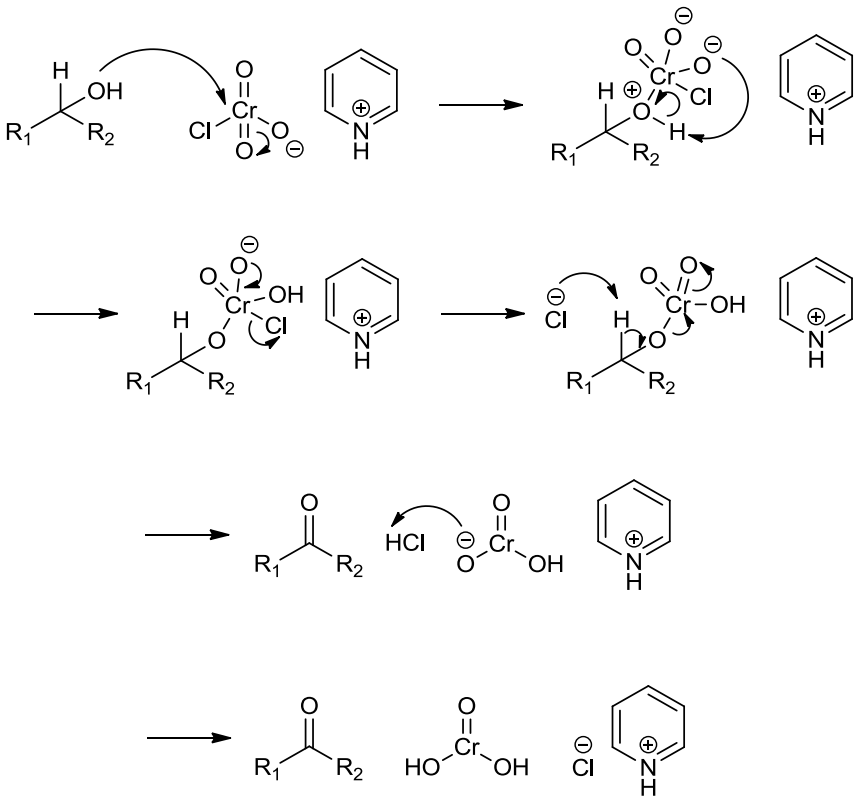

Scheme 8. Mechanism of Corey-Suggs oxidation.

In the Pfitzner-Moffatt oxidation, primary and secondary alcohols are oxidised by dimethyl sulfoxide activated by dicyclohexylcarbodiimide (DCC) in acidic conditions, as shown in scheme 9. Despite the sensitivity of the silyl ether to acidic conditions, the method has been used for the conversion of 3,5-*O*-(tetraisopropyldisiloxane-1,3-diyl)-1-*O*-methyl-α-D-ribofuranose to the corresponding ketone compound.[48] However, treatment of compound **46** with DCC in anhydrous DMSO and diethyl ether in acidic conditions gave an inseparable mixture of the desired ketone compound **47** and a second 2-ketosugar (20% overall yield, ratio 1:1). In fact, the absence of singlets at approximately δ 3.00 ppm for the 2-OH in the ^{1}H NMR spectrum of the mixture demonstrated that the two species were oxidised at the 2-position. The side-product differs by the presence of a singlet at δ 4.39 ppm for the 5'-OH or 3'-OH, suggesting that its formation was due to the partial hydrolysis of the acid-labile protecting group from one hydroxyl group. The identity of products was further confirmed by mass spectrometry (*m/z* 427.2 [MNa^{+}] and 445.2 [MNa^{+}] observed for compound **47** and for the side-product, respectively).

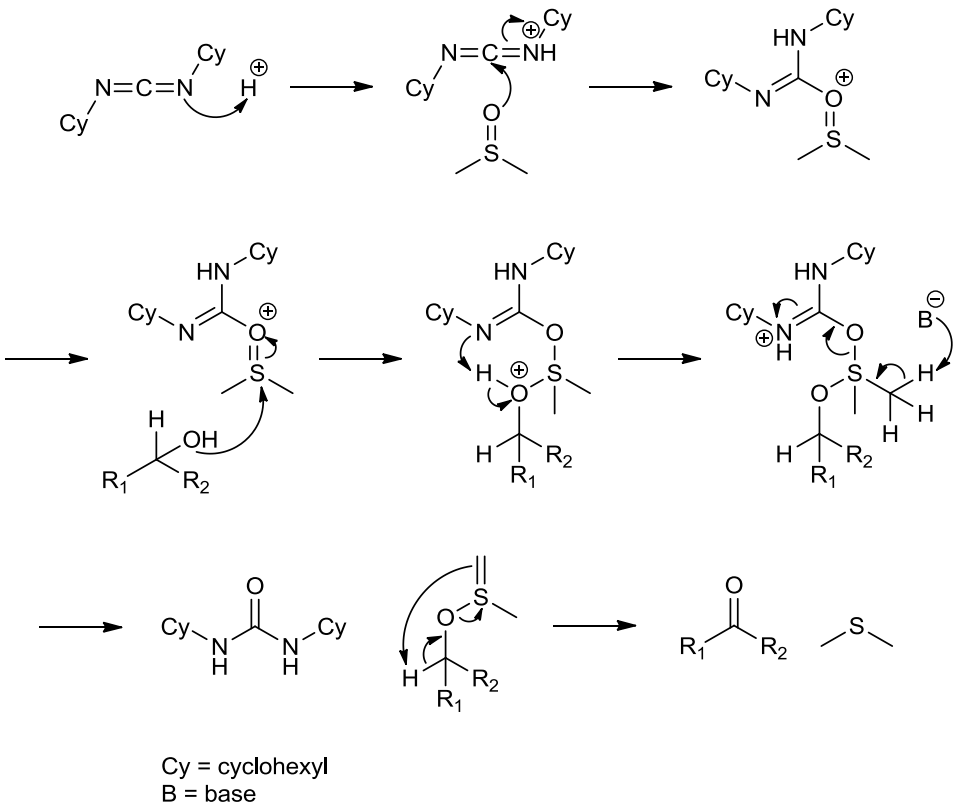

Scheme 9. Mechanism of Pfitzner-Moffatt oxidation.

Finally, the broadly used oxidising agent Dess-Martin periodinane (DMP) was employed. Although the Dess-Martin reagent offers mild oxidation of primary and secondary alcohols to aldehyde and ketone respectively, acetic acid is a by-product of the reaction (scheme 10). As a consequence, oxidation of the 2-hydroxyl group of compound **46** using DMP in DCM for 24 hours at room temperature[49] was associated with partial hydrolysis of the silyl ether due to the inherent acidic conditions, as observed in the Pfitzner-Moffatt oxidation, and an inseparable mixture of desired product and side-product was obtained (30% overall yield, ratio 2:1). When compound **46** was treated with DMP at 0 °C for 2 hours, no conversion occurred and the TIPDS-protected starting material **46** was recovered. In an attempt to isolate the desired product only, the reaction was quenched after 8 hours at room temperature. However, ^{1}H NMR spectroscopy of the crude residue showed the presence of three species corresponding to the unreacted starting material **46**, the desired product **47** and a second 2-ketosugar (ratio 1:2:0.7). The side-product was obtained due to the cleavage of TIPDS-protecting group from one hydroxyl group, as previously observed in the Pfitzner-Moffatt oxidation.

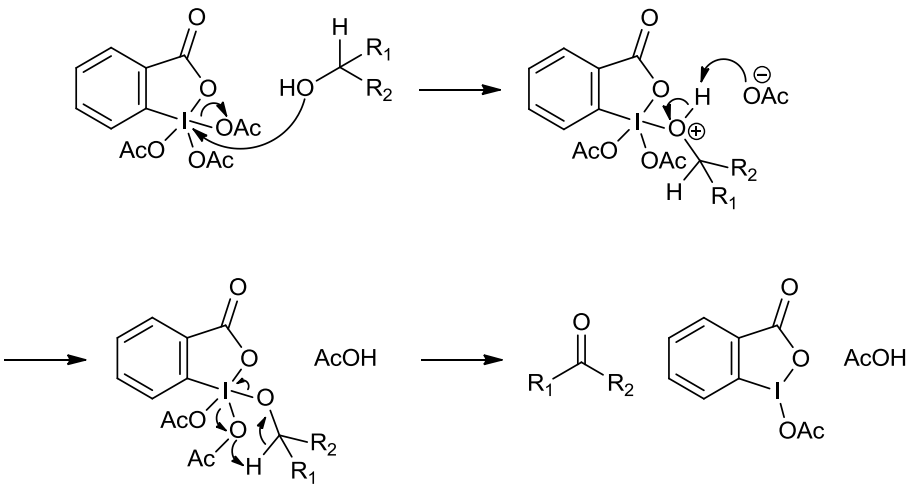

Scheme 10. Mechanism of Dess-Martin periodinane oxidation.

The attempts described above demonstrated that the 1,1,3,3-tetraisopropyldisiloxane was not a suitable protecting group in this work as compound 3,5-*O*-(tetraisopropyldisiloxane-1,3-diyl)-1-*O*-methyl-β-D-ribofuran-2-ulose **47** could not be isolated.

Protection of the 3' and 5'-hydroxyl groups as 2,4-dichlorobenzyl ethers was found to be a valid alternative and the 2-ketone sugar intermediate 3,5-bis-*O*-(2,4-dichlorobenzyl)-1-*O*-methyl-α-D-ribofuran-2-ulose **49** was easily obtained by treatment of commercially available 1-*O*-methyl-3,5-bis-*O*-(2,4-dichlorobenzyl)-α-D-ribofuranose **48** with DMP in DCM at room temperature (scheme 11).[42] The reaction was monitored by thin layer chromatography, which showed full conversion of the starting material after 72 hours. The following introduction of the methyl group in the 2-position was carried out using either methyllithium or methylmagnesium bromide. Reaction of the keto-sugar with organolithium reagent (3 equivalents) in Et_2O at -78 °C to room temperature for 4 hours did not show a clean profile on thin layer chromatography and the 2-*C*-methyl derivative could not be isolated after column chromatography. Treatment with Grignard reagent (4 equivalents) in Et_2O at -55 °C to room temperature for 7 hours[42] furnished **50** in 22% yield. As expected, the 1-*O*-methyl substituent in the α-position of the ribofuranose ring contributed to the stereochemistry of the addition, so that the 2-β-*C*-methyl derivative was the only product. In another attempt, two additions of methylmagnesium bromide were performed and the work-up procedure was changed from a filtration through celite pad to an extraction with Et_2O. Although the ratio between the desired product and unreacted starting material did not vary, the yield of compound **50** increased to 54% thanks to the more appropriate work-up procedure.

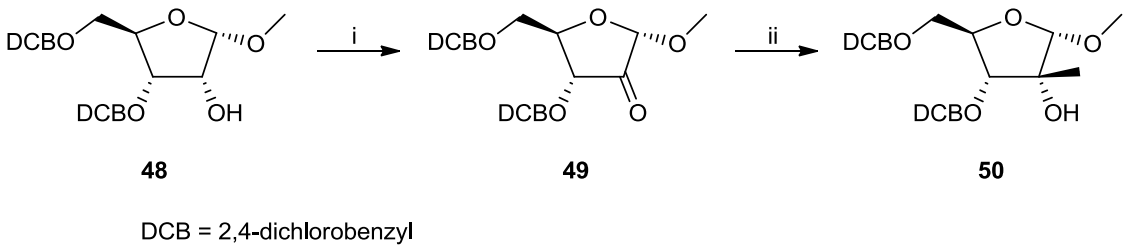

48 **49** **50**

DCB = 2,4-dichlorobenzyl

Scheme 11. Synthesis of the 2'-*C*-methyl glycosylating agents **50**. *Reagents and conditions:* i) DMP, DCM, 0 °C to rt, 72h (**49**, 90% yield); ii) CH_3MgBr, Et_2O, -78 °C to 0 °C, 7h (**50**, 54% yield).

The application of the Vorbrüggen procedure is generally effective for the glycosylation of 7-*N* purines.[41, 50] In contrast, the coupling reaction of the glycosylating agent to 7-deaza purine analogues requires the generation of the nucleobase anion *in situ*.[42, 51]

The ribofuranose **50** was converted to the corresponding 1-bromo derivative by treatment with hydrogen bromide/acetic acid in dichloromethane and reacted with an excess of the sodium salt of commercially available 6-chloro-7-deazapurine, which was formed *in situ* by reaction with sodium hydride.[42] The coupling step was initially performed over 1 day at room temperature and furnished the β-nucleoside **51** with 10% yield. A slightly greater yield (20%) was obtained by prolonging the reaction time to 60 hours (scheme 12). An optimisation of the glycosylation was achieved by adding the reactive 1-bromo intermediate directly to a mixture of 6-chloro-7-deazapurine, potassium hydroxide and tris[2-(2-methoxyethoxy)ethyl]amine. These conditions are reported to yield stereospecifically the β-anomer[51] and allowed for the isolation of the desired compound **51** with an yield of approximately 40%. NMR spectra were in agreement with the literature and the anomeric identity was further confirmed by a 2D NOESY experiment showing correlation peaks between H-1' and H-4' as well as between H-3' and H-8.

The following deprotection was attempted by treatment of **51** with boron trichloride in DCM at low temperature.[42] However, degradation occurred and **52** was not obtained (scheme 12).

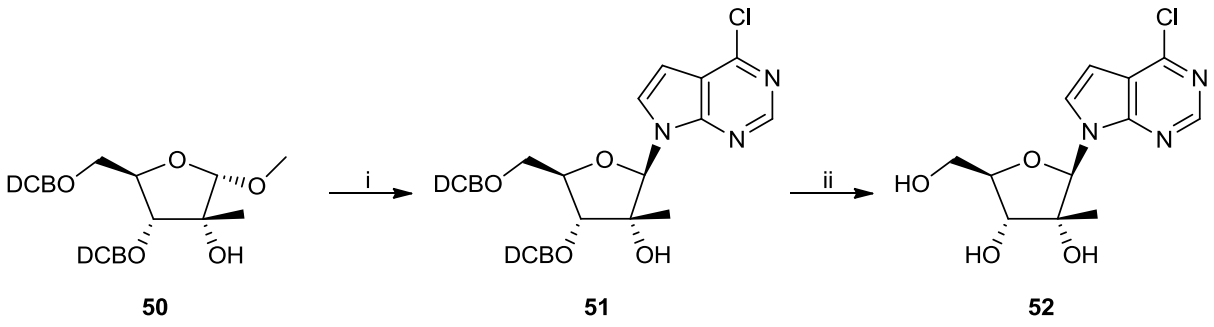

DCB = 2,4-dichlorobenzyl

Scheme 12. Glycosylation of 6-chloro-7-deazapurine. *Reagents and conditions:* i) Procedure *a*: HBr/acetic acid, DCM, 0 °C to rt, 4h, then sodium salt of 6-chloro-7-deazapurine, CH_3CN, rt, 60h (**51**, 20% yield); Procedure *b*: HBr/acetic acid, DCM, 0 °C to rt, 2h, then 6-chloro-7-deazapurine, KOH, TDA-1, CH_3CN, rt, 1h (**51**, 39% yield); ii) BCl_3, DCM, -78 °C to -20 °C, 3h, degradation.

The BCl_3-assisted cleavage of the 2,4-dichlorobenzyl ethers was attempted at an early stage of the synthetic route. However, the deprotection of the 2,4-dichlorobenzyl ethers of the glycosylating agent **50** (scheme 13) led to the degradation of the starting material.

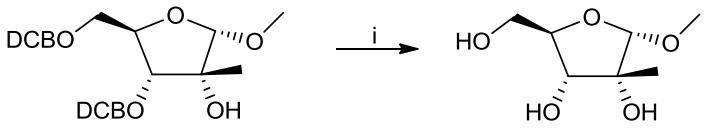

DCB = 2,4-dichlorobenzyl

Scheme 13. Attempt of deprotection of the glycosylating agent **50**. *Reagents and conditions:* i) BCl_3, DCM, -78 °C to -30 °C, 4h, degradation.

Alternatively, treatment of the β-nucleoside **51** with commercially available methanolic solution of ammonia (7M) over 48 hours at 85 °C afforded the protected 7-deazaadenosine derivative **54** in excellent yield (scheme 14) as well as the 6-*O*-methylinosine derivative **55** as a minor product of the reaction (figure 58).

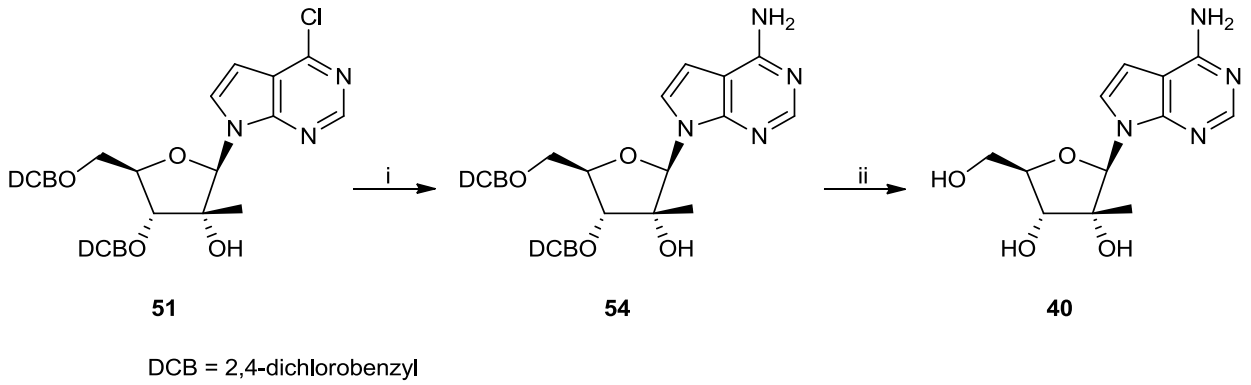

Scheme 14. Amination and deprotection of the target nucleoside 2'-*C*-methyl-7-deazaadenosine **56**. *Reagents and conditions:* i) NH_3, MeOH, 85 °C, 72h (**54**, 87% yield); ii) Procedure *a*: H_2, Pd/C, MeOH, AcOH, rt, 48h (**40**, 70% yield); Procedure *b*: $HCOONH_4$, Pd/C, MeOH, reflux, 16h (**40**, 77% yield).

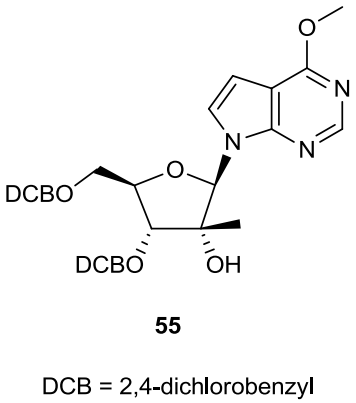

Figure 58. Side-product **55** isolated from the amination of compound **54**.

The following hydrogenolysis of the 2,4-dichlorobenzyl ethers furnished the target nucleoside 2'-*C*-methyl-7-deazaadenosine **40** in good yield. Compound **40** could also be obtained by transfer hydrogenation with ammonium formate in refluxing methanol in the presence of 10% palladium on carbon (scheme 14). ^{1}H and ^{13}C NMR spectra of **40** were in agreement with the literature[42] and confirmed identity and anomeric configuration. Overall, the synthesis of 2'-*C*-methyl-7-deazaadenosine consists of five steps with an overall yield of 6%.

The anti-DENV activity and cytotoxicity *in vitro* of 2'-*C*-methyl-7-deazaadenosine **40** were evaluated by our collaborators (see section 2.3 for details).

2.2.2.2 Synthesis of 2'-*C*-methyladenosine and 7-deazaadenosine ProTides

The nucleoside 2'-*C*-methyladenosine was originally developed as an anti-HCV agent (EC_{50} 0.26 μM), but did not undergo further development due to its poor oral bioavailability.[42] The application of the ProTide strategy to 2'-*C*-methyladenosine and to the 7-deaza analogue aims at reducing the toxicity and boosting the activity of the parent nucleosides.

Without prior protection of the nucleoside, the ProTide bearing the L-alanine benzyl ester as amino acid moiety was synthesised according to the conventionally used procedure using *t*BuMgCl as a base.[30] Treatment of commercially available **56** with the phosphorochloridate **35** (refer to section 2.2.1 for the preparation of **35**) in the presence of *t*BuMgCl afforded the 5'-*O*-phosphoramidate **57** as main product of the coupling reaction (scheme 15). Purification by column chromatography and semi-preparative HPLC were required to remove traces of the parent nucleoside and of the 3'-*O*-phosphoramidate isomer. NMR spectroscopy and analytical HPLC confirmed the identity and purity (94%) of the phosphoramidate, that was obtained as an even mixture of two diastereoisomers in 9% yield.

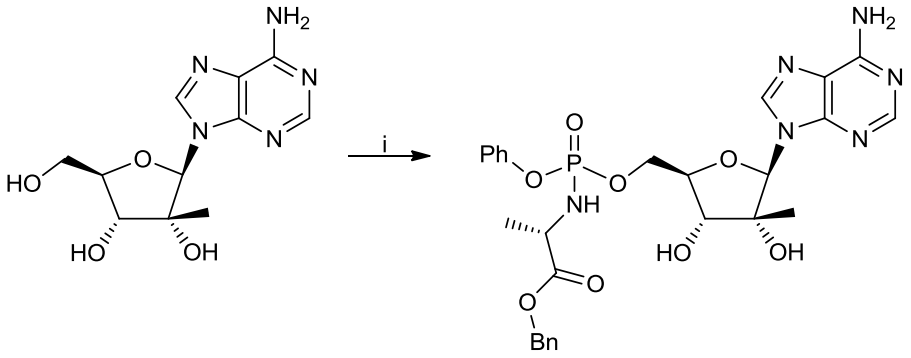

56 **57**

Scheme 15. Synthesis of 2'-*C*-methyladenosine ProTide **57**. *Reagents and conditions:* i) *t*BuMgCl, phosphorochloridate **35**, THF, rt, 72h (**57**, 9% yield).

For the preparation of the ProTide of the previously synthesised 2'-*C*-methyl-7-deazaadenosine **40**, a modified procedure was applied. The coupling to the phosphoramidate moiety bearing the L-alanine isopropyl ester was carried out in DMF as solvent. Additionally, the *p*-nitrophenolate phosphoramidating reagent **38** (refer to section 2.2.1 for the preparation of **38**) was employed in place of the conventional phosphorochloridate (scheme 16). Treatment of **40** with 1 equivalent of **38** in the presence of *t*BuMgCl furnished the 5'-*O*-phosphoramidate **58** as sole product after 4

hours at room temperature. Purification by column chromatography allowed for the isolation of the ProTide **58** in 46% yield with a purity of 99% according to analitycal HPLC.

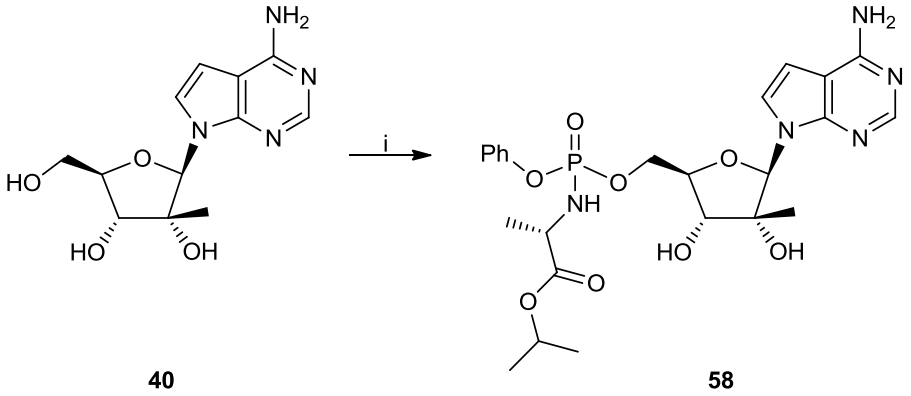

40 **58**

Scheme 16. Synthesis of 2'-*C*-methyl-7-deazaadenosine ProTide **58**. *Reagents and conditions:* i) *t*BuMgCl, *p*-nitrophenolate **38**, DMF, rt, 4h (**58**, 46% yield).

The anti-DENV activity and cytotoxicity *in vitro* of the synthesised 2'-*C*-methyladenosine ProTide **57** and of the parent nucleoside **56** were evaluated by our collaborators (see section 2.3 for details). The prepared 2'-*C*-methyl-7-deazaadenosine ProTide **58** was also sent for biological evaluation and results are currently being awaited.

2.2.2.3 Synthesis of 1'-*C*-modified adenosine analogues

The first synthetic pathway towards 1'-*C*-substituted nucleosides involved photochemical radical reactions, by using high pressure mercury or tungsten lamps, either on the glycosylating agent[34] or on the intact nucleoside.[35] In 2002 Cappellacci *et al.*[37] reported a method for the synthesis of 1'-*C*-methyladenosine based on the chemistry of organolithium compounds (scheme 17). According to the authors, the introduction of the methyl moiety at the anomeric position had been performed on 5-*O*-benzyl-2,3-*O*,*O*-benzylidene-D-ribono-1,4-lactone **59**. Compound **60** had been converted to its acetoxy derivative **61**, then coupled to 6-chloropurine in the presence of ethylaluminum dichloride to furnish the nucleoside as an anomeric mixture **62**. Amination at the 6-position of the purine, separation from the undesired α-anomer and finally deprotection of hydroxyl groups by hydrogenation had afforded the target molecule **41**.

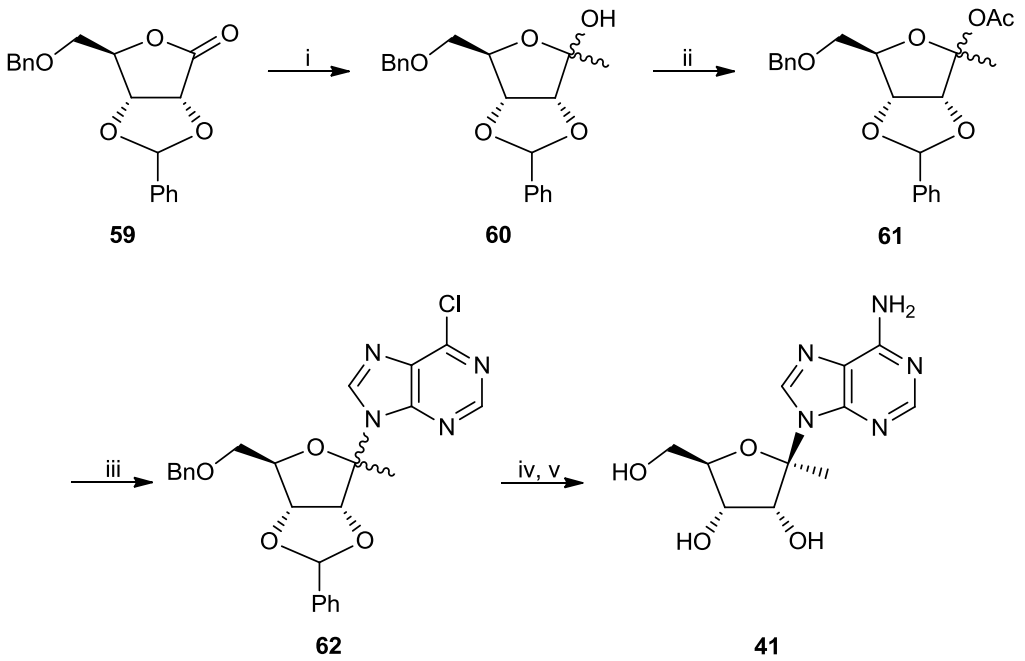

Scheme 17. Reported synthesis of 1'-*C*-methyladenosine **41.**[37] *Reagents and conditions:* i) CH_3Li, Et_2O, -78 °C to rt, 45 min; ii) Ac_2O, 4-(dimethylamino)pyridine, pyridine, rt, 48h; iii) 6-chloropurine, $EtAlCl_2$, CH_3CN, rt, 2h; iv) NH_3, 60 °C, 5h; v) $HCOONH_4$, 10% Pd/C, CH_3OH, reflux.

The protected D-ribono-1,4-lactone **59** used in the synthetic route described above was an attractive sugar intermediate in order to introduce carbon substituents at the anomeric position. Therefore, the synthesis of **59** was attempted, as illustrated in scheme 18.

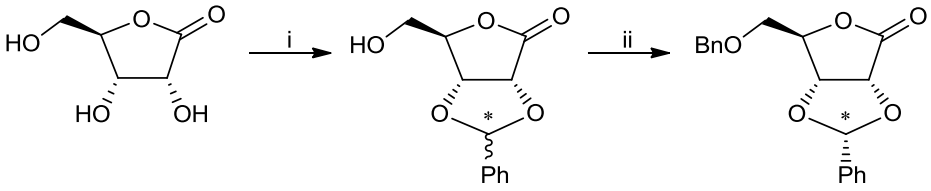

Scheme 18. 2,3-*O*,*O*-Benzylidene and 5-*O*-benzyl ether protection of D-ribonic acid 1,4-lactone **63**. *Reagents and conditions:* i) benzaldehyde dimethyl acetal, $POCl_3$, CH_3CN, 0 °C, 1h (**64** and **65**, 68% yield) or benzaldehyde dimethyl acetal, $SnCl_2$, DME, reflux, 1h (**64** and **65**, 40% yield); ii) benzyl bromide, NaH, THF, 0 °C-rt, 16h (**67**, 20% yield). SE: slow-eluting; FE: fast-eluting.

2,3-*O*,*O*-Benzylidene protection of commercially available D-ribonic acid 1,4-lactone **63** was carried out using phosphorus (V) oxychloride (2 equivalents) and benzaldehyde dimethyl acetal (1 equivalent) in acetonitrile at 0 °C for 1 hour. The benzylidene protection induces the formation of a chiral carbon atom in the product, hence two diastereoisomers were obtained with a ratio between slow-eluting (SE) (*R*)-isomer **64** and fast-eluting (FE) (*S*)-isomer **65** of 3:1, which were separated by column chromatography. NMR spectra of the (*R*)-isomer **64** and (*S*)-isomer **65** were in agreement with the literature.[52] In one previous attempt performed with an excess of benzaldehyde dimethyl acetal (5 equivalents),[53] the free 5-hydroxyl group further reacted with benzaldehyde and methanol, a by-product of the reaction, leading to the formation of side-product **66** as a mixture of four stereoisomers (scheme 19). The identity of side-product **66** was confirmed by mass spectrometry (the observed *m/z* was 379.1 [MNa^+]).

In another attempt, the 2,3-*O*,*O*-benzylidene protected intermediates **64** and **65** were prepared by treatment of **63** with benzaldehyde dimethyl acetal (1.2 equivalents) in the presence of the catalyst tin (II) chloride (0.2 equivalents) in refluxing 1,2-dimethoxyethane for 1 hour.[54] These conditions allowed for the isolation of the product in 40% yield as an even mixture of the two diastereoisomers **64** and **65**. The use of fewer equivalents of the catalyst, as in the reported procedure,[54] led to a poor formation of the desired product whereas the replacement of 1,2-dimethoxyethane with THF did not improve the yield of the mixture of **64** and **65**.

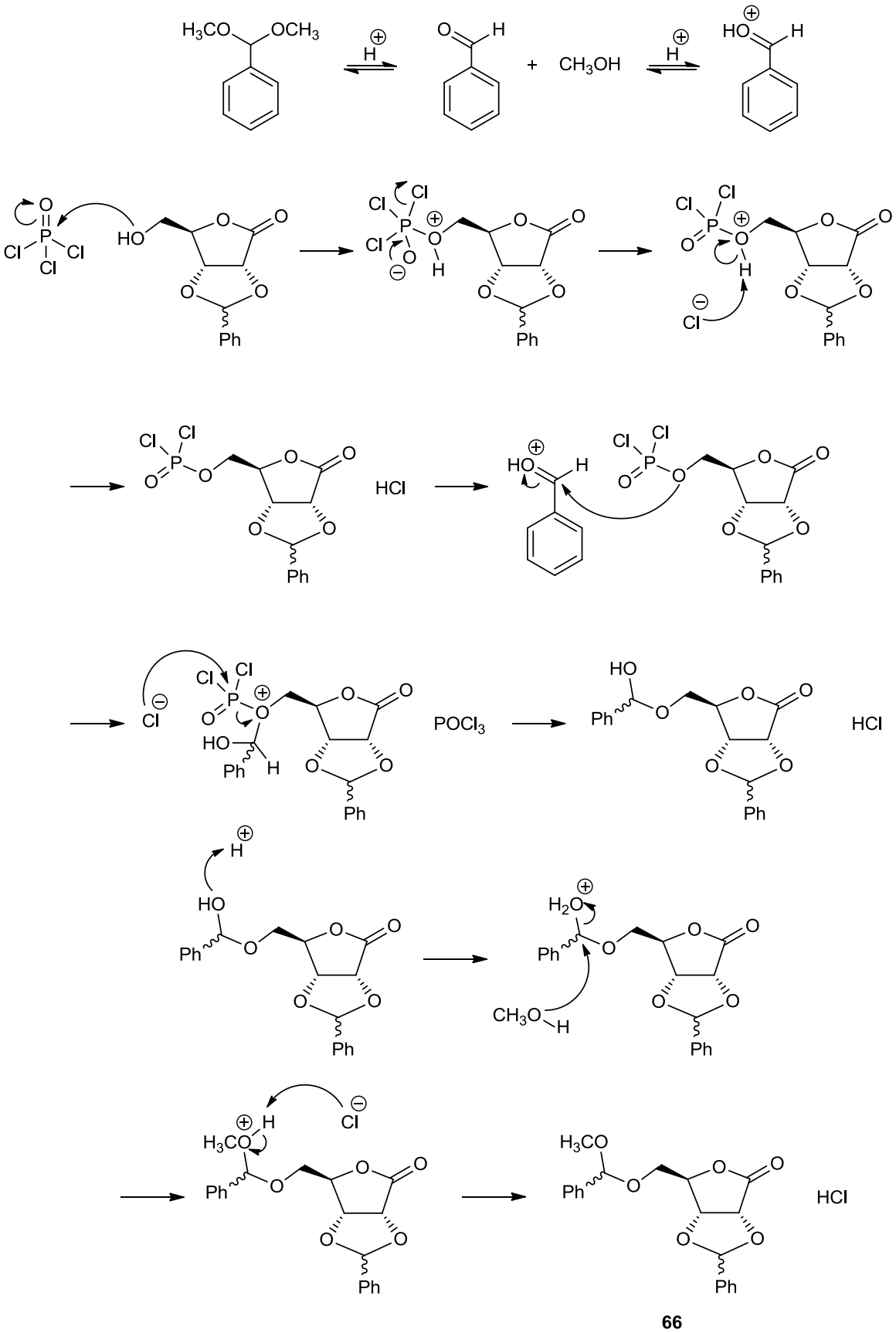

Scheme 19. Mechanism of formation of side-product **66**.

The following protection of the 5-hydroxyl group by benzyl ether was performed by treatment of the (*R*)-isomer **64** with benzyl bromide (1.2 equivalents) in the presence of sodium hydride in anhydrous THF at room temperature for 16 hours (scheme 18).[37] The reaction furnished 5-*O*-benzyl-2,3-*O*,*O*-(*R*)-benzylidene-D-ribofuran-1-ulose **67** in poor yield (20%) as a large amount of the starting material was left unreacted. In an attempt to increase the yield, the reaction was carried out using an excess of benzyl bromide (2 equivalents) in the presence of sodium hydride and catalytic amount of tetrabutylammonium iodide.[54] After 24 hours at room temperature, no significant formation of **67** was observed, hence the reaction mixture was heated to 75 °C for additional 48 hours (monitoring by thin layer chromatography). In another attempt, the (*R*)-isomer **64** was treated with an excess of benzyl bromide (2 equivalents) and sodium hydride at 75 °C for 48 hours. In both cases, the formation of several side-products was observed and, among them, the desired product **67** could be isolated by column chromatography in poor yield (27% and 20% respectively). Further optimisation of the protection of the 5-hydroxyl group was not performed.
The introduction of a carbon group at the anomeric position was attempted by treatment of **67** with an excess of methyl lithium or ethynylmagnesium bromide (scheme 20).

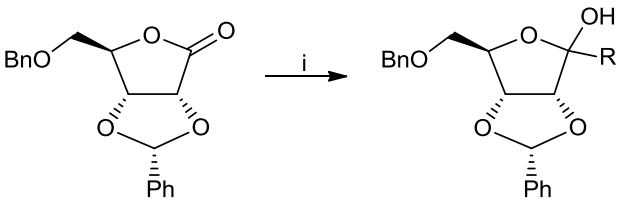

67

68 R = CH_3
69 R = CCH

Scheme 20. Attempts of alkylation at the anomeric position resulted in the formation of side-products, but not of the desired product (see text). *Reagents and conditions:* i) CH_3Li (2.8 eq.), Et_2O, -78 °C to rt, 3h or HCCMgBr (4.0 eq.), THF, -78 °C to rt, 3h.

Both reactions led to the formation of the bis-alkylated side-product **70** and **71**, respectively (scheme 21). In particular, in the NMR spectra of compound **71**, which was purified and fully characterised, the two ethynyl moieties were clearly visible (two singlets at δ 2.57 ppm and δ 2.54 ppm in the ^{1}H NMR spectrum, two signals at δ 74.64 ppm and 72.20 ppm in the ^{13}C NMR spectrum). Furthermore, the presence of two broad singlets in the ^{1}H NMR spectrum (at δ 5.60 ppm and at δ 3.57 – 3.54 ppm, overlapping with the multiplet of one H-5) suggested that opening

of the lactone ring had occurred. The identity of **71** was finally confirmed by mass spectrometry (the observed *m/z* was 401.1 [MNa^+]). The formation of the bis-alkylated derivatives was assumed to be due to the further reaction of the mono-alkylated products with a second equivant of the organolithium compound or the Grignard reagent respectively, allowed by the equilibrium shown in scheme 21. The formation of the bis-alkylated side-product suggested that the number of equivalents of reagent and the reaction time may be crucial for the isolation of the desired mono-alkylated derivative.

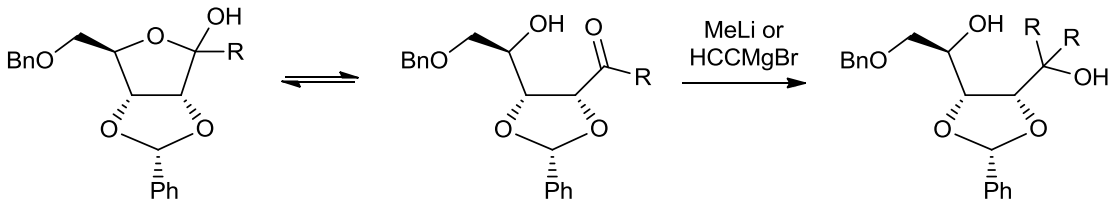

68 R = CH_3
69 R = CCH

70 R = CH_3
71 R = CCH

Scheme 21. Equilibrium at the basis of the formation of bis-alkylated side-products **70** and **71**.

As a proof-of-concept, the synthesis of 2-*O*-acetyl-1-deoxy-D-psicofuranose **72** was attempted on a small scale (starting from 100 mg of **67**) without purification of compounds (scheme 22). The protected lactone **67** was treated with 1.4 equivalent of methyl lithium in Et_2O over 45 minutes.[37] The reaction was quenched despite the incomplete conversion of the starting material according to thin layer chromatography to prevent the formation of the bis-alkylated side-product. The ^1H NMR spectrum of the crude residue showed the presence of unreacted **67** together with the desired product **68** in a ratio of 1.4:1. The ^1H NMR spectrum of compound **68** was characterised by the presence of a D_2O-exchanging singlet at δ 4.95 ppm for the anomeric OH. The crude residue was used for the following acetylation, carried out with acetic anhydride and 4-(dimethylamino) pyridine in pyridine over 48 hours.[37] The disappearance of the singlet at δ 4.95 ppm in the ^1H NMR spectrum of the crude residue showed that the acetylation had occurred. The identity of **72** was confirmed by mass spectrometry (the observed *m/z* was 407.1 [MNa^+]). The other species in the crude mixture were identified as the starting material **67** and the intermediate **68** (*m/z* 349.1 [MNa^+] and 365.1 [MNa^+], respectively), whereas the bis-alkylated side-product **70** was not observed. Although **72** was not purified from the reaction mixture and was not submitted to

glycosylation, the performed reactions demonstrated the feasibility of the synthetic pathway towards 1-*C*-substituted ribose moieties.

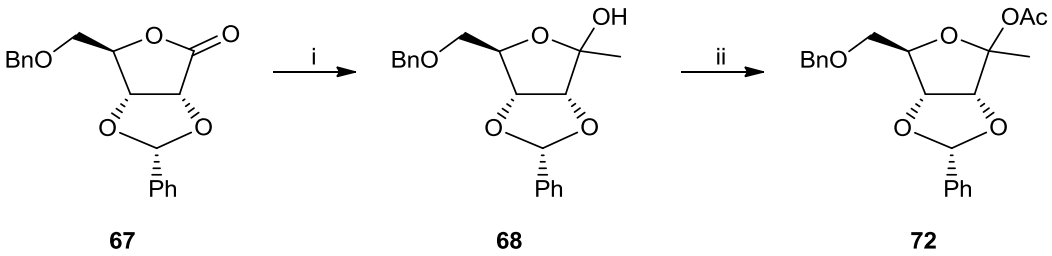

67 **68** **72**

Scheme 22. Synthesis of the glycosylating agent **72** as proof-of-concept. *Reagents and conditions:* i) CH_3Li (1.4 eq.), Et_2O, -78 °C to 0 °C, 45 min; ii) Ac_2O, 4-(dimethylamino)pyridine, pyridine, rt, 48h.

As the protection of the 5-hydroxyl group of **64** as benzyl ether could not be optimised, the possibility of an alternative protective group was explored. According to the reported procedure,[37] the use of the benzyl ether and the benzylidene protecting groups offers the advantage of a simultaneous deprotection of all functionalities by catalytic transfer hydrogenation to furnish 1'-*C*-methyladenosine **41**. On the other hand, the protection as silyl ether of the 5-OH of the lactone would allow for the selective deprotection of the functionality to provide the benzylidene-protected nucleoside, which represents a convenient precursor for the synthesis of phosphoramidate ProTides of **41**. Furthermore, the fluoride-mediated cleavage of silyl ethers occurs under mild conditions and in particular avoids acidic conditions that are reported to cause cleavage of anomeric-substituted nucleoside analogues.[37, 38]

The mixture of **64** and **65** was treated with *tert*-butylchlorodiphenylsilane in the presence of 1*H*-imidazole in DMF to obtain an even mixture of two diastereoisomers **73** and **74**, which could be separated by column chromatography (scheme 23). With the aim to define the configuration of **73** and **74**, the (*S*)-isomer **65**, which was the FE diastereoisomer on silica gel, was converted into the corresponding (*S*)-isomer **74**. By comparing the NMR spectra of the prepared (*S*)-isomer **74** and of the previously synthesised two species, the (*S*)-isomer **74** was identified as the SE diastereoisomer on silica gel.

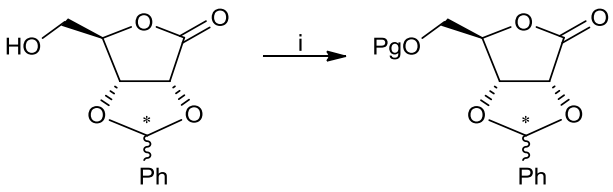

64 (*R*)-isomer (SE)
65 (*S*)-isomer (FE)

73 (*R*)-isomer (FE)
74 (*S*)-isomer (SE)

Pg = TBDPSi

Scheme 23. 5-*O*-Silylation of the 2,3-*O*,*O*-benzylidene protected lactone **64** and **65**. *Reagents and conditions:* i) TBDPSiCl, 1*H*-imidazole, DMF, 0 °C to rt, 4h (**73** and **74**, 48% yield). SE: slow-eluting; FE: fast-eluting.

The protection as *tert*-butyldiphenylsilyl ether may also be performed selectively on the 5-hydroxyl group of D-ribonic acid 1,4-lactone **63**, followed by the 2,3-*O*,*O*-benzylidene protection of the remaining free functionalities (scheme 24). In fact, the reaction of **63** with 1.1 equivalents of *tert*-butylchlorodiphenylsilane in the presence of 1*H*-imidazole in DMF led to the isolation of protected compound **75** in good yield. Additionally, the crude residue could be used in the subsequent step without the need for purification by column chromatography. The 5-*O*-silylated lactone **75** was further protected using benzaldehyde dimethyl acetal and tin (II) chloride in refluxing DME. When the benzylidene group was introduced on either the purified or the crude lactone **75**, almost exclusively the (*S*)-isomer **74** was obtained in 55% yield, whereas traces of the (*R*)-isomer **73** were formed and could be removed by chromatographical purification. The method based on the 5-*O*-silylation followed by the 2,3-*O*,*O*-benzylidation was superior to the previously described procedure, not only because of higher obtained yields but also because of the possibility for easily isolation of **74** as one single diastereoisomer.

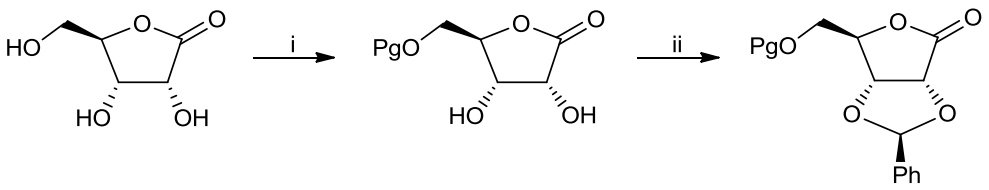

63 **75** **74** (S)-isomer

Pg = TBDPSi

Scheme 24. 5-*O*-Silyl ether and 2,3-*O*,*O*-benzylidene protection of D-ribonic acid 1,4-lactone **63**. *Reagents and conditions:* i) TBDPSiCl, 1*H*-imidazole, DMF, 0 °C to rt, 4h (**75**, 57% yield); ii) benzaldehyde dimethyl acetal, $SnCl_2$, DME, reflux, 1h (**74**, 55% yield).

The fully protected lactone **74** underwent alkylation using a 1.6M solution of methyllithium in Et_2O (scheme 25).

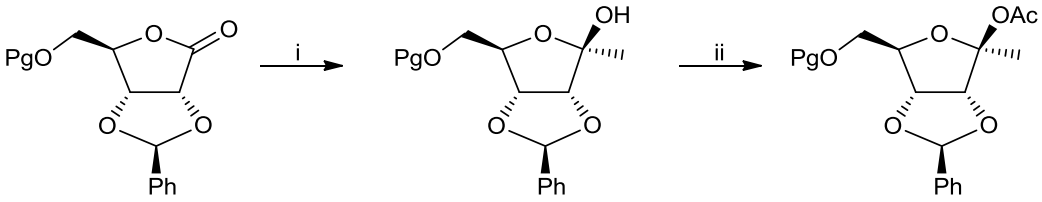

74 **76** **77**

Pg = TBDPSi

Scheme 25. Synthesis of the glycosylating agent **77**. *Reagents and conditions:* i) CH_3Li, Et_2O/THF, -78 °C to 0 °C, 1h (**76**, crude); ii) Ac_2O, 4-(dimethylamino)pyridine, Et_3N, DCM, rt, 48h (**77**, 48% yield).

In the first attempt, alkylation using a slight excess of the organolithium reagent (1.4 equivalents) over 30 minutes at -78 °C followed by treatment with acetic anhydride (1 equivalent) and the catalyst 1-(dimethylamino)pyridine in pyridine[37] produced a mixture of species, among which the bis-acetylated bis-alkylated side-product **78** (figure 59) and the mono-alkylated intermediate **76** were isolated with 34% yield and 20% yield, respectively.

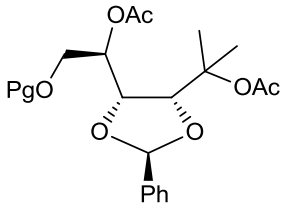

78

Pg = TBDPSi

Figure 59. Bis-acetylated bis-alkylated side-product **78**.

When 1 equivalent of methyllithium reagent was employed, full conversion of the starting material was observed over 1 hour at -78 °C and was not accompanied by the formation of the undesired bis-alkylated product (scheme 25). The crude mono-alkylated product **76** underwent acetylation by treatment with an excess of acetic anhydride and 4-(dimethylamino)pyridine in pyridine. Purification by column chromatography allowed for the isolation of the 2-*O*-acetyl-1-deoxy-D-psicofuranose derivative **77** with 35% yield among other species. Furthermore, the NMR spectra of the crude **76** and of the purified acetylated derivative **77** demonstrated that the addition of the methyl moiety on the starting material **74** occurred in a stereoselective fashion. A 2D NOESY experiment was performed on **76** and suggested that the β-D-psicofuranose derivative was obtained: indeed, the broad singlet at δ 4.89 ppm for the 2-hydroxyl group correlated with the two doublets of doublets at δ 3.79 and 3.61 ppm for the methylene group in the 6-position.

In an attempt to increase the yield of the acetylation, compound **76** was treated with 1.2 equivalents of acetic anhydride in the presence of 4-(dimethylamino)pyridine in pyridine. However, the reaction did not reach completion over 48 hours and furnished the product **77** in a low yield (20%). The reaction carried out using an excess of acetic anhydride (3 equivalents), 4-(dimethylamino)pyridine and Et_3N in DCM showed a clean profile and afforded **77** in 48% yield.

The glycosylation of the 6-chloropurine was achieved by treatment with the prepared 2-*O*-acetyl-1-deoxy-β-D-psicofuranose derivative **77** in the presence of ethylaluminum dichloride in acetonitrile (scheme 26).

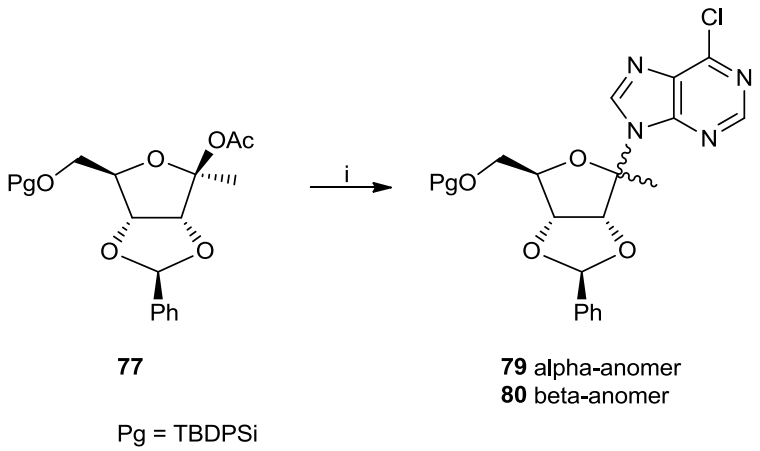

Scheme 26. Glycosylation of 6-chloropurine using **77**. *Reagents and conditions:* i) 6-chloropurine, $EtAlCl_2$, CH_3CN, rt, 2h (α-anomer and β-anomer **79**/**80**, 40% yield; *N*-7 adduct, 17% yield)

The reaction reached completion after 2 hours at room temperature and afforded an unseparable mixture of α-nucleoside and β-nucleoside **79**/**80** in 40% yield. The obtained nucleosides were hypothesised to be the *N*-9 coupling derivatives because they were the major products of the glycosylation reaction. A 2D NOESY experiment demonstrated that the major product in the mixture was the desired β-nucleoside **80**: indeed, the doublet at δ 4.70 ppm of the H-4' of the D-psicofuranose moiety correlated with the singlet at δ 8.44 ppm of the H-8. Furthermore, the observation of a correlation signal between the singlet at δ 6.05 ppm of the methyne of the 2,3-*O*,*O*-benzylidene group and the singlet at δ 8.43 ppm of the H-8 belonging to the minor product demonstrated the α-anomeric configuration of the minor nucleoside **79** in the mixture. The ratio between the α and the β-nucleosides **79**/**80** was 1:1.7. A third nucleoside was isolated from the coupling reaction of 6-chloropurine with **77** in low yield (17%). Characterisation by NMR spectroscopy and mass spectrometry showed that the side-product was a structural isomer of nucleosides **79** and **80** (the observed *m/z* was 649.2 for $[MNa^+]$ as for **79**/**80**), hypothesised as the *N*-7 coupling product. Additionally, a 2D NOESY experiment was performed, however the anomeric configuration could not be defined.

The anomeric mixture of **79**/**80** was efficiently converted into the corresponding mixture of α and β-adenosine nucleosides **81**/**82** using a saturated (7M) methanolic solution of ammonia at 80 °C (scheme 27).

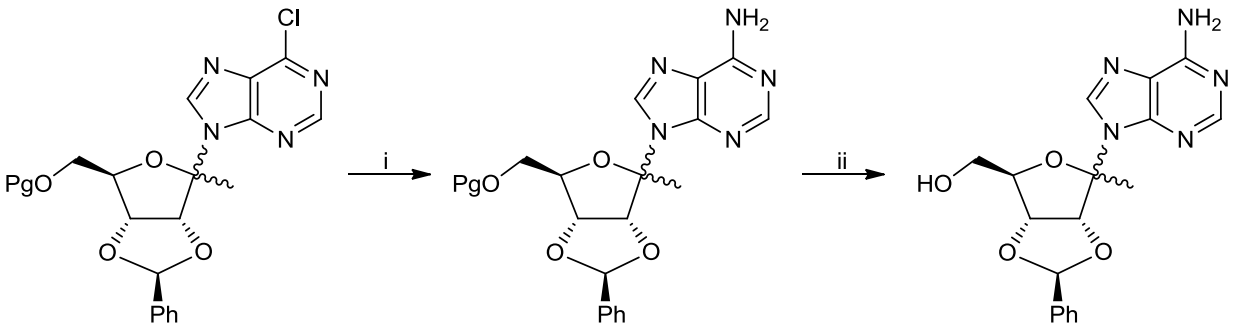

79 alpha-anomer
80 beta-anomer

81 alpha-anomer
82 beta-anomer

85 alpha-anomer
86 beta-anomer

Pg = TBDPSi

Scheme 27. Amination and 6'-*O*-deprotection of the anomeric mixture of nucleosides **79**/**80**. Reagents and conditions: i) NH_3, MeOH, 80 °C, 48h (α-anomer and β-anomer **81**/**82**, 63% yield); ii) TBAF·$3H_2O$, THF, 0 °C, 2h (α-anomer and β-anomer **85**/**86**, 85% yield).

The reaction afforded the anomeric mixture of the 6-*O*-methyl inosine derivatives **83**/**84** as side-products in 12% yield (figure 60).

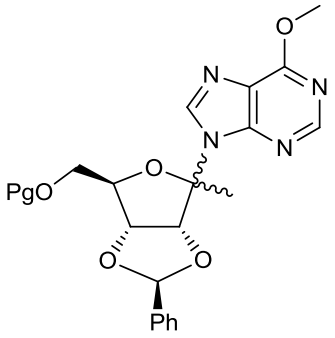

83 alpha-anomer
84 beta-anomer

Pg = TBDPSi

Figure 60. Side-products **83**/**84** isolated from the amination of **79**/**80**.

As the separation of the two anomers by column chromatography was unsuccessful, the mixture of α and β-nucleosides **81**/**82** underwent selective cleavage of the 6'-*O*-silyl ether by tetrabutylammonium fluoride in THF to obtain the corresponding 6'-*O*-deprotected mixture of **85**/**86** (scheme 27). Also at this stage, the two anomers **85** and **86** showed identical

chromatographical behaviour and could not be separated. Figure 61 shows the ^{1}H NMR of the mixture of α and β-nucleosides **85**/**86**.

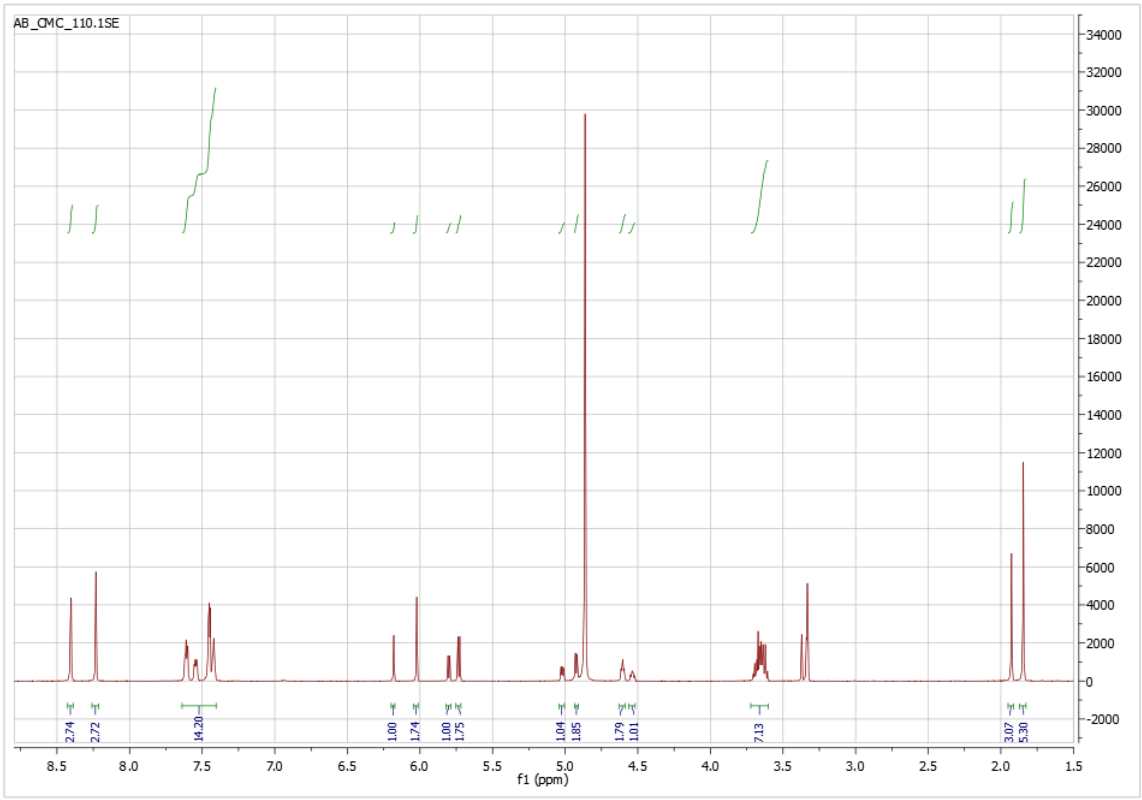

Figure 61. ^{1}H NMR of the mixture of α and β-nucleosides **85**/**86**.

In an attempt to improve the anomeric ratio during the glycosylation of the 6-chloropurine, the application of Vorbrüggen conditions was investigated (scheme 28). Silylation of the 6-chloropurine by treatment with *N*,*O*-bis(trimethylsilyl)acetamide in refluxing acetonitrile was followed by the reaction with the glycosylating reagent **77** in the presence of trimethylsilyl triflate at low temperature (from -20 °C to 0 °C), according to a procedure that was reported for the preparation of 1',4'-bis-substituted uridine analogues.[38] Althoug the reaction was not regioselective and afforded the hypothetised *N*-7 adduct as well, the desired β-nucleoside **80** was the only *N*-9 nucleoside formed and could be easily isolated in 14% yield after chromatographical purification. Therefore, the Vorbrüggen glycosylation by the 1-deoxy-β-D-psicofuranose derivative **77** was found to occur with stereoselectivity. The 2',3'-*O*,*O*-benzylidene group, rather than the methyl substituent at the anomeric position, may play a role in the stereoselective control of the reaction. However the exact role of the additional carbon group remains unclear as only one other

example of stereoselective glycosylation by anomeric-modified ribose moiety is reported in the literature to date.[38]

The following amination and deprotection of the 6'-hydroxyl group of the β-nucleoside **80** were carried out according to the procedures previously developed for the anomeric mixture. Treatment with a saturated (7M) methanolic solution of ammonia at 80 °C, followed by the reaction with tetrabutylammonium fluoride in THF at 0 °C, provided the β-nucleoside **86** in good yield (scheme 28).

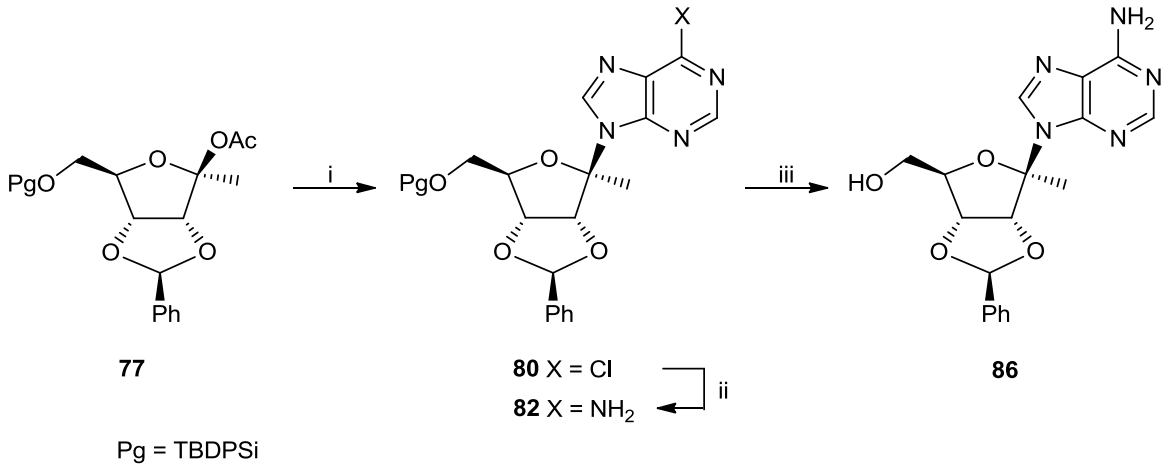

Scheme 28. Stereoselective glycosylation of **77** followed by amination and 6'-*O*-deprotection. *Reagents and conditions:* i) 6-chloropurine, *N,O*-bis(trimethylsilyl)acetamide, CH_3CN, rt to 50 °C, then TMSOTf, CH_3CN, -20 °C to 0 °C, 1h (β-nucleoside **80**, 14% yield; *N*-7 adduct, 8% yield); ii) NH_3, MeOH, 80 °C, 48h (β-anomer **82**, 66% yield); iii) TBAF·$3H_2O$, THF, 0 °C, 2h (β-anomer **86**, 74% yield).

The anomeric configuration of **86** was demonstrated by the observation of correlation signals of the singlet at δ 8.19 ppm of the H-2 with both multiplets at δ 3.43 – 3.37 ppm and 3.35 – 3.28 ppm for the 6'-methylene as well as with the triplet at δ 5.03 ppm for the 6'-OH in the 2D NOESY experiment. Furthermore, the 6-amino group did not show any correlation signals, suggesting that **86** corresponded to the desired *N*-9 derivative.

In contrast, the cleavage of the 3',4'-*O*,*O*-benzylidene group (scheme 29) was not straightforward (table 10). Treatment of the protected nucleoside with ammonium formate in the presence of palladium on carbon as catalyst in refluxing methanol was reported to furnish the target nucleoside in high yield.[37] However, when up to 16 equivalents of ammonium formate and 80%

of palladium on carbon were used, only traces of the deprotected nucleoside **41** were formed according to thin layer chromatography and mass spectrometry. The attempts of deprotection using hydrogen gas (1 atm) catalysed by either palladium on carbon or palladium hydroxide on carbon were unsuccessful. Catalytic transfer hydrogenation conditions using a large excess of both ammonium formate and palladium on carbon were finally applied to the starting material **86** and allowed for the isolation of the target nucleoside **41** in a low yield of 18% after purification by column chromatography.

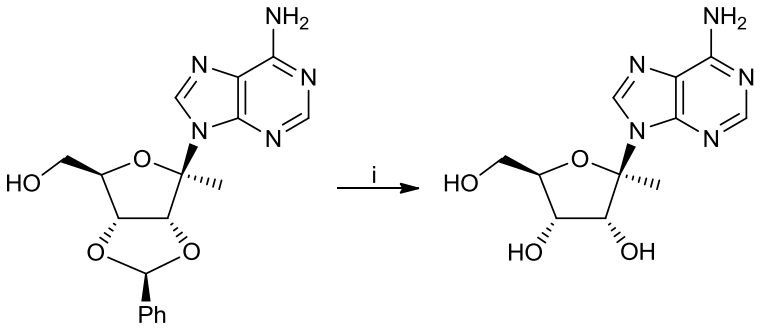

86 **41**

Scheme 29. Cleavage of the 3',4'-*O*,*O*-benzylidene group of the β-nucleoside **86**. *Reagents and conditions:* i) $HCOONH_4$, 10% Pd/C, CH_3OH, reflux, 20h (**41**, 18% yield).

Table 10. Attempts of cleavage of the 3',4'-*O*,*O*-benzylidene group of β-nucleoside **86**.

Reagents and conditions	**Products**
$HCOONH_4$ (8 eq.), 20% w/w Pd/C, CH_3OH, reflux, 20h	traces of **41**
$HCOONH_4$ (8 eq.), 40% w/w Pd/C, CH_3OH, reflux, 20h	traces of **41**
$HCOONH_4$ (16 eq.), 80% w/w Pd/C, CH_3OH, reflux, 48h	traces of **41**
$HCOONH_4$ (48 eq.), 100% w/w Pd/C, CH_3OH, reflux, 20h	incomplete reaction (**41**, 18% yield)
H_2 (1 atm), 40% w/w Pd/C, EtOH, rt, 48h	starting material **86**
H_2 (1 atm), 80% w/w $Pd(OH)_2$/C, EtOH, rt, 24h	starting material **86**

The comparison of the ^{1}H NMR spectrum of **41** to the available literature[37] confirmed that the β-nucleoside isolated from the glycosylation reaction was the desired *N*-9 adduct, as previously suggested by NMR analysis performed on the precursor **86**.

In conclusion, a synthetic procedure for the preparation of 1'-*C*-methyladenosine **41** was developed. The synthesis involved eight steps starting from the commercially available D-ribonic acid 1,4-lactone **63**, with an overall yield less than 1%, and thus further optimisation of the method is required.

The prepared nucleoside **41** was sent to our collaborators for biological evaluation *in vitro* (see section 2.3 for details). The results are currently being awaited.

2.2.3 SYNTHESIS OF BENZO-FUSED ADENOSINE ANALOGUES

Benzo-fused 7-deaza adenosine analogues were designed by Tichý *et al*.[14, 15] as potential agents against RNA viruses, with the aim of exploring substitutions at the 7-deaza position of adenosine. As previously mentioned, some analogues within this family were found to inhibit DENV RdRp (see paragraph 1.2.2.2 and table 20 in the APPENDIX for details). Molecular modelling studies confirmed that the presence of large substituents at the 7-deaza position of adenosine, such as a benzene ring fused in a tricyclic heterobase, is well tolerated by the active site of the DENV RdRp (see paragraph 2.1.1.2 for details). In addition, docking studies suggested that modifications at the ribose moiety are compatible with the large tricyclic base (see paragraph 2.1.2.1).

This section describes the synthesis of known benzo-fused 7-deazaadenosine analogues (**87** and **88**, figure 62) and the application of the phosphoramidate ProTide strategy in an attempt to enhance their antiviral potency and overcome a reported issue of cytotoxicity of these compounds.[14, 15] Given the promising docking results, the combination of a modified glycosylating agent to the synthesised tricyclic heterobase was also explored.

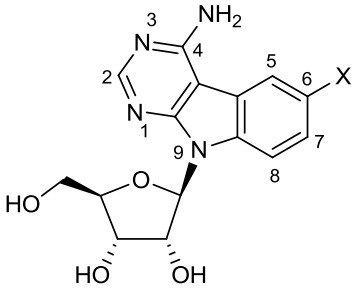

87 X = Cl
88 X = H

Figure 62. Structures of **87** and **88** as examples of tricyclic nucleosides.

2.2.3.1 Synthesis of benzo-fused 7-deazaadenosine analogues

For the preparation of benzo-fused 7-deazaadenosine analogues, such as **87** and **88**, the synthesis of the corresponding pyrimido[4,5-*b*]indole heterocycles was performed, which was then followed by glycosylation, amination and deprotection steps. The synthesis of the tricyclic heterobases had been reported by Tichý *et al.*[15] in 2012. The strategy was applied to the synthesis of 4,6-dichloro **97** as well as 4-chloro-9*H*-pyrimido[4,5-*b*]indole **98**, starting from commercially available 2,4-dichloronitrobenzene **89** and 2-chloronitrobenzene **90**, respectively (scheme 30).

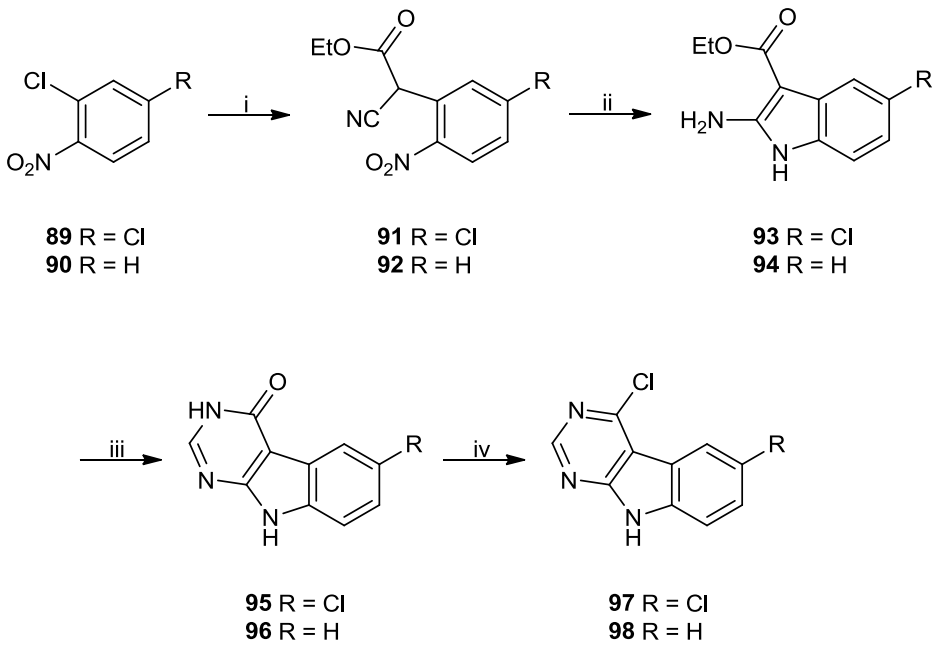

89 R = Cl
90 R = H

91 R = Cl
92 R = H

93 R = Cl
94 R = H

95 R = Cl
96 R = H

97 R = Cl
98 R = H

Scheme 30. Synthesis of pyrimido[4,5-*b*]indole heterocycles **97** and **98**. *Reagents and conditions:* i) $CNCH_2COOEt$, tBuOK, DMF, 70 °C, 16h (**91**, 77% yield; **92**, 72% yield); ii) Zn, AcOH, rt, 4h (**93**, 89% yield; **94**, crude); iii) formamide, 190 °C, 18h (**95**, 62% yield; **96**, crude); iv) $POCl_3$, reflux, 48h (**97**, 83% yield; **98**, 17% for last 3 steps).

The first step was a nucleophilic aromatic substitution on the starting material by ethyl cyanoacetate, activated *in situ* by an excess of potassium *tert*-butoxide. In the reported procedure anhydrous THF had been used as solvent and the reaction mixture had been refluxed for 48 hours.[15, 55] However, in this work, the reaction did not go to completion under these conditions and was characterised by a moderate yield (45% yield for **91**, 35% yield for **92**). When the reaction was performed in anhydrous DMF at 70 °C, full conversion of the starting material was observed after 16 hours with higher yields (77% yield for **91**, 72% yield for **92**). Additionally, purification by column chromatography was not required and the crude products could be used directly for the following step. Reduction of the nitro group by treatment with zinc dust in glacial acetic acid[15, 56] and spontaneous cyclisation of the amino intermediates afforded the desired indole derivatives **93** and **94** in good yields. Cyclocondensation with formamide at 190 °C furnished the fused pyrimidone derivatives **95** and **96**, which were then converted to 4,6-dichloro-9*H*-pyrimido[4,5-*b*]indole **97** and 4-chloro-9*H*-pyrimido[4,5-*b*]indole **98** by treatment with phosphorus (V) oxychloride under reflux for 48 hours, monitored by thin layer chromatography.

The synthesis of 4-chloro-9*H*-pyrimido[4,5-*b*]indole **98** did not involve any purification of the intermediates, however was characterised by an overall yield of 12%. In contrast, the 4,6-dichloro analogue **97** was prepared with an overall yield of 35%. Purification by column chromatography of intermediate **95** was performed in order to isolate the desired product among several side-products and significantly contributed to the increase in the yield of the subsequent step. The heterobase **97** was then submitted to glycosylation, amination and deprotection steps to obtain the target nucleoside **87**, whereas the final steps towards nucleoside **88** were not performed because of the low-yielding synthesis of its precursor **98**.

In the reported procedure, the coupling reaction of a protected D-ribofuranose and a 9*H*-pyrimido[4,5-*b*]indole derivative had been performed as a one-pot reaction according to the Vorbrüggen procedure.[15] The 4,6-dichloro-9*H*-pyrimido[4,5-*b*]indole **97** was coupled to commercially available 1-*O*-acetyl-2,3,5-tri-*O*-benzoyl-β-D-ribofuranose (scheme 31): silylation of **97** by *N*,*O*-bis(trimethylsilyl)acetamide and reaction with the glycosylating agent catalysed by trimethylsilyl triflate, were carried out in anhydrous acetonitrile under reflux and afforded nucleoside **99** in good yield (55%). The desired β-nucleoside could be separated by column chromatography from the α-nucleoside that was formed with a 10% yield (ratio α:β = 1:5). The ^{1}H NMR and ^{13}C NMR spectra of the β-nucleoside were in agreement with the literature.[15] NOESY 2D NMR experiments of both species were performed and further confirmed their anomeric identity: a correlation peak was observed between H-1' and H-2' in the α-anomer, whereas the anomeric proton of the β-anomer correlated to H-4'.

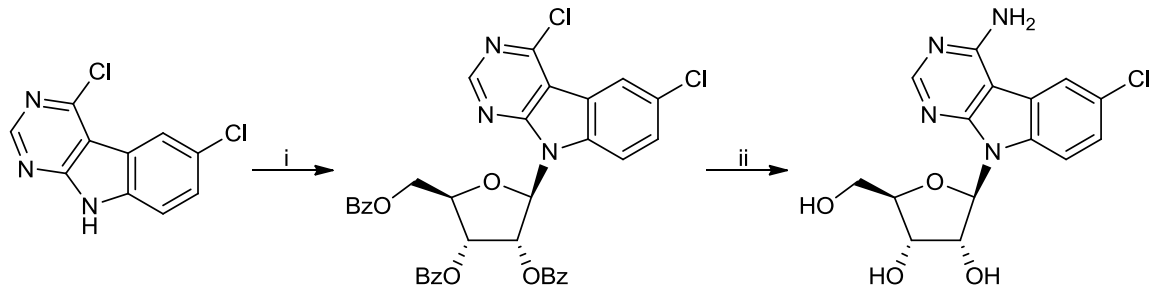

97 **99** **87**

Scheme 31. Glycosylation of 4,6-dichloro-9*H*-pyrimido[4,5-*b*]indole **97**. *Reagents and conditions:* i) 1-*O*-acetyl-2,3,5-tri-*O*-benzoyl-β-D-ribofuranose, *N,O*-bis(trimethylsilyl)acetamide, TMSOTf, 60 °C, 20h (**99**, 55% yield); ii) NH_3, MeOH, 75 °C, 48h (**87**, 44%).

The last step was the amination of the 4-position and simultaneous cleavage of the protecting groups by treatment of **99** with a saturated (7M) methanolic solution of ammonia in a sealed tube at 75 °C for 48 hours (scheme 31). The target nucleoside benzo-fused 7-deazaadenosine analogue **87** was isolated by filtration from the reaction mixture in 44% yield.[14] NMR spectra were in agreement with the literature reported for the β-nucleoside.[14] In the NOESY experiment, the observed correlation peaks between H-1' and 2'-OH, H-2' and the aromatic H-8 of the nucleobase as well as the absence of correlation between H-1' and H-3' confirmed that the desired β-nucleoside was obtained.

The anti-DENV activity and cytotoxicity *in vitro* of the synthesised tricyclic adenosine analogue **87** were evaluated by our collaborators (see section 2.3 for details).

2.2.3.2 Synthesis of benzo-fused adenosine analogue ProTides

In order to increase the anti-DENV activity and reduce the cytotoxic effect of the parent nucleoside **87** (refer to section 2.3 for details), the phosphoramidate ProTide approach was applied (scheme 32).

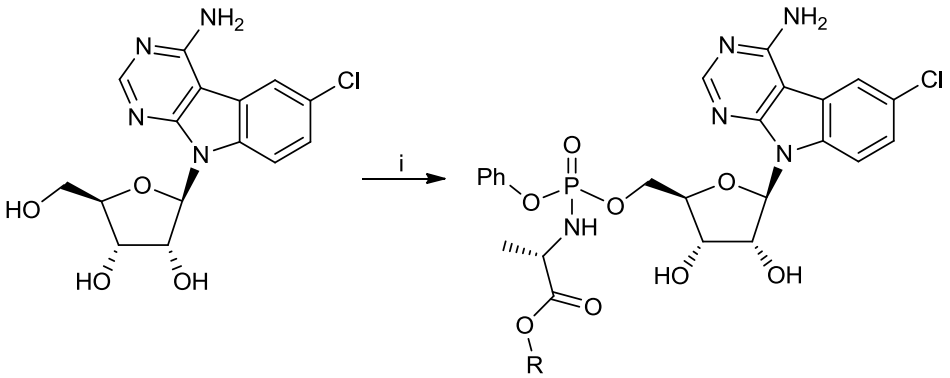

Scheme 32. Synthesis of benzo-fused adenosine analogue ProTides **100** and **101**. *Reagents and conditions:* i) coupling reaction using phosphorochloridate or *p*-nitrophenolate reagents (see text for details).

The coupling reaction was initially attempted on the unprotected nucleoside **87** according to the standand procedure using *t*BuMgCl as a base.[30] As previously mentioned, the method based on the use of the Grignard reagent does not provide selectivity towards primary hydroxyl groups, but

it is generally accociated with relatively high yields and the formation of the desired 5'-*O*-phosphoramidate as main product of the reaction.[30] Compound **87** was treated with the phosphochloridate **35** (refer to section 2.2.1 for the preparation of **35**) and *t*BuMgCl in anhydrous THF. However, purification by column chromatography led to the isolation of two species in very poor yield, which were showing similar chromatographic behaviour. In fact, the presence of two couples of peaks at the ^{31}P NMR (at δ 3.44 ppm and 3.32 ppm, at δ 2.14 ppm and 2.01 ppm) suggested that the 5'-*O*-phoshoramidate and the 3'-*O*-phosphoramidate, each as a mixture of diastereoisomers, were obtained. Further purification by column chromatography of the mixture did not lead to the isolation of compound **100**.

The use of NMI in place of *t*BuMgCl for the preparation of ProTides generally allows for the selective reaction at the 5'-hydroxyl group of the parent nucleoside. In an attempt to avoid the formation of the undesired 3'-*O*-phosphoramidate and the inconvenient separation of the two couples of diastereoisomers, compound **87** was treated with the phosphochloridate **35** (refer to section 2.2.1 for the preparation of **35**) in the presence of an excess of NMI in a mixture of THF and pyridine under anhydrous conditions. The reaction was characterised by poor conversion of the starting material, therefore the desired ProTide **100** could not be isolated after column chromatography.

In a methodology study that will be described in section 2.2.5, innovative microwave irradiation (MWI) conditions for the preparation of ProTides were investigated. The methods using either NMI or the Grignard reagent *t*BuMgCl, conventionally carried out at room temperatute, were found to be compatible with heating by MWI and were applied for the synthesis of ProTide **101** bearing the L-alanine isopropyl ester moiety. A mixture of the parent nucleoside **87** and the phosphorochloridate bearing the isopropyl ester moiety **36** (see section 2.2.1 for the synthesis of **36**) in the presence of an excess of NMI in a mixture of THF and pyridine was heated under MWI conditions at 65 °C for 4 hours. Progress of the reaction was monitored by thin layer chromatography, however poor conversion of the starting material **87** was observed and the ProTide **101** was not isolated after purification by column chromatography. Finally, nucleoside **87** was treated with 1 equivalent of the *p*-nitrophenolate reagent **38** (refer to section 2.2.1 for the preparation of **38**) in the presence of *t*BuMgCl in DMF. Heating of the reaction mixture by MWI at 65 °C over 30 minutes, followed by purification by column chromatography, furnished the target ProTide **101** in 13% yield with a purity of 98% according to analytical HPLC.

The prepared tricyclic adenosine phosphoramidate **101** was sent to our collaborators for biological evaluation *in vitro* (see section 2.3 for details). The results are currently being awaited.

2.2.3.3 Synthesis of ribose-modified benzo-fused 7-deazaadenosine analogues

For the preparation of ribose-modified benzo-fused 7-deazaadenosine analogues, an appropriate glycosylating agent needed to be synthesised before the coupling to the pyrimido[4,5-*b*]indole heterocycles. Specifically, the synthetic strategy towards the tricyclic nucleoside bearing a methyl group at the 2'-position **102** (figure 63) was investigated.

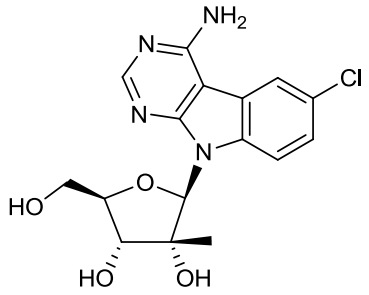

102

Figure 63. Structure of 2'-*C*-methyl substituted tricyclic nucleoside **102**.

The synthesis of the 2'-*C*-methyl glycosylating agent **107** for the following Vorbrüggen coupling reaction was accomplished according to a published procedure (scheme 33).[57] Commercially available 2-*C*-methyl-D-ribono-1,4-lactone **103** was treated with benzoyl chloride to obtain the fully protected lactone **104**, that was used in the subsequent step without purification. Reduction of **104** using sodium bis(2-methoxyethoxy)aluminum dihydride (Red-Al®) afforded the anomeric mixtures of **105** and **106**, whose formation was due to transbenzoylation. The mixture of four species was submitted without purification for the protection of the remaining free hydroxyl group as benzoyl ester. The glycosylating agent 1,2,3,5-tetra-*O*-benzoyl-2-*C*-methyl-D-ribofuranose **107** was obtained in 35% yield after extraction and trituration. The synthetic pathway consists of three steps, does not involve purification by column chromatography of any of the intermediates and is characterised by an overall yield of 22%.

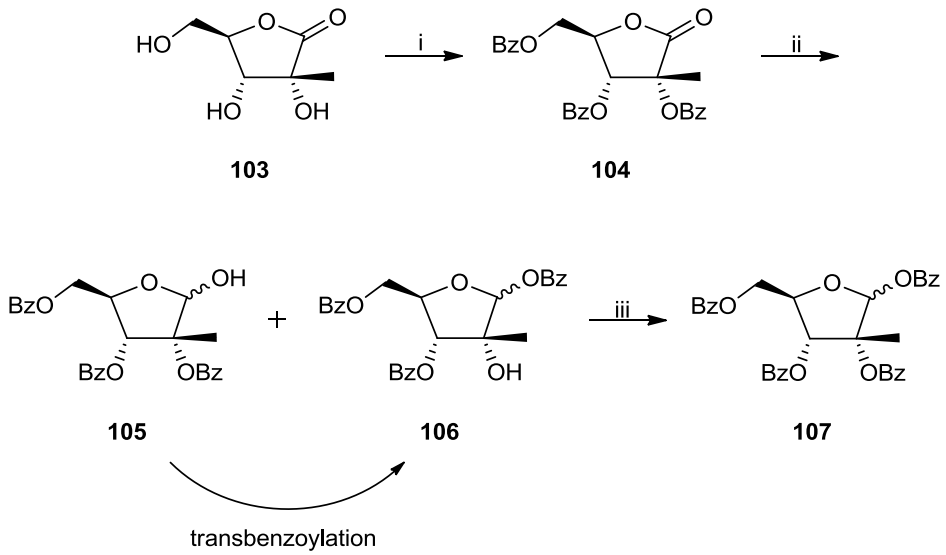

Scheme 33. Synthesis of the 2'-*C*-methyl glycosylating agent **107**. *Reagents and conditions:* i) BzCl, 4-(dimethylamino)pyridine, Et_3N, DME, rt, 16h (**104**, 77% yield); ii) Red-Al®, EtOH, -5 °C, 1.5h (**105** and **106**, 82% yield); iii) BzCl, 4-(dimethylamino)pyridine, Et_3N, THF, 5 °C to rt, 24h (**107**, 35% yield).

The glycosylating agent **107** was then used as an anomeric mixture for the coupling reaction with 4,6-dichloro-9*H*-pyrimido[4,5-*b*]indole **97** (scheme 34). According to Vorbrüggen conditions for the glycosylation,[15] **97** was activated *in situ* by treatment with *N,O*-bis(trimethylsilyl)acetamide and reacted with **107** in the presence of the catalyst trimethylsilyl triflate to afford the protected β-nucleoside **108** with a yield of 21%. Compound **108** was identified by NMR spectroscopy and mass spectrometry (the observed *m/z* was 696.2 [MH^+]), whereas the anomeric configuration was not determined as the benzoyl protective groups interfere with the analysis of the 2D NOESY experiment.

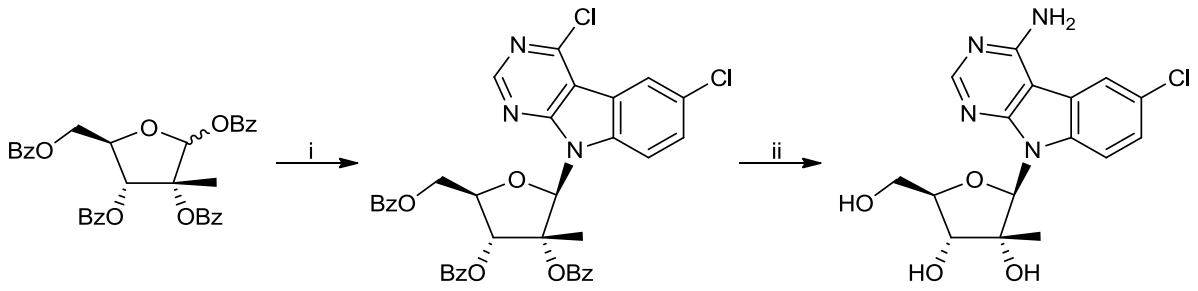

107 **108** **102**

Scheme 34. Glycosylation of 4,6-dichloro-9*H*-pyrimido[4,5-*b*]indole **97** using **107**. *Reagents and conditions:* i) **97**, *N,O*-bis(trimethylsilyl)acetamide, TMSOTf, 60 °C, 20h (**108**, 21% yield); ii) NH_3, MeOH, 80 °C, 24h (**102**, 52% yield).

Compound **108** underwent amination and deprotection by treatment with a saturated (7M) methanolic solution of ammonia at 80 °C for 24 hours (scheme 34). Chromatographical purification allowed for the isolation of the desired product **102** with 52% yield as well as the side-product **109** with 14% yield (figure 64). Characterisation of the anomeric configuration was performed on the final nucleoside **102**. A correlation signal between the singlet at δ 6.46 ppm for the H-1' and the broad singlet at δ 5.00 ppm for the free hydroxyl group in the 2'-position was observed in the 2D NOESY experiment of **102**; the lack of correlation of the singlet for the H-1' with the methyl group in the 2'-position further confirmed that the desidered β-nucleoside was obtained.

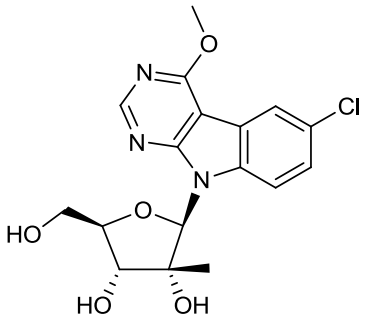

3.23

Figure 64. Side-product **109** isolated from the amination of compound **108**.

The prepared 2'-*C*-methyl benzo-fused nucleoside analogues **102** and **109** were sent to our collaborators for the biological evaluation *in vitro* (see section 2.3 for details) and the results are currently being awaited.

2.2.4 SYNTHESIS OF ACYCLIC ADENOSINE ANALOGUES

Acyclic nucleoside analogues represent an important class of DAAs as exemplified by the fact that almost half of the nucleoside analogues approved to date as antiviral agents are acyclic nucleosides, acyclic nucleoside phosphonates (ANPs) or their prodrugs.[58, 59]

With regard to DENV RdRp inhibitors, this field is still unexplored. With the aim of identifying potential anti-DENV acyclic nucleoside analogues, molecular modelling studies were performed using the model of the DENV RdRp *de novo* initiation complex. As previously described, two scaffolds replacing the 5-membered ring of the ribose were selected following screening of a database of linear linkers and docking studies (see paragraph 2.1.2.2 for details). The corresponding adenosine derivatives **27** and (*R*)-enantiomer of **28** are shown in figure 65 and are representative of two families of acyclic adenosine analogues, whose synthesis is reported in this section.

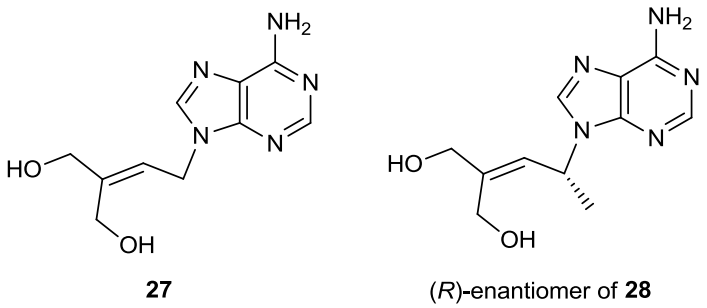

Figure 65. Acyclic adenosine analogues **27** and (*R*)-enantiomer of **28** designed *in silico*.

2.2.4.1 Synthesis of acyclic adenosine analogues – first scaffold

Compound 1-[3,3'-bis-(hydroxymethyl)-prop-2-enyl]adenine **27** (figure 66) had been developed as an unsaturated derivative of pencyclovir **110** (figure 66), an acyclic guanosine analogue approved for the treatment of herpes simplex virus (HSV) and varicella zoster virus (VZV).[58] The additional double bond had been introduced to mimic the carbocycle of the naturally occurring antibiotic neplanocin A **111** (figure 64).[19]

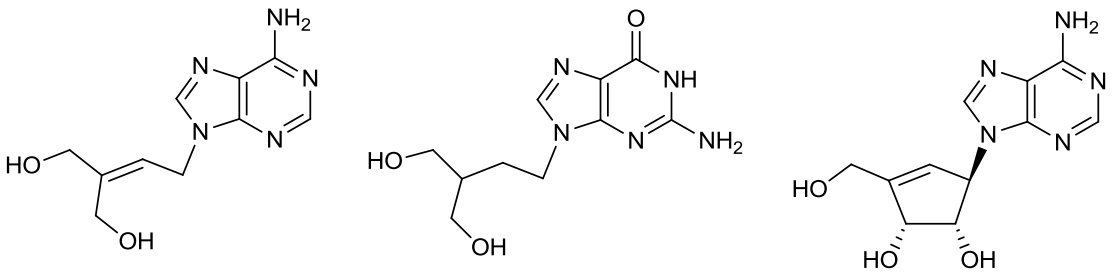

Figure 66. Structures of pencyclovir **110** and neplanocin A **111** as rationale for compound **27**.[19]

In this work, the synthesis of **27** and 7-deaza analogues involved the alkylation of a 6-chloropurine base by primary allylic halides, which were synthesised according to the four steps pathway shown in scheme 35.

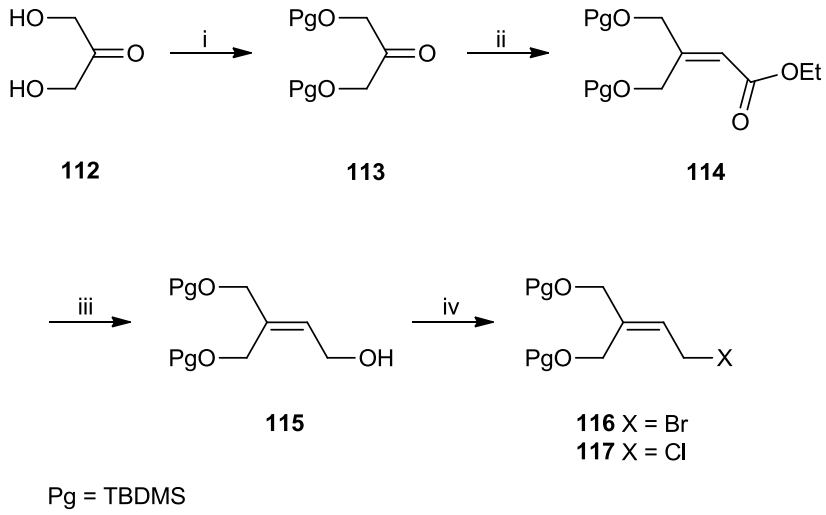

Scheme 35. Synthesis of the allylic halides **116** and **117**. *Reagents and conditions:* i) TBDMSCl, Et_3N, 4-(dimethylamino)pyridine, DCM, 0 °C to rt, 24h (**113**, 87% yield); ii) triethyl phosphonoacetate, NaH, THF, 0 °C to rt, 2h (**114**, 94% yield); iii) DIBALH, DCM, -20 °C to 0 °C, 1h (**115**, 79% yield); iv) attempts of bromination (**116**, see text) or *p*TsCl, 4-(dimethylamino)pyridine, Et_3N, DCM, rt, 4h (**117**, 40% yield).

The inexpensive starting material 1,3-dihydroxyacetone **112**, which is commercially available as a dimer, was initially protected as *tert*-butyldimethylsilyl ethers. In the reported procedure[19] the protection had been performed using *tert*-butyldimethylchlorosilane in the presence of 1*H*-imidazole in anhydrous DMF. However formation of **113** occured neither when the reaction was

monitored by thin layer chromatography over 60 hours, nor when a second addition of both reagents was performed over 96 hours. In these attempts, the starting material was converted to a more lipophilic product that could not be extracted from the aqueous phase during the work-up. In a third attempt, the protected 1,3-dihydroxyacetone **113** was obtained after treatment of the starting material **112** with *tert*-butyldimethylchlorosilane and Et_3N in anhydrous Et_2O for 72 hours in poor yield (26%). Finally, the reaction was performed using *tert*-butyldimethylchlorosilane in the presence of Et_3N and 4-(dimethylamino)pyridine in anhydrous DCM and afforded the desired product **113** after 24 hours in good yield (87%).

The following reaction of **113** with triethyl phosphonoacetate in the presence of sodium hydride in THF, according to Wittig-Emmons conditions, furnished the ethyl ester derivative 3,3'-bis-(*tert*-butyldimethylsilyloxymethyl)prop-2-en-1-oate **114** with excellent yield (94%). Reduction to the allylic primary alcohol **115** was carried out using DIBALH and was characterised by a good yield (79%).

According to the published procedure,[19] the conversion of **115** to the bromo derivative **116** had been accomplished using *N*-bromosuccinimide and triphenylphosphine in DCM. Although attempts of bromination of the allylic alcohol **115** were performed using a variety of bromine sources, the desired product **116** could not be obtained in good yield. As summarised in table 11, bromination of the allylic alcohol of **115** using *N*-bromosuccinimide or carbon tetrabromide was associated with several side-reactions. After treatment with 2 equivalents of *N*-bromosuccinimide, the allylic bromide **116** was isolated from the mixture of species in 14% yield. Treatment with phosphorus tribromide did not lead to the formation of **116** according to the ^1H NMR spectrum of the crude residue, whereas treatment with bromotrimethylsilane in DCM led to the formation of a mixture of deprotected species.

Table 11. Attempts of bromination of the allylic primary alcohol **115**.

Reagents and conditions	**Products**
N-Bromosuccinimide (1.07 eq.), Ph_3P (1.1 eq.), DCM, 0 °C to rt, 4h	mixture of species
N-Bromosuccinimide (2.0 eq.), Ph_3P (1.1 eq.), DCM, 0 °C to rt, 4h	bromide **116** (14% yield)
Bromotrimethylsilane (1.2 eq.), DCM, 0 °C to rt, 6h	deprotected species
Bromotrimethylsilane (1.2 eq.), DCM, 0 °C to rt, 1h	deprotected species
CBr_4 (1.25 eq.) Ph_3P (1.5 eq.), DCM, 0 °C to rt, 1h	mixture of species
PBr_3 (2 x 0.5 eq.), Et_3N (2 x 2.0 eq.), DCM, 0 °C to rt, 20h	mixture of species

In contrast, chlorination of **115** was easily achieved by treatment with *p*-toluenesulfonyl chloride, in the presence of 4-(dimethylamino)pyridine and Et_3N in DCM[60] with 40% yield. Conversion into the chloro derivative **117** was confirmed by NMR spectroscopy. The upfield shift of the signals of the methylene bound to the halogen atom was observed in both the ^1H NMR and ^{13}C NMR spectra: the doublet integrating for two protons, which overlapped with the singlet of 3-CH_2, shifted from δ 4.15 ppm to δ 4.12 ppm in the ^1H NMR spectrum, the singlet for the carbon atom shifted from δ 58.70 ppm to δ 39.67 ppm in the ^{13}C NMR spectrum (figure 67).

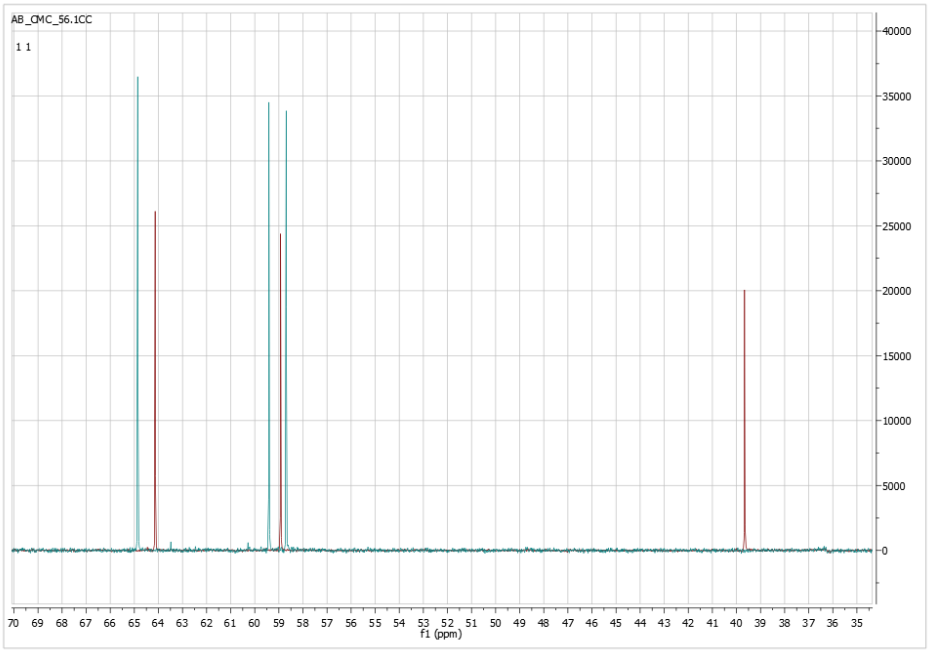

Figure 67. Expansion of the ^{13}C NMR of the allylic chloride **117** (red) superimposed to the ^{13}C NMR of the allylic alcohol **115** (blue).

The coupling reaction of the allylic chloride **117** with commercially available 6-chloropurine **118** was performed in the presence of caesium carbonate as a base catalyst in DMF.[19] Alkylation of **118** provided the desired *N*-9 adduct **119** in 56% yield (scheme 36). The NMR spectra of **119** were in agreement with the literature[19] and confirmed the identity of the compound. The *N*-7 alkylated isomer was obtained as a minor product of the reaction (23% yield), with a ratio *N*-9:*N*-7 of 2.5:1. Deprotection of the *tert*-butyldimethylsilyl groups using tetrabutylammonium fluoride trihydrate in THF at low temperature (-10 °C to 0 °C) furnished **120** in excellent yield (94%). The following amination by treatment with a saturated (7M) methanolic solution of ammonia at 75 °C over 48 hours afforded **27** in 56% yield.

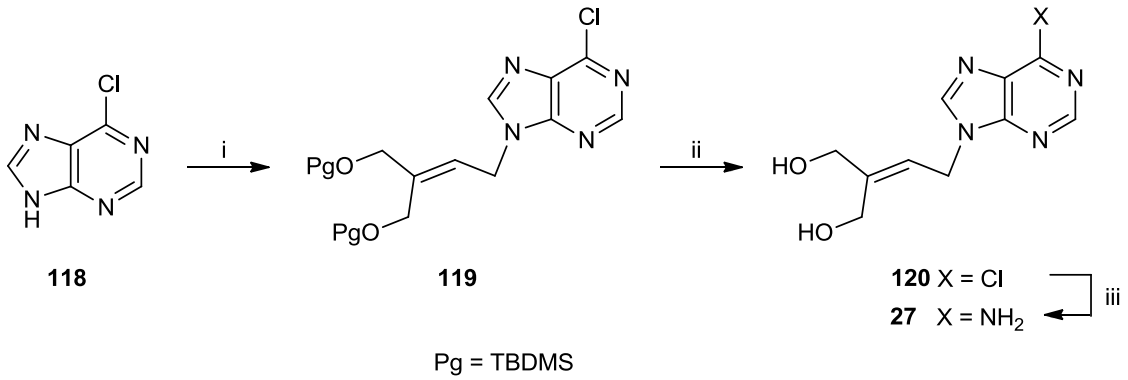

Scheme 36. Alkylation of 6-chloropurine **118**. *Reagents and conditions:* i) Cs_2CO_3, allylic chloride **117**, DMF, rt, 20h (**119**, 56% yield; *N*-7 adduct, 23% yield); ii) TBAF·$3H_2O$, THF, -10 °C to 0 °C, 2h (**120**, 94% yield); iii) NH_3, MeOH, 75 °C, 48h (**27**, 56% yield).

To investigate the possibility of increasing anti-DENV activity and selectivity of acyclic adenosine analogues, structurally modified heterobases were combined to the linear linker. The general procedure of alkylation was applied to a series of 6-chloro-7-deazapurine derivatives. Besides the commercially available 6-chloro-7-deazapurine **121** and the benzo-fused 7-deaza-6-chloropurine **97** (refer to paragraph 2.2.3.1 for the synthesis of **97**), the methyl 7-carboxylate derivative **123** was used in the alkylation procedure as well. This heterobase was selected because it is a readily accessible intermediate for the synthesis of 7-carbamoyl-7-deazaadenosine analogues, such as the DENV RdRp inhibitor NITD449 (see paragraph 1.2.2.2 for details). A two-step synthetic procedure for **123** had been reported by Chen *et al*.[11] and was performed in this work (scheme 37).

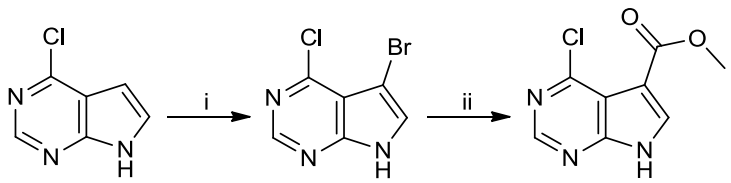

121 **122** **123**

Scheme 37. Synthesis of methyl 7-deaza-6-chloropurine-7-carboxylate **123**. *Reagents and conditions:* i) *N*-bromosuccinimide, DCM, rt, 3h (**122**, 72% yield); ii) *n*-butyllithium, THF, -78 °C, 0.5h, then methyl chloroformate, -78 °C to rt, 3h (**123**, 61% yield).

Commercially available 6-chloro-7-deazapurine **121** was converted into the 7-bromo derivative **122** by treatment with *N*-bromosuccinimide with 72% yield. Lithium-bromine exchange and following reaction of the organolithium compound (generated *in situ*) with the carbonyl group of methyl chloroformate afforded the methyl 7-carboxylate derivative **123** in good yield (61%).
The alkylation of 6-chloro-7-deazapurine **121** and the synthesised analogues **97** and **123** is illustrated in schemes 38 and 39.

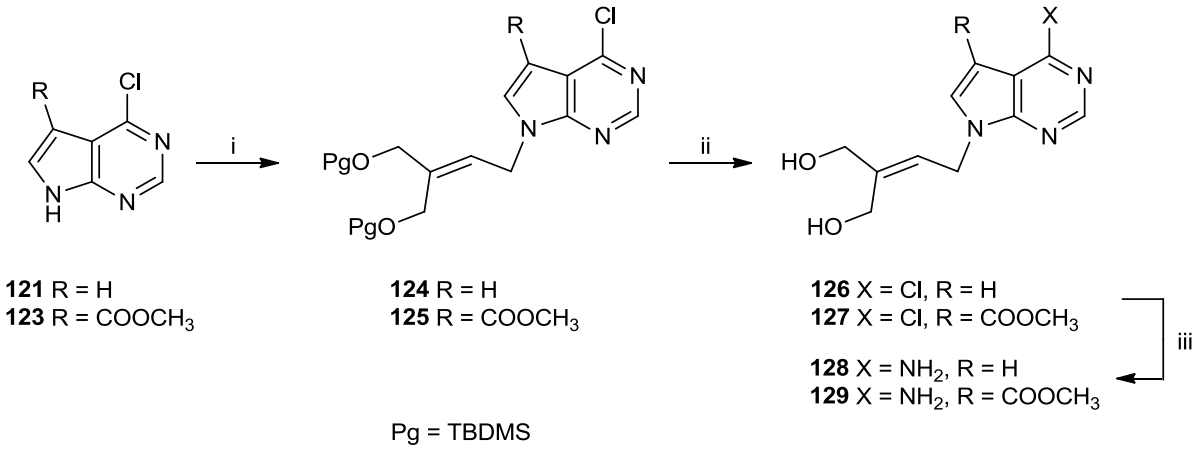

121 R = H
123 R = $COOCH_3$

124 R = H
125 R = $COOCH_3$

126 X = Cl, R = H
127 X = Cl, R = $COOCH_3$
128 X = NH_2, R = H
129 X = NH_2, R = $COOCH_3$

Pg = TBDMS

Scheme 38. Alkylation of 6-chloro-7-deazapurine **121** and methyl 7-carboxylate derivative **123**. *Reagents and conditions:* i) Cs_2CO_3, allylic chloride **117**, DMF, rt, 20h (**124**, 69% yield; **125**, 78% yield); ii) TBAF·$3H_2O$, THF, -10 °C to 0 °C, 2h (**126**, 76% yield; **127**, 100% yield); iii) NH_4OH aq. solution, 1,4-dioxane, 90 °C, 48h (**128**, 85% yield) or NH_3, MeOH, 75 °C, 48h (**129**, 34% yield).

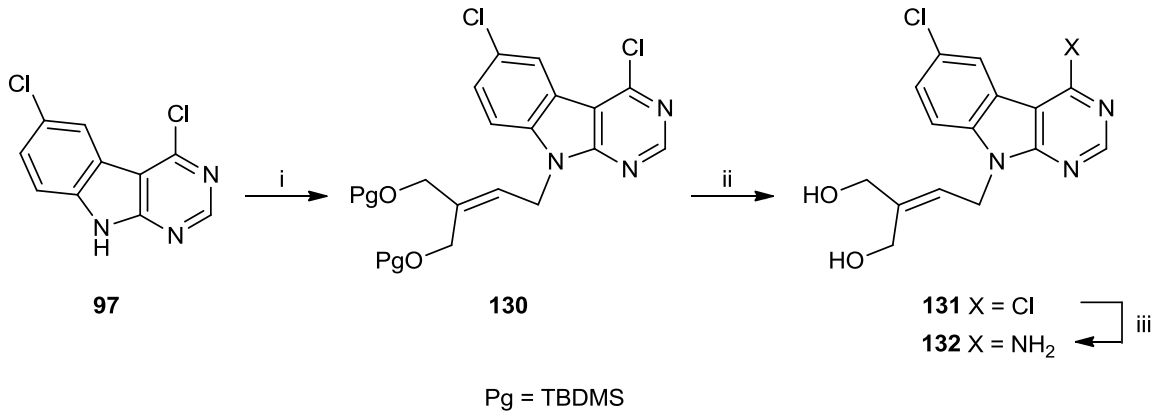

Scheme 39. Alkylation of 4,6-dichloro-9*H*-pyrimido[4,5-*b*]indole **97**. *Reagents and conditions:* i) Cs_2CO_3, allylic chloride **117**, DMF, rt, 20h (**130**, 65% yield); ii) TBAF·$3H_2O$, THF, -10 °C to 0 °C, 2h (**131**, 71% yield); iii) NH_3, MeOH, 75 °C, 48h (**132**, 26% yield).

Compounds **124**, **125** and **130** were obtained in good yields (from 65% to 78%) and submitted to the TBAF-mediated cleavage of silyl ethers (schemes 38 and 39). Amination of the deprotected acyclic purine nucleosides **127** and **131** by treatment with a saturated (7M) methanolic solution of ammonia at 75 °C over 48 hours afforded the corresponding target nucleosides **129** and **132** in moderate yields. For the preparation of the 7-deazaadenine analogue **128**, the application of the standard procedure using the methanolic ammonia solution did not lead to the isolation of the desired product. A different procedure consisting of treatment of **126** with a 30% aqueous ammonia solution in 1,4-dioxane then allowed for full conversion of the starting material and furnished the target nucleoside **128** in excellent yield after chromatographical purification.

Before applying the phosphoramidate ProTide approach to the acyclic nucleoside analogues, an optimisation of the synthesis of the representative compounds **27** and **128** was performed (schemes 40 and 41). In an attempt to improve the yield of the coupling with the heterobase, the allylic alcohol **115** was converted into the mesylate derivative by treatment with methanesulfonyl chloride in the presence of Et_3N in Et_2O at low temperature (from -78 °C to 0 °C). Filtration of the reaction mixture was crucial to avoid the further conversion of the mesylate intermediate to the chloro derivative **117**. The mesylate intermediate was used directly in the reaction with either 6-chloropurine **118** or 6-chloro-7-deazapurine **121** in the presence of caesium carbonate in DMF to afford **119** and **124**, respectively, allowing for a substancial increase of the yield compared to the previously described method (32% and 40% against 22% and 28% for two steps from the allylic alcohol **115** to **119** and **124**, respectively).

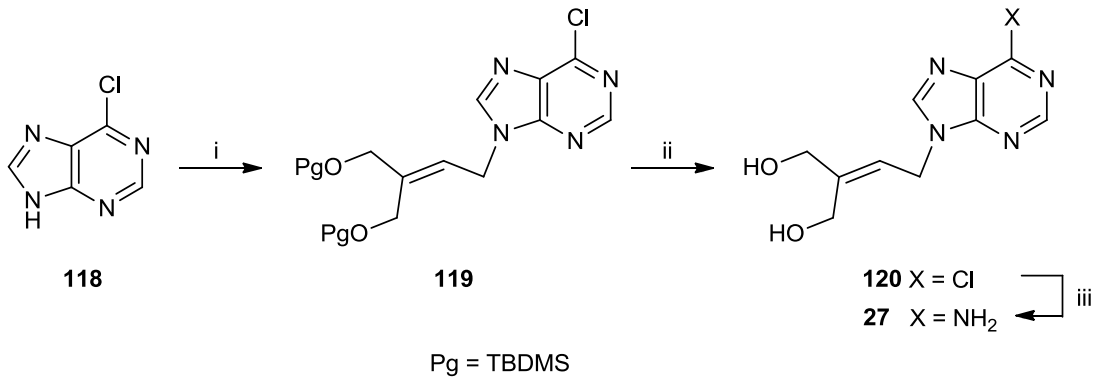

Scheme 40. Optimised synthesis of the acyclic nucleoside **27**. *Reagents and conditions:* i) allylic alcohol **115**, MsCl, Et_3N, Et_2O, -78 °C to 0 °C, 3h, then Cs_2CO_3, DMF, rt, 20h (**119**, 32% yield; *N*-7 adduct, 17% yield); ii) TBAF·$3H_2O$, THF, -10 °C to 0 °C, 2h (**120**, 94% yield); iii) NH_4OH aq. solution, 1,4-dioxane, 90 °C, 48h (**27**, 90% yield).

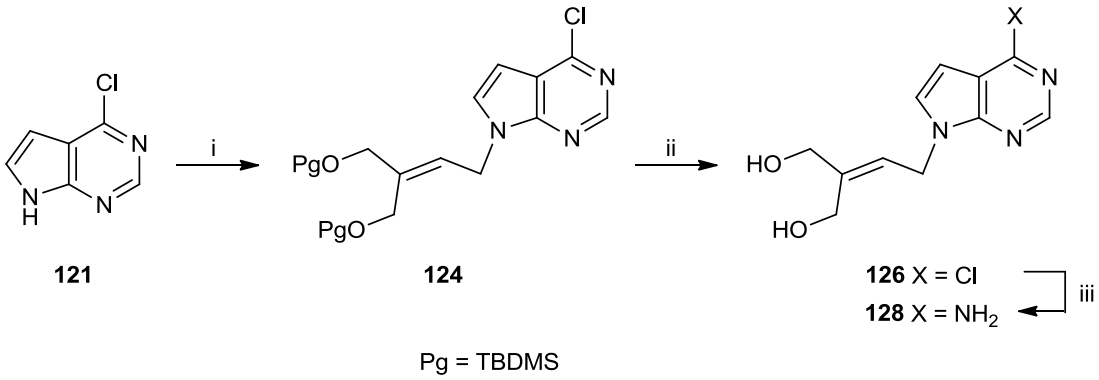

Scheme 41. Optimised synthesis of the acyclic nucleoside **128**. *Reagents and conditions:* i) allylic alcohol **115**, MsCl, Et_3N, Et_2O, -78 °C to 0 °C, 3h, then Cs_2CO_3, DMF, rt, 20h (**124**, 40% yield); ii) 80% aq. AcOH, THF, rt, 24h (**126**, 80% yield); iii) NH_4OH aq. solution, 1,4-dioxane, 90 °C, 48h (**127**, 85% yield).

The optimised procedure for preparation of the adenosine analogue **27** involved fluoride-mediated deprotection, followed by amination carried out using a 30% aqueous ammonia solution in 1,4-dioxane at 90 °C (scheme 40). Trituration of the crude compound in ethanol afforded **27** in 90% yield. In the optimised synthesis of the acyclic 7-deaza nucleoside **128**, the cleavage of the *tert*-butyldimethylsilyl ethers in acidic conditions was found to be superior to the previously described method based on the use of tetrabutylammonium fluoride. In fact, treatment of **124** with a 80% aqueous acetic acid solution in THF at room temperature afforded the fully

deprotected nucleoside **126** in excellent yield and was used directly in the amination step without need for chromatographical purification (scheme 41).

The anti-DENV activity and cytotoxicity *in vitro* of the synthesised acyclic adenosine and 7-deazaadenosine analogues **27**, **128**, **129** and **132** were evaluated by our collaborators (see section 2.3 for details).

2.2.4.2 Synthesis of acyclic adenosine analogue ProTides

The phosphoramidate ProTide strategy was applied to the acyclic nucleoside analogues with the aim to boost the anti-DENV activity of the adenosine analogue **27** as well as to overcome an issue of cytotoxicity common among the nucleosides within this family. Additionally, the nucleotide prodrug approach may improve the biological profile of inactive acyclic nucleoside analogues, such the 7-deaza derivative **128** (refer to section 2.3 for details). The linear scaffold designed to replace the ribose moiety is characterised by the presence of two primary hydroxyl groups with similar reactivity towards the phosphoramidating reagent, regardless of the employed methodology. According to the predicted binding mode of the acyclic adenosine analogues in the active site of the DENV RdRp (see paragraph 2.1.2.2 for details), phosphorylation of the hydroxyl group in *trans* position of the alkene should occur. Therefore, the *trans* mono-*O*-phosphoramidate (figure 68) represents the target nucleotide prodrug. The *O*-*O*-cyclic phosphoramidate (figure 68) is a nucleotide prodrug of interest as well, due to the similarity to 3'-*O*-5'-*O*-cyclic phosphate ester nucleotide prodrugs that were recently reported as anti-HCV agents.[61, 62, 63]

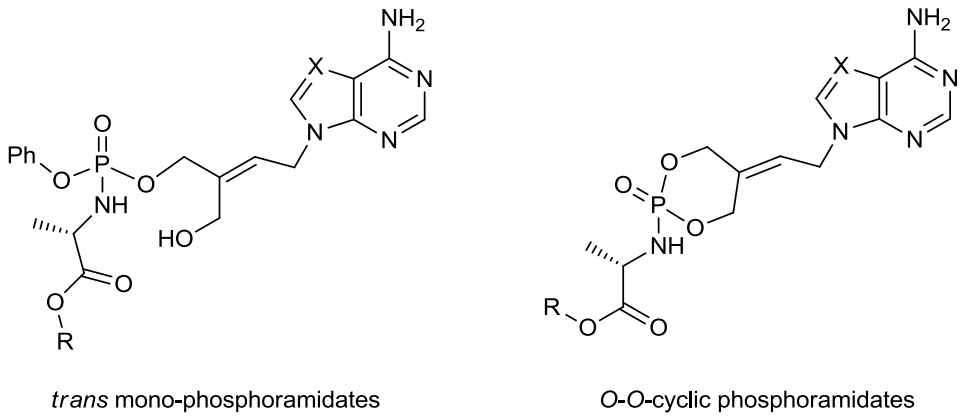

trans mono-phosphoramidates *O*-*O*-cyclic phosphoramidates

Figure 68. General structures of target phosphoramidate ProTides.

The bis-*O*,*O*-phosphoramidates and the *cis* isomer mono-*O*-phosphoramidate are side-products of the coupling reaction performed on unprotected acyclic adenosine analogues (figure 69).

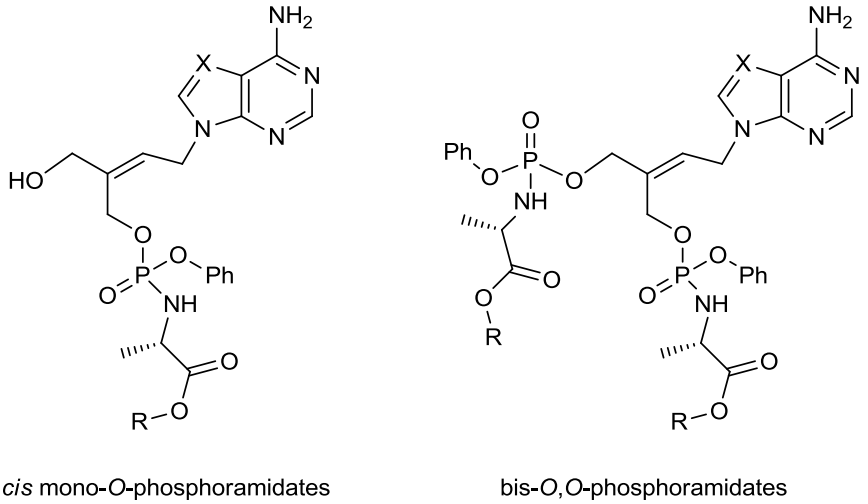

cis mono-*O*-phosphoramidates bis-*O*,*O*-phosphoramidates

Figure 69. General structures of the phosphoramidate side-products of the coupling reaction.

For the preparation of phosphoramidate ProTides of acyclic nucleosides, the method based on *t*BuMgCl and *p*-nitrophenolate reagent was first investigated (scheme 42). The acyclic adenosine analogue **27** was treated with 1 equivalent of **38** (refer to section 2.2.1 for the preparation of **38**) in the presence of *t*BuMgCl in DMF. Complete consumption of the starting material was achieved in few hours at room temperature and the corresponding *O*-*O*-cyclic L-alanine isopropyl ester phosphoramidate **133** was isolated in 39% yield with a purity of 96% according to analytical HPLC. The same reaction conditions were successfully applied to the 7-deazaadenosine analogue **128** and provided the *O*-*O*-cyclic phosphoramidate **134** in 26% yield with a purity of 96% according to analytical HPLC.

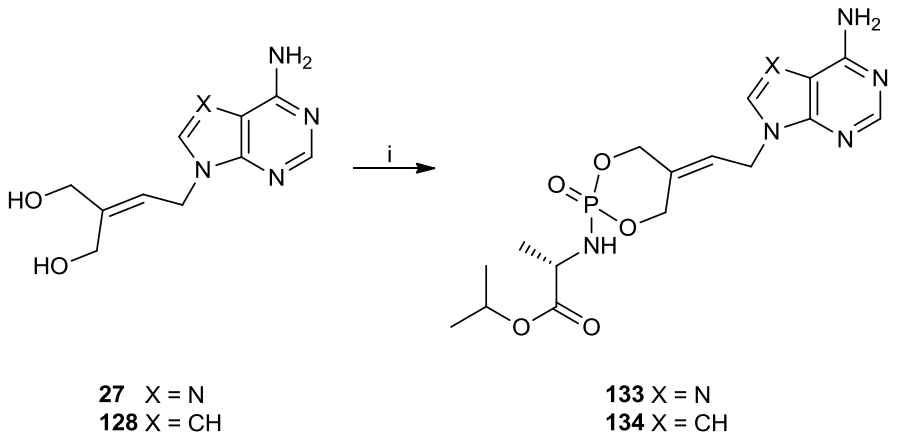

27 X = N
128 X = CH

133 X = N
134 X = CH

Scheme 42. Synthesis of *O*-*O*-cyclic phosphoramidate ProTides **133** and **134**. *Reagents and conditions:* i) *t*BuMgCl, *p*-nitrophenolate reagent **38**, DMF, 4h (**133**, 39% yield; **134**, 26% yield).

With the aim to facilitate the preparation of the desired *trans* mono-*O*-phosphoramidate ProTides, the deprotection of only one of the hydroxyl groups of **124** was attempted using aqueous acetic acid solution (scheme 43). Different ratios between acetic acid, water and THF were explored, as summarised in table 12, and the reactions were monitored by thin layer chromatography. Deprotection of both functionalities occurred simultaneously when the fully protected nucleoside **124** was treated at room temperature, whereas no conversion of the starting material was observed upon reaction at 0 °C. Traces of the mono-protected species **135** and **136** were formed according to thin layer chromatography and NMR spectroscopy when acetic acid, water and THF were used at a ratio of 2:1:1, however the fully deprotected compound **126** was the main product of the reaction and the mono-protected intermediates **135** and **136** could not be isolated.

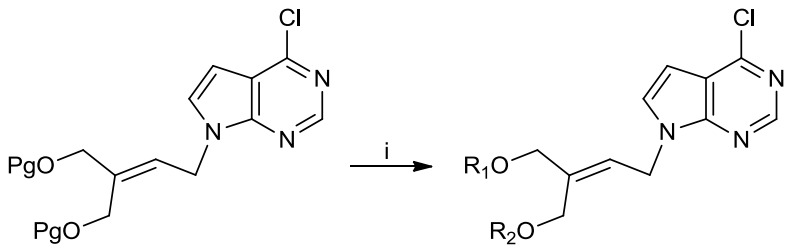

124

Pg = TBDMS

126 $R_1 = R_2 = Pg$
135 $R_1 = H$, $R_2 = Pg$
136 $R_1 = Pg$, $R_2 = H$

Scheme 43. Attempts of partial deprotection of acyclic nucleoside **124**. *Reagents and conditions:* i) as in table 12.

Table 12. Attempts of partial deprotection of acyclic nucleoside **124**.

Reagents and conditions	**Products**
AcOH, H_2O, THF (4:1:1), rt, 24h	fully deprotected **126**
AcOH, H_2O, THF (4:1:1), 0 °C, 6h	fully protected **124**
AcOH, H_2O, THF (2:3:1), rt, 24h	fully deprotected **126**
AcOH, H_2O, THF (2:1:1), rt, 48h	fully deprotected **126** and traces of mono-protected **135** and **136**

As a procedure for the partial deprotection of acyclic nucleosides could not be developed, the synthesis of *trans* mono-*O*-phosphoramidates was attempted on unprotected acyclic nucleosides. The application of innovative MWI conditions (refer to section 2.2.5 for a description of the developed methodology) to the preparation of this class of phosphoramidates was investigated (scheme 44).

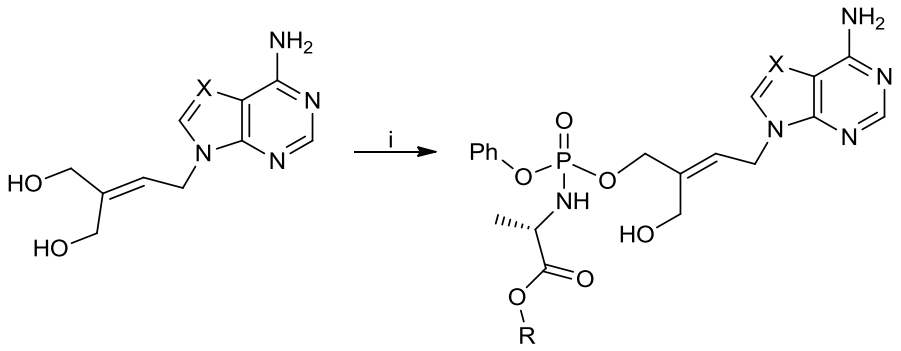

27 X = N
128 X = CH

137 X = N
138 X = CH, R = *i*Pr
139 X = CH, R = Bn

Scheme 44. Synthesis of mono-*O*-phosphoramidate ProTides **137**, **138** and **139**. *Reagents and conditions:* i) NMI, phosphorochloridate **36**, THF/pyridine, MWI (300W), 50 °C, 10 min (**137**, 3% yield; **138**, 6% yield) or NMI, phosphorochloridate **35**, THF/pyridine, MWI (300W), 50 °C, 30 min (**139**, 4% yield).

When the reaction mixture containing the acyclic adenosine analogue **27**, phosphorochloridate **36** (1.7 equivalents) (see section 2.2.1 for the preparation of **36**) and an excess of NMI in THF and pyridine was heated by MWI at 50 °C for a time as short as 10 minutes, the starting material was converted into three different products according to thin layer chromatography. Intense chromatographical purification allowed for the separation of the bis-*O*,*O*-phosphoramidates (14% yield, **140** in section 4.2.5) and a mixture of *cis* and *trans* mono-*O*-phosphoramidates (17% yield).

The number of equivalents of phosphoramidating reagent was found to influence the ratio of bis-*O*,*O*-phosphoramidates and mono-*O*-phosphoramidate. In fact, a slight reduction of the number of equivalents from 1.7 to 1.5 halved the amount of the undesired bis-*O*,*O*-phosphoramidates **140** (6% yield) whereas the mixture containing the *cis* and the *trans* mono-*O*-phosphoramidates was obtained in a comparable yield of 13% after purification by column chromatography. In order to separate the mixture of the two isomers, repetitive purification by column chromatography was performed and allowed for the isolation of the FE isomer, that was characterised by two signals at δ 2.91 and 2.79 ppm in the ^{31}P NMR spectrum, in 3% yield. The isolated ProTide was characterised by NMR spectroscopy and mass spectrometry (the observed *m/z* was 527.2 for [MNa^+]). The methylene bearing the phosphoramidate moiety could be distinguished thanks to the coupling between its carbon atom and the phosphorus atom observed in the ^{13}C NMR spectrum: in fact, the CH_2OP appeared as a triplet at δ 68.27 ppm due to the overlapping of the two doublets (one for each diastereoisomer), whereas the CH_2 bound to the free hydroxyl group was characterised by two singlets at δ 57.31 ppm and δ 57.28 ppm. In the 2D HSQC spectrum, the apparent triplet for the CH_2OP in the ^{13}C NMR spectrum correlated to the multiplet for the methylene group at δ 4.62 – 4.54 ppm in the ^{1}H NMR spectrum. Finally, the 2D NOESY experiment allowed for the characterisation of the configuration of isomer. The observation of a correlation signal between the multiplet for the methylene bearing the phosphoramidate moiety and the proton in the 2-position demonstrated that the desired *trans* isomer of the alkene **137** was obtained (figure 70).

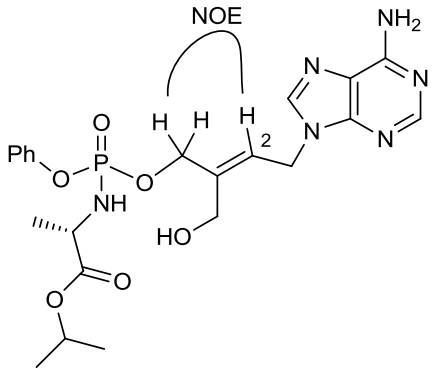

137

Figure 70. The NOESY correlation signal observed for the *trans* mono-*O*-phosphoramidate **137**.

The *trans* mono-*O*-phosphoramidate of the acyclic 7-deazaadenosine analogue **128** were prepared and characterised as described for the ProTide **137** (scheme 44). The reaction of **128** with the

phosphorochloridate bearing the isopropyl ester **36** in the presence of NMI in a mixture of THF and pyridine under MWI conditions, followed by purification by column chromatography, afforded the ProTide **138** in 6% yield as well as the bis-*O*,*O*-phosphoramidates in 4% yield (**141** in section 4.2.5) as a side-product. Similarly, the benzyl ester derivatives **139** were obtained from the microwave-assisted coupling reaction between the parent nucleoside **128** and the phosphorochloridate **35** (scheme 44). Intense chromatographical purification furnished the desired product in 4% yield and the bis-*O*,*O*-phosphoramidates in 5% yield (**142** in section 4.2.5).

Previous attempts for the synthesis of *trans* mono-*O*-phosphoramidate ProTides of acyclic nucleosides were performed using NMI under conventionally used conditions.[30] The 7-deazaadenosine derivative **128** was treated with the phosphorochloridate **35** (see section 2.2.1 for the preparation of **35**) and an excess of NMI either in THF or in a mixture of THF and pyridine at room temperature. However, the formation of phosphoramidate products was not observed despite the long reaction time (40 hours). These observations demonstrated that heating by MWI significantly increased the reactivity of the acyclic nucleoside analogues in the coupling with the phosphorochloridate, despite the lack of selectivity between the two primary alcohol groups.

The synthesised *trans* mono-*O*-phosphoramidates **137**, **138** and **139** were found to be prone to spontaneous conversion to the corresponding *O*-*O*-cyclic phosphoramidates. The instability was confirmed by analytical HPLC analysis, which revealed the formation of a second set of diastereoisomers with the same retention times observed for compounds **133** and **134**. In the case of ProTide **139**, the identity of the second species was confirmed by mass spectrometry: in fact, the *m/z* of 458.2 and 480.2 were observed for the *O*-*O*-cyclic phosphoramidate bearing the L-alanine benzyl ester moiety ([MH^+] and [MNa^+], respectively). Further decomposition may also occur over time, as suggested by the presence of a third peak in the HPLC chromatogram of the ProTides **138** and **139**, corresponding to a more hydrophilic product that could not be identified.

The prepared *O*-*O*-cyclic Protides **133** and **134**, the *trans* mono-*O*-phosphoramidate ProTides **137**, **138** and **139** as well as the corresponding bis-*O*,*O*-phosphoramidates **140**, **141** and **142** were sent to our collaborators for biological evaluation *in vitro* (see section 2.3 for details). The results are currently being awaited.

2.2.4.3 Synthesis of acyclic adenosine analogues – second scaffold

The structural modification of the acyclic adenosine analogue **28** is the additional methyl group in the position corresponding to the α-anomeric position of nucleosides. For the preparation of **28**,

alkylation of 6-chloropurine **118** by the secondary allylic chloride **146** was initially attempted (scheme 45).

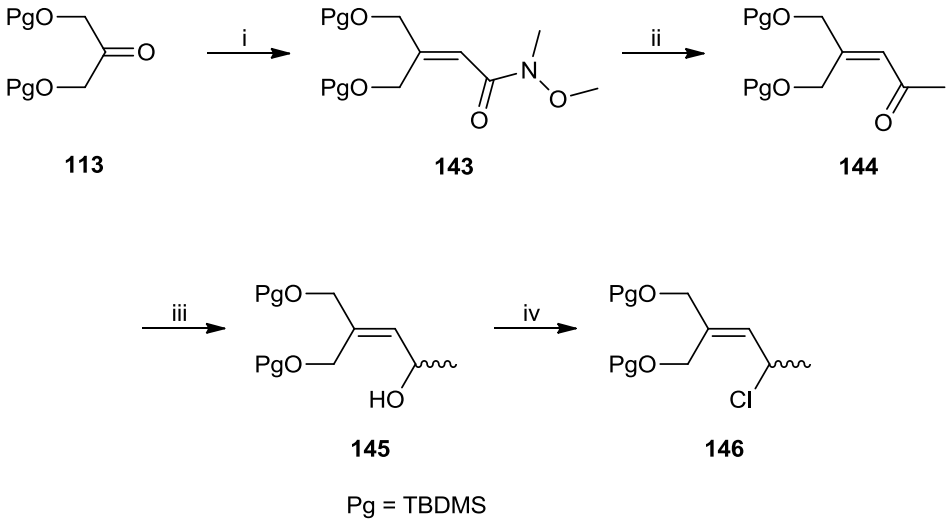

Scheme 45. Synthesis of the secondary allylic chloride **146**. *Reagents and conditions:* i) *N*-methoxy-*N*-methyldiethylphosphonoacetate, NaH, THF, 0 °C to rt, 1h (**143**, 87% yield); ii) MeLi, Et_2O, -78 °C to 0 °C, 2h (**144**, 73% yield); iii) DIBALH, DCM, -20 °C to 0 °C, 1h (**145**, 60% yield); iv) MsCl, pyridine, 0 °C to rt, 2h (**146**, 33% yield).

The secondary allylic chloride **146** was synthesised from the protected 1,3-dihydroxyacetone **113**, whose preparation was described in paragraph 2.2.4.1. The *N*-methoxy-*N*-methylamide (Weinreb amide) derivative **143** was prepared under Wittig-Emmons conditions[64] as intermediate for the synthesis of the ketone **144**. The derivatisation to the Weinreb amide is an effective strategy for the synthesis of ketones,[65] as this functional group reduces the propensity of Grignard reagents or organolithium compounds to overadd to the substrate, thus preventing the formation of a tertiary alcohol.[65]

The reactivity of methyl lithium towards the previously prepared ester intermediate **114** and towards the Weinreb amide **143** were compared. Treatment of **114** with one equivalent of methyl lithium at -78 °C led to the isolation of the bis-adduct **147** (scheme 46), whereas no traces of the ketone compound **144** were observed in the ^1H NMR spectrum of the crude residue.

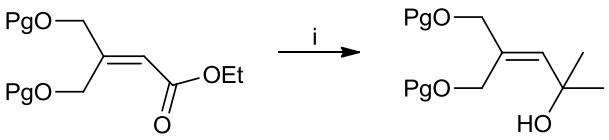

114 **147**

Pg = TBDMS

Scheme 46. Reaction of the ester intermediate **114** with methyl lithium. *Reagents and conditions:* i) MeLi (1.0 eq.), Et_2O, -78 °C, 2h (**147**, crude).

The presence of a singlet integrating for six protons at δ 1.28 ppm in the ^{1}H NMR spectrum confirmed the identity of side-product **147**. In contrast, the nucleophilic addition of methyl lithium to the Weinreb amide **143** afforded the desired ketone **144** (scheme 45) as only product of the reaction in good yield (73%).

The following reduction of **144** was accomplished by treatment with DIBALH and furnished the allylic secondary alcohol **145** in 60% yield. A second compound was isolated in 15% yield and identified as the isomer **148** (scheme 47), whose formation was due to transsilylation. Compared to the ^{1}H NMR spectrum of compound **145**, in the ^{1}H NMR spectrum of **148** the multiplet for the H-2 shifted upfield (from δ 4.62 – 4.56 to 4.59 to δ 3.71 – 3.66 ppm) and two doublets of doublets were observed at δ 2.09 and 1.80 ppm for one of the methylene groups in 4-position, rather than the singlet at δ 4.06 ppm observed in **145**. Additionally, the free hydroxyl group gave a broad singlet at δ 3.73 ppm, rather than at δ 2.45 ppm observed for the 2-OH of **145**. The identity of the isomers was confirmed by mass spectrometry (the observed *m/z* was 383.2 [MNa^+]).

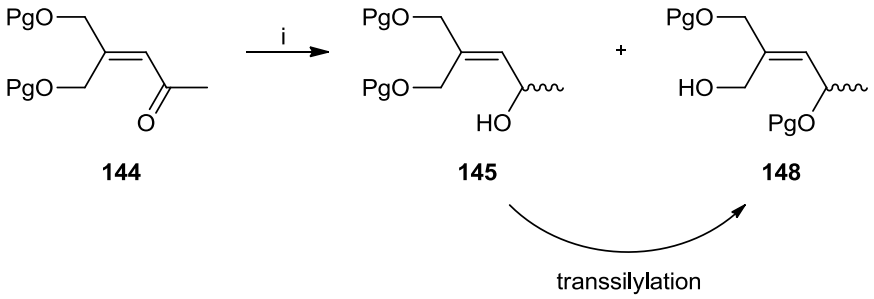

144 **145** **148**

Scheme 47. Reduction of the ketone **144** associated with transsilylation. *Reagents and conditions:* i) DIBALH, DCM, -20 °C to 0 °C, 1h (**145**, 60% yield, **148**, 15% yield).

For the chlorination of the secondary allylic alcohol **145** (scheme 48), the conditions previously employed for the preparation of the primary allylic chloride **117** were applied (refer to paragraph 2.2.4.1). However, treatment of **145** with *p*-toluenesulfonyl chloride, in the presence of 4-(dimethylamino)pyridine and Et_3N in DCM did not lead to the formation of the corresponding chloro derivative **146**. In contrast, the use of methanesulfonyl chloride and Et_3N in DCM at room temperature provided the secondary allylic chloride **146** in 24% yield. A better yield (33%) could be obtained by performing the reaction with methanesulfonyl chloride in pyridine. As described for the primary allylic chloride **117**, an upfield shift of the methyne bound to the chlorine atom was observed in the ^{13}C NMR spectrum, from δ 63.65 ppm to δ 52.97 ppm.

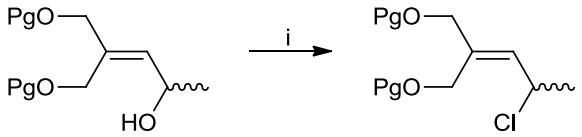

145 **146**

Pg = TBDMS

Scheme 48. Chlorination of the secondary allylic alcohol **145**. *Reagents and conditions:* i) MsCl, pyridine, 0 °C to rt, 2h (**146**, 33% yield).

The secondary allylic chloride **146** was used in the coupling reaction with the heterobase (scheme 49). 6-Chloropurine **118** was treated with **146** in the presence of caesium carbonate in DMF over 20 hours. However, the formation of the alkylated product **149** was observed neither at room temperature nor at higher temperature (60 °C or 120 °C).

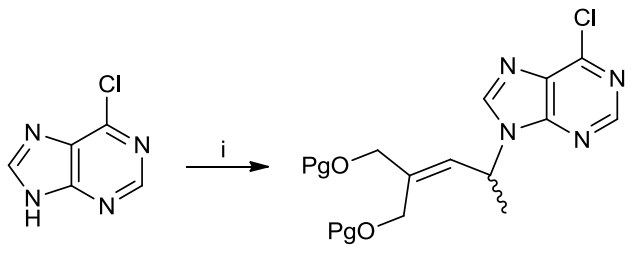

118 **149**

Pg = TBDMS

Scheme 49. Synthesis of the acyclic nucleoside **149** from the secondary allylic chloride **146**. *Reagents and conditions:* i) Cs_2CO_3, allylic chloride **146**, DMF (see text for details).

Therefore, the synthesis of the target compound **149** via the mesylate derivative of **145** was attempted by treating the secondary allylic alcohol **145** with methanesulfonyl chloride in the presence of Et_3N in Et_2O at low temperature (from -78 °C to 0 °C). These conditions were not successful and the mesylate intermediate could not be prepared.

Finally, Mitsunobu reaction conditions were employed (scheme 50):[66] the coupling reaction between the alcohol **145** and 6-chloropurine **118** was carried out in the presence of triphenylphosphine and di-isopropyl azodicarboxilate in THF at reflux and afforded the desired product **149** in 22% yield. Performing the reaction in refluxing 1,4-dioxane failed to improve the yield as compound **149** could not be isolated among other species.

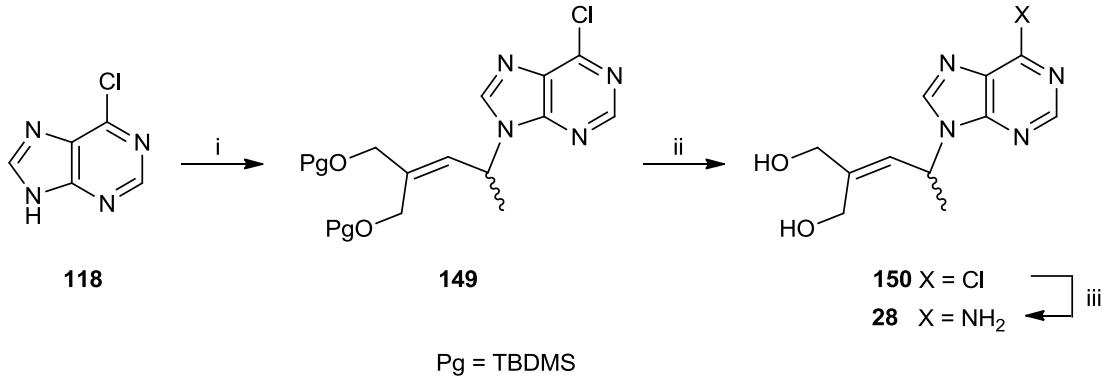

Scheme 50. Synthesis of the target acyclic nucleoside **28** as enantiomeric mixture from the secondary allylic alcohol **145**. *Reagents and conditions:* i) allylic alcohol **145**, Ph_3P, DIAD, THF, reflux, 20h (**149**, 22% yield); ii) 80% aq. AcOH, THF, rt, 24h (**150**, 71% yield); iii) NH_4OH aq. solution, 1,4-dioxane, 90 °C, 40h (**28**, 64% yield).

The target nucleoside **28** was obtained as a mixture of two enantiomers, following deprotection of the *tert*-butyldimethylsilyl groups in acidic conditions and amination that was performed by treatment with a 30% aqueous ammonia solution in 1,4-dioxane at 90 °C (scheme 50).

The prepared acyclic adenosine analogue **28** was sent to our collaborators for biological evaluation *in vitro* (see section 2.3 for details) and the results are currently being awaited.

2.2.5 MICROWAVE-ASSISTED SYNTHESIS OF PROTIDES

Nucleoside analogues represent an important class of anticancer and antiviral agents.[59] They are prodrugs that become active upon intracellular conversion to their triphosphate derivative in a cascade of phosphorylation catalysed by cellular kinases. The triphosphate nucleotide analogue then acts a competitive inhibitor of RNA or DNA polymerases, by mimicking the natural substrates of the enzymes, and is incorporated into the nascent nucleic acid.[59]

The development of effective nucleoside analogues is often a challenging process. Besides being toxic and sensitive to metabolic degradation, these compounds are polar and thus they have limited membrane permeability, resulting in both low bioavailability and cellular uptake by passive diffusion. Furthermore, nucleoside analogues as well as their monophosphate and diphosphate derivatives are poor substrates of cellular kinases resulting in an inefficient conversion to the bioactive triphosphates. In particular, the first phosphorylation generally represents the rate-limiting step in the cascade of activation and may compromise the biological activity of the nucleoside analogue.[25, 26]

To overcome these common limitations, nucleotide prodrug strategies have been developed. These prodrugs deliver the monophosphate directly into cells, therefore bypassing the first phosphorylation.[25, 26] The negative charges of the monophosphate moiety are masked by hydrophobic groups resulting in a neutral and lipophilic molecule. The prodrug reaches the intracellular compartment by passive diffusion and releases the monophosphate nucleotide into cells, where it is further phosphorylated to the bioactive triphosphate. As a consequence, the application of nucleotide prodrug strategies has the potential to improve the pharmacokinetic properties and boost the biological activity of the parent nucleoside.[26] The developed nucleotide monophosphate prodrug approaches are summarised in paragraph 1.2.2.1.

Among the number of available strategies, the phosphoramidate ProTide technology has gained validation in the clinic and currently represents the most promising pronucleotide approach. Remarkable examples of the success of phosphoramidate ProTides include the anti-HCV agent Sofosbuvir (PSI-7977, **21**, figure 71)[67] and Tenofovir alafenamide (GS-7340, **22**, figure 71), which was recently approved for the treatment of HIV infections.[68]

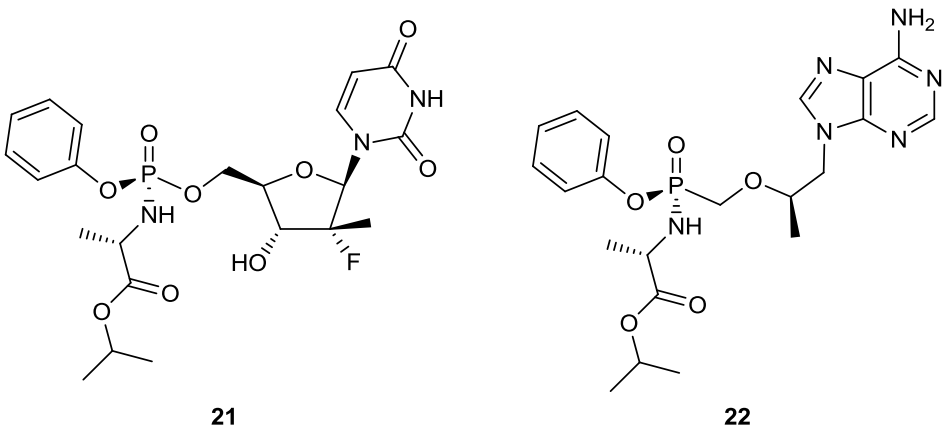

21 22

Figure 71. Structures of Sofosbuvir (PSI-7977, **21**) and Tenofovir alafenamide (GS-7340, **22**).

Structurally, the ProTide consists of an amino acid alkyl or aryl ester, most commonly L-alanine isopropyl or benzyl esters, and a second aryl moiety attached to the phosphorus centre in a chiral molecule.[26, 30] The common methods for the preparation of phosphoramidate ProTides involve the coupling reaction between the parent nucleoside and the chosen aryl amino acid phosphorochloridate in the presence of a base, namely NMI or *t*BuMgCl (scheme 51).[30]

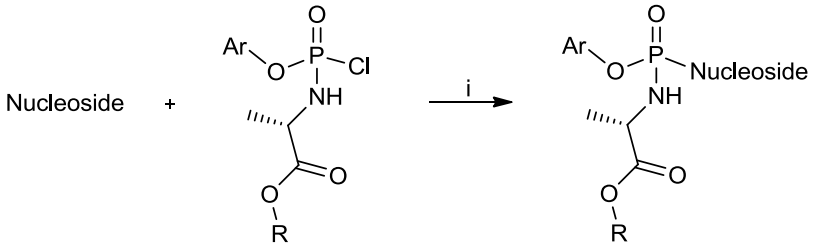

Scheme 51. Standard synthesis of phosphoramidate ProTides.[30] *Reagents and conditions:* i) *t*BuMgCl or NMI, solvent(s), rt, 16-20h.

These procedures are conventionally used, however they are characterised by major limitations: i) use of labile reagents; ii) long reaction time at room temperature; iii) need for additional steps of protection and deprotection; iv) inefficient conversion especially of highly modified nucleoside analogues; v) need for intense purification procedures, resulting in low yields.

Microwave-assistance has become an increasingly popular method to carry out a variety of reactions within short times and has been demonstrated to provide better yields and higher selectivity in nucleoside chemistry.[69] With the aim of developing an improved method for the

synthesis of phosphoramidate ProTides, the application of innovative MWI conditions was investigated and is described in the following section (scheme 52).

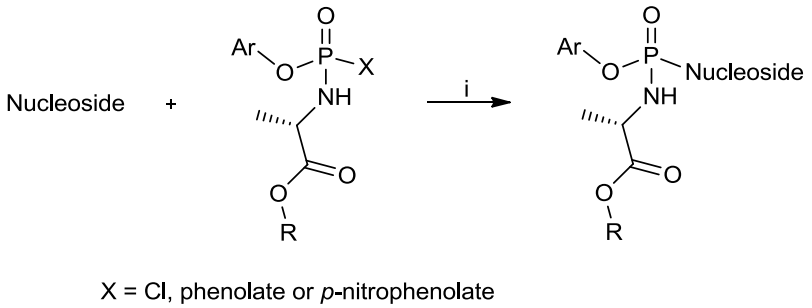

X = Cl, phenolate or *p*-nitrophenolate

Scheme 52. Microwave-assisted synthesis of phosphoramidate ProTides. *Reagents and conditions:* i) *t*BuMgCl or NMI, solvent(s), MWI.

2.2.5.1 Synthesis of phosphoramidating reagents

As the stability of the sensitive phosphorochloridate reagent of the type of **35** and **36** was uncertain, alternative phosphoramidating reagents containing phenolate and *p*-nitrophenolate as leaving groups were prepared to test their reactivity in the coupling reaction (scheme 52). The ideal phosphoramidating reagent should be more stable than the phosphorochloridate, while maintaining sufficient reactivity towards the 5'-hydroxyl group of the nucleoside. The syntheses of the phosphorochloridates **35** and **36** bearing the L-alanine benzyl and isopropyl ester moieties were accomplished as previously described in section 2.2.1, starting from the corresponding L-alanine benzyl and isopropyl ester salts **32** and **33**, respectively. The *p*-nitrophenolate derivatives **37** and **38** were synthesised either from the corresponding phosphorochloridate or from 4-nitrophenyldichlorophosphate, phenol and the chosen L-alanine ester salt, according to procedures that were described in section 2.2.1.

The phosphoramidating reagents **152** and **154** characterised by the phenolate as leaving group were prepared from commercially available starting materials, diphenylchlorophosphate **151** and the corresponding L-alanine benzyl and isopropyl ester salts **32** and **33**, respectively (scheme 53). The reaction was carried out in the presence of Et_3N in DCM under anhydrous conditions and was monitored by ^{31}P NMR. The appearance of a single ^{31}P signal at δ -2.79 ppm or at δ -2.81 ppm suggested the formation of the phenolate reagents **152** and **153**, which were obtained in high yields (96% and 83% respectively) after chromatographical purification.

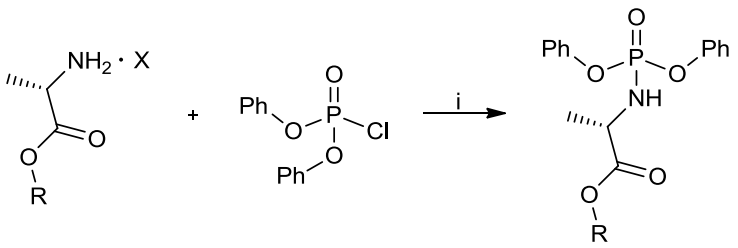

32 X = *p*-TsOH and R = Bn
33 X = HCl and R = *i*Pr

151

152 R = Bn
153 R = *i*Pr

Scheme 53. Synthesis of the phenolate phosphoramidating reagents **152** and **153**. *Reagents and conditions:* i) Et_3N, DCM, -78 °C to rt, 3h (**152**, 96% yield; **153**, 83% yield).

2.2.5.2 Synthesis of ProTides

To explore the potential of microwave-assistance in the synthesis of phosphoramidate ProTides, the natural nucleoside adenosine was chosen as a starting model.

According to the conventional procedures for the synthesis of phosphoramidate ProTides, the use of a different base, NMI or *t*BuMgCl, affects the reaction outcome.[30] The latter does not provide selectivity towards primary hydroxyl groups, whereas the former allows the coupling reaction to occur exclusively at the 5'-hydroxyl group of the nucleoside. As a consequence, the method based on the use of NMI is generally applied on unprotected nucleosides in the presence of multiple reactive functionalities.[30]

First, the applicability of microwave-assistance for the preparation of phosphoramidate ProTides was probed using NMI on the unprotected nucleoside adenosine **154** (scheme 54). Irradiation of the reaction mixture containing the phosphorochloridate **35** in 1,4-dioxane at 85 °C for a short time of 15 minutes allowed for complete consumption of the starting material **154** according to thin layer chromatography, however the desired 5'-*O*-phosphoramidate **155** was only furnished in a very low yield of 4% after chromatographical purification. Additionally, a mixture of bis-*O*,*O*-phosphoramidate adducts was obtained (2% yield). These results suggested that the method based on the use of NMI lacks efficiency and selectivity at high temperature and under MWI conditions.

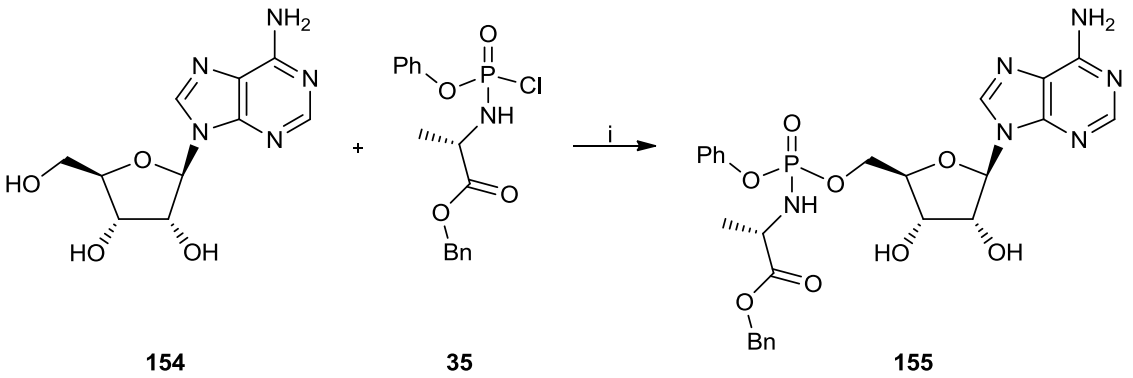

154 **35** **155**

Scheme 54. Microwave-assisted synthesis of the phosphoramidate ProTide **155** using NMI. *Reagents and conditions:* i) NMI, dioxane, MWI (300W), 85 °C, 15 min (**155**, 4% yield).

Following this, the application of microwave-assistance to the method based on the use of the Grignard reagent was investigated on 2',3'-*O*,*O*-protected adenosine **156**. The 2' and 3'-hydroxyl groups of adenosine were protected by treatment of the nucleoside **154** with acetone and a commercially available 70% aqueous solution of perchloric acid (scheme 55), as described in a reported procedure.[70] Full conversion into the desired isopropylidene derivative **156** was observed when the mixture was reacted for 30 minutes at room temperature according to thin layer chromatography. Purification by column chromatography allowed for the isolation of **156** in high yield (95%).

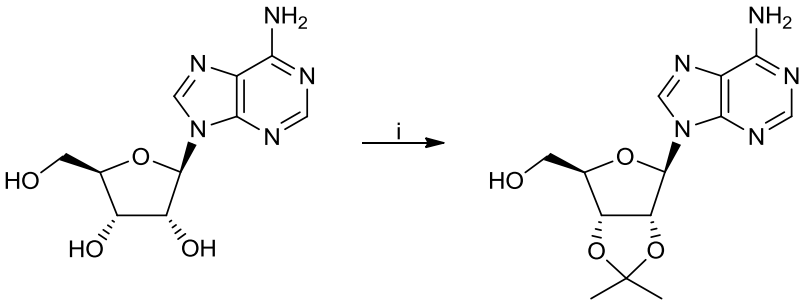

154 **156**

Scheme 55. 2',3'-*O*,*O*-isopropylidene protection of adenosine **154**. *Reagents and conditions:* i) 70% aq. $HClO_4$, acetone, rt, 30 min (**156**, 95% yield).

When 2',3'-*O*,*O*-isopropylidene adenosine **156** in a mixture of THF and NMP in the presence of *t*BuMgCl and of the phosphorochloridate **35** was heated at 65 °C by MWI for a short time of 15

minutes, the desired product was isolated in 28% yield after purification by column chromatography as compared with 55% yield from the corresponding reaction carried out by conventional heating over a time of 2 hours at 55 °C (scheme 56). These results suggested that the method based on the use of the Grignard reagent was compatible with the application of microwave-assistance even when the sensitive phosphorochloridate **35** was employed.

The reactivity of the two alternative phosphoramidating reagents was then evaluated under MWI conditions and compared to the corresponding reactions performed by conventional heating (scheme 56). Both reactions irradiated and conventionally heated carried out in the presence of the phenolate derivatives **152** and **153** were inefficient. However, the use of the *p*-nitrophenolate derivatives **37** and **38** allowed for the complete and clean conversion of the parent nucleoside **156** into the 2',3'-*O*,*O*-protected adenosine phosphoramidate ProTides **157** and **158**, respectively. The yields obtained for **157** and **158** from the reactions by MWI and by conventional heating were found to be comparable. Furthermore, a time of only 2 minutes was found to be sufficient for the full consumption of the starting material **156**, as compared with 30 minutes by conventional heating.

To evaluate the influence of NMP, the coupling reactions were performed under the same conditions in the absence of the second solvent (scheme 56). The reactions, both irradiated as well as conventionally heated, did not reach completion, resulting in lower yields as well as in purification issues. Therefore, NMP was demonstrated to substantially affect the reaction outcome.

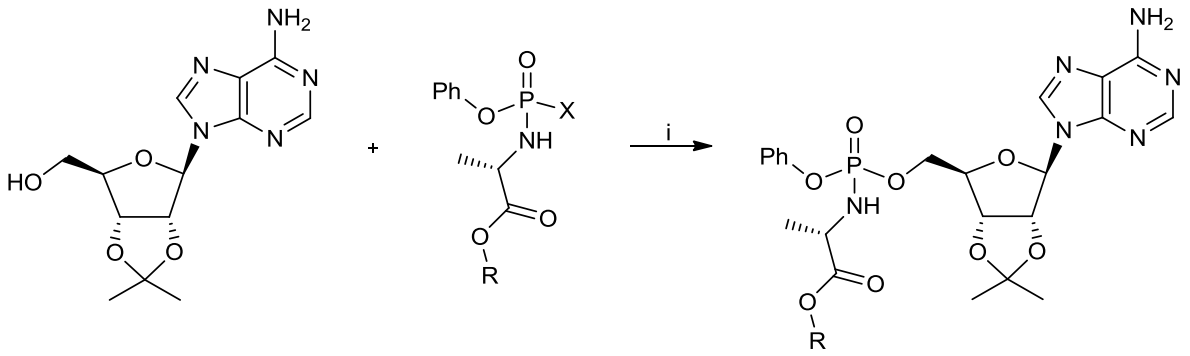

156

35 X = Cl and R = Bn
36 X = Cl and R = *i*Pr
37 X = *p*-nitrophenolate and R = Bn
38 X = *p*-nitrophenolate and R = *i*Pr
152 X = phenolate and R = Bn
153 X = phenolate and R = *i*Pr

157 R = Bn
158 R = *i*Pr

Scheme 56. Synthesis of the phosphoramidate ProTides **157** and **158** using *t*BuMgCl. *Reagents and conditions:* i) *t*BuMgCl (2 equivalents), solvent(s) as described in table 13.

Table 13. Microwave-assisted synthesis of the phosphoramidate ProTides **157** and **158** using *t*BuMgCl compared to reactions by conventional heating.

		Conventional heating to 55 °C		**Heating by MWI to 65 °C**	
Phosphoramidating reagent (equivalents)	**Solvent(s)**	**Time**	**Product(s)**	**Time**	**Product(s)**
35 (2)	THF/NMP	2h	**157** (55%)	15 min	**157** (28%)
36 (2)	THF/NMP	15 min	**158** (52%)	2 min	**158** (36%)
37 (2)	THF/NMP	30 min	**157** (46%)	2 min	**157** (41%)
38 (2)	THF/NMP	30 min	**158** (77%)	2 min	**158** (67%)
152 (2)	THF/NMP	8h (incomplete)	mixture of species	1h (incomplete)	mixture of species
153 (2)	THF/NMP	8h (incomplete)	**158** (15%)	1h (incomplete)	**158** (28%)
37 (2)	THF	8h (incomplete)	mixture of species	1h (incomplete)	mixture of species

Finally, the obtained 2',3'-*O*,*O*-isopropylidene phosphoramidate ProTide **157** was submitted to the final step of deprotection under acidic conditions. Treatment of **157** with a 60% aqueous solution of acetic acid at 95 °C over 16 hours afforded the deprotected phosphoramidate ProTide **155** in a moderate yield of 40% (scheme 57).[71] The process of protection of the parent nucleoside **154**,

coupling with the phosphoramidate reagent **37** followed by the cleavage of the isopropylidene protected group was characterised by a low yield of 15%, thus the multi-step synthesis of **155** was inconvenient.

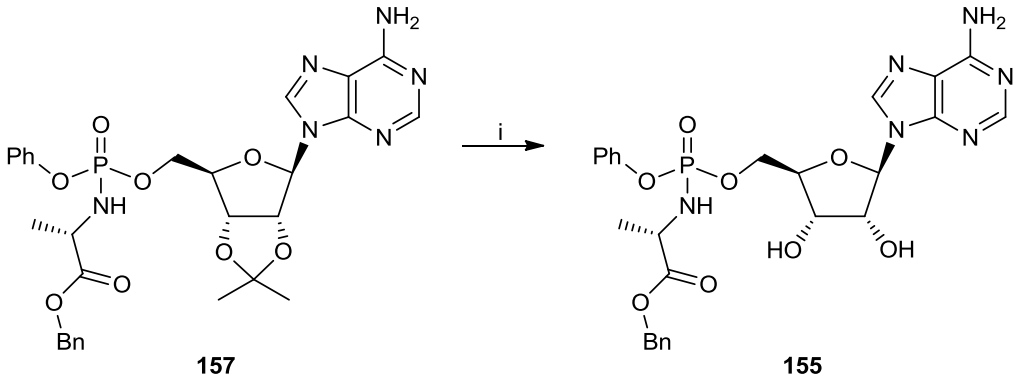

157 **155**

Scheme 57. Deprotection of 2',3'-*O*,*O*-isopropylidene phosphoramidate ProTide **157**. *Reagents and conditions:* i) 60% aq. AcOH, 95 °C, 16h (**155**, 40% yield).

With the aim of reducing the number of steps and increasing the overall yield, the application of the microwave-assisted method using *t*BuMgCl and the *p*-nitrophenolate reagent **37**, selected from the previously described study, was investigated on the unprotected nucleoside **154** (scheme 58). When **154** was treated with 2 equivalents of *t*BuMgCl and **37** in a mixture of THF and NMP and irradiated by microwave at 65 °C, the reaction proceeded smoothly and reached completion within 5 minutes. The 5'-*O*-phosphoramidate **155** was furnished in approximately 40% yield after purification by column chromatography. The increase of the amount of *t*BuMgCl to 3 equivalents resulted in a fast and clean reaction, characterised by a similar yield for the desired product **155**. However, when an even larger excess of *t*BuMgCl (4 equivalents) was employed a mixture of species was obtained according to thin layer chromatography and ^{31}P NMR spectroscopy, suggesting that the selectivity towards the 5'-hydroxyl group was lost.

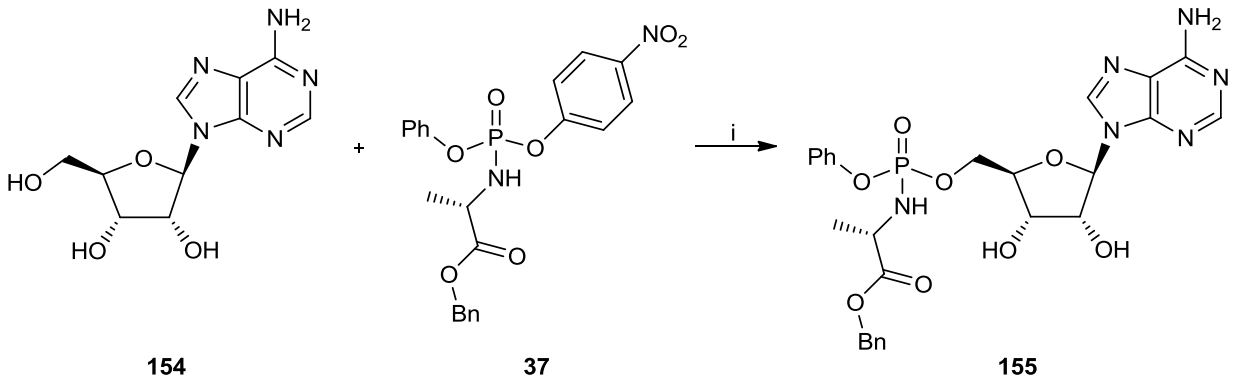

154 **37** **155**

Scheme 58. Synthesis of the phosphoramidate ProTide **155** using *t*BuMgCl and the *p*-nitrophenolate **37**. *Reagents and conditions:* i) *t*BuMgCl, solvent(s) as described in table 14.

Table 14. Microwave-assisted synthesis of the phosphoramidate ProTide **155** using *t*BuMgCl and the *p*-nitrophenolate **37** (2 equivalents) compared to reactions by conventional heating.

		Conventional heating to 55 °C		**Heating by MWI to 65 °C**	
Reagent (equivalents)	**Solvent(s)**	**Time**	**Product(s)**	**Time**	**Product(s)**
*t*BuMgCl (2)	THF/NMP	1h	**155** (49%)	5 min	**155** (38%)
*t*BuMgCl (3)	THF/NMP	1h	**155** (42%)	2 min	**155** (40%)
*t*BuMgCl (4)	THF/NMP	1h	mixture of species	2 min	mixture of species
*t*BuMgCl (2)	THF	20h (incomplete)	**155** (47%)	1h (incomplete)	**155** (14%)

Microwave-assistance induced a reduction of the reaction time from 1 hour with conventional heating to as low as 2 minutes. Of note, the yields obtained under MWI conditions were comparable with the corresponding conventionally heated reactions (table 14). Furthermore, comparable yields were afforded with the reactions performed on the 2',3'-*O*,*O*-protected adenosine **156** (table 13). Therefore, the one-step methodology on the unprotected nucleoside **154** was found to be highly efficient under MWI conditions as well as superior to the protection-coupling-deprotection method.

In conclusion, in the course of this PhD, an improved methodology for the preparation of phosphoramidate ProTides was developed under MWI conditions. The application of the method to the model nucleoside adenosine was demonstrated using the Grignard reagent *t*BuMgCl.

Noteworthy points of the innovative method include the use of stable phosphoramidating reagents, the reduction in reaction time and the ease of chromatographical purification thanks to the full consumption of the parent nucleoside.

Following the described study, the microwave-assisted synthesis of phosphoramidate ProTides was further optimised by Dr Cinzia Bordoni at the School of Pharmacy and Pharmaceutical Sciences, Cardiff University, and Dr Elisa Azzali at the School of Pharmacy, University of Parma. Further studies were carried out by our collaborators to validate the applicability of the methodology to the other natural nucleosides cytidine, uridine, thymidine and guanosine (figure 72).

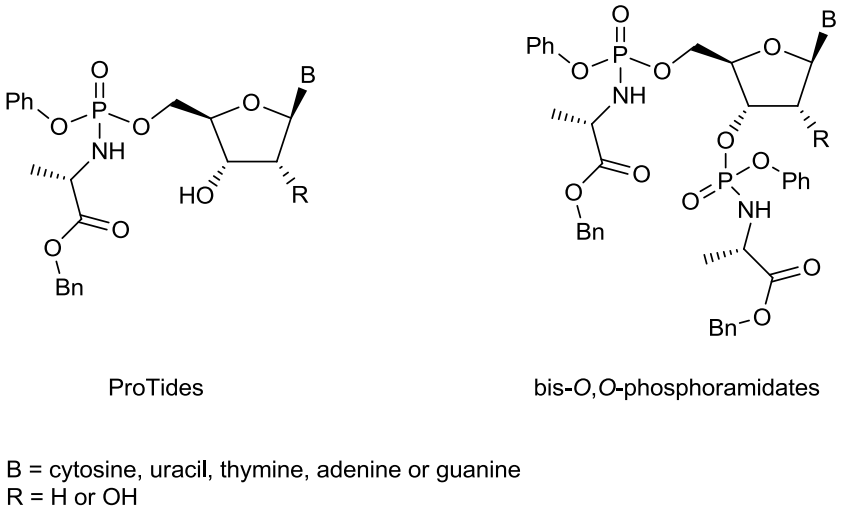

Figure 72. General structures of natural nucleoside ProTides and possible bis-*O*,*O*-phosphoramidates side-products.

The microwave-assisted coupling reactions were compared to the corresponding conventionally heated reactions on the basis of the percentage of formation of the phosphoramidate products, which was measured by analytical HPLC of the reaction mixture. The main results of these studies are summarised in the following tables (tables 15, 16, 17 and 18).

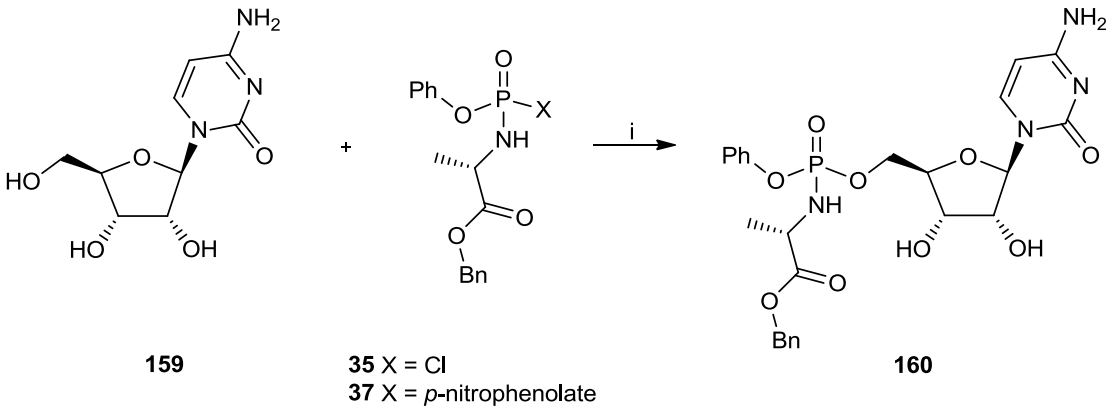

159 **35** X = Cl
37 X = *p*-nitrophenolate **160**

Scheme 59. Synthesis of cytidine phosphoramidate ProTide **160**. *Reagents and conditions:* i) as described in table 15.

Table 15. Microwave-assisted synthesis of cytidine phosphoramidate ProTide **160** compared to reactions by conventional heating.

		Conventional heating to 55 °C				**Heating by MWI to 65 °C**			
Reagents (equivalents)	**Solvent(s)**	**Time**	**HPLC analysis**			**Time**	**HPLC analysis**		
			159	**160**	bis		**159**	**160**	bis
*t*BuMgCl (3) **37** (2)	DMF	4h	-	45%	3%	30 min	19%	81%	-
NMI (6.3) **35** (3)	THF/pyridine	24h	89%	11%	-	30 min	89%	8%	-

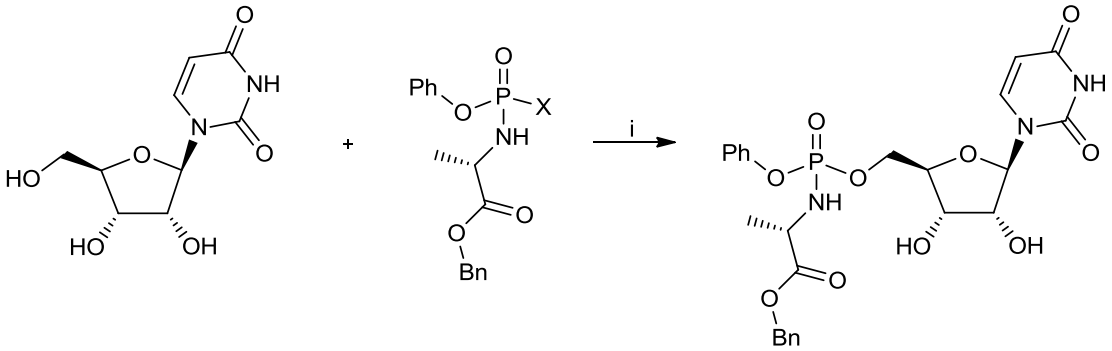

Scheme 60. Synthesis of uridine phosphoramidate ProTide **162**. *Reagents and conditions:* i) as described in table 16.

Table 16. Microwave-assisted synthesis of uridine phosphoramidate ProTide **162** compared to reactions by conventional heating.

		Conventional heating to 55 °C				**Heating by MWI to 65 °C**			
Reagents (equivalents)	**Solvent(s)**	**Time**	**HPLC analysis**			**Time**	**HPLC analysis**		
			161	**162**	bis		**161**	**162**	bis
*t*BuMgCl (3) **37** (2)	THF/NMP	5.5h	62%	38%	-	30 min	66	29%	5%
NMI (6.3) **35** (3)	THF	4.5h	13%	28%	59%	35 min	42%	50%	8%

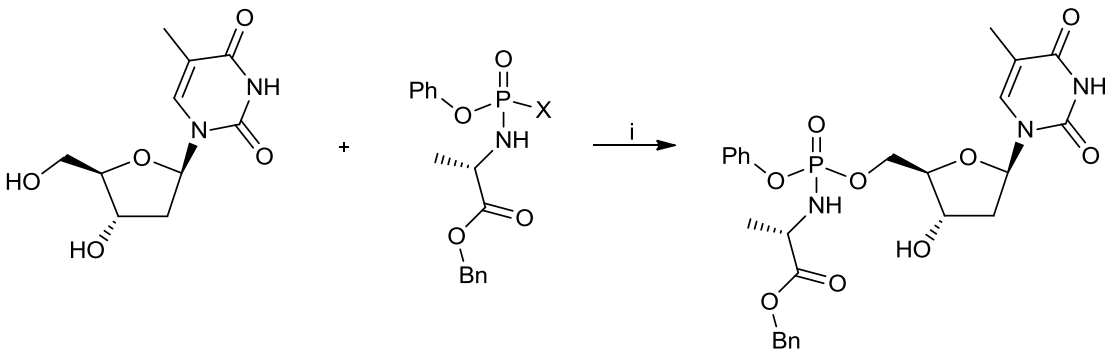

163 **35** X = Cl
37 X = *p*-nitrophenolate **164**

Scheme 61. Synthesis of thymidine phosphoramidate ProTide **164**. *Reagents and conditions:* i) as described in table 17.

Table 17. Microwave-assisted synthesis of thymidine phosphoramidate ProTide **164** compared to reactions by conventional heating.

		Conventional heating to 55 °C				**Heating by MWI to 65 °C**			
Reagents (equivalents)	**Solvent(s)**	**Time**	**HPLC analysis**			**Time**	**HPLC analysis**		
			163	**164**	bis		**163**	**164**	bis
*t*BuMgCl (2) **37** (2)	DMF	40 min	5%	29%	66%	20 min	30%	45%	25%
NMI (6.3) **35** (3)	THF	4h	13%	72%	14%	5 min	1%	70%	29%

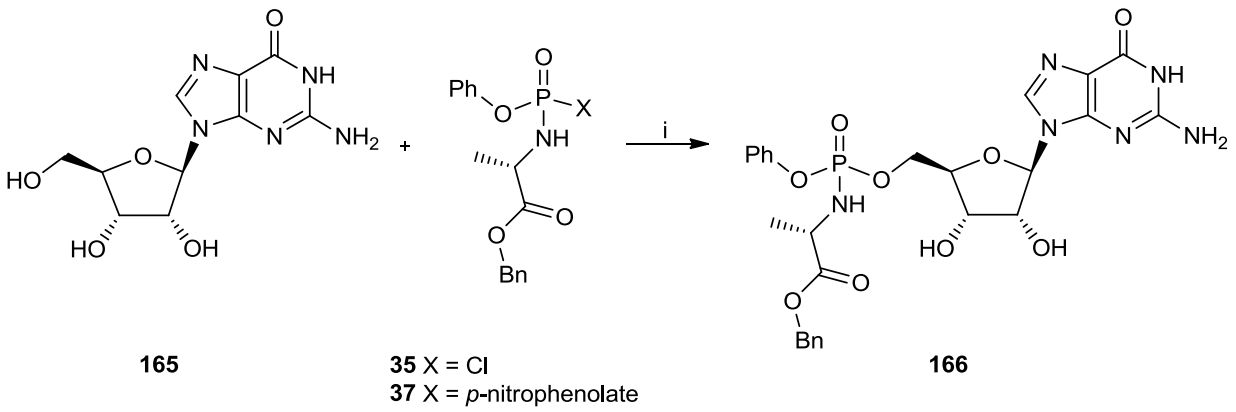

Scheme 62. Synthesis of guanosine phosphoramidate ProTide **166**. *Reagents and conditions:* i) as described in table 18.

Table 18. Microwave-assisted synthesis of guanosine phosphoramidate ProTide **166** compared to reactions by conventional heating.

		Conventional heating to 55 °C				**Heating by MWI to 65 °C**			
Reagents (equivalents)	**Solvent(s)**	**Time**	**HPLC analysis**			**Time**	**HPLC analysis**		
			165	**166**	bis		**165**	**166**	bis
*t*BuMgCl (4) **37** (4)	DMF	4h	-	12%	3%	30 min	18%	79%	3%
NMI (6.3) **35** (3)	THF/pyridine	24h	51%	49%	-	35 min	87%	13%	-

Microwave-assistance was successfully applied to the synthesis of phosphoramidate ProTides. Different reagents, solvents and reaction conditions were explored for the natural nucleosides, which were employed as models.

In the course of this PhD, this innovative methodology found great utility in the preparation of phosphoramidate ProTides of structurally modified nucleoside analogues as described in paragraphs 2.2.3.2 and 2.2.4.2.

2.3 BIOLOGICAL EVALUATION

The anti-DENV activity and cytotoxicity of the synthesised nucleosides and phosphoramidate ProTides were tested *in vitro* by Dr Joachim J. Bugert, Institute for Microbiology, Armed Forces Medical Academy in Munich.

The virus-induced cytopathic effect (CPE) inhibition assay[72] was performed to evaluate the antiviral activity (EC_{50}) in DENV-infected cells (human hepatoma cells, Huh7). The reduction of the viability of non-infected cells was measured to evaluate the cytotoxicity (CC_{50}) of compounds. The nucleoside 2',5'-di-*O*-trityluridine **167** (figure 73) was reported to be selectively active against flaviviruses[72] and was adopted as reference compound in the cell-based assays. The available biological data for the synthesised compounds are summarised in table 19.

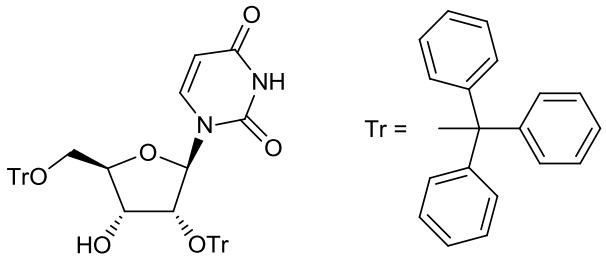

167

Figure 73. Structure of the reference compound 2',5'-di-*O*-trityluridine **167**.

Table 19. The anti-DENV activity (EC_{50}) and cytotoxicity (CC_{50}) of synthesised compounds in CPE-reduction assays.

Compounds	**EC_{50}[a]**	**CC_{50}[a]**
40	> 10 µM	5 µM
56	8.96/10.40 µM	> 20 µM
57	4.50/4.58 µM	> 20 µM
87	> 10 µM	10 µM
27	9.1 µM	10 µM
128	> 10 µM	10 µM
129	> 10 µM	10 µM
132	> 10 µM	10 µM
reference compound[b]	9.50 µM	> 10 µM

[a]Human hepatoma cells (Huh7) were used. [b]2',3'-di-*O*-trityluridine.[72]

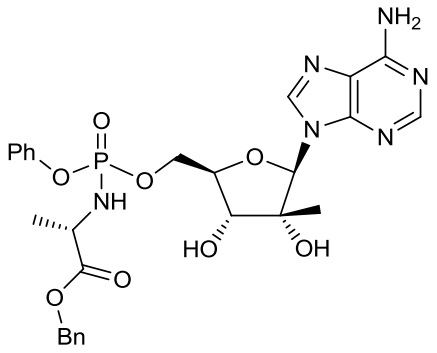

57

Figure 74. Structure of 2'-*C*-methyladenosine ProTide **57**.

The nucleoside 2'-*C*-methyladenosine **56** was poorly active against DENV, showing an EC_{50} of 8.96/10.40 μM. However, the corresponding phenyl L-alanine benzyl ester phosphoramidate **57** (figure 74) was characterised by a two-fold increase of the anti-DENV activity (EC_{50} 4.50/4.58 μM), compared to the parent nucleoside **56** and to 2',3'-di-*O*-trityluridine. Therefore, the application of the phosphoramidate ProTide approach to **56** was successful in increasing the activity of the parent nucleoside **56**, suggesting that the activity of that compound was limited by pharmacokinetics factors, such as poor cellular permeation, intracellular conversion to inactive metabolites and poor activation by host kinases.

The 2'-*C*-methyl-7-deazaadenosine **40** and the benzo-fused 7-deazaadenosine analogue **87** were found to be inactive against DENV and were found to elicit a certain degree of cytotoxicity (CC_{50} 5 μM and 10 μM, respectively). As observed for **56**, the application of the phosphoramidate ProTide strategy may improve the pharmacokinetic properties of the parent nucleosides **40** and **87**. However, the biological data for the corresponding phenyl L-alanine isopropyl ester phosphoramidates **58** and **101**, respectively, are still missing.

When comparing the biological profile of the 7-deaza analogue **40** to the *N*-7 analogue **56**, it is interesting to note that the 7-deaza modification of the nucleobase resulted in a loss of potency and a significant increase of cytotoxicity (CC_{50} 5 μM).

Within the series of acyclic nucleoside analogues, the adenosine derivative **27** showed an anti-DENV activity that was comparable to the nucleoside 2'-*C*-methyladenosine **56** and to the reference compound, with an EC_{50} of 9.1 μM. However, this poor antiviral activity of **27** was also accompanied by cytotoxicity (CC_{50} 10 μM). The 7-deaza, the methyl 7-carboxylate and the benzo-

fused 7-deaza analogues **128**, **129** and **132** failed to inhibit DENV and were also found to be cytotoxic (CC_{50} 10 µM).

The biological data for the *trans* mono-*O*-phosphoramidates **137**, **138** and **139** as well as the *O*-*O*-cyclic phosphoramidates **133** and **134** are not available yet, therefore the capability of the phosphoramidate ProTide approach to boost the *in vitro* anti-DENV activity of the acyclic adenosine analogues **27** and **128** remains to be explored.

Currently, the prepared nucleosides and nucleotide phosphoramidates are also being evaluated for their inhibiting effect on ZIKV, a member of the genus *flavivirus* that is the cause of an increasing number of infections worldwide.[73, 74] Besides the great concern for the recent re-emergence of ZIKV, the availability of the virus as well as the ease of the cell-based assays prompted the biological evaluation of the compounds against ZIKV. Furthermore, the active site of RdRp is highly conserved among flaviviruses, therefore nucleoside and nucleotide analogues designed as anti-DENV agents may show an antiviral activity against related viruses such as ZIKV.

The anti-ZIKV activity of the 2'-*C*-methyladenosine ProTide **57** was determined in ZIKV-infected cells (human lung carcinoma cells, A549) using xCELLigence system (figure 75). This system monitors the cells by measuring their electrical impedance. The loss of tight junctions between cells, which is induced by the viral infection (virus-induced CPE), can then be measured as a reduction of electric resistance of the cells (**A** in figure 75). The L-dideoxy furanopyrimidine bicyclic nucleoside analogue (L-ddBCNA) cf2642 **168** (figure 76), which was originally developed as an autophagy inhibitor effective against vaccinia and measles viruses,[75] was employed as reference compound. In the presence of an antiviral agent such as cf2642, the reduction of the virus-induced CPE decreases the loss of tight junctions between cells and therefore an increase of the electric resistance (violet line, **B** in figure 75) is observed. Natural killer cells (pink line, figure 75) were used as a positive control. Similarly, the 2'-*C*-methyladenosine ProTide **57** was found to inhibit ZIKV (blue line, **B** in figure 75). Finally, a synergistic effect was observed when **57** was combined with cf2642 (light green line, **B** in figure 75).

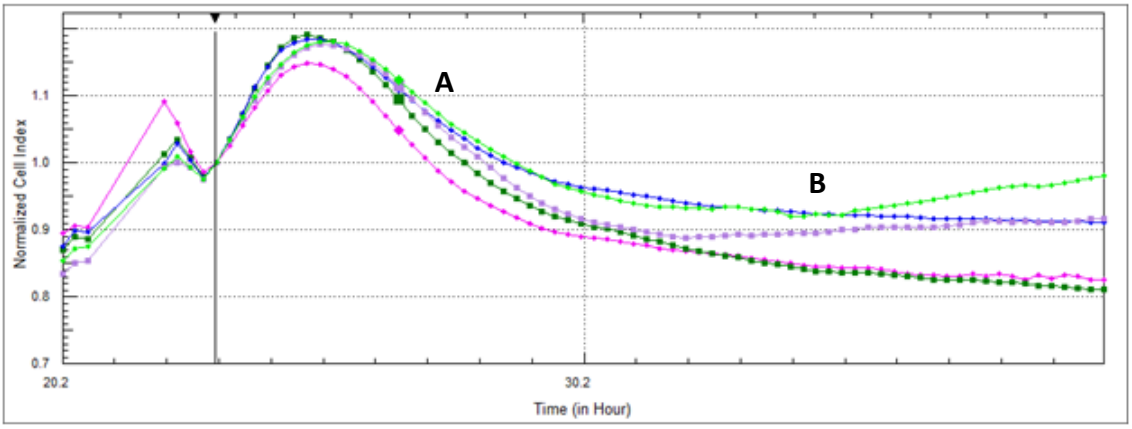

Pink: natural killer cells
Dark green: ZIKV
Blue: ZIKV + **57**
Violet: ZIKV + reference compound **168**
Light green: ZIKV + **57** + reference compound **168**

Human lung carcinoma cells (A549) and xCELLigence system were used.

Figure 75. Inhibition of ZIKV by the 2'-*C*-methyladenosine ProTide **57** and synergistic effect of **57** with the reference compound cf2642 **168**. Solid line: time of addition of ZIKV and compounds/natural killer cells; dotted line: time selected for comparison of treatments; **A**: reduction of electric resistance due to virus-induced cytopathic effect; **B**: effect of treatments. Figure and data by Dr Joachim J. Bugert.

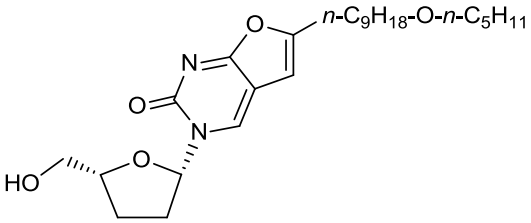

168

Figure 76. Structure of the autophagy inhibitor cf2642 **168**, which was employed as reference compound.

The EC_{50} of the 2'-*C*-methyladenosine ProTide **57** and of the combination of **57** with the L-ddBCNA cf2642 **168** were determined to be 4 ± 0.2 µM and 1 ± 0.2 µM, respectively, whereas the cytotoxicity was found to be very low with CC_{50} values > 20 µM for the single-drug treatments. The promising results obtained for the combination of the RdRp inhibitor 2'-*C*-methyladenosine

ProTide **57** with the autophagy inhibitor cf2642 **168** warrant further investigation towards an effective treatment of ZIKV infection.

Finally, the biological data obtained for the 2'-*C*-methyladenosine ProTide **57** highlight the great utility of the nucleotide phosphoramidate ProTide strategy against DENV as well as closely related viruses.

2.4 REFERENCES

[1] T. L. Yap, T. Xu, Y.-L. Chen, H. Malet, M.-P. Egloff, B. Canard, S. G. Vasudevan, J. Lescar. Crystal structure of the dengue virus RNA-dependent RNA polymerase catalytic domain at 1.85-angstrom resolution. *J. Virol.*, 81(9): 4753-4765, 2007.

[2] C. G. Noble, S. P. Lim, y.-L- Chen, C. W. Liew, L. Yap, J. Lescar, P.-Y. Shi. Conformational flexibility of the dengue virus RNA-dependent RNA polymerase revealed by a complex with an inhibitor. *J. Virol.*, 87(9): 5291-5295, 2013.

[3] S. P. Lim, J. H. Koh, C. C. Seh, C. W. Liew, A. D. Davidson, L. S. Chua, R. Chandrasekaran, T. C. Cornvik, P.-Y. Shi, J. Lescar. A crystal structure of the dengue virus NS5 polymerase delineates inter-domain amino acids that enhance its thermostability and *de novo* initiation activities. *J. Biol. Chem.*, 288: 31105-31114, 2013.

[4] Y. Zhao, T. S. Soh, J. Zheng, K. W. K. Chan, W. W. Phoo, C. C. Lee, M. Y. F. Tay, K. Swaminathan, T. C. Cornvik, S. P. Lim, P.-Y. Shi, J. Lescar, S. G. vasudevan, D. Luo. A crystal structure of the dengue virus NS5 protein reveals a novel inter-domain interface essential for protein flexibility and virus replication. *PLoS Pathog.*, 11(3): e1004682, 2015.

[5] K. H. Choi, M. G. Rossmann. RNA-dependent RNA polymerases from *Flaviviridae*. *Curr. Opin. Struct. Biol.*, 19 : 746-751, 2009.

[6] B. Selisko, S. Potisopon, R. Agred, S. Priet, I. Varlet, Y. Thillier, C. Sallamand, F. Debart, J.-j. Vasseur, B. Canard. Molecular basis for nucleotide conservation at the ends of the Dengue virus genome. *PLoS Phatog.*, 8(9): e1002912, 2012.

[7] G. Migliaccio, J. E. Tommassini, S. S. Carroll, L. Tomei, S. Altamura, B. Bhat, L. Bartholomew, M. R. Bosserman, A. Ceccacci, L. F. Colwell, R. Cortese, R. De Francesco, A. B. Eldrup, K. L. Getty, X. S. Hou, R. L. LaFemina, S. W. Ludmerer, M. MacCoss, D. R. McMasters, M. W. Stahlhut, D. B. Olsen, D. J. Hazuda, O. A. Flores. Characterization of resistance to non-obligate chain-terminating ribonucleoside analogs that inhibit Hepatitis C Virus replication *in vitro*. *J. Biol. Chem.*, 278: 49164-49170, 2003.

[8] R. T. Mosley, T. E. Edwards, E. Murakami, A. M. Lam, R. L. Grice, J. Du, M. J. Sofia, P. A. Furman, M. J. Otto. Structure of Hepatitis C virus polymerase in complex with primer-template RNA. *J. Virol.,* 86: 6503-6511, 2012.

[9] D. B. Olsen, A. B. Eldrup, L. Bartholomew, B. Bhat, M. R. Bosserman, A. Ceccacci, L. F. Colwell, J. F. Fay, O. A. Flores, K. L. Getty, J. A. Grobler, R. L. LaFemina, E. J. Markel, G. Migliaccio, M. Prhavc,

M. W. Stahlhut, J. E. Tomassini, M. MacCoss, D. J. Hazuda, S. S. Carroll. A 7-deaza-adenosine analog is a potent and selective inhibitor of hepatitis C virus replication with excellent pharmacokinetic properties. *Antimicr. Agents Chemother.*, 48(10): 3944-3953, 2004.

[10] Z. Yin, Y.-L. Chen, W. Schul, Q.-Y. wang, F. Gu, J. Duraiswamy, R.R. Kondreddi, P. Niyomrattanakit, S. B. Lakshminarayana, A. Goh, H. Y. Xu, W. Liu, B. Liu, J. Y. H. Lim, C. Y. Ng, M. Qing, C. C. Lim, A. Yip, G. Wang, W. L. Chan, H. P. Tan, K. Lin, B. Zhang, G. Zou, K. A. Bernard, C. Garrett, K. Beltz, M. Dong, M. Weaver, H. He, A. Pichota, V. Dartois, T. H. Keller, P.-Y. Shi. An adenosine nucleoside inhibitor of dengue virus. *Proc. Natl. Acad. Sci.*, 106(48): 20435-20439, 2009.

[11] Y.-L. Chen, Z. Yin, J. Duraiswamy, W. Schul, C. C. Lim, H. Y. Xu, M. Qing, A. Yip, G. Wang, W. L. Chan, H. P. Tan, M. Lo, S. Liung, R. R. Kondreddi, R. Rao, H. Gu, H. He, T. H. Keller, P.-Y. Shi. Inhibition of dengue virus RNA synthesis by an adenosine nucleoside. *Antimicrob. Agents Chemother.*, 54(7): 2932-2939, 2010.

[12] Y.-L. Chen, Z. Yin, S. B. Lakshminarayana, M. Qing, W. Schul, J. Duraiswamy, R. R. Kondreddi, A. Goh, H. Y. Xu, A. Yip, B. Liu, M. Weaver, V. Dartois, T. H. Keller, P.-Y. Shi. Inhibition of dengue virus by an ester prodrug of an adenosine analog. *Antimicrob. Agents Chemother.*, 54(8): 3255-3261, 2010.

[13] L. Bassit, P. Chatterjee, B. Kim, S. J. Coats, R. F. Schinazi. 2,6-Diaminopurine nucleosides are a novel class of anti-DENV inhibitors. *First International Symposium of Human Vector-Borne Diseases HVBD DART*. December 12-13, 2013.

[14] M. Tichý, R. Pohl, E. Tlousťová, J. Weber, G. Bahador, Y.-J. Lee, M. Hocek. Synthesis and biological activity of benzo-fused 7-deazaadenosine analogues. 5- and 6-substituted 4-amino- or 4-alkylpyrimido[4,5-*b*]indole ribonucleosides. *Bioorg. Med. Chem.*, 21: 5362-5372, 2013.

[15] M. Tichý, R. Pohl, H. Y. Xu, Y.-L. Chen, F. Yokokawa, P.-Y. Shi, M. Hocek. Synthesis and antiviral activity of 4,6-disubstituted pyrimido[4,5-*b*]indole ribonucleosides. *Bioorg. Med. Chem.*, 20: 6123-6133, 2012.

[16] A. C. Anderson. The process of structure-based drug design. *Chem. Biol.*, 10: 787-797, 2003.

[17] D. B. Kitchen, H. Decornez, J. R. Furr, J. Bajorath. Docking and scoring for drug discovery: methods and applications. *Nat. Rev. Drug Discov.*, 3: 935-949, 2004.

[18] A. R. Leach. Molecular dynamics simulation methods. Molecular modelling – Principles and applications. *Pearson Education Limited, Harlow*, 2nd edition: 353-409, 2001.

[19] J. H. Hong, H. O. Kim, H. R. Moon, L. S. Jeong. Synthesis and antiviral activity of fluoro-substituted apio dideoxynucleosides. *Arch. Pharm. Res.*, 24(2): 95-99, 2001.

[20] G. Lu, P. Gong. Crystal structure of the full-length Japanese encephalitis virus NS5 reveals a conserved methyltransferase-polymerase interface. *PLoS Phatog.*, 9(8): e1003549, 2013.

[21] D. Tarantino, R. Cannalire, E. Mastrangelo, R. Croci, G. Querat, M. L. Barreca, M. Bolognesi, G. Manfroni, V. Cecchetti, M. Milani. Targeting flavivirus RNA dependent RNA polymerase through a pyridobenzothiazole inhibitor. *Antiviral Res*., 134: 226-235, 2016.

[22] F. Yokokawa, S. Nilar, C. G. Noble, S. P. Lim, R. Rao, S. Tania, G. Wang, G. Lee, J. Hunziker, R. Karuna, U. Manjunatha, P.-Y. Shi, P. W. Smith. Discovery of potent non-nucleoside inhibitors of dengue viral RNA-dependent RNA polymerase from a fragment hit using structure-based drug design. *J Med Chem.*, 59(8): 3935-3952, 2016.

[23] S. P. Lim, C. G. Noble, C. C. Seh, T. S. Soh, A. E. Sahili, G. K. Y. Chan, J. Lescar, R. Arora, T. Benson, S. Nilar, U. Manjunatha, K. F. Wan, H. Dong, X. Xie, P.-Y. Shi, F. Yokokawa. Potent allosteric dengue virus NS5 polymerase inhibitors: mechanism of action and resistance profiling. *PLoS Pathog.*, 12(8): e1005737, 2016.

[24] C. G. Noble, Y.-L. Chen, H. Dong, F. Gu, S. P. Lim, W. Schul, Q.-Y. Wang, P.-Y. Shi. Strategies for development of dengue virus inhibitors. *Antiviral Res.*, 85: 450-462, 2010.

[25] S. P. Lim, Q.-Y. Wang, C. G. Noble, Y.-L. Chen, H. Dong, B. Zou, F. Yokokawa, S. Nilar, P. Smith, D. Beer, J. Lescar, P.-Y. Shi. Ten years of dengue drug discovery: progress and prospects. *Antiviral Res.*, 100: 500-519, 2013.

[26] U. Pradere, E. C. Garnier-Amblard, S. J. Coats, F. Amblards, R. F. Schinazi. Synthesis of nucleoside phosphate and phosphonate prodrugs. *Chem. Rev.*, 114: 9154-9218, 2014.

[27] K. L. Yeo,Y.-L. Chen, H. Y. Xu, H. Dong, Q.-Y. Wang, F. Yokokawa, P.-Y. Shi. Synergistic suppression of dengue virus replication using a combination of nucleoside analogs and nucleoside synthesis inhibitors. *Antimicrob. Agents. Chemother.*, 59(4): 2086-2093, 2015.

[28] J. H. Boom, P. M. Burgers, R. Crea, W. C. M. Luyten, A. B. J. Vink, C. B. Reese. Phosphorylation of nucleoside derivatives with aryl phosphoramidochloridate. *Tetrahedron*, 31: 2953-2959, 1975.

[29] M. Uchiyama, Y. Aso, R. Noyori, Y. Hayakawa. *O*-selective phosphorylation of nucleosides without *N*-protection. *J. Org. Chem.*, 58: 373-379, 1993.

[30] M. Serpi, K. Madela, F. Pertusati, M. Slusarczyk. Synthesis of phosphoramidate prodrugs: ProTide approach. *Curr. Protoc. Nucleic Acid Chem.*, supplement 53, 15.5.1-15.5.15, June 2013.

[31] B. S. Ross, P. Ganapadi Reddy, H.-R. Zhang, S. Rachakonda, M. J. Sofia. Synthesis of diastereomerically pure nucleotide phosphoramidates. *J. Org. Chem.*, 76: 8311-8319, 2011.

[32] M. Derudas, D. Carta, A. Brancale, C. Vanpouille, A. Lisco, L. Margolis, J. Balzarini, C. McGuigan. The application of phosphoramidate ProTide technology to acyclovir confers anti-HIV inhibition. *J. Med. Chem.*, 52: 5520-5530, 2009.

[33] S. S. Carroll, D. B. Olsen. Nucleoside analog inhibitors of hepatitis C virus replication. *Infect. Disord. Drug Targets*, 6(1): 17-29, 2006.

[34] V. Uteza, G.-R. Chen, J. Le Quan Tuoi. G. Descotes, B. Fenet, A. Grouiller. Synthesis and structure determination of the first 1'-C-cyano-β-D-nucleosides. *Tetrahedron*, 49(38): 8579-8588, 1993.

[35] T. Kodama, S. Shuto, M. Nomura, A. Matsuda. An efficient method for the preparation of 1'-α-branched-chain sugar pyrimidine ribonucleosides from uridine: the first conversion of a natural nucleoside into 1'-substituted ribonucleosides. *Chem. Eur. J.*, 7(11): 2332-2340, 2001.

[36] K. Haraguchi, Y. Itoh, H. Tanaka, K. Yamaguchi, T. Miyasaka. Anomeric manipulation of nucleosides: stereospecific entry to 1'-*C*-branched uracil nucleosides. *Tetrahedron Lett.*, 34(43): 6913-6916, 1993.

[37] L. Cappellacci, G. Barboni, M. Palmieri, M. Pasqualini, M. Grifantini, B. Costa, C. Martini, P. Franchetti. Ribose-modified nucleosides as ligands for adenosine receptors: synthesis, conformational analysis, and biological evaluation of 1'-*C*-methyl adenosine analogues. *J. Med. Chem.*, 45 (6): 1196-1202, 2002.

[38] G. Sautrey, D. Bourgeois, C. Périgaud. Diastereoselective synthesis of (±)-1',4'-dimethyluridine. *Org. Biomol. Chem.*, 8, 378-383, 2010.

[39] A. Matsuda, H. Itoh, K. Takenuki, T. Sasaki, T. Ueda. Alkyl addition reaction of pyrimidine 2'-ketonucleosides: synthesis of 2'-branched-chain sugar pyrimidine nucleosides (nucleosides and nucleotides. LXXXI). *Chem. Pharm. Bull.*, 36(3): 945-953, 1988.

[40] J.-L. Girardet, E. Gunic, C. Esler, D. Cieslak, Z. Pietrzkowski, G. Wang. Synthesis and cytotoxicity of 4-amino-5-oxopyrido[2,3-*d*]pyrimidine nucleosides. *J. Med. Chem.*, 43: 3704-3713, 2000.

[41] R. E. Harry-O'kuru, J. M. Smith, M. S. Wolfe. A short, flexible route toward 2'-*C*-branched ribonucleosides. *J. Org. Chem.*, 62: 1754-1759, 1997.

[42] A. B. Eldrup, M. Prhavc, J. Brooks, B. Bhat, T. P. Prakash, Q. Sing, S. Bera, N. Bhat, P. Dande, P. D. Cook, C. F. Bennett, S. S. Carroll, R. G. Ball, M. Bosserman, C. Burlein, L. F. Colwell, J. F. Fay, O. A. Flores, K. Getty, R. L. LaFemina, J. Leone, M. MacCoss, D. R. McMasters, J. E. Tommassini, D. Von Langen, B. Wolanski, D. B. Olsen. Structure-activity relationship of heterobase-modified 2'-*C*-

methyl ribonucleosides as inhibitors of hepatitis C virus RNA replication. *J. Med. Chem.*, 47: 5284-5297, 2004.

[43] T. Maeda, H. Uehara, N. Harada, M. Katsurada, M. Sano. Process for producing 5-deoxyribofuranose derivatives by hydrogenation of 5-deoxy-5-haloribofuranose. API Corporation, Japan. WO 2009044886 A1, Apr 09, 2009.

[44] G. Parmentier, G. Schmitt, F. Dolle, B. Luu. A convergent synthesis of 2'-*O*-methyl uridine. *Tetrahedron*, 50(18): 5361-5368, 1994.

[45] F. W. D'Souza, J. D. Ayers, P. R. McCarren, T. L. Lowary. Arabinofuranosyl oligosaccharides from mycobacteria: synthesis and effect of glycosylation on ring conformation and hydroxymethyl group rotamer populations. *J. Am. Chem. Soc.*, 122(7): 1251-1260, 2000.

[46] S. D. Osborne, V. E. C. Powers, D. A. Rusling, O. Lack, K. R. Fox, T. Brown. Selectivity and affinity of triplex-forming oligonucleotides containing 2'-aminoethoxy-5-(3-aminoprop-1-ynyl)uridine for recognizing At base pairs in duplex DNA. *Nucleic Acids Res.*, 32(15): 4439-4447, 2004.

[47] Y. Cen, A. A. Sauve. Transition state of ADP-ribosylation of acetyllysine catalyzed by Archaeoglobus fulgidus Sir2 determined by kinetic isotope effects and computational approaches. *J. Am. Chem. Soc.*, 132(35): 12286-12298, 2010.

[48] G. Wang, J. L. Girardet, E. Gunic. Conformationally locked nucleosides. Synthesis and stereochemical assignments of 2'-C,4'-C-bridged bicyclonucleosides. *Tetrahedron*, 55: 7707-7724, 1999.

[49] N. S. Li, J. Lu, J. A. Piccirilli. Efficient synthesis of methyl 3,5-di-O-benzyl-alpha-D-ribofuranoside and application to the synthesis of 2'-C-beta-alkoxymethyluridines. *Org. Lett.*, 9(16): 3009-3012, 2007.

[50] C. Simons. Synthesis of conventional D-nucleosides. Nucleoside mimetics – Their chemistry and biological properties. *Advanced Chemistry Texts, Gordon and Breach Science Publishers*, volume 3: 29-62, 2001.

[51] F. Seela, B. Westermann, U. Bindig. Liquid-liquid and solid-liquid phase-transfer glycosylation of pyrrolo[2,3-*d*]pyrimidines: stereospecific synthesis of 2-deoxy-β-D-ribofuranosides related to 2'-deoxy-7-carbaguanosine. *J. Chem. Soc. Perkin Trans.*, 1: 697-702, 1988.

[52] S.-Y. Han, M. M. Joullié. Investigations of the formation of cyclic acetal and ketal derivatives of D-ribono-1,4-lactone and 2-deoxy-D-ribono-1,4-lactone. *Tetrahedron*, 49(2): 349-362, 1993.

[53] E. Klein, S. Mons, A. Valleix, C. Mioskowski, L. Lebeau. Synthesis of Enzymatically non-hydrolyzable analogues of dinucleoside triphosphates Ap3A and Gp3G. *J. Org.Chem.*, 67(1): 146-153, 2002.

[54] M. S. Valle, A. Tarrade-Matha, P. Dauban, R. H. Dodd. Regioselective electrophilic substitution of 2,3-aziridino-γ-lactones: preliminary studies aimed at the synthesis of α,α-disubstituted α- or β-amino acids. *Tetrahedron*, 64: 419-432, 2008.

[55] F. Stazi, W. Maton, D. Castoldi, P. Westerduin, O. Curcuruto, S. Bacchi. Efficient methods for the synthesis of arylacetonitriles. *Synthesis*, 19: 3332-3338, 2010.

[56] K. Kobayashi, T. Komatsu, Y. Yokoi, H. Konishi. Synthesis of 2-aminoindole-3-carboxylic acid derivatives by the copper(I) iodide catalyzed reaction of *N*-2-iodophenyl)formamides with malononitrile or cyanoacetates. *Synthesis*, 5: 764-768, 2011.

[57] R. Storer, A. Moussa, N. Chaudhuri, F. Waligora. Process for the production of 2'-branched nucleosides. Idenix Cayman Limited. WO 2004052899 A2. Jun 24, 2004.

[58] E. De Clercq. Antiviral drugs in current clinical use. *J. Clin. Virol.*, 30: 115-133, 2004.

[59] L. P. Jordheim, D. Durantel, F. Zoulim, C. Dumontet. Advances in the development of nucleoside and nucleotide analogues for cancer and viral diseases. *Nat. Rev. Drug Disc.*, 12: 447-464, 2013.

[60] D. R. Haines, C. K. H. Tseng, V. E. Marquez. Synthesis and biological activity of unsaturated carboacyclic purine nucleoside analogues. *J. Med. Chem.*, 30(5): 943-947, 1987.

[61] T. H. M. Jonckers, A. Tahri, L. Vijgen, J. M. Berke, S. Lachau-Durand, B. Stoops, J. Snoeys, L. Leclercq, L. Tambuyzer, T. Lin, K. Simmen, P. Raboisson. Discovery of 1-((2*R*,4a*R*,6*R*,7*R*,7a*R*)-2-isopropoxy-2-oxidodihydro-4*H*,6*H*-spiro[furo[3,2-*d*][1,3,2]dioxaphosphinine-7,2'-oxetan]-6-yl)pyrimidine-2,4(1*H*,3*H*)-dione (JNJ-54257099), a 3'-5'-cyclic phosphate ester prodrug pf 2'-deoxy-2'-spirooxetane uridine triphosphate useful for HCV inhibition. *J. Med. Chem.*, 59(12): 5790-5798, 2016.

[62] E. Gunic, J.-L. Girardet, K. Ramasamy, V. Stoisavljevic-Petkov, S. Chow, L.-T. Yeh, R. K. Hamatake, A. Raney, Z. Hong. Cyclic monophosphate prodrugs of base-modified 2'-*C*-methyl ribonucleosides as potent inhibitors of hepatitis C virus RNA replication. *Bioorg. Med. Chem. Lett.*, 17: 2452-2455, 2007.

[63] P. Reddy, B. Chun, H. Zhang, S. Rachakonda, B. S. Ross, M. J. Sofia. Stereoselective synthesis of PSI-352938: a β-D-2'-deoxy-2'-α-fluoro-2-β-*C*-methyl-3'-5'-cyclic phosphate nucleotide prodrug for the treatment of HCV. *J. Org. Chem.*, 76: 3782-3790, 2011.

[64] D. F. Netz, J. L. Seidel. Diethyl (*N*-methoxy-*N*-methylcarbamoylmethyl)phosphonate – a useful Emmons-Horner Wittig reagent. *Tetrahedron Lett.*, 33(15): 1957-1958, 1992.

[65] M. Mentzel, H. M. R. Hoffmann. *N*-methoxy-*N*-methylamides (Weinreb amides) in modern organic synthesis. *J. prakt. Chem.*, 339: 517-524, 1997.

[66] M. Bessières, O. Sari, V. Roy, D. Warszycki, A. J. Bojarski, S. P. Nolan, R. Snoeck, G. Andrei, R. F. Schinazi, L. A. Agrofoglio. Sonication-assisted synthesis of (*E*)-2-methyl-but-2-enyl nucleoside phosphonate prodrugs. *ChemistrySelect*, 1: 3108, 2016.

[67] M. J. Sofia, D. Bao, W. Chang, J. Du, D. Nagarathnam, S. rachakonda, P. G. Reddy, B. S. Ross, P. Wang, H.-R. Zhang, S. Bansal, C. Espiritu, M. Keilman, A. M. Lam, H. M. M. Steuer, C. Niu, M. J. Otto, P. A. Furman. Discovery of a β-D-2'-deoxy-2'-α-fluoro-2'-β-*C*-methyluridine nucleotide prodrug (PSI-7977) for the treatment of hepatitis C virus. *J. Med. Chem.*, 53: 7202-7218, 2010.

[68] A. S. Ray, M. W. Fordyce, J. M. Hitchcock. Tenofovir alafenamide: a novel prodrug of tenofovir for the treatment of Human Immunodeficiency virus. *Antiviral Res.*, 125, 63-70, 2016.

[69] V. Roy, U. Pradère, L. A. Agrofoglio. Microwave-assisted synthesis of nucleosides and their precursors. *Future Med. Chem.*, 2, 177-192, 2010.

[70] J.-H. Cho, S. J. Coats, R. F. Schinazi. Efficient synthesis of exo-*N*-carbamoyl nucleosides: application to the synthesis of phosphoramidate prodrugs. *Org. Lett.*, 14(10): 2488-2491, 2012.

[71] C. McGuigan, P. Perrone, K. Madela, J. Neyts. The phosphoramidate ProTide approach greatly enhances the activity of β-2'-*C*-methylguanosine against hepatitis C virus. *Bioorg. Med. Chem. Lett.*, 19: 4316-4320, 2009.

[72] T. De Burghgraeve, B. Selisko, S. Kaptein, G. Chatelain, P. Leyssen, Y. Debing, M. Jacobs, A. Van Aerschot, B. Canard, J. Neyts. 3',5'-di-*O*-trityluridine inhibits *in vitro* flavivirus replication. *Antiviral Res.*, 98: 242-247, 2013.

[73] World Health Organisation. Zika virus. Fact sheet, updated September 2016. http://www.who.int/mediacentre/factsheets/zika/en, accessed January 2017.

[74] World Health Organisation. WHO statement on the first meeting of the International Health Regulations (2005) (IHR 2005) Emergency Committee on Zika virus and observed increase in neurological disorders and neonatal malformations. WHO statement, 1st February 2016. http://www.who.int/mediacentre/news/statements/2016/1st-emergency-committee-zika/en/, accessed January 2017.

[75] C. McGuigan, K. Hinsinger, L. Farleigh, R. N. Pathirana. Novel antiviral activity of L-dideoxy bicyclic nucleoside analogues versus vaccinia and measles viruses *in vitro*. *J. Med. Chem.*, 56: 1311-1322, 2013.

3 CONCLUSIONS

3. CONCLUSIONS

The development of effective antiviral therapeutics for the treatment of DENV infection has been a major field of research in the last decades. The RdRp represents one of the most attractive targets for the identification of potent and selective anti-DENV agents. Therefore, the overarching aim of this PhD project was the *in silico* design and synthesis of RdRp targeted nucleoside and nucleotide analogues as potential inhibitors of viral replication.

With the aim of providing an essential tool for the application of computer-aided drug design approaches, a model of the DENV RdRp *de novo* initiation complex was generated using molecular modelling techniques and validated through docking studies on known DENV RdRp inhibiting nucleoside analogues.

Docking studies on families of nucleoside analogues were performed using the novel model and were used to select the most promising structural modifications of the natural nucleoside adenosine. In particular, DENV RdRp accepted modifications at the 7-deaza position of the nucleobase, from the substitution with a variety of functional groups to the addition of a benzene ring to form a tricyclic heterocycle. In addition, the introduction of carbon groups at the 2' and 1'-positions of the ribose ring was examined. The combination of modified nucleobases and *C*-substituted ribose moieties was generally well tolerated by the active site of the DENV RdRp. LBDD approaches, such as scaffold replacement and pharmacophore search, were combined with the docking process to design acyclic nucleoside analogues in which the ribose moiety was replaced by allylic linkers. Taken together, molecular modelling studies led to the creation of a novel model of the DENV RdRp and the identification of three families of nucleoside analogues as potential RdRp inhibitors.

To investigate the mechanistic aspects of the DENV RdRp activity, different complexes of the DENV RdRp and the nucleic acid, which are representative of the pre-initiation, initiation and elongation phases of the RNA synthesis, were modelled and submitted to MD simulations. This study allowed for the identification of the main loops of the enzyme that are involved in its conformational changes during the synthesis of the viral genome. Specifically, residues that may interact with the priming NTP in the *de novo* initiation phase were identified. The results highlighted the role of specific key loops, including the priming loop, in the DENV RdRp activity and provided valuable knowledge for future drug design studies.

With regards to the preparation of nucleosides, the synthetic strategies towards the three families of adenosine analogues that were selected by the molecular modelling studies were investigated. These families were the ribose-modified, the benzo-fused and finally the acyclic derivatives. The

conditions for the preparation of nucleotide phosphoramidate ProTides of specific members of these families were studied as well.

- The first, ribose-modified, family included 2'-*C*-substituted and 1'-*C*-substituted nucleoside analogues. A convergent method consisting of five steps was developed for the preparation of 2'-*C*-substituted 7-deazaadenosine analogues. The strategy was successfully applied to the synthesis of 2'-*C*-methyl-7-deazaadenosine. The combination of 7-modified 7-deaza 6-chloropurines with different 2'-*C*-substituted glycosylating agents could furnish various adenosine derivatives as potential anti-DENV agents. The ProTide approach was applied to commercially available 2'-*C*-methyladenosine and the synthesised 7-deaza analogue. Standard conditions were employed for the preparation of the former. In contrast, a newly developed method, which was based on the use of an alternative solvent and a *p*-nitrophenolate reagent, was applied to 2'-*C*-methyl-7-deazaadenosine and allowed for a significant increase in yield compared to standard conditions.

  The synthetic route towards 1'-*C*-substituted nucleosides, a largely unexplored class of compounds, was developed and consists of eight steps. The method successfully furnished 1'-*C*-methyladenosine. However, an optimisation of the synthetic procedures would be required to ease the preparation of nucleoside analogues within this family and their corresponding nucleotide phosphoramidates. Furthermore, docking studies suggested that 1',2'-*C*,*C*-bis-substituted adenosine analogues may represent attractive antiviral agents. Further investigations will be required to adapt the developed procedure for the synthesis of this novel class of nucleosides.

- The second family were the benzo-fused 7-deazaadenosine analogues bearing natural or 2'-*C*-substituted ribose moieties. A published procedure consisting of six steps was employed to prepare one derivative in which the ribose ring was unmodified. The application of the ProTide strategy to this class of tricyclic nucleosides was novel, and therefore was investigated on the prepared derivative. The application of innovative MWI conditions, which were developed in an independent methodology study, proved to be essential for the synthesis of the phosphoramidate prodrug of the benzo-fused 7-deazaadenosine analogue.

  The preparation of the 2'-*C*-substituted derivative involved the glycosylation of the tricyclic heterobase by a modified glycosylating agent, whose synthesis required three steps. Docking studies suggested that nucleosides bearing various substituents at the level of the

benzo-fused purine base may fit well in the active site of DENV RdRp. Both the prepared tricyclic nucleosides could be used as intermediates in the synthesis of these nucleosides.

- The third family were acyclic adenosine analogues characterised by two allylic scaffolds replacing the ribose ring. The initially developed synthetic strategy for the first scaffold was based on the alkylation of the heterobase using the appropriate allylic chloride, which was synthesised using a four step method. The following coupling to a variety of purine bases afforded a series of novel acyclic adenosine analogues. Further investigations resulted in an optimised procedure for the synthesis of these acyclic nucleosides. The preparation of ProTides of this class of acyclic nucleosides was inconvenient due to the presence of two primary hydroxyl groups in the linear linker. Nevertheless, suitable MWI conditions were identified for the synthesis of the desired *trans* mono-*O*-phosphoramidates of the adenosine and 7-deazaadenosine derivatives. To overcome the issue of selectivity of the coupling reaction with the phosphoramidating reagent, the corresponding cyclic *O*-*O*-phosphoramidates were synthesised as well.

  With regards to the second scaffold, the synthetic route that was previously developed for the nucleosides containing the first scaffold was adapted in order to introduce a methyl group in the 1-position of the allylic linker. The method consisting of seven steps was successfully applied to the synthesis of the corresponding acyclic adenosine analogue.

As previously mentioned, innovative MWI conditions for the preparation of phosphoramidate ProTides were investigated in this work. First, the applicability of the microwave-assistance was demonstrated on unmodified adenosine, which was employed as a model nucleoside. Then, the conditions were successfully applied to the synthesis of phosphoramidate ProTides of structurally modified analogues as potential anti-DENV agents. The new methodology has proven of great utility in the preparation of phosphoramidate ProTides of nucleoside analogues and was superior than conventionally used methods for the reaction time and, in some cases, for the reaction yield.

Finally, preliminary data from the biological evaluation, which as of yet are only available for a limited number of the synthesised nucleosides and nucleotides, confirmed that the phosphoramidate ProTide approach represents a useful strategy for boosting the antiviral activity of adenosine analogues in infected cells. The 2'-*C*-methyladenosine ProTide inhibited the cytopathy by DENV as well as the closely related ZIKV *in vitro*. Further characterisation of the antiviral activity of the ProTide in ZIKV-infected cells revealed that a significant synergistic effect is observed in combination with an autophagy inhibitor. These encouraging results warrant further

development of both antiviral agents and suggested that the combination of two drugs, of which one is an NI targeting the viral RdRp, may provide potent inhibition of the replication of flaviviruses.

In conclusion, this PhD study has provided a novel model of the DENV RdRp *de novo* initiation complex. As demonstrated in this work, the new model is a valuable tool for *in silico* design of novel NIs of DENV RdRp. An increased understanding of the mechanism of RNA synthesis by the viral RdRp was achieved and will aid future *in silico* design studies on NNIs of DENV RdRp. Finally, the synthetic procedures for the preparation of novel nucleoside analogues and nucleotide phosphoramidate ProTides, which were developed in the course of this PhD, give access to a variety of biologically relevant compounds.

4 EXPERIMENTAL PART

4.1 COMPUTATIONAL METHODS

4.1.1 METHODS – SECTION 2.1.1

The crystal structures of the DENV RdRp and the HCV NS5B in complex with the nucleic acid were downloaded from the Protein Data Bank website (codes 4HHJ and 4E78, respectively).[1, 2] Water molecules, non-catalytic ions and glycerol were removed using MOE2014.09. The model of the DENV RdRp *de novo* initiation complex was built using the same modelling program, as described in paragraph 2.1.1.1. Modifications on the nucleic acid were applied using the MOE Builder tool. The Mg^{2+} ions were imported from Protein Data Bank code 2J7U[3] and re-positioned manually using MOE2014.09. Minimisation of the protein complex was performed with AMBER99 force field, using MOE2014.09.

Docking simulations of DENV RdRp inhibitors were performed using Protein-Ligand ANT System (PLANTS). Small molecule databases were prepared using MOE2014.09. The nucleotides monophosphate and triphosphate were designed with the Builder tool and energy minimised with MMFF94x force field. Databases were converted to a format PLANTS-compatible. To identify the docking site, the centre was set at the oxygen atom of ATP with radius of 10Å. In each docking simulation, 20 poses were generated and visually inspected using MOE2014.09.

The MD simulation on the model of the DENV RdRp *de novo* initiation complex was performed using the application Desmond of Schrödinger Maestro 9.5. Firstly, the missing loops in the protein (spanning residues from 406 to 420 and from 457 to 469) were constructed using the MOE Structure Preparation tool. Secondly, the protein complex was prepared with the Protein Preparation Wizard tool using Schrödinger Maestro 9.5. The model system was built by employing an orthorhombic box of 10Å side and by adding molecules of water as SPC solvent model. The total charges of the system were neutralised by adding 2 Na^{2+} ions. Solvation was run using OPLS_2005 force field. An initial energy minimization was performed to relax the system before the MD simulation. The maximum number of iterations was set at 2 000 steps. The MD simulation was 50 ns long and trajectory and energy values were recorded every 100 ps (500 steps). The simulation was run in NPT conditions (constant number of atoms N, pressure P and temperature T) at the temperature of 300 K and pressure of 1.01325 bar.

Results were visually inspected using VMD 1.9.1. Additionally, the final step of the MD simulation and the system before the MD simulation were superposed using MOE2014.09.

4.1.2 METHODS – SECTION 2.1.2

Docking simulations of nucleoside analogues were performed using Protein-Ligand ANT System (PLANTS). Small molecule databases were prepared using MOE2014.09. The nucleotides monophosphate were designed with the Builder tool and energy minimised with MMFF94x force field. Databases were converted to a format PLANTS-compatible. To identify the docking site, the centre was set at the oxygen atom of ATP with radius of 10Å. In each docking simulation, 5 poses were generated and visually inspected using MOE2014.09.

The scaffold replacement was performed using MOE2014.09. The database of linkers that was used for the screening was available in MOE2014.09. Linkers were selected for a Tanimoto index of similarity less than 0.8, a molecular weight of the corresponding NTP less than 525 Da and for the essential feature of hydrogen bond donor (pharmacophore). The pharmacophore was built using MOE2014.09.

Docking simulations of acyclic nucleoside analogues were performed using Protein-Ligand ANT System (PLANTS). Small molecule databases were prepared using MOE2014.09. The nucleotides triphosphate were designed with the Builder tool and energy minimised with MMFF94x force field. Databases were converted to a format PLANTS-compatible. To identify the docking site, the centre was set at the oxygen atom of ATP with radius of 10Å. In each docking simulation, 20 poses were generated and visually inspected using MOE2014.09.

4.1.3 METHODS – SECTION 2.1.3

All MD simulations were performed using the application Desmond of Schrödinger Maestro 9.5. Protein complexes were prepared with the Protein Preparation Wizard tool using Schrödinger Maestro 9.5. The model system was built by employing an orthorhombic box of 10Å side and by adding molecules of water as SPC solvent model. The total charges of the system were neutralised by adding either Na^+ or Cl^- ions. Solvation was run using OPLS_2005 force field. An initial energy minimization was performed to relax the system before the MD simulation. The maximum number of iterations was set at 2 000 steps. The MD simulation was 50 ns long and trajectory and energy values were recorded every 100 ps (500 steps). The simulation was run in NPT conditions (constant number of atoms N, pressure P and temperature T) at the temperature of 300 K and pressure of 1.01325 bar. Results were visually inspected using VMD 1.9.1. Additionally, the final step of the MD simulation and the system before the MD simulation were superposed using MOE2014.09.

For the model of the complete *apo* DENV RdRp, the DENV RdRp crystal structure, downloaded from the Protein Data Bank website (codes 4HHJ),[1] was used. Water molecules, non-catalytic ions and glycerol were removed using MOE2014.09. The missing loops in the protein (spanning residues from 406 to 420 and from 457 to 469) were constructed using the MOE Structure Preparation tool. The Mg^{2+} ions were imported from Protein Data Bank code 2J7U[3] and re-positioned manually using MOE2014.09. The protein complex was prepared following the standard procedure, by adding 8 Cl^- ions to neutralise the molecular system, minimised and submitted to the MD simulation.

For the construction of the model of the complete *de novo* initiation complex, the final step of the previous MD simulation was used. Using MOE2014.09, the water molecules (SPC) were removed and the nucleic acid was imported from the crystal structure of the HCV NS5B complex, downloaded from the Protein Data Bank website (codes 4E78).[2] Using the same modelling program, an incomplete nucleotide present in the original crystal structure was bound to a copy of the ssRNA and the molecules of 3dGTP were converted to GMP. Loops spanning residues from 406 to 420 (loop **L1**), from 457 to 469 (loop **L2**) and the priming loop (residues 782 to 809) were deleted and constructed using the MOE Loop Modeller tool. The *de novo* method was applied to generate multiple loop conformations, setting RMSD limit at 0.5, loop limit at 100 and energy window at 5.0. The new conformations were inspected visually to select the most conservative

and appropriate conformations for each loop. The protein complex was prepared following the standard procedure, by adding 11 Na^+ ions to neutralise the molecular system, minimised and submitted to the MD simulation.

For the construction of the model of the elongation complex, the nucleic acid of the crystal structure of the HCV NS5B complex, downloaded from the Protein Data Bank website (codes 4E78),[2] was duplicated and the copy bound to the original one to build the 8-nucleotide long dsRNA, using MOE2014.09. The molecules of 3dGTP were converted to GMP. The dsRNA was minimised using AMBER99 force field and imported into the final step of the previous MD simulation, after removing the water molecules (SPC). Part of the priming loop spanning residues from 782 to 796 was deleted and constructed using the MOE Loop Modeller tool. The *de novo* method was applied to generate multiple loop conformations, setting RMSD limit at 0.25, loop limit at 100 and energy window at 5.0. The new conformations were inspected visually and the most conservative one was selected. The protein complex was minimised using AMBER99 force field. The protein complex was prepared following the standard procedure, by adding 14 Na^+ ions to neutralise the molecular system, minimised and submitted to the MD simulation.

The crystal structure of the DENV RdRp bound to the allosteric inhibitor NITD107 was downloaded from the Protein Data Bank website (code 3VWS)[1] and superposed to the final step of the MD simulation on the elongation complex using MOE2014.09.

4.2 SYNTHETIC PROCEDURES

4.2.1 GENERAL INFORMATION

All reagents and anhydrous solvents were used as supplied from Sigma-Aldrich, Fisher Scientific or other commercial sources without further purification or treatment.

Reactions under MWI conditions were performed in a CEM Discover microwave system in closed vessel mode.

Thin layer chromatography (TLC) was carried out on commercial Merck silica gel 60 F_{254} plates. Compounds were visualized under UV light (254 nm) or potassium permanganate stain.

Column chromatography was performed using Fisher Scientific silica gel 60A particle size 35-70 micron as a stationary phase. Flash column chromatography was performed on a Interchim PuriFlash 430 using high performance silica gel particle size 50 micron cartridges.

Melting points were measured on a Griffin 220V melting point apparatus.

^{1}H NMR spectra were recorded on a BrukerAvance Ultra Shield (500 MHz) spectrometer and tetramethylsilane was used as the internal standard. ^{13}C NMR spectra were recorded on a BrukerAvance Ultra Shield (126 MHz) spectrometer and the solvent resonance was employed as the internal standard. ^{31}P NMR spectra were recorded on a BrukerAvance Ultra Shield (202 MHz) spectrometer and were proton-decoupled. MestReNova (v6.0.2-5475) NMR processing software was used for the assignment of peaks and calculation of coupling constants. Chemical shifts δ are given in ppm (parts per million) relative to the internal standard and accompanied by multiplicity (s for singlet, br s for broad singlet, d for doublet, t for triplet, q for quartet and m for multiplet), coupling constants $J_{H,H}$ in Hz and relative assignment.

Low resolution mass spectrometry (MS) was performed on a Bruker MicroTOF-LC in positive mode and electron spray ionization (ES+). High resolution mass spectrometry (HRMS) was performed as a service by Cardiff University (School of Chemistry).

Reverse-phase analytical and semi-preparative high performance liquid chromatography (HPLC) experiments were carried out on a Variant ProStar (LC work station – Varian ProStar 335LC detector, Varian fraction collector, ProStar 201 delivery system) using a XSelect CSH C18 (5 µm, 4.6 x 150 mm) column and a Variant Pursuit XRs 5C18 (150 x 21.2 mm) column, respectively. Galaxie Chromatography Data System was used as software. Elution systems used were: mobile phase water/methanol in gradient from 10% to 100% of methanol in 30 minutes (system 1), mobile phase water/methanol in gradient from 100% to 70% of water in 15 minutes, then to 100%

methanol in 15 minutes (system 2) for analytical experiments; mobile phase water/acetonitrile in gradient from 10% to 100% of acetonitrile in 30 minutes (system 3) for semi-preparative experiments.

4.2.2 PROCEDURES AND SPECTRAL DATA – SECTION 2.2.1

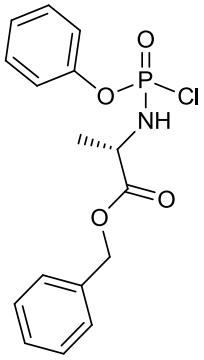

$C_{16}H_{17}ClNO_4P$, MW 353.74

***N*-(chlorophenoxyphosphinyl)-L-alanine benzyl ester** (**35**).[4]

L-alanine benzyl ester *p*-tosylate salt **32** (0.50 g, 1.42 mmol) was suspended in anhydrous dichloromethane under an argon atmosphere and phenyl dichlorophosphate **34** (0.21 mL, 1.42 mmol) was added at room temperature. The mixture was cooled to -78 °C before adding triethylamine (0.40 mL, 2.84 mmol) dropwise. After stirring 1 hour at -78 °C, the reaction mixture was allowed to attain room temperature and stirred for additional 2 hours. The solvent was removed under reduced pressure and the crude residue was purified by quick column chromatography on silica gel eluting with hexane/ethylacetate (50:50 v/v) to obtain compound **35** (0.47 g, 94% yield) as a colourless oil.

^{31}P NMR (202 MHz, $CDCl_3$) δ 8.03, 7.79.

^{1}H NMR (500 MHz, $CDCl_3$) δ 7.31 – 7.10 (m, 10H, Harom), 5.12, 5.10 (2s, 2H, C*H*$_2$(C_6H_5)), 4.57 – 4.46 (m, 1H, N*H*), 4.22 – 4.06 (m, 1H, C*H*CH_3), 1.43, 1.42 (2d, *J* = 7.0 Hz, 3H, CHC*H*$_3$).

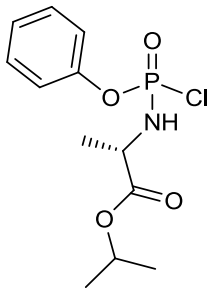

$C_{12}H_{17}ClNO_4P$, MW 305.69

***N*-(chlorophenoxyphosphinyl)-L-alanine isopropyl ester** (**36**).[5]

L-alanine isopropyl ester hydrochloride **33** (1.00 g, 5.97 mmol) was dissolved in anhydrous dichloromethane under an argon atmosphere and phenyl dichlorophosphate **34** (0.90 mL, 5.97 mmol) was added at room temperature. The mixture was cooled to -78 °C before adding triethylamine (1.66 mL, 11.93 mmol) dropwise. After stirring 1 hour at -78 °C, the reaction mixture was allowed to attain room temperature and stirred for additional 2 hours. The solvent was removed under reduced pressure. The crude residue was suspended in anhydrous diethyl ether under an argon atmosphere and stirred for 15 minutes, then filtered under vacuo protected by a flow of nitrogen. The ethereal filtrate was evaporated under reduced pressure to obtain compound **36** (1.81 g, 95% yield) as a colourless oil.

^{31}P NMR (202 MHz, $CDCl_3$) δ 8.09, 7.72.

^{1}H NMR (500 MHz, $CDCl_3$) δ 7.34 – 7.16 (m, 5H, Harom), 5.06 – 4.97 (m, 1H, *H*-*i*Pr), 4.29, 4.21 (2 br s, 1H, N*H*), 4.13 – 3.99 (m, 1H, C*H*CH_3), 1.43, 1.42 (2d, *J* = 2.4 Hz, 1H, CHC*H*$_3$), 1.23 – 1.18 (m, 6H, 2 C*H*$_3$-*i*Pr).

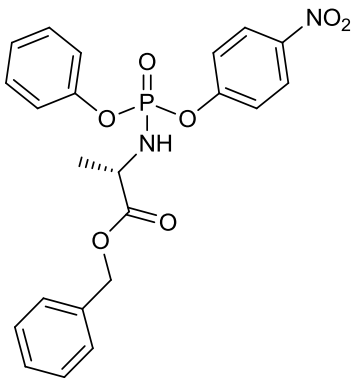

$C_{22}H_{21}N_2O_7P$, MW 456.39

***N*-[(4-nitrophenoxy)phenoxyphosphinyl]-L-alanine benzyl ester** (**37**).[6]

Procedure *a*:

A solution of **35** (0.66 g, 1.87 mmol) in anhydrous dichloromethane was cooled to -78 °C under a nitrogen atmosphere (solution A). In another flask, 4-nitrophenol (0.29 mg, 2.05 mmol) was suspended in dichloromethane and triethylamine (0.52 mL, 3.73 mmol) was added dropwise at room temperature under a nitrogen atmosphere (solution B). The resulting solution (solution B) was added slowly to solution A at -78 °C under a nitrogen atmosphere. The reaction mixture was stirred at a temperature from -78 °C to -40 °C for 2 hours, then the solvent was removed under reduced pressure. The crude residue was suspended in diethyl ether and stirred for 15 minutes, then filtered under vacuo. The ethereal filtrate was evaporated under reduced pressure and the crude residue was purified by flash column chromatography on silica gel (hexane to hexane/ethylacetate 80:20 v/v) to obtain compound **37** (0.62 g, 73% yield) as a colourless oil.

Procedure *b*:

A solution of 4-nitrophenyldichlorophosphate **39** (1.00 g, 3.91 mmol) in dichloromethane was cooled to -78 °C under a nitrogen atmosphere (solution A). In another flask, phenol (0.37 g, 3.91 mmol) was dissolved in dichloromethane and triethylamine (0.60 mL, 4.30 mmol) was added dropwise at room temperature under a nitrogen atmosphere (solution B). Solution B was added slowly to solution A at -78 °C under a nitrogen atmosphere. The resulting solution was stirred at -78 °C for 1 hour, then added to a stirred solution of L-alanine benzyl ester *p*-tosylate salt **32** (1.37 g, 3.91 mmol) in dichloromethane at -50 °C. Triethylamine (1.14 mL, 8.21 mmol) was added dropwise at -50 °C and the resulting reaction mixture was stirred for 1 hour at the same temperature, then allowed to attain 0 °C and stirred for additional 2 hours. The solvent was removed under reduced pressure. The crude residue was suspended in ethylacetate and stirred

for 15 minutes, then filtered under vacuo. The filtrate was evaporated under reduced pressure and the crude residue was purified by flash column chromatography on silica gel (hexane to hexane/ethylacetate 80:20 v/v) to obtain compound **37** (1.61 g, 90% yield) as a colourless oil.

^{31}P NMR (202 MHz, CDCl3) δ -3.22, -3.35.

^{1}H NMR (500 MHz, $CDCl_3$) δ 8.08 (m, 2H, Harom), 7.31 – 7.09 (m, 12H, Harom), 5.10 – 5.00 (m, 2H, C*H*$_2$(C_6H_5)), 4.17 – 3.95 (m, 2H, N*H* and C*H*CH_3), 1.34, 1.33 (2d, *J* = 4.0 Hz, 3H, CHC*H*$_3$).

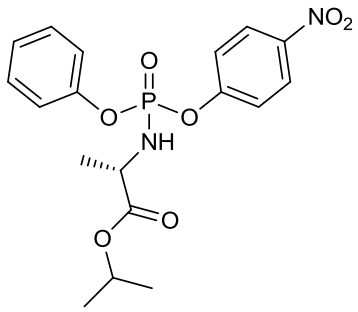

$C_{19}H_{23}N_2O_7P$, MW 408.34

***N*-[(4-nitrophenoxy)phenoxyphosphinyl]-L-alanine isopropyl ester** (**38**).[7, 8]

Procedure *a*:

A solution of **36** (1.76 g, 5.76 mmol) in anhydrous dichloromethane was cooled to -78 °C under a nitrogen atmosphere (solution A). In another flask, 4-nitrophenol (0.80 g, 5.76 mmol) was suspended in dichloromethane and triethylamine (1.6 mL, 11.51 mmol) was added dropwise at room temperature under a nitrogen atmosphere (solution B). The resulting solution (solution B) was added slowly to solution A at -78 °C under a nitrogen atmosphere. The reaction mixture was stirred at a temperature from -78 °C to -40 °C for 2 hours, then the solvent was removed under reduced pressure. The crude residue was suspended in diethyl ether and stirred for 15 minutes, then filtered under vacuo. The ethereal filtrate was evaporated under reduced pressure and the crude residue was purified by flash column chromatography on silica gel (hexane to hexane/ethylacetate 75:25 v/v) to obtain compound **38** (1.49 g, 63% yield) as a colourless oil.

Procedure *b*:

A solution of 4-nitrophenyldichlorophosphate **39** (2.00 g, 7.81 mmol) in dichloromethane was cooled to -78 °C under a nitrogen atmosphere (solution A). In another flask, phenol (0.74 g, 7.81 mmol) was dissolved in dichloromethane and triethylamine (1.20 mL, 8.59 mmol) was added dropwise at room temperature under a nitrogen atmosphere (solution B). Solution B was added

slowly to solution A at -78 °C under a nitrogen atmosphere. The resulting solution was stirred at -78 °C for 1 hour, then added to a stirred solution of L-alanine isopropyl ester hydrochloride **33** (1.31 g, 7.81 mmol) in dichloromethane at -50 °C. Triethylamine (2.30 mL, 16.41 mmol) was added dropwise at -50 °C and the resulting reaction mixture was stirred for 1 hour at the same temperature, then allowed to attain 0 °C and stirred for additional 2 hours. The solvent was removed under reduced pressure. The crude residue was suspended in ethylacetate and stirred for 15 minutes, then filtered under vacuo. The filtrate was evaporated under reduced pressure and the crude residue was purified by flash column chromatography on silica gel (hexane to hexane/ethylacetate 75:25 v/v) to obtain compound **38** (2.72 g, 86% yield) as a colourless oil.

^{31}P NMR (202 MHz, $CDCl_3$) δ -3.15, -3.19.

^{1}H NMR (500 MHz, $CDCl_3$) δ 8.25 (m, 2H, Harom), 7.44 – 7.35 (m, 4H, Harom), 7.28 – 7.21 (m, 3H, Harom), 5.08 – 4.98 (m, 1H, *H*-*i*Pr), 4.17 – 4.06 (m, 1H, C*H*CH_3), 3.93 (m, 1H, N*H*), 1.43, 1.41 (2d, *J* = 2.9 Hz, 3H, CHC*H*$_3$), 1.26, 1.24 (2d, *J* = 4.2 Hz, 6H, 2 C*H*$_3$-*i*Pr).

4.2.3 PROCEDURES AND SPECTRAL DATA – SECTION 2.2.2

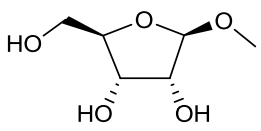

$C_6H_{12}O_5$, MW 164.16

1-*O*-Methyl-β-D-ribofuranose (**44**).[8]

To a stirred suspension of D-ribose **42** (4,00 g, 26.60 mmol) in anhydrous methanol (40 mL) concentrated sulfuric acid (0.26 mL, 2.66 mmol) was added dropwise at -5°C under a nitrogen atmosphere. The reaction mixture was allowed to attain room temperature and the resulting clear solution was stirred for 24 hours. Then the solution was neutralised with the addition of sodium acetate (0.66 g, 7.98 mmol) and concentrated under reduced pressure. The cloudy oily residue was purified by column chromatography on silica gel eluting with ethyl acetate/methanol (90:10 v/v) to obtain compound **44** (2.81 g, 64% yield) as a colourless syrup.

^{1}H NMR (500 MHz, DMSO-d_6) δ 4.95 (br s, 1H, 2-OH), 4.76 (d, $J_{3\text{-}OH,3}$ = 4.8 Hz, 1H, 3-OH), 4.63 (s, 1H, H-1), 4.58 (t, $J_{5\text{-}OH,5}$ = 5.6 Hz, 1H, 5-OH), 3.86 – 3.81 (m, 1H, H-3), 3.78 – 3.70 (m, 2H, H-4 and H-2), 3.54 – 3.49 (m, 1H, H-5a), 3.38 – 3.32 (m, 1H, H-5b), 3.23 (s, 3H, 1-OCH_3).

^{13}C NMR (126 MHz, DMSO-d_6) δ 108.03 (CH, C1), 83.55 (CH, C4), 74.20 (CH, C2), 70.92 (CH, C3), 63.14 (CH_2, C5), 54.21 (CH_3, 1-OCH_3).

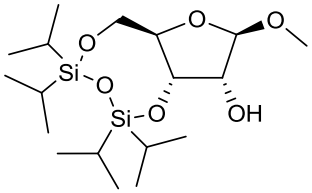

$C_{18}H_{38}O_6Si_2$, MW 406.66

3,5-*O*-(Tetraisopropyldisiloxane-1,3-diyl)-1-*O*-methyl-β-D-ribofuranose (**46**).[8]

Compound **44** (0.51 g, 3.11 mmol) was dried by several coevaporations with anhydrous acetonitrile and dissolved in anhydrous pyridine (8 mL). The solution was cooled to 0 °C and 1,3-dichloro-1,1,3,3-tetraisopropyldisiloxane (0.90 mL, 2.80 mmol) was added dropwise under an argon atmosphere. Then the cooling bath was removed and the reaction mixture was stirred at

room temperature for 1 hour. The solvent was evaporated and the residue was dissolved in ethyl acetate (50 mL), washed with water (50 mL) and brine (50 mL). The organic layer was dried over anhydrous Na_2SO_4, filtered and concentrated under reduced pressure. The residue was purified by column chromatography on silica gel eluting with hexane/ethyl acetate (80:20 v/v) to give compound **46** (0.85 g, 67% yield) as a colourless syrup.

^{1}H NMR (500 MHz, $CDCl_3$) δ 4.83 (s, 1H, H-1), 4.51 (apparent t, 1H, H-4), 4.09 – 4.00 (m, 3H, H-2, H-3 and H-5a), 3.77 (dd, *J* = 10.9, 9.1 Hz, 1H, H-5b), 3.33 (s, 3H, 1-OC*H*$_3$), 2.99 (s, 1H, 2-OH), 1.14 – 1.03 (m, 28H, 4 C*H*-*i*Pr and 8 C*H*$_3$-*i*Pr).

^{13}C NMR (126 MHz, $CDCl_3$) δ 107.28 (CH, C1), 82.64, 75.77 (2 CH, C2 and C3), 75.00 (CH, C4), 66.15 (CH_2, C5), 54.85 (CH_3, 1-O*C*H_3), 17.48, 17.39, 17.36, 17.33, 17.15, 16.99, 16.96, 16.93 (8 CH_3, 8 *C*H_3-*i*Pr), 13.28, 12.82, 12.59 (3 CH, 4 *C*H-*i*Pr).

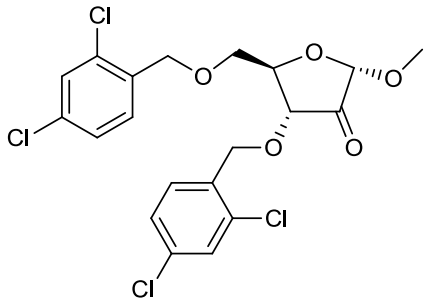

$C_{20}H_{18}Cl_4O_5$, MW 480.17

3,5-Bis-*O*-(2,4-dichlorobenzyl)-1-*O*-methyl-α-D-ribofuran-2-ulose (**49**).[9]

To a stirred suspension of Dess-Martin periodinane (1.13 g, 2.65 mmol) in anhydrous dichloromethane (8 mL) was added a solution of commercially available 1-*O*-methyl-3,5-bis-*O*-(2,4-dichlorobenzyl)-α-D-ribofuranose **48** (0.80 g, 1.66 mmol) in anhydrous dichloromethane (6 mL) dropwise at 0 °C under a nitrogen atmosphere. The suspension was stirred at this temperature for 0.5 hour and then at room temperature for 72 hours. The mixture was diluted with diethyl ether (15 mL), poured into a solution of $Na_2S_2O_3{\cdot}5H_2O$ (3 g) in saturated aqueous $NaHCO_3$ solution (30 mL) and stirred for 0.5 hour. The phases were separated and the aqueous solution was further extracted with diethyl ether (2 x 30 mL). The combined organic layer was washed with saturated aqueous $NaHCO_3$ solution (50 mL), water (50 mL) and brine (50 mL), dried over anhydrous Na_2SO_4, filtered and concentrated to dryness. The oily residue was purified by column chromatography on silica gel eluting with hexane/ethyl acetate (60:40 v/v) to give compound **49** (0.72 g, 90% yield) as a colourless oil. ^{1}H NMR (500 MHz, $CDCl_3$) δ 7.33 – 7.22 (m, 4H, Harom), 7.20 – 7.09 (m, 2H,

Harom), 4.93 (d, J_{gem} = 12.5 Hz, 1H, *H*-CH($C_6H_3Cl_2$)), 4.78 (d, $J_{1,3}$ = 1.0 Hz, 1H, H-1), 4.69 (d, J_{gem} = 12.5 Hz, H, *H*-CH($C_6H_3Cl_2$)), 4.50 (d, J_{gem} = 13.0 Hz, 1H, *H*-CH($C_6H_3Cl_2$)), 4.60 (d, J_{gem} = 13.0 Hz, H, *H*-CH($C_6H_3Cl_2$)), 4.29 (ddd, $J_{4,3}$ = 8.3 Hz, $J_{4,5b}$ = 3.4 Hz, $J_{4,5a}$ = 2.5 Hz, 1H, H-4), 4.12 (dd, $J_{3,4}$ = 8.4, $J_{3,1}$ = 1.2 Hz, 1H, H-3), 3.85 (dd, $J_{5a,5b}$ = 11.3 Hz, $J_{5a,4}$ = 2.4 Hz, 1H, H-5a), 3.72 (dd, $J_{5b,5a}$ = 11.3 Hz, $J_{5b,4}$ = 3.6 Hz, 1H, H-5b), 3.41 (s, 3H, 1-OCH_3).

^{13}C NMR (126 MHz, $CDCl_3$) δ 207.25 (C, C=O), 134.45, 134.11, 133.96, 133.89, 133.56, 133.47 (6 C, Carom), 130.59, 129.91, 129.22, 127.16 (4 CH, Carom), 98.71 (CH, C1), 77.80 (CH, C4), 76.31 (CH, C3), 70.19 (CH_2, *C*H_2($C_6H_3Cl_2$)), 69.47 (CH_2, *C*H_2($C_6H_3Cl_2$)), 68.91 (CH_2, C5), 55.87 (CH_3, 1-O*C*H_3).

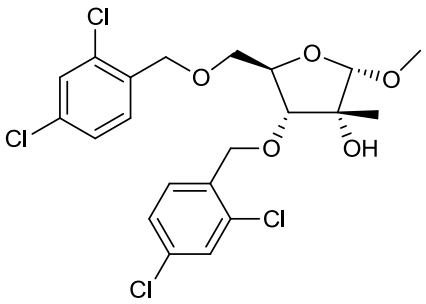

$C_{21}H_{22}Cl_4O_5$, MW 496.21

3,5-Bis-*O*-(2,4-dichlorobenzyl)-2-*C*-methyl-1-*O*-methyl-α-D-ribofuranose (**50**).[9]

A solution of 3.0M methylmagnesium bromide in diethyl ether (0.83 mL, 2.50 mmol) was diluted in diethyl ether (4.5 mL) and cooled to -55°C, before adding dropwise a solution of compound **49** (0.30 g, 0.63 mmol) in diethyl ether (2 mL) under a nitrogen atmosphere. The reaction mixture was allowed to warm to -30 °C and stirred at -30 °C to -15°C for 2 hours, then a solution of 3.0M methylmagnesium bromide in diethyl ether (0.83 mL, 2.50 mmol) was added dropwise. The reaction mixture was allowed to attain 0 °C, stirred for additional 5 hours and quenched with saturated NH_4Cl aqueous solution (50 mL). After vigorous stirring over 30 minutes at room temperature, the mixture was extracted with diethyl ether (3 x 50 mL). The combined organic layer was washed with water (60 mL) and brine (60 mL), dried over anhydrous Na_2SO_4, filtered and concentrated to dryness. The crude oily residue was purified by column chromatography on silica gel eluting with hexane/ethyl acetate (70:30 v/v) to give compound **50** (0.17 g, 54% yield) as a colourless oil.

^{1}H NMR (500 MHz, $CDCl_3$) δ 7.34 – 7.25 (m, 4H, Harom), 7.19 – 7.10 (m, 2H, Harom), 4.72 (d, J_{gem} = 13.2 Hz, 1H, *H*-CH($C_6H_3Cl_2$)), 4.56 – 4.50 (m, 3H, *H*-CH($C_6H_3Cl_2$) and CH_2($C_6H_3Cl_2$)), 4.43 (s, 1H, H-1),

4.10 (apparent q, 1H, H-4), 3.58 (d, $J_{5,4}$ = 4.6 Hz, 2H, H-5a and H-5b), 3.37 (s, 3H, 1-OCH_3), 3.33 (d, $J_{3,4}$ = 4.2 Hz, 1H, H-3), 3.25 (s, 1H, 2-OH), 1.27 (s, 3H, 2-CH_3).

^{13}C NMR (126 MHz, $CDCl_3$) δ 134.40, 134.26, 133.95, 133.91, 133.56, 133.46 (6 C, Carom), 130.11, 129.80, 129.14, 129.12, 127.09 (5 CH, Carom), 107.42 (CH, C1), 82.86 (CH, C3), 81.96 (CH, C4), 76.85 (C, C2), 70.70 (CH_2, C5), 70.03 (CH_2, $CH_2(C_6H_3Cl_2)$), 69.72 (CH_2, $CH_2(C_6H_3Cl_2)$), 55.20 (CH_3, 1-OCH_3), 24.69 (CH_3, 2-CH_3).

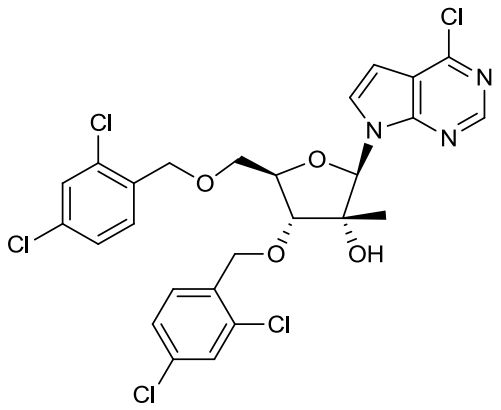

$C_{26}H_{22}Cl_5N_3O_4$, MW 617.74

6-Chloro-7-deaza-9-[3,5-bis-*O*-(2,4-dichlorobenzyl)-2-*C*-methyl-β-D-ribofuranosyl]purine (**51**).[9]

Procedure *a*:

To a solution of compound **50** (0.10 g, 0.20 mmol) in anhydrous dichloromethane (3 mL) at 0 °C was added dropwise a solution of 5.7M bromine hydride in acetic acid (0.21 mL, 1.21 mmol) under an argon atmosphere. The resulting solution was stirred at 0 °C for 1 hour, then allowed to attain room temperature and stirred for additional 3 hours. After full conversion of the starting material (monitored by TLC), the solution was evaporated under reduced pressure and coevaporated with anhydrous toluene (3 x 0.5 mL). The oily residue was dissolved in anhydrous acetonitrile (0.5 mL) and added to a stirring solution of the sodium salt of 6-chloro-7-deazapurine **121** in acetonitrile (generated in situ from commercially available 6-chloro-7-deazapurine **121** (0.09 g, 0.60 mmol) in anhydrous acetonitrile (10 mL), and sodium hydride 60% dispersion in mineral oil (0.02 g, 0.60 mmol), after vigorously stirring for 4 hours at room temperature under a nitrogen atmosphere). The combined mixture was stirred at room temperature for 60 hours, then evaporated to dryness. The residue was suspended in water (30 mL) and extracted with ethyl acetate (3 x 30 mL). The combined organic layer was washed with water (50 mL) and brine (50 mL), dried over anhydrous Na_2SO_4, filtered and concentrated to dryness. The crude residue was purified by column

chromatography on silica gel eluting with hexane/ethyl acetate (70:30 v/v) to give compound **51** (0.021 g, 17% yield) as a colourless foam.

Procedure *b*:

To a solution of compound **50** (0.52 g, 1.04 mmol) in anhydrous dichloromethane (20 mL) at 0 °C was added dropwise a solution of 5.7M bromine hydride in acetic acid (1.22 mL, 6.97 mmol) under a nitrogen atmosphere. The resulting solution was allowed to attain room temperature and stirred for 2 hour. After full conversion of the starting material (monitored by TLC), the solution was evaporated under reduced pressure and coevaporated with anhydrous toluene (2 mL). The oily residue was dissolved in anhydrous acetonitrile (2 mL) and added to a stirring suspension of 6-chloro-7-deazapurine **121** (0.16 g, 1.04 mmol), potassium hydroxide 85% powder (0.21 g, 3.12 mmol) and tris[2-(2-methoxyethoxy)ethyl]amine (0.07 mL, 0.21 mmol) in anhydrous acetonitrile (20 mL) under a nitrogen atmosphere at room temperature. The reaction mixture was stirred for 1 hour, then filtered under vacuo and the filtrate was concentrated to dryness. The crude residue was purified by flash column chromatography on silica gel (hexane to hexane/ethyl acetate 70:30 v/v) to give compound **51** (0.25 g, 39% yield) as a colourless foam.

^{1}H NMR (500 MHz, $CDCl_3$) δ 8.56 (s, 1H, H-2), 7.61 (d, $J_{8,7}$ = 3.7 Hz, 1H, H-8), 7.37 – 7.16 (m, 6H, Harom), 6.47 (d, $J_{7,8}$ = 3.7 Hz, 1H, H-7), 6.34 (s, 1H, H-1'), 4.71 (d, J_{gem} = 12.0 Hz, 1H, *H*-CH($C_6H_3Cl_2$)), 4.65 (d, J_{gem} = 12.1 Hz, 1H, *H*-CH($C_6H_3Cl_2$)), 4.61 (d, J_{gem} = 12.6 Hz, 1H, *H*-CH($C_6H_3Cl_2$)), 4.56 (d, J_{gem} = 12.6 Hz, 1H, *H*-CH($C_6H_3Cl_2$)), 4.22 (dt, $J_{4',3'}$ = 7.9 Hz, $J_{4',5'}$ = 2.7 Hz, 1H, H-4'), 4.17 (d, $J_{3',4'}$ = 8.0 Hz, 1H, H-3'), 3.91 (dd, $J_{5'a,5'b}$ = 10.9, $J_{5'a,4'}$ = 2.5 Hz, 1H, H-5'a), 3.72 (dd, $J_{5'b,5'a}$ = 10.9 Hz, $J_{5'b,4'}$ = 2.9 Hz, 1H, H-5'b), 3.09 (s, 1H, 2'-OH), 0.86 (s, 3H, 2'-CH_3).

^{13}C NMR (126 MHz, $CDCl_3$) δ 152.26 (C, Carom), 150.96 (C, Carom), 150.86 (CH, C2), 134.99, 134.53, 134.17, 134.12, 133.79, 133.32 (6 C, Carom), 130.76, 130.35, 129.55, 129.51, 127.35, 127.24 (6 CH, Carom), 126.83 (CH, C8), 117.99 (C, Carom), 100.33 (CH, C7), 90.93 (CH, C1'), 80.90 (CH, C3'), 80.22 (CH, C4'), 79.36 (C, C2'), 70.54 (CH_2, *C*H_2($C_6H_3Cl_2$)), 70.21 (CH_2, *C*H_2($C_6H_3Cl_2$)), 68.94 (CH_2, C5'), 21.11 (CH_3, 2'-*C*H_3).

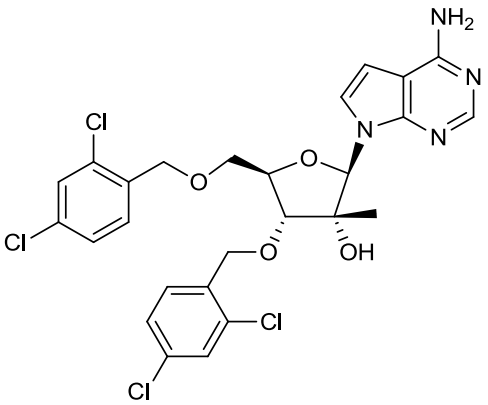

$C_{26}H_{24}Cl_4N_4O_4$, MW 598.31

7-Deaza-3',5'-bis-*O*-(2,4-dichlorobenzyl)-2'-*C*-methyladenosine (**54**).

Compound **51** (0.18 g, 0.29 mmol) was dissolved in a saturated (7M) solution of ammonia in methanol (10 mL). The reaction mixture was stirred in a screw-cap pressure glass tube at 80 °C for 48 hours, then cooled to room temperature. The solvent was evaporated and the crude residue was purified by column chromatography on silica gel eluting with hexane/ethylacetate (10:90 v/v to 0:100 v/v) to obtain the protected adenosine analogue **54** (0.15 g, 87% yield) as a white foam; mp: 60-62 °C.

^{1}H NMR (500 MHz, $CDCl_3$) δ 8.23 (s, 1H, H-2), 7.35 – 7.26 (m, 5H, Harom and H-8), 7.16 (ddd, 2H, Harom), 6.25 (s, 1H, H-1'), 6.23 (d, $J_{7,8}$ = 3.7 Hz, 1H, H-7), 5.23 (br s, 2H, 4-NH_2), 4.74 (d, J_{gem} = 12.3 Hz, 1H, *H*-CH($C_6H_3Cl_2$)), 4.65 (d, J_{gem} = 12.3 Hz, 1H, *H*-CH($C_6H_3Cl_2$)), 4.60 (d, J_{gem} = 12.8 Hz, 1H, *H*-CH($C_6H_3Cl_2$)), 4.56 (d, J_{gem} = 12.8 Hz, 1H, *H*-CH($C_6H_3Cl_2$)), 4.26 – 4.20 (m, 1H, H-4'), 4.13 (d, $J_{3',4'}$ = 7.7 Hz, 1H, H-3'), 3.88 (dd, $J_{5'a,5'b}$ = 10.8 Hz, $J_{5'a,4'}$ = 2.7 Hz, 1H, H-5'a), 3.73 (dd, $J_{5'b,5'a}$ = 10.8 Hz, $J_{5'b,4'}$ = 3.4 Hz, 1H, H-5'b), 0.90 (s, 3H, 2'-CH_3).

^{13}C NMR (126 MHz, $CDCl_3$) δ 156.73 (C, Carom), 151.83 (CH, C2), 150.32 (C, Carom), 134.65, 134.21, 134.09, 133.96, 133.87, 133.71 (6 C, Carom), 130.64, 130.16, 129.38, 129.34, 127.26, 127.16 (6 CH, Carom), 122.43 (CH, C8), 103.52 (C, Carom), 98.34 (CH, C7), 91.16 (CH, C1'), 81.57 (CH, C3'), 80.19 (CH, C4'), 79.28 (C, C2'), 70.33 (CH_2, *C*H_2($C_6H_3Cl_2$)), 70.09 (CH_2, *C*H_2($C_6H_3Cl_2$)), 69.38 (CH_2, C5'), 21.29 (CH_3, 2'-*C*H_3).

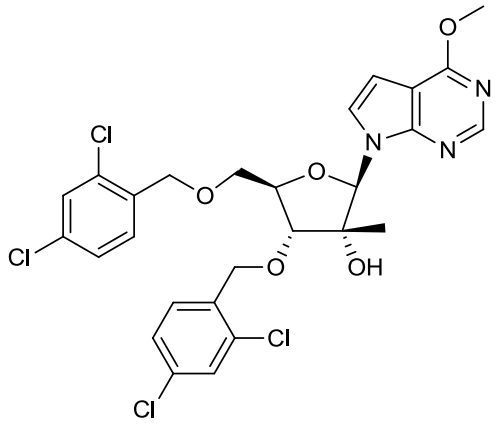

$C_{27}H_{25}Cl_4N_3O_5$, MW 613.32

7-Deaza-3',5'-bis-*O*-(2,4-dichlorobenzyl)-2'-*C*-methyl-6-*O*-methylinosine (**55**).

Compound **55** was isolated as a side-product of the synthesis of compound **54** and obtained as a white powder (0.018 g, 10% yield); mp: 71-73 °C.

^{1}H NMR (500 MHz, CD_3OD) δ 8.38 (s, 1H, H-2), 7.64 (d, $J_{8,7}$ = 3.7 Hz, 1H, H-8), 7.53 (d, J = 8.3 Hz, 1H, Harom), 7.49 – 7.43 (m, 3H, Harom), 7.35 – 7.31 (m, 2H, Harom), 6.47 (d, $J_{7,8}$ = 3.7 Hz, 1H, H-7), 6.34 (s, 1H, H-1'), 4.83 (d, 1H, J_{gem} = 12.7 Hz, 1H, *H*-CH($C_6H_3Cl_2$)), 4.73 (d, J_{gem} = 12.7 Hz, 1H, *H*-CH($C_6H_3Cl_2$)), 4.70 (d, J_{gem} = 12.6 Hz, 1H, *H*-CH($C_6H_3Cl_2$)), 4.62 (d, J_{gem} = 12.6 Hz, 1H, *H*-CH($C_6H_3Cl_2$)), 4.30 (m, 1H, H-4'), 4.27 (d, $J_{3',4'}$ = 8.7 Hz, 1H, H-3'), 4.12 (s, 3H, 4-OCH_3), 4.00 (dd, $J_{5'a,5'b}$ = 11.1 Hz, $J_{5'a,4'}$ = 1.9 Hz, 1H, H-5'a), 3.82 (dd, $J_{5'b,5'a}$ = 11.1 Hz, $J_{5'b,4'}$ = 2.6 Hz, 1H, H-5'b), 0.92 (s, 3H, 2'-CH_3).

^{13}C NMR (126 MHz, CD_3OD) δ 163.07, 151.52 (2 C, Carom), 150.41 (CH, C2), 134.47, 134.34, 134.08, 134.04, 133.93, 133.63 (6 CH, Carom), 130.94, 130.68, 128.87, 128.69, 126.96, 126.94 (6 C, Carom), 123.69 (CH, C8), 105.55 (C, Carom), 98.70 (CH, C7), 91.22 (CH, C1'), 80.44 (CH, C3'), 79.98 (CH, C4'), 79.11 (C, C2'), 69.73 (CH_2, CH_2($C_6H_3Cl_2$)), 69.51 (CH_2, CH_2($C_6H_3Cl_2$)), 68.53 (CH_2, C5'), 52.94 (CH_3, 4-OCH_3), 19.55 (CH_3, 2'-CH_3).

MS (ES+) *m/z* 614.1 [MH^+], 636.1 [MNa^+].

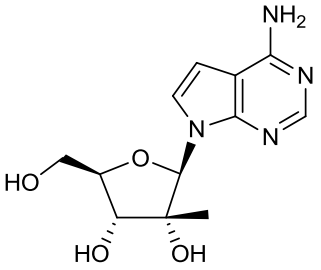

$C_{12}H_{16}N_4O_4$, MW 280.28

7-Deaza-2'-*C*-methyladenosine (**40**).[9]

Procedure *a*:

To a solution of compound **54** (0.11 g, 0.18 mmol) in anhydrous methanol and 10% glacial acetic acid, palladium on carbon (10% w/w, 0.011 g) was added and the reaction mixture was stirred under an hydrogen atmosphere (1 atm) for 48 hours (monitored by TLC). Then the reaction mixture was filtered through a celite pad, that was washed with methanol. The filtrate was evaporated and the crude residue was purified by column chromatography on silica gel eluting with ethylacetate/methanol (90:10 v/v) to obtain the nucleoside **40** (0.036 g, 70% yield) as a white foam; mp: 218-220 °C (lit. 222 °C).

Procedure *b*:

To a solution of **54** (0.32 g, 0.54 mmol) in anhydrous methanol, ammonium formate (0.27 g, 4.28 mmol) and palladium on carbon (20% w/w, 0.064 g) were added under a nitrogen atmosphere and the reaction mixture was heated at reflux for 16 hours, then cooled to room temperature and diluted with methanol. The suspension was filtered and the filtrate concentrated to dryness. The crude residue was purified by flash column chromatography on silica gel (ethylacetate to ethylacetate/methanol 90:10 v/v) to obtain the nucleoside **40** (0.12 g, 77% yield) as a white foam.

^{1}H NMR (500 MHz, CD_3OD) δ 8.11 (s, 1H, H-2), 7.50 (d, $J_{8,7}$ = 3.7 Hz, 1H, H-8), 6.63 (d, $J_{7,8}$ = 3.7 Hz, 1H, H-7), 6.24 (s, 1H, H-1'), 4.14 (d, $J_{3',4'}$ = 8.8 Hz, 1H, 3'-H), 4.06 – 4.02 (m, 2H, H-4' and H-5'a), 3.87 (dd, $J_{5'b,5'a}$ = 12.9 Hz, $J_{5'b,4'}$ = 3.8 Hz, 1H, H-5'b), 0.83 (s, 3H, 2'-CH_3).

^{13}C NMR (126 MHz, CD_3OD) δ 159.04 (C, Carom), 152.13 (CH, C2), 150.58 (C, Carom), 123.59 (CH, C8), 104.66 (C, Carom), 100.73 (CH, C7), 93.30 (CH, C1'), 83.75 (CH, C4'), 80.50 (C, C2'), 73.98 (CH, C3'), 61.48 (CH_2, C5'), 20.00 (CH_3, 2'-*C*H_3).

MS (ES+) *m/z* 281.1 [MH^+].

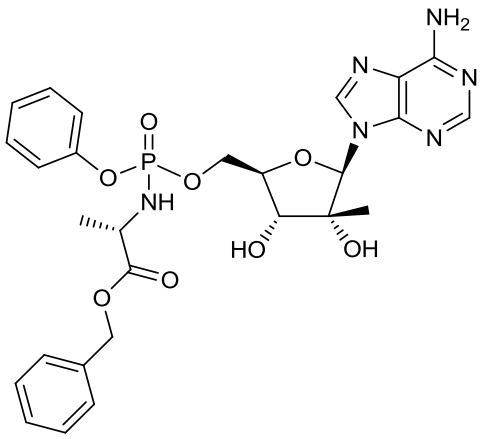

$C_{27}H_{31}N_6O_8P$, MW 598.54

2'-*C*-Methyladenosine 5'-*O*-[phenyl-(benzyloxy-L-alaninyl)] phosphate (**57**).

Commercially available 2'-*C*-methyl adenosine **56** (0.045 g, 0.16 mmol) was suspended in anhydrous tetrahydrofuran (0.3 mL) under an argon atmosphere and *tert*-butylmagnesium chloride 1M in tetrahydrofuran (0.16 mL, 0.16 mmol) was added dropwise at room temperature. After stirring 30 minutes, a solution of the phosphorochloridate **35** (0.11 g, 0.32 mmol) in anhydrous tetrahydrofuran (0.7 mL) was added slowly. The reaction mixture was stirred at room temperature for 48 hours (monitored by TLC), then the solvent was evaporated under reduced pressure and the residue was washed three times with chloroform. The crude residue was purified by column chromatography on silica gel eluting with chloroform/methanol (92:8 v/v) to isolate the titled compound. Compound **57** was further purified by semi-preparative HPLC (system 3) and obtained as a white solid (0.009 g, 9% yield).

^{31}P NMR (202 MHz, CD_3OD) δ 4.01, 3.75.

^{1}H NMR (500 MHz, CD_3OD) δ 8.24 - 8.22 (m, 2H, H-2 and H-8), 7.35 – 7.17 (m, 10H, Harom), 6.13, 6.11 (2s, 1H, H-1'), 5.16 – 5.02 (m, 2H, C*H*$_2$(C_6H_5)), 4.57 – 4.44 (m, 2H, H-4' and H-5'a), 4.27 – 4.18 (m, 2H, H-3' and H-5'b), 4.07 – 3.99 (m, 1H, C*H*CH_3), 1.35 – 1.32 (m, 3H, CHC*H*$_3$), 0.96, 0.93 (2s, 3H, 2'-C*H*$_3$).

^{13}C NMR (126 MHz, CD_3OD) δ 174.80 (d, $J_{C\text{-}C\text{-}N\text{-}P}$ = 4.4 Hz, C, C=O), 174.61 (d, $J_{C\text{-}C\text{-}N\text{-}P}$ = 5.4 Hz, C, C=O), 157.42, 157.41 (C, Carom), 154.02, 153.99 (CH, C2), 152.19, 152.13 (C, Carom), 150.44, 150.37 (C, Carom), 140.73, 140.46 (CH, C8), 137.24, 137.19 (C, Carom), 130.81, 130.78, 129.56, 129.53, 129.35, 129.29, 129.24, 129.13, 128.27, 128.00, 126.15, 121.45, 121.44, 121.42, 121.40 (CH, Carom) 120.38 (C, Carom), 93.37, 93.08 (CH, C1'), 82.26 (d, $J_{C\text{-}C\text{-}O\text{-}P}$ = 8.2 Hz, CH, C4'), 82.06 (d, $J_{C\text{-}C\text{-}O\text{-}P}$ = 7.8 Hz, CH, C4'), 80.02, 79.94 (C, C2'), 74.46, 73.93 (CH, C3'), 67.95, 67.89 (CH_2, *C*H_2(C_6H_5)),

67.31 (d, $J_{C\text{-}O\text{-}P}$ = 5.2 Hz, CH_2, C5'), 66.39 (d, $J_{C\text{-}O\text{-}P}$ = 4.8 Hz, CH_2, C5'), 51.77, 51.60 (CH, *C*HCH_3), 20.51 (d, $J_{C\text{-}C\text{-}N\text{-}P}$ = 6.2 Hz, CH_3, CH*C*H_3), 20.26 (d, $J_{C\text{-}C\text{-}N\text{-}P}$ = 7.2 Hz, CH_3, CH*C*H_3), 20.16 (CH_3, 2'-*C*H_3).

HPLC (system 1) t_R = 22.91, 23.24 min.

HPLC (system 2) t_R = 22.36 min.

MS (ES+) *m/z* 621.18 [MNa^+].

HRMS calculated for $C_{27}H_{32}N_6O_8P$: 599.2019; found 599.2037.

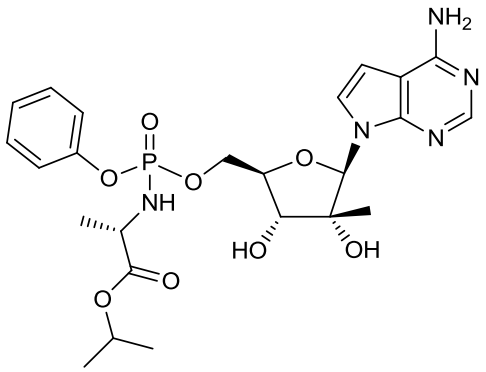

$C_{24}H_{32}N_5O_8P$, MW 549.51

7-Deaza-2'-*C*-methyladenosine 5'-*O*-[phenyl-(isopropoxy-L-alaninyl)] phosphate (**58**).

Compound **40** (0.05 g, 0.18 mmol) was dissolved in anhydrous dimethylformamide (1 mL) under a nitrogen atmosphere and *tert*-butylmagnesium chloride 1M in tetrahydrofuran (0.18 mL, 0.18 mmol) was added dropwise at room temperature. After stirring 10 minutes, a solution of the compound **38** (0.07 g, 0.18 mmol) in anhydrous dimethylformamide (1 mL) was added slowly. The reaction mixture was stirred for 4 hours at room temperature, then quenched by adding water (0.5 mL) slowly. The mixture was concentrated under reduced pressure by coevaporation with toluene. The crude residue was purified by flash column chromatography on silica gel (dichloromethane to dichloromethane/methanol 93:7 v/v) to isolate the titled compound. Compound **58** was further purified by flash column chromatography on silica gel (dichloromethane to dichloromethane/methanol 93:7 v/v) and obtained as a colourless wax (0.045 g, 46% yield).

^{31}P NMR (202 MHz, $CDCl_3$) δ 3.38, 3.11.

^{1}H NMR (500 MHz, $CDCl_3$) δ 8.19 (s, 1H, H-2), 7.22 – 7.13 (m, 4H, Harom), 7.05 – 6.93 (m, 2H, Harom and H-8), 6.32 – 6.22 (m, 1H, H-7 and H-1'), 5.81, 5.77 (2 br s, 2H, 6-NH_2), 4.93 – 4.83 (m, 1H, *H*-*i*Pr), 4.62 – 4.32 (m, 3H, N*H*, H-5'a and H-5'b), 4.18 – 4.12 (m, 1H, H-3'), 3.98 – 3.89 (m, 2H,

C*H*CH_3 and H-4'), 1.26, 1.25 (s, 3H, CHC*H_3*), 1.12 – 1.04 (m, 3H, 2 C*H_3*-*i*Pr), 0.71, 0.69 (2 s, 3H, 2'-C*H_3*).

^{13}C NMR (126 MHz, $CDCl_3$) δ 173.24, 173.19, 173.14 (C, C=O), 156.91, 156.89 (C, Carom), 151.55, 151.48 (CH, C2), 150.71, 150.66 (C, Carom), 149.69, 149.58 (C, Carom), 129.75 (CH, Carom), 125.04, 124.97 (CH, C8), 121.84, 121.71, 120.13, 120.11, 120.09, 120.07 (CH, Carom), 103.43, 103.35 (C, Carom), 99.16 (CH, C7), 91.43, 91.27 (CH, C1'), 80.70, 80.64 (CH, C3'), 73.93, 73.58 (CH, C4'), 69.34, 69.28 (CH, *C*H-*i*Pr), 65.89, 65.85 (d, $J_{C\text{-}O\text{-}P}$ = 4.4 Hz, CH_2, C5'), 65.26, 65.23 (d, $J_{C\text{-}O\text{-}P}$ = 4.1 Hz, CH_2, C5'), 50.48, 50.36 (CH, *C*HCH_3), 21.65, 21.57 (CH_3, 2 *C*H_3-*i*Pr), 20.93, 20.89 (d, $J_{C\text{-}C\text{-}N\text{-}P}$ = 5.1 Hz, CH_3, CH*C*H_3), 20.84, 20.80 (d, $J_{C\text{-}C\text{-}N\text{-}P}$ = 5.2 Hz, CH_3, CH*C*H_3), 19.89, 19.86 (CH_3, 2'-*C*H_3).

HPLC (system 1) t_R = 21.51, 21.54 min.

HPLC (system 2) t_R = 27.23, 27.84 min.

MS (ES+) *m/z* 550.2 [MH^+], 572.2 [MNa^+].

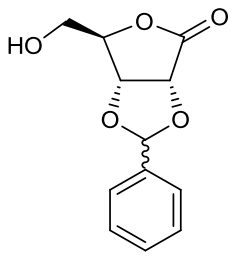

$C_{12}H_{12}O_5$, MW 236.22

2,3-*O*-(*R*,*S*)-Benzylidene-D-ribonic-γ-lactone (**64** and **65**).[10]

Procedure *a*:

To a stirred suspension of D-ribonic acid 1,4-lactone **63** (0.40 g, 2.70 mmol) in anhydrous acetonitrile (10 mL) was added benzaldehyde dimethyl acetal (0.40 mL, 2.70 mmol) under an argon atmosphere at 0 °C, followed by the addition of phosphorus (V) oxychloride (0.50 mL, 5.40 mmol) dropwise at the same temperature. The initial suspension was stirred for 1 hour at 0 °C. The resulting solution was poured slowly into iced saturated aqueous $NaHCO_3$ solution (30 mL) and stirred for 1.5 h at 0 °C. The solvent was distilled off and the aqueous solution was extracted with ethyl acetate (3 x 30 mL), the combined organic layer was washed with water (30 mL) and brine (30 mL), dried over anhydrous Na_2SO_4, filtered and concentrated to dryness under reduced pressure. The residue was purified by column chromatography on silica gel eluting with

hexane/ethyl acetate (70:30 v/v to 40:60 v/v) to give (*R*)-isomer **64** (SE) and (*S*)-isomer **65** (FE) as white powders (0.44 g, 68% yield, SE:FE = 3:1).

Procedure *b*:

To a stirred suspension of D-ribonic acid 1,4-lactone **63** (0.40 g, 2.70 mmol) in anhydrous dimethoxyethane (2 mL) was added benzaldehyde dimethyl acetal (0.50 mL, 3.24 mmol) and anhydrous tin(II) chloride (0.10 g, 0.54 mmol) under a nitrogen atmosphere at room temperature. The reaction mixture was heated at reflux for 1 hour, then cooled to room temperature and evaporated under reduced pressure. The crude residue was purified by flash column chromatography on silica gel (hexane to hexane/ethyl acetate 60:40 v/v) to give (*R*)-isomer **64** (SE) and (*S*)-isomer **65** (FE) as white powders (0.26 g, 41% yield, SE:FE = 1:1).

(*R*)-isomer **64** (SE):

^{1}H NMR (500 MHz, DMSO-d_6) δ 7.45 – 7.40 (m, 5H, Harom), 5.97 (s, 1H, C*H*(C_6H_5)), 5.42 (t, $J_{5\text{-}OH,5}$ = 4.9 Hz, 1H, 5-OH), 4.96 – 4.90 (m, 2H, H-2 and H-3), 4.79 (t, $J_{4,5}$ = 2.1 Hz, 1H, H-4), 3.72 (ddd, $J_{5a,5b}$ = 12.0 Hz, $J_{5a,5\text{-}OH}$ = 4.7 Hz, $J_{5a,4}$ = 1.8 Hz, 1H, H-5a), 3.66 (ddd, $J_{5b,5a}$ = 12.0 Hz, $J_{5b,5\text{-}OH}$ = 5.0 Hz, $J_{5b,4}$ = 2.7 Hz, 1H, 5b-H).

^{13}C NMR (126 MHz, DMSO-d_6) δ 173.48 (C, C=O), 135.83 (C, Carom), 129.83, 128.40, 126.71 (3 CH, Carom), 105.04 (CH, *C*H(C_6H_5)), 81.83 (CH, C4), 79.83, 75.19 (2 CH, C2 and C3), 60.36 (CH_2, C5).

(*S*)-isomer **65** (FE):

^{1}H NMR (500 MHz, DMSO-d_6) δ 7.51 – 7.40 (m, 5H, Harom), 5.94 (s, 1H, C*H*(C_6H_5)), 5.37 (t, $J_{5\text{-}OH,5}$ = 5.0 Hz, 1H, 5-OH), 5.12 (d, $J_{2,3}$ = 5.7 Hz, 1H, H-2), 4.83 (d, $J_{3,2}$ = 5.8 Hz, 1H, H-3), 4.80 (t, $J_{4,5}$ = 2.2 Hz, 1H, H-4), 3.72 (ddd, $J_{5a,5b}$ = 12.1 Hz, $J_{5a,5\text{-}OH}$ = 4.8 Hz, $J_{5a,4}$ = 2.2 Hz, 1H, H-5a), 3.65 (ddd, $J_{5b,5a}$ = 12.1 Hz, $J_{5b,5\text{-}OH}$ = 5.2 Hz, $J_{5b,4}$ = 2.9 Hz, 1H, H-5b).

^{13}C NMR (126 MHz, DMSO-d_6) δ 173.29 (C, C=O), 136.13 (C, Carom), 129.70, 128.34, 126.66 (3 CH, Carom), 103.59 (CH, *C*H(C_6H_5), 84.35 (CH, C4), 77.39 (CH, C3), 75.64 (CH, C2), 60.57 (CH_2, C5).

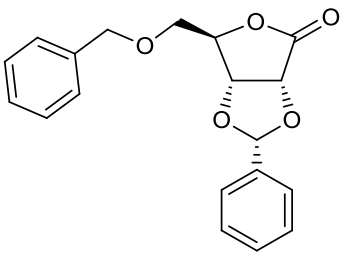

$C_{19}H_{18}O_5$, MW 326.34

5-*O*-Benzyl-2,3-*O*-(*R*)-benzylidene-D-ribonic-γ-lactone (**67**).[11]

To a cold (0 °C) solution of (*R*)-isomer **64** (0.40 g, 1.69 mmol) in anhydrous tetrahydrofuran (8 mL), sodium hydride 60% dispersion in mineral oil (0.082 g, 2.03 mmol) was added portionwise over 5 minutes under a nitrogen atmosphere. Then benzyl bromide (0.24 mL, 2.03 mmol) was added dropwise at the same temperature. The reaction mixture was allowed to attain room temperature and stirred for 16 hours. Ice was added slowly, then the reaction mixture was poured into ice-water and extracted with dichloromethane (3 x 30 mL). The combined organic layer was washed with water (60 mL) and brine (60 mL), dried over anhydrous Na_2SO_4, filtered and concentrated to dryness. The crude residue was purified by column chromatography on silica gel eluting with petroleum ether/ethyl acetate (80:20 v/v) to give **67** (0.14 g, 20% yield) as a white powder.

^{1}H NMR (500 MHz, DMSO-d_6) δ 7.45 – 7.31 (m, 10H, Harom), 5.98 (s, 1H, C*H*(C_6H_5)), 5.01 (d, $J_{3,2}$ = 5.8 Hz, 1H, H-3), 4.94 (t, $J_{4,3}$ = 2.3 Hz, 1H, H-4), 4.91 (d, $J_{2,3}$ = 5.8 Hz, 1H, H-2), 4.56 (s, 2H, CH_2(C_6H_5)), 3.80 (dd, $J_{5a,5b}$ = 10.8 Hz, $J_{5a,4}$ = 2.1 Hz, 1H, H-5a), 3.71 (dd, $J_{5b,5a}$ = 10.8 Hz, $J_{5b,4}$ = 2.6 Hz, 1H, H-5b).

^{13}C NMR (126 MHz, DMSO-d_6) δ 173.38 (C, C=O), 137.62, 135.67 (2 C, Carom), 129.90, 128.42, 128.38, 127.68, 127.35, 126.70 (6 CH, Carom), 105.30 (CH, *C*H(C_6H_5)), 80.22 (CH, C4), 79.70 (CH, C3), 75.15 (CH, C2), 72.61 (CH_2, *C*H_2(C_6H_5)), 68.72 (CH_2, C5).

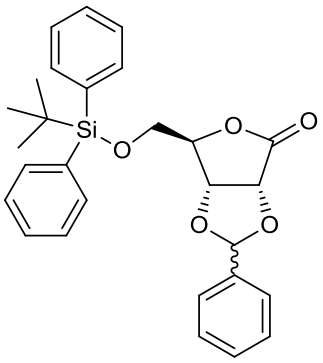

$C_{28}H_{30}O_5Si$, MW 474.62

5-*O*-(*tert*-butyldiphenylsilyl)-2,3-*O*-(*R*,*S*)-benzylidene-D-ribonic-γ-lactone (**73** and **74**).

To a solution of the mixture of (*R*)-isomer **64** and (*S*)-isomer **65** (0.25 g, 1.05 mmol) and 1*H*-imidazole (0.16 g, 2.30 mmol) in anhydrous dimethylformamide (2 mL) cooled to 0 °C, *tert*-butyldiphenylsilyl chloride (0.41 mL, 1.57 mmol) was added dropwise under a nitrogen atmosphere. After stirring 10 minutes at 0 °C, the reaction mixture was allowed to attain room temperature and stirred for 4 hours. The reaction mixture was poured into water (40 mL) and ethyl acetate (40 mL), the aqueous phase was separated and further extracted with ethyl acetate (2 x 40 mL). The combined organic layer was washed several times with brine (150 mL), dried over anhydrous $MgSO_4$, filtered and concentrated to dryness. The crude residue was purified by flash column chromatography on silica gel (hexane/ethyl acetate 97:3 v/v to hexane/ethyl acetate 90:10 v/v) to give (*R*)-isomer **73** (FE) and (*S*)-isomer **74** (SE) (0.24 g, 48% yield) as colourless oils.

(*R*)-isomer **73** (FE):

^{1}H NMR (500 MHz, $CDCl_3$) δ 7.56 – 7.51 (m, 4H, Harom), 7.40 – 7.28 (m, 11H, Harom), 5.87 (s, 1H, C*H*(C_6H_5)), 5.05 (d, *J* = 5.7 Hz, 1H), 4.76 (d, *J* = 5.7 Hz, 1H), 4.66 – 4.64 (m, 1H, H-4), 3.83 (dd, $J_{5a,5b}$ = 11.6 Hz, $J_{5a,4}$ = 2.0 Hz, 1H, H-5a), 3.69 (dd, $J_{5b,5a}$ = 11.5 Hz, $J_{5b,4}$ = 1.1 Hz, 1H, H-5b), 0.96 (s, 9H, *t*BuSi).

^{13}C NMR (126 MHz, $CDCl_3$) δ 173.10 (C=O), 135.66 (CH, Carom), 135.59 (C, Carom), 135.48 (CH, Carom), 132.23, 131.50 (2 C, Carom), 130.30, 129.95, 128.56, 128.12, 126.54 (5 CH, Carom), 104.68 (CH, *C*H(C_6H_5)), 84.24 (CH, C4), 77.87 (CH), 76.48 (CH), 63.80 (CH_2, C5), 26.82 (CH_3, 3 *C*H_3-*t*BuSi), 19.14 (C, *C*-*t*BuSi).

(*S*)-isomer **74** (SE):

^{1}H NMR (500 MHz, $CDCl_3$) δ 7.60 – 7.50 (m, 4H, Harom), 7.42 – 7.25 (m, 11H, Harom), 5.90 (s, 1H, C*H*(C_6H_5)), 4.96 (d, *J* = 5.8 Hz, 1H), 4.83 (d, *J* = 5.8 Hz, 1H), 4.62 (s, 1H, H-4), 3.85 (d, $J_{5a,5b}$ = 11.4 Hz, 1H, H-5a), 3.70 (d, $J_{5b,5a}$ = 11.5 Hz, 1H, H-5b), 0.98 (s, 9H, *t*BuSi).

^{13}C NMR (126 MHz, $CDCl_3$) δ 172.99 (C, C=O), 135.66, 135.50 (2 CH, Carom), 135.24, 132.26, 131.45 (3 C, Carom), 130.29, 130.13, 128.58, 128.10, 126.88 (5 CH, Carom), 106.71 (CH, *C*H(C_6H_5)), 81.65 (CH, C4), 80.08 (CH), 76.00 (CH), 63.62 (CH_2, C5), 26.82 (CH_3, 3 *C*H_3-*t*BuSi), 19.13 (C, *C*-*t*BuSi).

MS (ES+) *m/z* 497.2 [MNa^+].

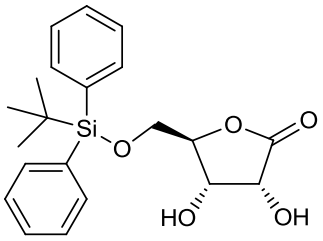

$C_{21}H_{26}O_5Si$, MW 386.51

5-*O*-(*tert*-butyldiphenylsilyl)-D-ribonic-γ-lactone (**75**).[12]

To a solution of D-ribonic acid 1,4-lactone **63** (0.40 g, 2.70 mmol) and 1*H*-imidazole (0.40 g, 5.94 mmol) in anhydrous dimethylformamide (3 mL) cooled to 0 °C, *tert*-butyldiphenylsilyl chloride (0.77 mL, 2.97 mmol) was added dropwise under a nitrogen atmosphere. After stirring 30 minutes at 0 °C, the reaction mixture was allowed to attain room temperature and stirred for 6 hours. The reaction mixture was poured into water (20 mL) and ethyl acetate (20 mL), the aqueous phase was separated and further extracted with ethyl acetate (2 x 20 mL). The combined organic layer was washed several times with brine (80 mL), dried over anhydrous $MgSO_4$, filtered and concentrated to dryness to give compound **75** (0.60 g, 57% yield) as a white solid, that was used in the next step without purification. For analysis, the crude residue was purified by flash column chromatography on silica gel (dichloromethane to dichloromethane/methanol 90:10 v/v).

^{1}H NMR (500 MHz, $CDCl_3$) δ 7.71 – 7.66 (m, 4H, Harom), 7.45 – 7.40 (m, 6H, Harom), 5.05 (br s, 1H, O*H*), 4.95 (d, *J* = 5.5 Hz, 1H, H-2), 4.61 (d, *J* = 5.5 Hz, 1H, H-3), 4.54 (s, 1H, H-4), 4.46 (br s, 1H, O*H*), 3.90 (dd, $J_{5a,5b}$ = 11.8 Hz, $J_{5a,4}$ =2.6 Hz, 1H, H-5a), 3.85 (dd, $J_{5b,5a}$ = 11.7 Hz, $J_{5b,4}$ = 1.8 Hz, 1H, H-5b), 1.07 (s, 9H, *t*BuSi).

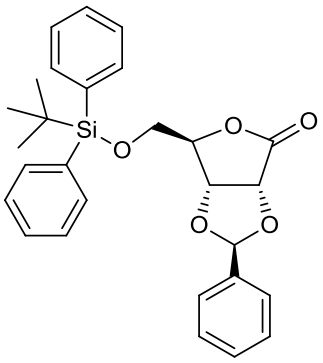

$C_{28}H_{30}O_5Si$, MW 474.62

5-*O*-(*tert*-butyldiphenylsilyl)-2,3-*O*-(*S*)-benzylidene-D-ribonic-γ-lactone (**74**).

To a stirred solution of crude compound **75** (0.25 g, 0.64 mmol) in anhydrous dimethoxyethane (2 mL) was added benzaldehyde dimethyl acetal (0.12 mL, 0.76 mmol) and anhydrous tin(II) chloride (0.024 g, 0.13 mmol) under a nitrogen atmosphere at room temperature. The reaction mixture was heated at reflux for 45 minutes, then cooled to room temperature and evaporated under reduced pressure. The crude residue was purified by flash column chromatography on silica gel (hexane/ethyl acetate 97:3 v/v to hexane/ethyl acetate 90:10 v/v) to give (*S*)-isomer **74** (0.12 g, 40% yield) as a colourless oil.

^{1}H NMR (500 MHz, $CDCl_3$) δ 7.60 – 7.50 (m, 4H, Harom), 7.42 – 7.25 (m, 11H, Harom), 5.90 (s, 1H, C*H*(C_6H_5)), 4.96 (d, *J* = 5.8 Hz, 1H), 4.83 (d, *J* = 5.8 Hz, 1H), 4.62 (s, 1H, H-4), 3.85 (d, $J_{5a,5b}$ = 11.4 Hz, 1H, H-5a), 3.70 (d, $J_{5b,5a}$ = 11.5 Hz, 1H, H-5b), 0.98 (s, 9H, *t*BuSi).

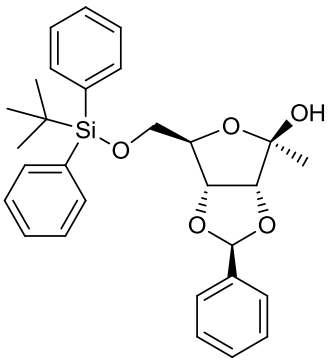

$C_{29}H_{34}O_5Si$, MW 490.66

6-*O*-(*tert*-butyldiphenylsilyl)-3,4-*O*-(*S*)-benzylidene-1-deoxy-β-D-psicofuranose (**76**).

A solution of compound **74** (0.22 g, 0.46 mmol) in anhydrous tetrahydrofuran was cooled to -78 °C under a nitrogen atmosphere before adding a solution of 1.6M methyllithium in diethylether (0.28

mL, 0.46 mmol) dropwise. The reaction mixture was stirred at -78 °C for 1 hour, then quenched with a 10% NH_4Cl aqueous solution (10 mL) and extracted with dichloromethane (3 x 20 mL). The combined organic layer was washed with brine (60 mL), dried over anhydrous $MgSO_4$, filtered and concentrated to dryness to give compound **76** (0.22 g, 100% yield) as a colourless oil. The crude residue was used in the following step without purification. For analysis, the crude residue was purified by flash column chromatography (hexane to hexane/ethyl acetate 80:20 v/v).

^{1}H NMR (500 MHz, $CDCl_3$) δ 7.63 – 7.57 (m, 5H, Harom), 7.43 – 7.28 (m, 10H, Harom), 5.74 (s, 1H, C*H*(C_6H_5)), 4.89 (br s, 1H, 2-O*H*), 4.85 (dd, $J_{4,3}$ = 6.2 Hz, $J_{4,5}$ = 1.0 Hz, 1H, H-4), 4.57 (d, $J_{3,4}$ = 6.2 Hz, 1H, H-3), 4.28 (m, 1H, H-5), 3.79 (dd, $J_{6a,6b}$ = 11.4 Hz, $J_{6a,5}$ = 2.6 Hz, 1H, H-6a), 3.61 (dd, $J_{6b,6a}$ = 11.4 Hz, $J_{6b,5}$ = 2.7 Hz, 1H, H-6b), 1.55 (s, 3H, H-1), 1.02 (s, 9H, *t*BuSi).

^{13}C NMR (126 MHz, $CDCl_3$) δ 136.10 (C, Carom), 135.81, 135.63 (2 CH, Carom), 131.60, 131.50 (2 C, Carom), 130.48, 130.28, 129.86, 128.49, 128.18, 128.11, 127.02 (7 CH, Carom), 106.58 (C, C2), 106.27 (CH, *C*H(C_6H_5)), 88.49 (CH, C3), 85.64 (CH, C5), 82.73 (CH, C4), 65.64 (CH_2, C6), 26.90 (CH_3, 3 *C*H_3-*t*BuSi), 21.69 (CH_3, C1), 19.17 (CH, *C*-*t*BuSi).

MS (ES+) *m/z* 513.2 [MNa^+].

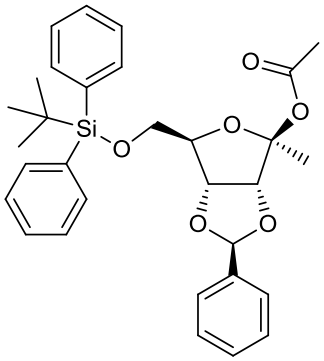

$C_{31}H_{36}O_6Si$, MW 532.70

2-*O*-Acetyl-6-*O*-(*tert*-butyldiphenylsilyl)-3,4-*O*-(*S*)-benzylidene-1-deoxy-β-D-psicofuranose (**77**).

To a stirred solution of compound **76** (0.22 g, 0.45 mmol) in anhydrous dichloromethane under a nitrogen atmosphere, 4-(dimethylamino)pyridine (0.055 g, 0.45 mmol) and acetic anhydride (0.13 mL, 1.34 mmol) were added at room temperature. Then triethylamine (0.2 mL, 1.34 mmol) was added dropwise at the same temperature and the reaction mixture was stirred for 48 hours, then poured into ice-cold water (10 mL). The aqueous phase was extracted with dichloromethane (3 x 10 mL). The combined organic layer was washed with saturated $NaHCO_3$ aqueous solution and

brine, dried over anhydrous $MgSO_4$, filtered and concentrated to dryness. The crude residue was purified by flash column chromatography on silica gel (hexane to hexane/ethyl acetate 90:10 v/v) to give compound **77** (0.12 g, 48% yield) as a colourless oil.

^{1}H NMR (500 MHz, $CDCl_3$) δ 7.60 – 7.56 (m, 5H, Harom), 7.44 – 7.41 (m, 2H, Harom), 7.36 – 7.27 (m, 8H, Harom), 5.76 (s, 1H, C*H*(C_6H_5)), 4.79 (d, *J* = 6.2 Hz, 1H), 4.75 (d, *J* = 6.2 Hz, 1H), 4.45 (dd, $J_{5,6b}$ = 9.0 Hz, $J_{5,6a}$ = 5.4 Hz, 1H, H-5), 3.70 (dd, $J_{6a,6b}$ = 10.2 Hz, $J_{6a,5}$ = 5.4 Hz, 1H, H-6a), 3.52 (t, $J_{6b,6a}$ = 10.2 Hz, 1H, H-6b), 1.70 (s, 3H, COCH_3), 1.66 (s, 3H, H-1), 0.99 (s, 9H, *t*BuSi).

^{13}C NMR (126 MHz, $CDCl_3$) δ 169.40 (C, C=O), 135.88 (C, Carom), 135.61 (CH, Carom), 133.26, 132.93 (2 C, Carom), 129.91, 128.48, 127.83, 127.06 (4 CH, Carom), 113.36 (C, C2), 106.51 (CH, *C*H(C_6H_5)), 86.42 (CH), 85.60 (CH), 82.92 (CH), 63.84 (CH_2, C6), 26.87 (CH_3, 3 *C*H_3-*t*BuSi), 22.21 (CH_3, C1), 19.61 (CH_3, CO*C*H_3), 19.27 (C, *C*-*t*BuSi).

MS (ES+) *m/z* 555.2 [MNa^+].

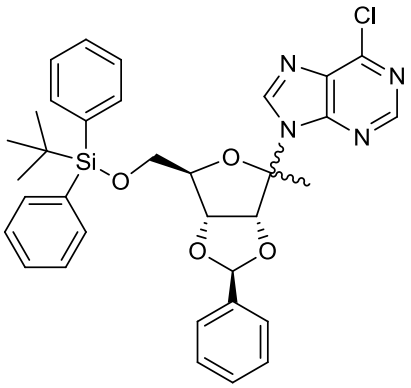

$C_{34}H_{35}ClN_4O_4Si$, MW 627.20

6-chloro-9*H*-[6-*O*-(*tert*-butyldiphenylsilyl)-3,4-*O*-(*S*)-benzylidene-1-deoxy-α,β-D-psicofuranosyl)]purine (**79**/**80**).

To a stirred mixture of compounds **77** (0.29 g, 0.54 mmol) and 6-chloropurine **118** (0.18 g, 1.18 mmol) in anhydrous acetonitrile under a nitrogen atmosphere, a 1.8M solution of ethylaluminum dichloride (0.95 mL, 1.72 mmol) was added dropwise at room temperature. The reaction mixture was stirred for 2 hours at the same temperature, then poured into an ice-cold mixture of saturated $NaHCO_3$ aqueous solution (20 mL) and dichloromethane (35 mL) and stirred vigorously for 10 minutes. The mixture was filtered through a celite pad and washed with dichloromethane. The separated organic layer was washed with saturated $NaHCO_3$ aqueous solution and brine, dried over anhydrous $MgSO_4$, filtered and concentrated to dryness. The crude residue was purified by

flash column chromatography on silica gel (hexane to hexane/ethyl acetate 80:20 v/v) to give the anomeric mixture **79**/**80** (0.14 g, 40% yield) as a colourless oil.

^{1}H NMR (500 MHz, $CDCl_3$) δ 8.70 (s, 1H, H-2 β), 8.65 (s, 1H, H-2 α), 8.44 (s, 1H, H-8 β), 8.43 (s, 1H, H-8 α), 7.65 – 7.17 (m, 30H, Harom), 6.05 (s, 1H, C*H*(C_6H_5) α), 5.92 (s, 1H, C*H*(C_6H_5) β), 5.75 (d, $J_{3',4'}$ = 6.0 Hz, 1H, H-3' α), 5.63 (d, $J_{3',4'}$ = 6.4 Hz, 1H, H-3' β), 4.78 – 4.74 (m, 1H, H-4' α), 4.70 (d, $J_{4',3'}$ = 6.4 Hz, 1H, H-4' β), 4.60 (t, $J_{5',6'}$ = 3.8 Hz, 1H, H-5' β), 4.50 – 4.45 (m, 1H, H-5' α), 3.64 (d, *J* = 4.7 Hz, 2H, H-6'a and H-6'b β), 3.62 – 3.59 (m, 2H, H-6'a and H-6'b α), 1.81 (s, 3H, H-1' α), 1.72 (s, 3H, H-1' β), 0.88 (s, 9H, *t*BuSi α), 0.84 (s, 9H, *t*BuSi β).

^{13}C NMR (126 MHz, $CDCl_3$) δ 151.71 (CH, C2 β), 151.66 (CH, C2 α), 151.18, 151.13, 150.52, 150.50 (4 C, Carom), 143.69 (CH, C8 α and β), 135.54, 135.52, 135.50, 135.44 (4 CH, Carom), 135.27 (C, Carom α and β), 133.03, 132.98, 132.21, 132.18 (4 C, Carom), 130.17, 130.13, 130.11, 130.08, 130.06, 129.95, 129.90, 128.57, 128.56, 128.09, 127.93, 127.83, 126.81, 126.62 (14 CH, Carom), 107.03 (CH, *C*H(C_6H_5) β), 105.18 (CH, *C*H(C_6H_5) α), 100.17 (C, C2' β), 99.85 (C, C2' α), 85.89 (CH, C5' α), 85.83 (CH, C5' β), 85.61 (CH, C3' β), 84.59 (CH, C3' α), 83.11 (CH, C4' β), 81.60 (CH, C4'α), 63.90 (CH_2, C6' β), 63.80 (CH_2, C6' α), 26.83 (CH_3, 3 *C*H_3-*t*BuSi α and β), 25.29 (CH_3, C1' β), 24.39 (CH_3, C1' α), 19.12 (C, *C*-*t*BuSi α), 19.08 (C, *C*-*t*BuSi β).

MS (ES+) *m/z* 649.2 [MNa^+].

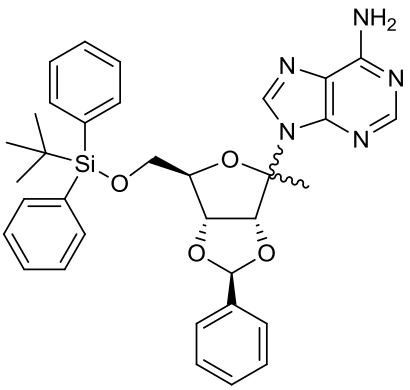

$C_{34}H_{37}N_5O_4Si$, MW 607.77

9*H*-[6-*O*-(*tert*-butyldiphenylsilyl)-3,4-*O*-(*S*)-benzylidene-1-deoxy-α,β-D-psicofuranosyl)]adenine (**81**/**82**).

The anomeric mixture **79**/**80** (0.05 g, 0.08) was dissolved in a saturated (7M) solution of ammonia in methanol (1 mL). The reaction mixture was stirred in a screw-cap pressure glass tube at 80 °C for 48 hours, then cooled to room temperature. The solvent was evaporated and the crude residue was purified by flash column chromatography on silica gel (dichloromethane to dichloromethane/methanol 98:2 v/v) to give the anomeric mixture **81**/**82** (0.03 g, 63% yield) as a colourless oil.

^{1}H NMR (500 MHz, $CDCl_3$) δ 8.32 (s, 1H, H-2 β), 8.27 (s, 1H, H-2 α), 8.13 (s, 1H, H-8 β), 8.11 (s, 1H, H-8 α), 7.54 – 7.21 (m, 30H, Harom), 6.03 (s, 1H, C*H*(C_6H_5) α), 5.93 (s, 1H, C*H*(C_6H_5) β), 5.88 (d, $J_{3',4'}$ = 5.9 Hz, 1H, H-3' α), 5.79 – 5.73 (m, 5H, H-3' β, 6-NH_2 α and β), 4.79 (d, $J_{4',3'}$ = 5.5 Hz, 1H, H-4' α), 4.70 (d, $J_{4',3'}$ = 6.3 Hz, 1H, H-4' β), 4.58 – 4.54 (m, 1H, H-5' β), 4.47 – 4.43 (m, 1H, H-5' α), 3.65 – 3.52 (m, 4H, H-6'a and H-6'b α and β), 1.80 (s, 1H, H-1' α), 1.73 (s, 1H, H-1' β), 0.93 (s, 9H, *t*BuSi α), 0.90 (s, 9H, *t*BuSi β).

^{13}C NMR (126 MHz, $CDCl_3$) δ 155.49 (C, Carom), 152.82 (CH, C2 β), 152.74 (CH, C2 α), 149.05, 149.00 (2 C, Carom), 138.95 (CH, C8 β), 138.92 (CH, C8 α), 136.25, 135.66 (2 C, Carom), 135.53, 135.51 (2 CH, Carom), 132.61, 132.56, 132.53 (3 C, Carom), 130.01, 129.97, 129.79, 129.76, 128.46, 127.84, 127.82, 126.88, 126.73 (9 CH, Carom), 121.00, 120.93 (2 C, Carom), 106.95 (CH, *C*H(C_6H_5) β), 104.95 (CH, *C*H(C_6H_5) α), 99.31 (C, C2' β), 99.13 (C, C2' α), 85.83 (CH, C5' β), 85.78 (CH, C5' α), 85.51 (CH, C3' β), 84.41 (CH, C3' α), 82.94 (CH, C4' β), 81.89 (CH, C4' α), 63.84 (CH_2, C6' α), 63.78 (CH_2, C6' β), 26.83 (CH_3, 3 *C*H_3-*t*BuSi α and β), 25.04 (CH_3, C1' β), 24.35 (CH_3, C1' α), 19.16 (C, *C*-*t*BuSi α), 19.13 (C, *C*-*t*BuSi β).

MS (ES+) *m/z* 608.3 [MH^+], 630.3 [MNa^+].

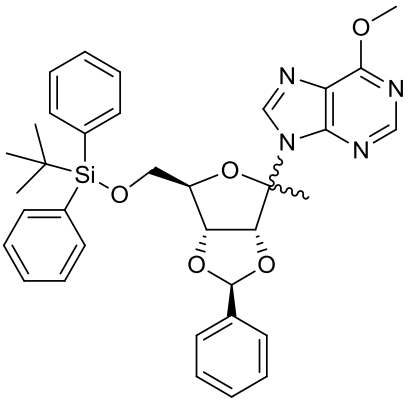

$C_{35}H_{38}N_4O_5Si$, MW 622.79

6-*O*-methyl-9*H*-[6-*O*-(*tert*-butyldiphenylsilyl)-3,4-*O*-(*S*)-benzylidene-1-deoxy-α,β-D-psicofuranosyl)]hypoxanthine (**83**/**84**).

The anomeric mixture **83**/**84** was isolated as a side-product of the synthesis of the anomeric mixture **81**/**82** and obtained as a colourless oil (0.006 g, 12% yield).

^{1}H NMR (500 MHz, $CDCl_3$) δ 8.51 (s, 1H, H-2 β), 8.45 (s, 1H, H-2 α), 8.25 (s, 1H, H-8 β), 8.23 (s, 1H, H-8 α), 7.54 – 7.21 (m, 30H, Harom), 6.04 (s, 1H, C*H*(C_6H_5) α), 5.93 (s, 1H, C*H*(C_6H_5) β), 5.82 (d, $J_{3',4'}$ = 6.0 Hz, 1H, H-3' α), 5.71 (d, $J_{3',4'}$ = 6.4 Hz, 1H, H-3' β), 4.80 – 4.76 (m, 1H, H-4' α), 4.73 – 4.69 (m, 1H, H-4' β), 4.56 (t, $J_{5',6'}$ = 4.7 Hz, 1H, H-5' β), 4.47 – 4.43 (m, 1H, H-5' α), 4.12 (s, 6H, 6-OCH_3 α and β), 3.65 – 3.54 (m, 4H, H-6'a and H-6'b α and β), 1.80 (s, 3H, H-1' α), 1.73 (s, 3H, H-1' β), 0.92 (s, 9H, *t*BuSi α), 0.89 (s, 9H, *t*BuSi β).

^{13}C NMR (126 MHz, $CDCl_3$) δ 161.11 (C, Carom α and β), 151.91 (CH, C2 β), 151.83 (CH, C2 α), 150.85 (C, Carom α), 150.82 (C, Carom β), 140.55 (CH, C8 β), 140.52 (CH, C8 α), 136.20 (C, Carom α and β), 135.57, 135.55, 135.49 (3 CH, Carom), 132.61, 132.53, 132.51, 132.47 (4 C, Carom), 130.01, 129.97, 129.94, 129.84, 129.80, 128.49, 127.86, 127.82, 126.87, 126.70 (10 CH, Carom), 123.00 (C, Carom β), 122.93 (C, Carom α), 107.04 (CH, *C*H(C_6H_5) β), 105.03 (CH, *C*H(C_6H_5) α), 99.49 (C, C2' β), 99.28 (C, C2' α), 85.76 (CH, C5' β), 85.71 (CH, C5' α), 85.65 (CH, C3' β), 84.57 (CH, C3' α), 83.00 (CH, C4' β), 81.84 (CH, C4'α), 63.83 (CH_2, C6' α), 63.78 (CH_2, C6' β), 54.17 (CH_3, 6-O*C*H_3 α and β), 26.84 (CH_3, 3 *C*H_3-*t*BuSi α and β), 25.04 (CH_3, C1' β), 24.27 (CH_3, C1' α), 19.15 (C, *C*-*t*BuSi α), 19.12 (C, *C*-*t*BuSi β).

MS (ES+) *m/z* 645.3 [MNa^+], 623.3 [MH^+].

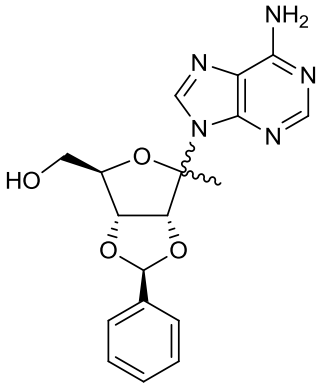

$C_{18}H_{19}N_5O_4$, MW 369.37

9*H*-[3,4-*O*-(*S*)-benzylidene-1-deoxy-α,β-D-psicofuranosyl)]adenine (**85**/**86**).

A solution of the anomeric mixture **81**/**82** (0.087 g, 0.14 mmol) in tetrahydrofuran was cooled to 0 °C before adding a solution of tetrabutylammonium fluoride trihydrate (0.054 g, 0.17 mmol) in tetrahydrofuran dropwise. The reaction mixture was stirred at the same temperature for 2 hours, then concentrated to dryness under reduced pressure. The crude residue was purified by flash column chromatography on silica gel (dichloromethane to dichloromethane/methanol 96:4 v/v) to give the anomeric mixture **85**/**86** (0.045 g, 85% yield) as a white powder.

^{1}H NMR (500 MHz, CD_3OD) δ 8.41 (s, 1H, H-2 α), 8.40 (s, 1H, H-2 β), 8.23 (s, 1H, H-8 α and β), 7.62 – 7.59 (m, 2H, Harom β), 7.56 – 7.53 (m, *2*H, Harom α), 7.47 – 7.41 (m, 3H, Harom α and β), 6.18 (s, 1H, C*H*(C_6H_5) α), 6.02 (s, 1H, C*H*(C_6H_5) β), 5.80 (d, $J_{3',4'}$ = 6.1 Hz, 1H, H-3' α), 5.73 (d, $J_{3',4'}$ = 6.5 Hz, 1H, H-3' β), 5.02 (dd, $J_{4',3'}$ = 6.1 Hz, $J_{4',5'}$ = 3.2 Hz, 1H, H-4' α), 4.92 (dd, $J_{4',3'}$ = 6.5 Hz, $J_{4',5'}$ = 2.2 Hz, 1H, H-4' β), 4.62 – 4.58 (m, 1H, H-5' β), 4.54 (m, 1H, H-5' α), 3.71 – 3.60 (m, 4H, H-6'a and H-6'b α and β), 1.93 (s, 3H, H-1' α), 1.84 (s, 3H, H-1' β).

^{13}C NMR (126 MHz, CD_3OD) δ 155.86 (C, Carom α and β), 152.05 (CH, C2 β), 152.02 (CH, C2 α), 148.46 (C, Carom α), 148.41 (C, Carom β), 139.20 (CH, C8 α and β), 136.72 (C, Carom α), 136.08 (C, Carom β), 129.38, 129.28, 128.05, 128.00, 126.54, 126.48 (6 CH, Carom), 119.89 (C, Carom α and β), 106.77 (CH, *C*H(C_6H_5) β), 104.77 (CH, *C*H(C_6H_5) α), 98.93 (C, C2' α and β), 86.26 (CH, C5' β), 85.85 (CH, C5' α), 85.72 (CH, C3' β), 84.71 (CH, C3' α), 82.72 (CH, C4' β), 81.60 (CH, C4'α), 61.76 (CH_2, C6' α), 61.64 (CH_2, C6' β), 23.32 (CH_3, C1' β), 22.72 (CH_3, C1' α).

MS (ES+) *m/z* 370.2 [MH^+], 392.2 [MNa^+].

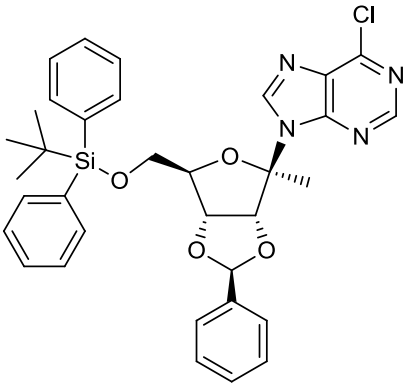

$C_{34}H_{35}ClN_4O_4Si$, MW 627.20

6-chloro-9*H*-[6-*O*-(*tert*-butyldiphenylsilyl)-3,4-*O*-(*S*)-benzylidene-1-deoxy-β-D-psicofuranosyl)]purine (**80**).

To a suspension of 6-chloropurine **118** (0.28 g, 1.82 mmol) in anhydrous acetonitrile was added *N*,*O*-bis(trimethylsilyl)acetamide (0.92 mL, 3.77 mmol) at room temperature under a nitrogen atmosphere. The resulting solution was heated to 50 °C for 1 hour, then cooled to room temperature. A solution of compound **77** (0.48 g, 0.91 mmol) in anhydrous acetonitrile was added at room temperature. The solution was then cooled to -20 °C before adding trimethylsilyl trifluoromethanesulfonate (0.16 mL, 0.91 mmol) dropwise. The reaction mixture was stirred at a temperature from -20 °C to 0 °C for 1 hour, then quenched by adding saturated $NaHCO_3$ aqueous solution and diluted with dichloromethane. The layers were separated and the organic phase was washed with water and brine, dried over anhydrous $MgSO_4$, filtered and concentrated to dryness. The crude residue was purified by flash column chromatography on silica gel (hexane to hexane/ethyl acetate 80:20 v/v) to give compound **80** (0.08 g, 14% yield) as a colourless oil.

^{1}H NMR (500 MHz, $CDCl_3$) δ 8.81 (s, 1H, H-2), 8.54 (s, 1H, H-8), 7.64 – 7.59 (m, 2H, Harom), 7.55 (d, *J* = 7.2 Hz, 4H, Harom), 7.49 – 7.40 (m, 5H, Harom), 7.35 (t, *J* = 7.4 Hz, 4H, Harom), 6.04 (s, 1H, C*H*(C_6H_5)), 5.75 (d, $J_{3',4'}$ = 6.4 Hz, 1H, H-3'), 4.83 – 4.81 (m, 1H, H-4'), 4.70 (t, $J_{5',6'}$ = 4.3 Hz, 1H, H-5'), 3.78 – 3.70 (m, 2H, H-6'a and H-6'b), 1.84 (s, 3H, H-1'), 0.96 (s, 9H, 3 CH_3-*t*BuSi).

^{13}C NMR (126 MHz, $CDCl_3$) δ 151.69 (CH, C2), 151.17, 150.52 (2 C, Carom), 143.64 (CH, C8), 135.53, 135.43 (2 CH, Carom), 135.33, 133.06, 132.25 (3 C, Carom), 130.13, 130.06, 129.91, 128.53, 127.90, 127.81.126.79 (7 CH, Carom), 107.06 (CH, *C*H(C_6H_5)), 100.11 (C, C2'), 85.86 (CH, C3'), 85.60 (CH, C5'), 83.05 (CH, C4'), 63.88 (CH_2, C6'), 26.83 (CH_3, 3 *C*H_3-*t*BuSi), 25.20 (CH_3, C1'), 19.08 (C, *C*-*t*BuSi).

MS (ES+) *m/z* 649.2 [MNa^+].

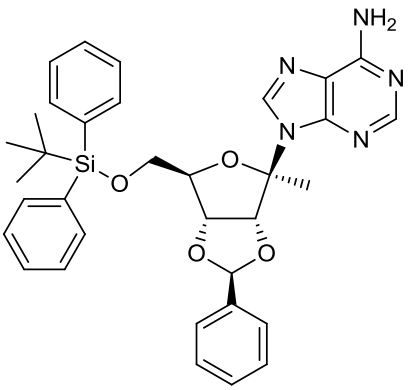

$C_{34}H_{37}N_5O_4Si$, MW 607.77

9*H*-[6-*O*-(*tert*-butyldiphenylsilyl)-3,4-*O*-(*S*)-benzylidene-1-deoxy-β-D-psicofuranosyl)]adenine (**82**).

Compound **82** was prepared as described for the anomeric mixture **81**/**82** from **80** (0.26 g, 0.41 mmol). The crude residue was purified by flash column chromatography on silica gel (dichloromethane to dichloromethane/methanol 99:1 v/v) to give compound **82** (0.17 g, 66% yield) as a colourless oil.

^{1}H NMR (500 MHz, $CDCl_3$) δ 8.43 (s, 1H, H-2), 8.23 (s, 1H, H-8), 7.64 – 7.53 (m, 6H, Harom), 7.48 – 7.40 (m, 5H, Harom), 7.35 (dd, *J* = 16.1, 7.8 Hz, 4H, Harom), 6.03 (s, 1H, C*H*(C_6H_5)), 5.87 (d, $J_{3',4'}$ = 6.4 Hz, 1H, H-3'), 5.67 (s, 2H, 6-NH_2), 4.80 (d, $J_{4',3'}$ = 6.3 Hz, 1H, H-4'), 4.66 (t, $J_{5',6'}$ = 5.0 Hz, 1H, H-5'), 3.72 (dd, $J_{6'a,6'b}$ = 11.3 Hz, $J_{6'a,5'}$ = 5.9 Hz, 1H, H-6'a), 3.67 (dd, $J_{6'b,6'a}$ = 11.3 Hz, $J_{6'b,5'}$ = 5.3 Hz, 1H, H-6'b), 1.83 (s, 3H, H-1), 1.01 (s, 9H, 3 CH_3-*t*BuSi).

^{13}C NMR (126 MHz, $CDCl_3$) δ 155.42 (C, Carom), 152.83 (CH, C2), 148.99 (C, Carom), 138.96 (CH, C8), 135.64 (C, Carom), 135.53, 135.49 (2 CH, Carom), 132.54, 132.53 (2 C, Carom), 130.01, 129.97, 129.80, 128.46, 127.84, 127.81, 126.88 (7 CH, Carom), 120.98 (C, Carom), 106.95 (CH, *C*H(C_6H_5)), 99.31 (C, C2'), 85.83 (CH, C5'), 85.51 (CH, C3'), 82.94 (CH, C4'), 63.78 (CH_2, C6'), 26.82 (CH_3, 3 *C*H_3-tBuSi), 25.05 (CH_3, C1), 19.13 (C, *C*-tBuSi).

MS (ES+) *m/z* 608.3 [MH^+], 630.3 [MNa^+].

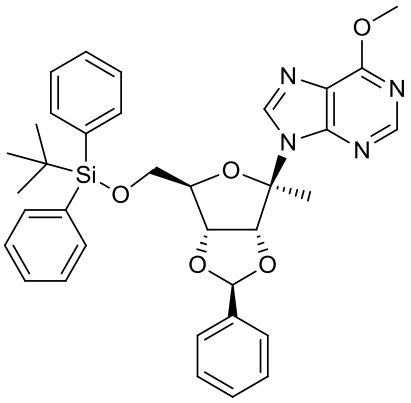

$C_{35}H_{38}N_4O_5Si$, MW 622.79

6-*O*-methyl-9*H*-[6-*O*-(*tert*-butyldiphenylsilyl)-3,4-*O*-(*S*)-benzylidene-1-deoxy-β-D-psicofuranosyl)]hypoxanthine (**84**).

Compound **84** was isolated as a side-product of the synthesis of compound **82** and obtained as a colourless oil (0.011 g, 4% yield).

^{1}H NMR (500 MHz, $CDCl_3$) δ 8.61 (s, 1H, H-2), 8.35 (s, 1H, H-8), 7.59 (dd, *J* = 17.2, 9.0 Hz, 6H, Harom), 7.48 – 7.39 (m, 5H, Harom), 7.38 – 7.32 (m, 4H, Harom), 6.04 (s, 1H, C*H*(C_6H_5)), 5.82 (d, $J_{3',4'}$ = 6.2 Hz, 1H, H-3'), 4.81 (d, $J_{4',3'}$ = 6.2 Hz, 1H, H-4'), 4.67 (t, $J_{5',6'}$ = 4.9 Hz, 1H, H-5'), 4.23 (s, 3H, 6-OCH_3), 3.73 (dd, $J_{6'a,6'b}$ = 11.3 Hz, $J_{6'a,5'}$ = 5.9 Hz, 1H, H-6'a), 3.68 (dd, $J_{6'b,6'a}$ = 11.3 Hz, $J_{6'b,5'}$ = 5.2 Hz, 1H, H-6'b), 1.84 (s, 3H, H-1'), 1.00 (s, 9H, 3 CH_3-*t*BuSi).

^{13}C NMR (126 MHz, $CDCl_3$) δ 161.11 (C, Carom), 151.91 (CH, C2), 150.82 (C, Carom), 140.56 (CH, C8), 135.57, 135.49 (2 CH, Carom), 132.51, 132.46 (2 C, Carom), 130.01, 129.94, 129.84, 128.49, 127.85, 127.82, 126.87 (7 CH, Carom), 122.99 (C, Carom), 107.04 (CH, *C*H(C_6H_5)), 99.49 (C, C2'), 85.75 (CH, C5'), 85.65 (CH, C3'), 83.00 (CH, C4'), 63.78 (CH_2, C6'), 54.17 (CH3, 6-O*C*H_3), 26.84 (CH_3, 3 *C*H_3-tBuSi), 25.04 (CH_3, C1), 19.11 (C, *C*-tBuSi).

MS (ES+) *m/z* 645.3 [MNa^+], 623.3 [MH^+].

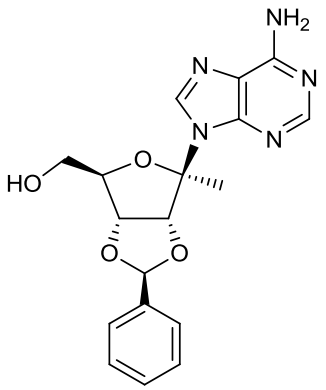

$C_{18}H_{19}N_5O_4$, MW 369.37

9*H*-[3,4-*O*-(*S*)-benzylidene-1-deoxy-β-D-psicofuranosyl)]adenine (**86**).

Compound **86** was prepared as described for the anomeric mixture **85**/**86** from **82** (0.16 g, 0.26 mmol). The crude residue was purified by flash column chromatography on silica gel (dichloromethane to dichloromethane/methanol 97:3 v/v) to give compound **86** (0.07 g, 74% yield) as a white powder; mp: 181-183 °C.

^{1}H NMR (500 MHz, DMSO-d_6) δ 8.19 (s, 1H, H-2), 8.09 (s, 1H, H-8), 7.53 – 7.48 (m, 2H, Harom), 7.42 – 7.38 (m, 3H, Harom), 7.19 (s, 2H, 6-NH_2), 5.91 (s, 1H, C*H*(C_6H_5)), 5.65 (d, $J_{3',4'}$ = 6.4 Hz, 1H, H-3'), 5.03 (t, $J_{6'\text{-}OH,6'}$ = 5.0 Hz, 1H, 6'-O*H*), 4.79 (d, $J_{4',3'}$ = 6.4 Hz, 1H, H-4'), 4.39 (t, $J_{5',6'}$ = 5.5 Hz, 1H, H-5'), 3.43 – 3.37 (m, 1H, H-6'a), 3.35 – 3.28 (m, 1H, H-6'b), 1.64 (s, 3H, H-1).

^{13}C NMR (126 MHz, DMSO-d_6) δ 156.59 (C, Carom), 152.71 (CH, C2), 148.85 (C, Carom), 138.83 (CH, C8), 136.48 (C, Carom), 130.21, 128.95, 127.32 (3 CH, Carom), 120.51 (C, Carom), 106.13 (CH, *C*H(C_6H_5)), 98.59 (C, C2'), 86.61 (CH, C5'), 85.64 (CH, C3'), 83.01 (CH, C4'), 61.61 (CH_2, C6'), 24.60 (CH_3, C1).

MS (ES+) *m/z* 370.2 [MH^+], 392.2 [MNa^+].

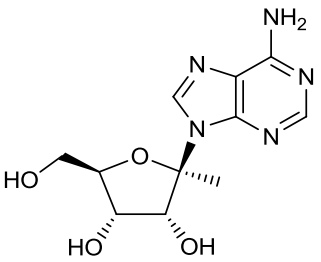

$C_{11}H_{15}N_5O_4$, MW 281.27

9*H*-(1-deoxy-β-D-psicofuranosyl)adenine (**41**).[11]

To a solution of **86** (0.03 g, 0.081 mmol) in anhydrous methanol, ammonium formate (0.25 g, 3.90 mmol) and palladium on carbon (100% w/w, 0.03 g) were added under a nitrogen atmosphere and the reaction mixture was heated at reflux for 20 hours, then cooled to room temperature and diluted with methanol. The suspension was filtered and the filtrate concentrated to dryness. The crude residue was purified by flash column chromatography on silica gel (dichloromethane to dichloromethane/methanol 87:13 v/v) to obtain compound **41** (0.004 g, 18% yield) as a white powder; mp: > 230 °C.

^{1}H NMR (500 MHz, DMSO-d_6) δ 8.39 (s, 1H, H-2), 8.13 (s, 1H, H-8), 7.22 (s, 2H, 6-NH_2), 5.68 (d, *J* = 4.5 Hz, 1H, O*H*), 5.24 – 5.17 (m, 1H, O*H*), 4.96 (d, *J* = 6.2 Hz, 1H, O*H*), 4.64 – 4.60 (m, 1H, H-3'), 4.03 – 3.84 (m, 2H, H-4' and H-5'), 3.80 – 3.73 (m, 1H, H-6'a), 3.59 – 3.52 (m, 1H, H-6'b), 1.75 (s, 3H, H-1').

MS (ES+) *m/z* 304.3 [MNa^+], 282.3 [MH^+].

4.2.4 PROCEDURES AND SPECTRAL DATA – SECTION 2.2.3

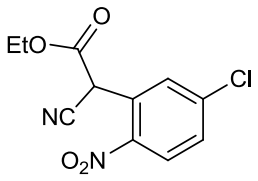

$C_{11}H_9ClN_2O_4$, MW 268.65

Ethyl 2-(5-chloro-2-nitrophenyl)-2-cyanoacetate (**91**).[13]

To a cold (0 °C) solution of ethyl cyanoacetate (4.43 mL, 41.66 mmol) in anhydrous dimethylformamide, potassium *tert*-butoxide (7.01 g, 62.49 mmol) was added portionwise under a nitrogen atmosphere. The resulting white suspension was allowed to attain room temperature and stirred for 30 minutes, before adding a solution of 2,4-dichloronitrobenzene **89** (4.00 g, 20.83 mmol) in 3 mL of anhydrous dimethylformamide dropwise at room temperature. The reaction mixture was heated to 70 °C for 16 hours (monitored by TLC), then was allowed to cool to room temperature and poured into ice-water. The aqueous mixture was acidified to pH 2 with HCl 6M and extracted with diethyl ether (3 x 100 mL). The combined organic layer was washed several times with brine (200 mL), dried over anhydrous $MgSO_4$, filtered and concentrated under reduced pressure to obtain a dark oil (4.32 g, 77% yield). The crude compound **91** was used in the next step without purification. For analysis, the crude residue was purified by column chromatography on silica gel eluting with hexane/ethyl acetate (80:20 v/v).

^{1}H NMR (500 MHz, DMSO-d_6) δ 8.32 (d, J = 8.1 Hz, 1H, Harom), 7.91 – 7.87 (m, 2H, Harom), 6.23 (s, 1H, H-2), 4.24 (q, J = 7.1 Hz, 2H, CH_2CH$_3$), 1.20 (t, J = 7.1 Hz, 3H, CH$_2$CH_3).

^{13}C NMR (126 MHz, DMSO-d_6) δ 163.51 (C, C=O), 145.40 (C, CN), 139.53 (C, C5), 132.97 (CH, Carom), 131.09 (CH, Carom), 128.03 (CH, Carom), 127.67 (C, Carom), 114.81 (C, Carom), 63.09 (CH$_2$, *C*H$_2$CH$_3$), 40.89 (CH, C2), 13.73 (CH$_3$, CH$_2$*C*H$_3$).

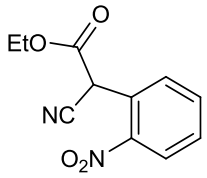

$C_{11}H_{10}N_2O_4$, MW 234.21

Ethyl 2-(2-nitrophenyl)-2-cyanoacetate (**92**).[14]

Compound **92** was prepared as described for **91** from 2-chloronitrobenzene **90** (2.0 g, 12.69 mmol) and obtained as a dark oil (2.14 g, 72% yield). The crude compound **92** was used in the next step without purification. For analysis, the crude residue was purified by column chromatography on silica gel eluting with hexane/ethyl acetate (90:10 v/v to 70:30 v/v).

^{1}H NMR (500 MHz, DMSO-d_6) δ 8.28 (d, *J* = 8.2 Hz, 1H, Harom), 7.92 (dd, *J* = 10.8, 4.3 Hz, 1H, Harom), 7.81 – 7.75 (m, 2H, Harom), 6.24 (s, 1H, H-2), 4.23 (q, *J* = 7.1 Hz, 2H, CH_2CH$_3$), 1.20 (t, *J* = 7.1 Hz, 3H, CH$_2$CH_3).

^{13}C NMR (126 MHz, DMSO-d_6) δ 164.01 (C, C=O), 146.74 (C, CN), 135.24 (CH, Carom), 133.15 (CH, Carom), 131.15 (CH, Carom), 125.99 (CH, Carom), 125.67 (C, Carom), 115.35 (C, Carom), 62.89 (CH$_2$, *C*H$_2$CH$_3$), 41.23 (CH, C2), 13.75 (CH$_3$, CH$_2$*C*H$_3$).

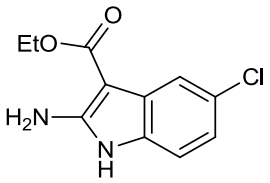

$C_{11}H_{11}ClN_2O_2$, MW 238.67

Ethyl 2-amino-5-chloro-1*H*-indole-3-carboxylate (**93**).[15]

To a solution of crude **91** (2.53 g, 9.42 mmol) in glacial acetic acid, zinc dust (1.85 g, 16.92 mmol) was added slowly at room temperature under a nitrogen atmosphere. The mixture was stirred for 4 hours without external heating (reaction is exothermic), then filtered through a celite pad. The pad was washed with acetic acid (400 mL) and the solution was evaporated. The residue was washed with water and dried under reduced pressure to obtain compound **93** as a brown powder (2.00 g, 89% yield), that was used in the following step without purification.

^{1}H NMR (500 MHz, DMSO-d_6) δ 11.34 (s, 1H, 1-N*H*), 7.56 (s, 1H, Harom), 7.12 (d, *J* = 8.3 Hz, 1H, Harom), 6.97 (dd, *J* = 8.3, 2.0 Hz, 1H, Harom), 6.94 (s, 2H, 2-NH_2), 4.25 (q, *J* = 7.1 Hz, 2H, CH_2CH$_3$), 1.33 (t, *J* = 7.1 Hz, 3H, CH$_2$CH_3).

^{13}C NMR (126 MHz, DMSO-d_6) δ 164.82 (C, C=O), 150.69 (C, Carom), 130.33 (C, Carom), 125.36 (C, Carom), 123.42 (C, Carom), 118.89 (CH, Carom), 117.08 (CH, Carom), 107.93 (CH, Carom), 79.14 (C, Carom), 58.32 (CH$_2$, *C*H$_2$CH$_3$), 14.69 (CH$_3$, CH$_2$*C*H$_3$).

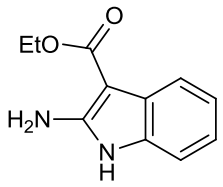

$C_{11}H_{12}N_2O_2$, MW 204.23

Ethyl 2-amino-1*H*-indole-3-carboxylate (**94**).[15]

Compound **94** was prepared as described for **93** from crude compound **92** (2.01 g, 8.58 mmol) and obtained as a brown powder, that was used directly in the next step.

^{1}H NMR (500 MHz, DMSO-d_6) δ 11.19 (s, 1H, 1-N*H*), 7.63 (d, *J* = 7.4 Hz, 1H, Harom), 7.13 (d, *J* = 7.2 Hz, 1H, Harom), 6.99 (dtd, *J* = 19.5, 7.3, 1.2 Hz, 2H, Harom), 6.79 (s, 2H, 2-NH_2), 4.24 (q, *J* = 7.1 Hz, 2H, CH_2CH$_3$), 1.33 (t, *J* = 7.1 Hz, 3H, CH$_2$CH_3).

^{13}C NMR (126 MHz, DMSO-d_6) δ 165.31 (C, C=O), 150.14 (C, Carom), 131.70 (C, Carom), 121.89 (C, Carom), 120.87 (CH, Carom), 119.34 (CH, Carom), 118.02 (CH, Carom), 106.62 (CH, Carom), 79.25 (C, Carom), 58.07 (CH$_2$, *C*H$_2$CH$_3$), 14.70 (CH$_3$, CH$_2$*C*H$_3$).

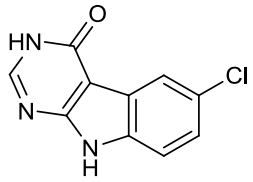

$C_{10}H_6ClN_3O$, MW 219.63

6-chloro-3*H*-pyrimido[4,5-*b*]indol-4(9*H*)-one (**95**).[13]

A suspension of crude compound **93** (2.00 g, 8.38 mmol) in formamide (8.0 mL, 201.4 mmol) was heated to 180 °C for 18 hours under a nitrogen atmosphere. The reaction mixture was cooled to room temperature and filtered under vacuo. The dark brown residue was washed with water,

dried under reduced pressure and purified by column chromatography on silica gel eluting with chloroform/methanol (92:8 v/v) to give **95** as an orange powder (0.73 g, 62% yield); mp: 182-184 °C (lit 188-193 °C).

^{1}H NMR (500 MHz, DMSO-d_6) δ 12.36 (br s, 1H, N*H*), 12.30 (br s, 1H, N*H*), 8.16 (s, 1H, H-2), 7.93 (d, $J_{5,7}$ = 1.9 Hz, 1H, H-5), 7.50 (d, $J_{8,7}$ = 8.6 Hz, 1H, H-8), 7.35 (dd, $J_{7,8}$ = 8.6 Hz, $J_{7,5}$ = 2.1 Hz, 1H, H-7).

^{13}C NMR (126 MHz, DMSO-d_6) δ 158.06 (C, C=O), 154.39 (C, Carom), 148.21 (CH, C2), 133.88 (C, Carom), 125.44 (C, Carom), 123.98 (CH, C7), 123.21 (C, Carom), 119.50 (CH, C5), 113.25 (CH, C8), 99.68 (C, Carom).

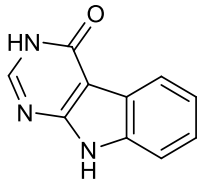

$C_{10}H_7N_3O$, MW 185.18

3*H*-Pyrimido[4,5-*b*]indol-4(9*H*)-one (**96**).[13]

Compound **96** was prepared as described for **95** from crude compound **94** (1.75 g, 8.58 mmol) and obtained as dark powder, that was used directly in the next step.

^{1}H NMR (500 MHz, DMSO-d_6) δ 12.19 (br s, 1H, N*H*), 12.16 (br s, 1H, N*H*), 8.13 (s, 1H, H-2), 8.00 (d, $J_{5,6}$ = 7.7 Hz, 1H, H-5), 7.48 (d, $J_{8,7}$ = 8.1 Hz, 1H, H-8), 7.36 – 7.31 (m, 1H, Harom), 7.27 – 7.21 (m, 1H, Harom).

^{13}C NMR (126 MHz, DMSO-d_6) δ 158.20 (C, C=O), 153.61 (C, Carom), 147.42 (CH, C2), 135.32 (C, Carom), 124.02 (CH, Carom), 122.03 (C, Carom), 121.00 (CH, Carom), 120.55 (CH, C5), 111.57 (CH, C8), 100.06 (C, Carom).

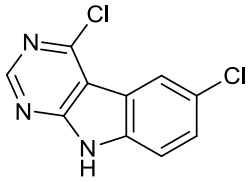

$C_{10}H_5Cl_2N_3$, MW 238.07

4,6-Dichloro-9*H*-pyrimido[4,5-*b*]indole (**97**).[13]

Compound **95** (0.72 g, 3.28 mmol) was suspended in phosphorus (V) oxychloride (10 mL, 108.2 mmol) under a nitrogen atmosphere and the suspension was heated at reflux for 48 hours (monitored by TLC). The reaction mixture was cooled to room temperature and the solvent evaporated under reduced pressure. The residue was diluted carefully with ice-cold water in a ice-bath and slowly neutralised with 10% aqueous ammonia to pH 7, then filtered under vacuo. The crude residue was washed with cold water, then with HCl 1M and again with cold water. After drying under reduced pressure the titled compound was obtained as a brown powder that was purified by flash colum chromatography on silica gel (hexane/acetone/isopropanol 89:10:1 v/v) to give compound **97** as a yellow powder (0.65 g, 83% yield); mp: > 230 °C (lit. > 300 °C).

^{1}H NMR (500 MHz, DMSO-d_6) δ 12.94 (s, 1H, 9-N*H*), 8.82 (s, 1H, H-2), 8.23 (s, 1H, H-5), 7.67 (m, 2H, H-7 and H-8).

^{13}C NMR (126 MHz, DMSO-d_6) δ 156.26 (C, Carom), 154.51 (CH, C2), 151.81, 136.98 (2 C, Carom), 128.33 (CH, Carom), 125.93 (C, C6), 121.45 (CH, C5), 118.90 (C, Carom), 113.97 (CH, Carom), 110.42 (C, Carom).

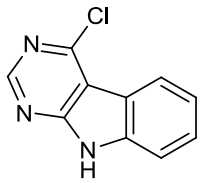

$C_{10}H_6ClN_3$, MW 203.63

4-Chloro-9*H*-pyrimido[4,5-*b*]indole (**98**).[13]

Compound **98** was prepared as described for **97** from crude compound **96** (1.59 g, 8.58 mmol). The crude residue was purified by flash colum chromatography on silica gel (hexane/acetone/isopropanol 94:5:1 v/v) to give compound **98** as a yellow powder (0.33 g, 17% yield for last three steps); mp: > 230 °C (lit. 258 °C).

^{1}H NMR (500 MHz, DMSO-d_6) δ 12.73 (s, 1H, N*H*), 8.74 (s, 1H, H-2), 8.23 (d, $J_{5,6}$ = 7.8 Hz, 1H, H-5), 7.62 – 7.58 (m, 2H, H-7 and H-8), 7.39 (ddd, $J_{6,5}$ = 8.0 Hz, $J_{6,7}$ = 6.0 Hz, $J_{6,8}$ = 2.2 Hz, 1H, H-6).

^{13}C NMR (126 MHz, DMSO-d_6) δ 156.44 (C, Carom), 154.37 (CH, C2), 151.70, 138.96 (2 C, Carom), 128.88 (CH, C7), 122.88 (CH, C5), 122.16 (CH, C6), 118.14 (C, Carom), 112.75 (CH, C8), 111.54 (C, Carom).

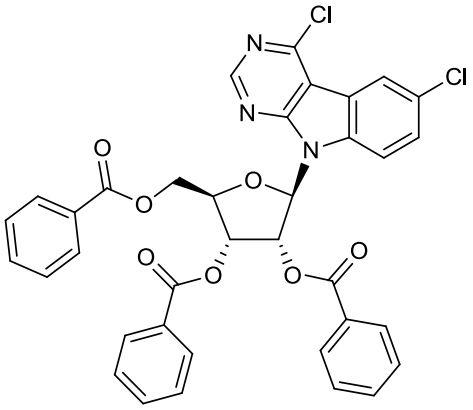

$C_{36}H_{25}Cl_2N_3O_7$, MW 681.11

4,6-Dichloro-9-(2,3,5-tri-*O*-benzoyl-β-D-ribofuranosyl)-pyrimido[4,5-*b*]indole (**99**).[13]

N,*O*-Bis(trimethylsilyl)acetamide (0.10 mL, 0.42 mmol) was added to a suspension of compound **97** (0.10 g, 0.42 mmol) in anhydrous acetonitrile at room temperature under a nitrogen atmosphere. After 10 minutes, trimethylsilyl trifluoromethanesulfonate (0.15 mL, 0.84 mmol) was added dropwise, followed by the addition of 1-*O*-acetyl-2,3,5-tri-*O*-benzoyl-β-D-ribofuranose (0.21 g, 0.42 mmol). The reaction mixture was heated to 60 °C for 20 hours, then cooled to room temperature and partioned between water and ethylacetate. The aqueous phase was further extracted with ethylacetate (2 x 20 mL), the combined organic layer was washed with saturated $NaHCO_3$ aqueous solution (40 mL) and water (40 mL), dried over anhydrous $MgSO_4$, filtered and concentrated. The crude residue was purified by column chromatography on silica gel eluting with hexane/ethyl acetate (70:30 v/v) to give compound **99** (0.16 g, 55% yield) as a white foam; mp: 160 – 162 °C (lit. 164 – 165 °C).

^{1}H NMR (500 MHz, DMSO-d_6) δ 8.81 (s, 1H, H-2), 8.30 (d, $J_{5,7}$ = 2.1 Hz, 1H, H-5), 8.15 (d, $J_{8,7}$ = 8.9 Hz, 1H, H-8), 8.02 – 7.98 (m, 2H, Harom), 7.93 – 7.90 (m, 2H, Harom), 7.86 – 7.83 (m, 2H, Harom), 7.71 – 7.66 (m, 2H, Harom), 7.63 – 7.60 (m, 2H, Harom and H-7), 7.51 – 7.48 (m, 4H, Harom), 7.44 – 7.41 (m, 2H, Harom), 7.02 (d, $J_{1',2'}$ = 4.5 Hz, 1H, H-1'), 6.60 (dd, $J_{2',3'}$ = 6.5 Hz, $J_{2',1'}$ = 4.5 Hz, 1H, H-

2'), 6.37 (t, $J_{3',2'} = J_{3',4'}$ = 6.6 Hz, 1H, H-3'), 4.93 – 4.89 (m, 1H, H-4'), 4.86 (dd, $J_{5'b,5'a}$ = 12.3 Hz, $J_{5'b,4'}$ = 3.1 Hz, 1H, H-5'b), 4.69 (dd, $J_{5'a,5'b}$ = 12.3 Hz, $J_{5'a,4'}$ = 4.2 Hz, 1H, H-5'a).

^{13}C NMR (126 MHz, DMSO-d_6) δ 165.30 (C, C=O), 164.77 (C, C=O), 164.58 (C, C=O), 155.33 (C, Carom), 154.36 (CH, C2), 152.47, 136.84 (2 C, Carom), 133.87 (CH, Carom), 133.53, 129.39, 129.29 (3 CH, Carom), 129.15 (C, Carom), 129.10, 128.73, 128.68, 128.67 (4 CH, Carom), 128.59 (CH, C7), 128.42, 127.42 (2 C, Carom), 121.74 (CH, C5), 119.18 (C, Carom), 113.72 (CH, C8), 111.51 (C, Carom), 86.24 (CH, C1'), 78.73 (CH, C4'), 72.20 (CH, C2'), 70.10 (CH, C3'), 62.87 (CH_2, C5').

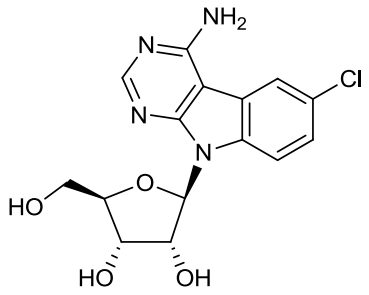

$C_{15}H_{15}ClN_4O_4$, MW 350.76

4-Amino-6-chloro-9-β-D-ribofuranosyl-pyrimido[4,5-*b*]indole (**87**).[16]

Compound **99** (0.15 g, 0.22 mmol) was dissolved in a saturated (7M) solution of ammonia in methanol (10 mL). The reaction mixture was stirred in a screw-cap pressure glass tube at 75 °C for 48 hours, then cooled to room temperature and filtered under vacuo to isolate pure compound **87** (0.034 g, 44% yield) as white crystals; mp: > 230 °C.

^{1}H NMR (500 MHz, DMSO-d_6) δ 8.51 (d, $J_{5,7}$ = 2.0 Hz, 1H, H-5), 8.31 (s, 1H, H-2), 7.89 (d, $J_{8,7}$ = 8.8 Hz, 1H, H-8), 7.46 (br s, 2H, 4-NH_2), 7.40 (dd, $J_{7,8}$ = 8.8 Hz, $J_{7,5}$ = 2.0 Hz, 1H, H-7), 6.34 (d, $J_{1',2'}$ = 7.3 Hz, 1H, H-1'), 5.41 (dd, $J_{5'\text{-}OH,5'a}$ = 6.3 Hz, $J_{5'\text{-}OH,5'b}$ = 4.7 Hz, 1H, 5'-OH), 5.20 (d, $J_{2'\text{-}OH,2'}$ = 6.6 Hz, 1H, 2'-OH), 5.14 (d, $J_{3'OH,3'}$ = 4.6 Hz, 1H, 3'-OH), 4.78 (dd, $J_{2',1' \text{ and } 2',3'}$ = 12.9 Hz, $J_{2',2'\text{-}OH}$ = 6.6 Hz, 1H, H-2'), 4.19 (dd, J = 7.3, 5.3 Hz, 1H, H-3'), 3.97 (dd, $J_{4',5'b \text{ and } 4',3'}$ = 6.2 Hz, $J_{4',5'a}$ = 3.2 Hz, 1H, H-4'), 3.74 – 3.69 (m, 1H, H-5'b), 3.64 (ddd, $J_{5'a,5'b}$ = 11.8 Hz, $J_{5'a,5'\text{-}OH}$ = 6.4 Hz, $J_{5'a,4'}$ = 3.6 Hz, 1H, H-5'a).

^{13}C NMR (126 MHz, DMSO-d_6) δ 157.77, 155.68 (2 C, Carom), 155.01 (CH, C2), 134.54, 125.86 (2 C, Carom), 124.42 (CH, C7), 121.54 (C, Carom), 120.59 (CH, C5), 113.07 (CH, C8), 95.11 (C, Carom), 87.08 (CH, C1'), 85.47 (CH, C4'), 70.63 (CH, C2'), 70.26 (CH, C3'), 61.81 (CH_2, C5').

MS (ES+) *m/z* 351.1 [MH^+].

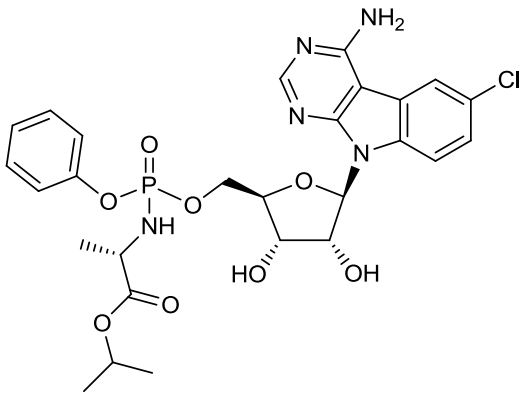

$C_{27}H_{31}ClN_5O_8P$, MW 619.99

4-Amino-6-chloro-9-β-D-ribofuranosyl-pyrimido[4,5-*b*]indole 5'-*O*-[phenyl-(isopropoxy-L-alaninyl)] phosphate (**101**).

Compound **87** (0.052 g, 0.15 mmol) was suspended in anhydrous dimethylformamide (1.5 mL) in a 10 mL sealed microwave tube under a nitrogen atmosphere and *tert*-butylmagnesium chloride 1M in tetrahydrofuran (0.14 mL, 0.15 mmol) was added dropwise at room temperature. After stirring 10 minutes, a solution of compound **38** (0.06 g, 0.15 mmol) in anhydrous dimethylformamide (0.8 mL) was added slowly. The reaction mixture was stirred for 30 minutes under MWI (100 W, 65 °C), then cooled to room temperature and quenched by adding water (0.5 mL) slowly. The mixture was concentrated under reduced pressure by coevaporation with toluene. The crude residue was purified by flash column chromatography on silica gel (dichloromethane to dichloromethane/methanol 90:10 v/v) to isolate the titled compound. Compound **101** was further purified by flash column chromatography on silica gel (dichloromethane to dichloromethane/methanol 92:8 v/v) and obtained as a white powder (0.012 g, 13% yield).

^{31}P NMR (202 MHz, CD_3OD) δ 3.80, 3.69.

^{1}H NMR (500 MHz, CD_3OD) δ 8.20, 8.19 (2 s, 1H, H-2), 8.12, 8.11 (2 d, $J_{5,7}$ = 1.9 Hz, 1H, H-5), 7.66, 7.63 (d, $J_{8,7}$ = 8.8 Hz, 1H, H-8), 7.30 – 7.24 (m, 1H, H-7), 7.22 – 7.16 (m, 2H, Harom), 7.10 – 7.03 (m, 3H, Harom), 6.33, 6.31 (2 d, $J_{1',2'}$ = 6.1 Hz, 1H, H-1'), 4.92, 4.88 (2 m, 1H, H-2'), 4.78 – 4.71 (m, 1H, *H*-*i*Pr), 4.47 – 4.43 (m, 1H, H-3'), 4.40 – 4.25 (m, 2H, H-5'a and H-5'b), 4.15 – 4.09 (m, 1H, H-4'), 3.78 – 3.71, 3.70 – 3.63 (2 m, 1H, C*H*CH_3), 1.15 – 0.99 (m, 9H, CHCH_3 and 2 CH_3-*i*Pr).

^{13}C NMR (126 MHz, CD_3OD) δ 173.15 (d, $J_{C\text{-}C\text{-}N\text{-}P}$ = 4.5 Hz, C, C=O), 172.96 (d, $J_{C\text{-}C\text{-}N\text{-}P}$ = 5.5 Hz, C, C=O), 157.75, 157.74, 155.93, 155.88 (C, Carom), 154.60, 154.56 (CH, C2), 150.76, 150.70, 135.02, 134.97 (C, Carom), 129.34, 129.32 (CH, Carom), 127.25 (C, Carom), 125.04, 124.98, 124.74, 124.74, 124.68, 124.67 (CH, Carom), 121.80, 121.73 (C, Carom), 120.36, 120.33 (CH, C5), 119.97, 119.96,

119.94, 119.93 (CH, Carom), 112.60, 112.43 (CH, C8), 95.95 (C, Carom), 88.36, 88.20 (CH, C1'), 82.47, 82.43 (d, $J_{C\text{-}C\text{-}O\text{-}P}$ = 6.8 Hz, CH, C4'), 82.40, 82.36 (d, $J_{C\text{-}C\text{-}O\text{-}P}$ = 6.6 Hz, CH, C4'), 71.08, 71.02 (CH, C2'), 69.81, 69.56 (CH, C3'), 68.73, 68.70 (CH, C*H*-*i*Pr), 66.47, 66.43 (d, $J_{C\text{-}O\text{-}P}$ = 5.4 Hz, CH_2, C5'), 65.94, 65.90 (d, $J_{C\text{-}O\text{-}P}$ = 5.2 Hz, CH_2, C5'), 50.31, 50.16 (CH, C*H*CH_3), 20.55, 20.47 (CH_3, 2 *C*H_3-*i*Pr), 19.11, 19.06 (d, $J_{C\text{-}C\text{-}N\text{-}P}$ = 6.3 Hz, CH_3, CH*C*H_3), 18.97, 18.91 (d, $J_{C\text{-}C\text{-}N\text{-}P}$ = 7.2 Hz, CH_3, CH*C*H_3).

HPLC (system 1) t_R = 25.71, 26.08 min.

HPLC (system 2) t_R = 29.59, 29.81 min.

MS (ES+) *m/z* 620.2 [MH^+], 642.2 [MNa^+].

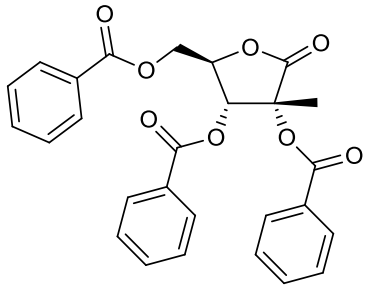

$C_{27}H_{22}O_8$, MW 474.46

2,3,5-Tri-*O*-benzoyl-2-*C*-methyl-D-ribonic-γ-lactone (**104**).[17]

To a solution of commercially available 2-*C*-methyl-D-ribono-1,4-lactone **103** (1.00 g, 6.17 mmol) in anhydrous dimethoxy ethane was added 4-(dimethylamino)pyridine (0.15 g, 1.23 mmol) and triethylamine (11.6 mL, 8.33 mmol) at room temperature under a nitrogen atmosphere. The resulting solution was stirred for 30 minutes, then cooled to -5 °C and benzoyl chloride (3.2 mL, 27.76 mmol) was added dropwise. The reaction mixture was allowed to attain room temperature and stirred for 16 hours. Ice-cold water (15 mL) was added and stirring was continued for 30 minutes, then the mixture was filtered under vacuo and washed with cold water. The crude product was vigorously stirred with *tert*-butyl methyl ether (20 mL) for 30 minutes, then filtered under vacuo, washed with *tert*-butyl methyl ether (20 mL) and dried to obtain compound **104** (2.27 g, 77% yield) as a white solid.

^{1}H NMR (500 MHz, $CDCl_3$) δ 8.06 (dd, *J* = 8.2, 1.0 Hz, 2H, Harom), 7.95 (dd, *J* = 8.2, 1.1 Hz, 2H, Harom), 7.75 (dd, *J* = 8.3, 1.1 Hz, 2H, Harom), 7.63 – 7.59 (m, 1H, Harom), 7.53 – 7.41 (m, 4H, Harom), 7.34 (t, *J* = 7.8 Hz, 2H, Harom), 7.20 (t, *J* = 7.9 Hz, 2H, Harom), 5.54 (d, $J_{3,4}$ = 5.9 Hz, 1H, H-3), 5.22 – 5.18 (m, 1H, H-4), 4.83 (dd, $J_{5a,5b}$ = 12.4 Hz, $J_{5a,4}$ = 3.2 Hz, 1H, H-5a), 4.72 (dd, $J_{5b,5a}$ = 12.4 Hz, $J_{5b,4}$ = 4.1 Hz, 1H, H-5b), 1.98 (s, 3H, 2-CH_3).

^{13}C NMR (126 MHz, $CDCl_3$) δ 172.62 (C, C=O), 165.97, 165.88, 165.39 (3 C, C=O), 133.85, 133.71, 133.51, 129.92, 129.69, 129.63 (6 CH, Carom), 129.25 (C, Carom), 128.59, 128.42, 128.31 (3 CH, Carom), 127.86, 127.80 (2 C, Carom), 79.49 (CH, C3), 75.34 (C, C2), 72.51 (CH, C4), 63.15 (CH_2, C5), 23.65 (CH_3, 2-*C*H_3).

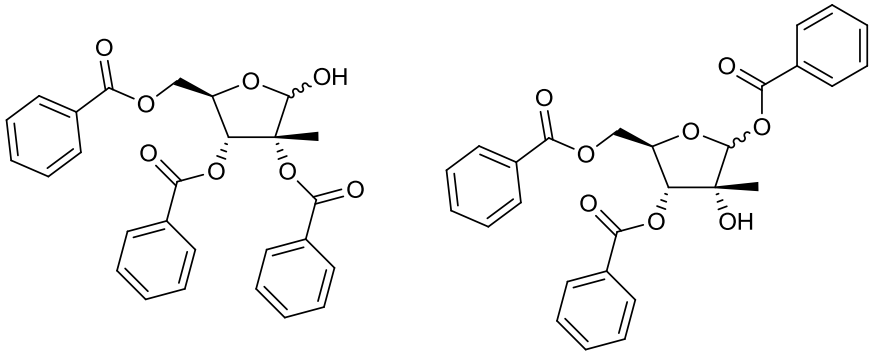

$C_{27}H_{24}O_8$, MW 476.47

2,3,5-Tri-*O*-benzoyl-2-*C*-methyl-β-D-ribofuranose (**105** and **106**).[17]

A solution of Red-Al® 65wt.% in toluene (2.0 mL, 6.56 mmol) was diluted with anhydrous toluene (2 mL) under a nitrogen atmosphere and cooled to 0 °C, then a solution of anhydrous ethanol (0.38 mL, 6.56 mmol) in anhydrous toluene (1.6 mL) was added dropwise over a period of 5 minutes. The resulting solution was stirred at 0 °C for 15 minutes, then 2 mL of the thus prepared reagent were added dropwise to a cold (-5 °C) solution of **104** in anhydrous toluene over a period of 10 minutes, under a nitrogen atmosphere. The reaction mixture was stirred at the same temperature for 1.5 hours, then quenched with acetone (0.2 mL), water (15 mL) and HCl 1M aqueous solution (15 mL) at 0 °C and allowed to attain room temperature. The mixture was extracted with ethyl acetate (3 x 30 mL). The combined organic layer was washed with brine (60 mL), dried over anhydrous $MgSO_4$, filtered and concentrated under reduced pressure to obtain compound **105** and **106** (0.39 g, 82% yield) as a colourless oil. The crude mixture of products was used for the following step without purification.

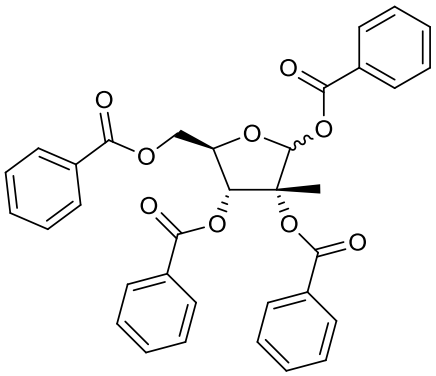

$C_{34}H_{28}O_9$, MW 580.58

1,2,3,5-Tetra-*O*-benzoyl-2-*C*-methyl-β-D-ribofuranose (**107**).[17]

To a solution of the mixture of crude compounds **105** and **106** (0.39 g, 0.82 mmol) and 4-(dimethylamino)pyridine (0.01 g, 0.08 mmol) in anhydrous tetrahydrofuran, triethylamine (0.60 mL, 4.09 mmol) was added dropwise at room temperature under a nitrogen atmosphere. The solution was cooled to 5 °C before adding benzoyl chloride (0.20 mL, 1.64 mmol) dropwise. The reaction mixture was allowed to attain room temperature and stirred for 24 hours, then was quenched by adding ice-cold water (10 mL) and saturated $NaHCO_3$ aqueous solution (10 mL), extracted with ethyl acetate (3 x 50 mL). The combined organic layer was washed with water (50 mL) and brine (50 mL), dried over anhydrous $MgSO_4$, filtered and concentrated under reduced pressure. The crude product was vigorously stirred with *tert*-butyl methyl ether (5 mL) for 5 minutes, then heptanes (5 mL) and water (0.1 mL) were added and the suspension was vigorously stirred for additional 2 hours. The solid was filtered under vacuo, washed with heptane/*tert*-butyl methyl ether (1:1 v/v, 10 mL), then with *tert*-butyl methyl ether (5 mL) and dried to obtain compound **107** (0.17 g, 35% yield) as a white solid.

^{1}H NMR (500 MHz, $CDCl_3$) δ 8.07 – 8.02 (m, 4H, Harom), 7.99 (dd, *J* = 8.3, 1.2 Hz, 2H, Harom), 7.82 (dd, *J* = 8.3, 1.2 Hz, 2H, Harom), 7.54 (td, *J* = 7.5, 0.9 Hz, 3H, Harom), 7.44 – 7.36 (m, 7H, Harom), 7.09 (dd, *J* = 8.1, 7.6 Hz, 2H, Harom), 6.99 (s, 1H, H-1), 5.88 (d, $J_{3,4}$ = 8.1 Hz, 1H, H-3), 4.74 – 4.69 (m, 1H, H-4), 4.61 (dd, $J_{5a,5b}$ = 12.1 Hz, $J_{5a,4}$ = 4.1 Hz, 1H, H-5a), 4.47 (dd, $J_{5b,5a}$ = 12.1, $J_{5b,4}$ = 4.8 Hz, 1H, H-5b), 1.88 (s, 3H, 2-CH_3).

^{13}C NMR (126 MHz, $CDCl_3$) δ 166.11, 165.64, 164.81, 164.56 (4 C, C=O), 133.78, 133.64, 133.48, 132.96 (4 CH, Carom), 130.31 (C, Carom), 129.95, 129.94, 129.79, 129.64 (4 CH, Carom), 129.47, 129.26, 128.94 (3 C, Carom), 128.65, 128.63, 128.56, 128.18 (4 CH, Carom), 97.90 (CH, C1), 86.71 (C, C2), 78.62 (CH, C3), 76.26 (CH, C4), 63.94 (CH_2, C5), 16.91 (CH_3, 2-CH_3).

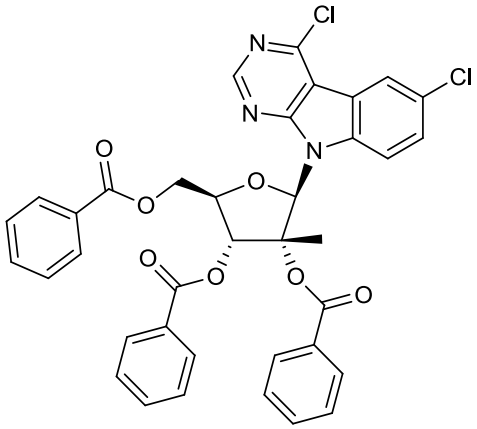

$C_{37}H_{27}Cl_2N_3O_7$, MW 696.53

4,6-Dichloro-9-(2,3,5-tri-*O*-benzoyl-2-*C*-methyl-β-D-ribofuranosyl)-pyrimido[4,5-*b*]indole (**108**).

N,*O*-Bis(trimethylsilyl)acetamide (0.10 mL, 0.42 mmol) was added to a suspension of compound **97** (0.10 g, 0.42 mmol) in anhydrous acetonitrile at room temperature under a nitrogen atmosphere. After 10 minutes, trimethylsilyl trifluoromethanesulfonate (0.15 mL, 0.84 mmol) was added dropwise, followed by the addition of compound **107** (0.24 g, 0.42 mmol). The reaction mixture was heated to 60 °C for 20 hours, then cooled to room temperature and partioned between water and ethylacetate. The aqueous phase was further extracted with ethylacetate (2 x 20 mL), the combined organic layer was washed with saturated $NaHCO_3$ aqueous solution (40 mL) and water (40 mL), dried over anhydrous $MgSO_4$, filtered and concentrated. The crude residue was purified by column chromatography on silica gel eluting with hexane/ethyl acetate (60:40 v/v) to give compound **108** (0.06 g, 21% yield) as a colourless oil.

^{1}H NMR (500 MHz, $CDCl_3$) δ 9.10 (s, 1H, H-2), 8.59 (d, $J_{5,7}$ = 2.0 Hz, 1H, H-5), 8.42 – 8.39 (m, 2H, H-8 and Harom), 8.35 – 8.32 (m, 2H, Harom), 8.24 – 8.20 (m, 2H, Harom), 8.13 (d, $J_{7,8}$ = 8.9 Hz, 1H, H-7), 7.85 – 7.77 (m, 4H, Harom), 7.73 – 7.69 (m, 4H, Harom), 7.67 – 7.63 (m, 3H, Harom), 7.55 (m, 2H, Harom), 7.41 (s, 1H, H-1'), 5.24 (dd, $J_{5'a,5'b}$ = 11.9 Hz, $J_{5'a,4'}$ = 3.6 Hz, 1H, H-5'a), 5.17 (dd, $J_{5'b,5'a}$ = 11.9 Hz, $J_{5'b,4'}$ = 6.4 Hz, 1H, H-5'b), 5.13 – 5.06 (m, 2H, H-3' and H-4'), 1.85 (s, 3H, 2'-CH_3).

^{13}C NMR (126 MHz, $CDCl_3$) δ 166.25 (C, C=O), 165.65 (C, C=O), 165.53 (C, C=O), 155.36 (C, Carom), 153.99 (CH, C2), 153.47 (C, Carom), 137.77 (C, Carom), 135.11 (CH, C8), 133.77, 133.73, 133.21 (3 CH, Carom), 130.06 (C, Carom), 129.93, 129.91, 129.71 (3 CH, Carom), 129.59 (C, Carom), 129.09, 129.01, 128.64, 128.59, 128.38 (5 CH, Carom), 125.45 (CH, C7), 122.74 (CH, C5), 119.80, 112.74 (2 C, Carom), 89.02 (CH, C1'), 87.19 (C, C2'), 76.32 (CH), 63.99 (CH_2, C5'), 18.19 (CH_3, 2'-*C*H_3).

MS (ES+) *m/z* 696.2 [MH^+].

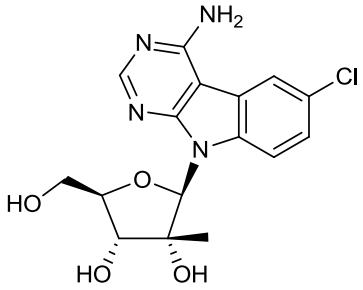

$C_{16}H_{17}ClN_4O_4$, MW 364.78

4-Amino-6-chloro-9-(2-*C*-methyl-β-D-ribofuranosyl)-pyrimido[4,5-*b*]indole (**102**).

Compound **108** (0.19 g, 0.27 mmol) was dissolved in a saturated (7M) solution of ammonia in methanol (4 mL). The reaction mixture was stirred in a screw-cap pressure glass tube at 80 °C for 24 hours, then cooled to room temperature. The solvent was evaporated under reduced pressure and the crude residue was purified by flash column chromatography on silica gel (dichloromethane to dichloromethane/methanol 90:10 v/v) to isolate the titled compound. Compound **102** was further purified by flash column chromatography on silica gel (dichloromethane to dichloromethane/methanol 90:10 v/v) and obtained as a white powder (0.052 g, 52% yield); mp: > 230 °C.

^{1}H NMR (500 MHz, DMSO-d_6) δ 8.50 (s, 1H, H-5), 8.31 (s, 1H, H-2), 7.95 (d, $J_{8,7}$ = 8.4 Hz, 1H, H-8), 7.46 (br s, 2H, 4-NH_2), 7.39 (d, $J_{7,8}$ = 8.4 Hz, 1H, H-7), 6.46 (s, 1H, H-1'), 5.24 (d, $J_{3',4'}$ = 7.0 Hz, 1H, H-3'), 5.21 (br s, 1H, O*H*), 5.00 (br s, 1H, O*H*), 4.17 (br s, 1H, O*H*), 3.91 – 3.84 (m, 2H, H-4' and H-5'a), 3.82 – 3.75 (m, 1H, H-5'b), 0.69 (s, 3H, 2'-CH_3).

^{13}C NMR (126 MHz, DMSO-d_6) δ 158.21 (C, Carom), 155.54 (CH, C2), 135.10 (C, Carom), 126.30 (C, Carom), 124.91 (CH, C7), 121.83 (C, Carom), 121.04 (CH, C5), 92.94 (CH, C1'), 82.47 (CH, C4'), 78.54 (C, C2'), 73.94 (CH, C3'), 60.42 (CH_2, C5'), 21.07 (CH_3, 2'-*C*H_3).

HPLC (system 1) t_R = 19.20 min.

HPLC (system 2) t_R = 25.82 min.

MS (ES+) *m/z* 365.1 [MH^+].

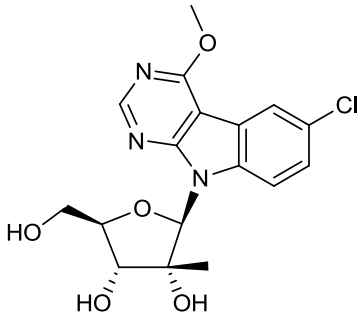

$C_{17}H_{18}ClN_3O_5$, MW 379.79

6-Chloro-4-methoxy-9-(2-*C*-methyl-β-D-ribofuranosyl)-pyrimido[4,5-*b*]indole (**109**).

Compound **109** was isolated as a side-product of the synthesis of compound **102** and obtained as an off-white powder (0.015 g, 14% yield); mp: > 230 °C.

^{1}H NMR (500 MHz, DMSO-d_6) δ 8.71 (s, 1H, H-2), 8.12 (d, $J_{8,7}$ = 8.6 Hz, 1H, H-8), 8.01 (d, $J_{5,7}$ = 2.1 Hz, 1H, H-5), 7.52 (dd, $J_{7,8}$ = 8.6 Hz, $J_{7,5}$ = 2.1 Hz, 1H, H-7), 6.53 (s, 1H, H-1'), 5.29 (d, $J_{3',4'}$ = 6.7 Hz, 1H, H-3'), 5.10 (t, *J* = 5.1 Hz, 1H, O*H*), 5.07 (br s, 1H, O*H*), 4.22 (s, 3H, 4-OCH_3), 4.16 (br s, 1H, O*H*), 3.94 – 3.86 (m, 2H, H-4' and H-5'a), 3.85 – 3.79 (m, 1H, H-5'b), 0.70 (s, 3H, 2'-CH_3).

^{13}C NMR (126 MHz, DMSO-d_6) δ 164.32, 156.50 (2 C, Carom), 155.32 (CH, C2), 135.86 (C, Carom), 126.74 (C, Carom), 126.66 (CH, C7), 121.64 (CH, C5), 120.51 (C, Carom), 98.82 (CH, C8), 93.17 (CH, C1'), 82.62 (CH, C4'), 78.53 (C, C2'), 74.09 (CH, C3'), 60.45 (CH_2, C5'), 54.73 (CH_3, 4-O*C*H_3), 21.07 (CH_3, 2'-*C*H_3).

HPLC (system 1) t_R = 26.54 min.

HPLC (system 2) t_R = 30.38 min.

MS (ES+) *m/z* 380.1 [MH^+], 402.1 [MNa^+].

4.2.5 PROCEDURES AND SPECTRAL DATA – SECTION 2.2.4

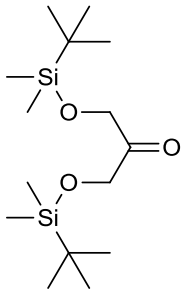

$C_{15}H_{34}O_3Si_2$, MW 318.60

Bis-(*tert*-butyldimethylsilyloxy)-acetone (**113**).[18]

To a solution of 1,3-dihydroxyacetone **112** dimer (0.80 g, 4.44 mmol) and 4-(dimethylamino)-pyridine (1.36 g, 11.10 mmol) in anhydrous dichloromethane, triethylamine (1.86 ml, 13.32 mmol) was added at room temperature under a nitrogen atmosphere. The solution was cooled to 0 °C and *tert*-butyldimethylchlorosilane (3.35 g, 22.20 mmol) was added slowly. The reaction mixture was allowed to attain room temperature and stirred for 24 hours. Then a saturated aqueous $NaHCO_3$ solution (20 mL) and extracted with petroleum ether (3 x 30 mL), the combined organic layer was washed with water (50 mL) and brine (50 mL), dried over anhydrous $MgSO_4$, filtered and concentrated under reduced pressure. The residue was purified by column chromatography on silica gel eluting with hexane/ethyl acetate (97:3 v/v) to give compound **113** (2.46 g, 87% yield) as a colourless syrup.

^{1}H NMR (500 MHz, $CDCl_3$) δ 4.32 (s, 4H, 2 C*H*$_2$), 0.83 (s, 18H, 2 *t*BuSi), 0.00 (s, 12H, 4 C*H*$_3$Si).

^{13}C NMR (126 MHz, $CDCl_3$) δ 208.51 (C, C=O), 67.87 (CH_2, 2 *C*H_2), 25.74 (CH_3, 6 *C*H_3-*t*BuSi), 18.30 (C, 2 *C*-*t*BuSi), -5.58 (CH_3, 4 *C*H_3Si).

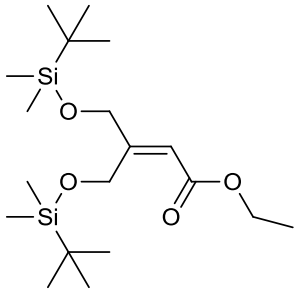

$C_{19}H_{40}O_4Si_2$, MW 388.69

Ethyl 3,3'-bis-(*tert*-butyldimethylsilyloxymethyl)prop-2-en-1-oate (**114**).[18]

Triethylphosphonoacetate (1.70 ml, 8.51 mmol) was added dropwise to a suspension of sodium hydride 60% dispersion in mineral oil (0.34 g, 8.51 mmol) in anhydrous tetrahydrofuran at 0 °C under a nitrogen atmosphere. The reaction mixture was stirred at room temperature for an hour, before cooling to 0 °C and adding slowly a solution of **113** (2.46 g, 7.74 mmol) in anhydrous tetrahydrofuran (1 mL). The reaction mixture was allowed to attain room temperature and stirred for 2 hours, then poured into water (30 mL) and extracted with ethyl acetate (3 x 30 mL), the combined organic layer was washed with water (30 mL) and brine (30 mL), dried over anhydrous $MgSO_4$, filtered and concentrated under reduced pressure. The residue was purified by column chromatography on silica gel eluting with hexane/ethyl acetate (96:4 v/v) to give compound **114** (2.83 g, 94% yield) as a colourless oil.

^{1}H NMR (500 MHz, $CDCl_3$) δ 5.90 – 5.88 (m, 1H, H-2), 4.79 – 4.77 (m, 2H, 3-CH_2), 4.35 – 4.33 (m, 2H, 3-CH_2), 4.06 (q, *J* = 7.1 Hz, 2H, CH_2CH$_3$), 1.19 (t, *J* = 7.1 Hz, 3H, CH$_2$CH_3), 0.84 (s, 9H, *t*BuSi), 0.80 (s, 9H, *t*BuSi), -0.00 (s, 6H, 2 CH_3Si), -0.03 (s, 6H, 2 CH_3Si).

^{13}C NMR (126 MHz, $CDCl_3$) δ 166.57 (C, C=O), 161.44 (C, C3), 111.92 (CH, C2), 63.22 (CH$_2$, 3-*C*H$_2$), 61.53 (CH$_2$, 3-*C*H$_2$), 59.72 (CH$_2$, *C*H$_2$CH$_3$), 25.91 (CH$_3$, 3 *C*H$_3$-*t*BuSi), 25.78 (CH$_3$, 3 *C*H$_3$-*t*BuSi), 18.39 (C, *C*-*t*BuSi), 18.16 (C, *C*-*t*BuSi), 14.31 (CH$_3$, CH$_2$*C*H$_3$), -5.49 (CH$_3$, 2 *C*H$_3$Si), -5.59 (CH$_3$, 2 *C*H$_3$Si).

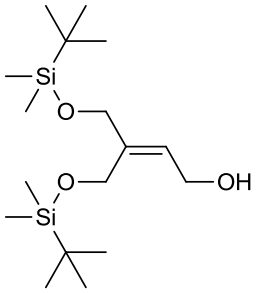

$C_{17}H_{38}O_3Si_2$, MW 346.65

3,3'-Bis-(*tert*-butyldimethylsilyloxymethyl)prop-2-en-1-ol (**115**).[19]

To a solution of **114** (2.52 g, 6.48 mmol) in anhydrous dichloromethane, a 1M solution of DIBALH in cyclohexane (13.6 mL, 13.62 mmol) was added slowly at -20 °C and the reaction mixture was stirred for 1 hour in the dry ice-acetone bath at the temperature of -20 °C to 0 °C. Then, methanol (15 mL) was added and the mixture poured into 10% Rochelle salt aqueous solution (200 mL) and ethyl acetate (200 mL). The two-phase solution was stirred vigorously for 1 hour at room temperature, until the two phases were clearly separated. The organic layer was separated, washed with brine/water (1:1 v/v, 2 x 100 mL), dried over $MgSO_4$, filtered and concentrated in vacuo. The residue was purified by column chromatography on silica gel eluting with hexane/ethyl acetate (90:10 v/v) to give compound **115** (1.58 g, 79% yield) as a colourless syrup.

^{1}H NMR (500 MHz, $CDCl_3$) δ 5.73 (t, $J_{2,1}$ = 6.8 Hz, 1H, H-2), 4.15 – 4.13 (m, 4H, 3-CH_2 and H-1), 4.08 (s, 2H, 3-CH_2), 2.04 (s, 1H, 1-O*H*), 0.84 (s, 9H, *t*BuSi), 0.83 (s, 9H, *t*BuSi), 0.01 (s, 6H, 2 CH_3Si), -0.00 (s, 6H, 2 CH_3Si).

^{13}C NMR (126 MHz, $CDCl_3$) δ 141.17 (C, C3), 125.41 (CH, C2), 64.86 (CH_2, 3-*C*H_2), 59.41 (CH_2, 3-*C*H_2), 58.70 (CH_2, C1), 25.94 (CH_3, 3 *C*H_3-*t*BuSi), 25.85 (CH_3, 3 *C*H_3-*t*BuSi), 18.40 (C, *C*-*t*BuSi), 18.25 (C, *C*-*t*BuSi), -5.34 (CH_3, 2 *C*H_3Si), -5.41 (CH_3, 2 *C*H_3Si).

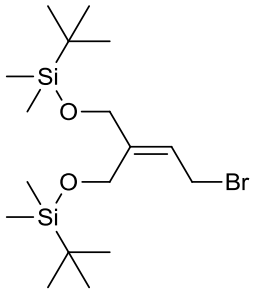

$C_{17}H_{37}BrO_2Si_2$, MW 409.55

3,3'-Bis-(*tert*-butyldimethylsilyloxymethyl)prop-2-enyl bromide (**116**).[20]

To a solution of **115** (0.18 g, 0.52 mmol) and triphenylphosphine (0.15 g, 0.57 mmol) in anhydrous dichloromethane, *N*-bromosuccinimide (0.18 g, 1.03 mmol) was added slowly at 0 °C under a nitrogen atmosphere. The reaction mixture was allowed to attain room temperature and stirred at room temperature for 4 hours, then diluted with dichloromethane. The organic layer was washed with water (10 mL) and brine (10 mL), dried over anhydrous $MgSO_4$, filtered and concentrated under reduced pressure. The residue was purified by column chromatography on silica gel eluting with hexane/ethyl acetate (98:2 v/v) to give compound **116** (0.03 g, 14% yield) as a colourless oil.

^{1}H NMR (500 MHz, $CDCl_3$) δ 5.78 (t, $J_{2,1}$ = 8.6 Hz, 1H, H-2), 4.20 (s, 2H, 3-CH_2), 4.14 (s, 2H, 3-CH_2), 4.04 (d, $J_{1,2}$ = 8.6 Hz, 2H, H-1), 0.85 (s, 9H, *t*BuSi), 0.83 (s, 9H, *t*BuSi), 0.01 (s, 6H, 2 CH_3Si), 0.00 (s, 6H, 2 CH_3Si).

^{13}C NMR (126 MHz, $CDCl_3$) δ 142.64 (C, C3), 119.84 (CH, C2), 63.08 (CH_2, 3-CH$_2$), 57.71 (CH_2, 3-CH$_2$), 26.42 (CH_2, C1), 24.90 (CH_3, 3 CH$_3$-*t*BuSi), 24.85 (CH_3, 3 CH$_3$-*t*BuSi), 17.36 (C, *C*-*t*BuSi), 17.22 (C, *C*-*t*BuSi), -6.38 (CH_3, 2 CH$_3$Si), -6.43 (CH_3, 2 CH$_3$Si).

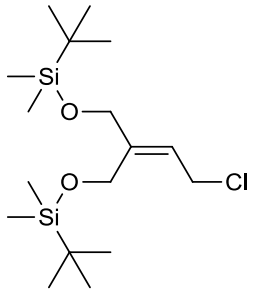

$C_{17}H_{37}ClO_2Si_2$, MW 365.10

3,3'-Bis-(*tert*-butyldimethylsilyloxymethyl)prop-2-enyl chloride (**117**).

To a solution of **115** (0.25 g, 0.72 mmol) in anhydrous dichloromethane at room temperature under a nitrogen atmosphere were added 4-(dimethylamino)pyridine (0.053 g, 0.43 mmol), *p*-toluenesulfonyl chloride (0.16 g, 0.86 mmol) and triethylamine (0.12 mL, 0.86 mmol) in sequence. The reaction mixture was stirred at room temperature for 4 hour, then quenched with a diluted aqueous solution of $NaHCO_3$ and extracted with dichloromethane (3 x 20 mL). The combined organic layer was washed with brine (50 mL), dried over anhydrous $MgSO_4$, filtered and concentrated under reduced pressure. The crude residue was purified by column chromatography on silica gel eluting with hexane/ethyl acetate (98:2 v/v) to give compound **117** (0.11 g, 40% yield) as a colourless oil.

^{1}H NMR (500 MHz, $CDCl_3$) δ 5.69 (t, $J_{2,1}$ = 8.1 Hz, 1H, H-2), 4.17 (s, 2H, 3-CH_2), 4.14 – 4.11 (m, 4H, H-1 and 3-CH_2), 0.84 (s, 9H, *t*BuSi), 0.82 (s, 9H, *t*BuSi), 0.00 (s, 6H, 2 CH_3Si), -0.00 (s, 6H, 2 CH_3Si).

^{13}C NMR (126 MHz, $CDCl_3$) δ 143.18 (C, C3), 120.95 (CH, C2), 64.13 (CH_2, 3-CH_2), 58.93 (CH_2, 3-CH_2), 39.67 (CH_2, C1), 25.93 (CH_3, 3 CH_3-*t*BuSi), 25.84 (CH_3, 3 CH_3-*t*BuSi), 18.39 (C, *C*-*t*BuSi), 18.24 (C, *C*-*t*BuSi), -5.36 (CH_3, 2 CH_3Si), -5.42 (CH_3, 2 CH_3Si).

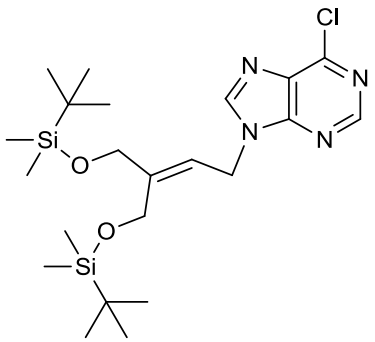

$C_{22}H_{39}ClN_4O_2Si_2$, MW 483.19

1-[3,3'-Bis-(*tert*-butyldimethylsilyloxymethyl)-prop-2-enyl]6-chloropurine (**119**).[20]

Procedure *a*:

To a suspension of 6-chloropurine **118** (0.15 g, 0.99 mmol) and caesium carbonate (0.18 g, 0.56 mmol) in anhydrous dimethylformamide was added a solution of compound **117** (0.16 g, 0.43 mmol) in anhydrous dimethylformamide at room temperature under a nitrogen atmosphere. The reaction mixture was stirred overnight, then was added of water (10 mL) and diluted with ethyl acetate (10 mL). The organic phase was separated and washed several times with brine (10 mL), dried over $MgSO_4$, filtered and concentrated under reduced pressure. The crude residue was purified by column chromatography on silica gel eluting with hexane/ethyl acetate (80:20 v/v) to give compound **119** (0.13 g, 63% yield) as a colourless oil.

Procedure *b*:

A solution of compound **117** (3.20 g, 9.24 mmol) in anhydrous diethyl ether was cooled to -78 °C under a nitrogen atmosphere, before adding triethylamine (3.86 mL, 27.73 mmol) and methanesulfonyl chloride (1.43 mL, 18.48 mmol) dropwise. The reaction mixture was stirred for 3 hours at a temperature from -78 °C to 0 °C, then filtered under vacuo and washed with diethyl ether. The filtrate was evaporated and the residue was dissolved in dichloromethane and washed with water and brine, dried over anhydrous $MgSO_4$, filtered and concentrated under reduced pressure. The crude residue was dissolved in anhydrous dimethylformamide and added to a stirred suspension of 6-chloropurine **118** (3.29 g, 21.26 mmol) and caesium carbonate (3.92 g, 12.02 mmol) in anhydrous dimethylformamide at room temperature under a nitrogen atmosphere. The reaction mixture was stirred overnight, then was added of water (100 mL) and diluted with ethyl acetate (100 mL). The organic phase was separated and washed several times with brine (100 mL), dried over $MgSO_4$, filtered and concentrated under reduced pressure. The

crude residue was purified by flash column chromatography on silica gel (hexane to hexane/acetone 80:20 v/v) to give compound **119** (1.41 g, 32% yield) as a colourless oil.

^{1}H NMR (500 MHz, $CDCl_3$) δ 8.70 (s, 1H, H-2_{base}), 8.14 (s, 1H, H-8_{base}), 5.76 (t, $J_{2,1}$ = 7.4 Hz, 1H, H-2), 5.03 (d, $J_{1,2}$ = 7.5 Hz, 2H, H-1), 4.33 (s, 2H, 3-CH_2), 4.15 (s, 2H, 3-CH_2), 0.86 (s, 9H, *t*BuSi), 0.83 (s, 9H, *t*BuSi), 0.06 (s, 6H, 2 CH_3Si), -0.00 (s, 6H, 2 CH_3Si).

^{13}C NMR (126 MHz, $CDCl_3$) δ 151.80 (CH, $C2_{base}$), 151.67 (C, Carom), 150.79 (C, Carom), 145.03 (CH, $C8_{base}$), 144.84 (C, C3), 131.54 (C, Carom), 117.71 (CH, C2), 64.26 (CH_2, 3-*C*H_2), 59.54 (CH_2, 3-*C*H_2), 40.93 (CH_2, C1), 25.81 (CH_3, 6 *C*H_3-*t*BuSi), 18.29 (C, *C*-*t*BuSi), 18.23 (C, *C*-*t*BuSi), -5.44 (CH_3, 4 *C*H_3Si).

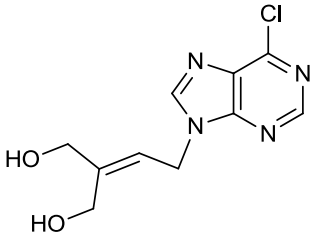

$C_{10}H_{11}ClN_4O_2$, MW 254.67

1-[3,3'-Bis-(hydroxymethyl)-prop-2-enyl]6-chloropurine (**120**).[20]

To a solution of **119** (0.24 g, 0.49 mmol) in tetrahydrofuran, tetrabutylammonium fluoride trihydrate (0.37 g, 1.18 mmol) was slowly added at -10 °C. The reaction mixture was stirred at -10 °C to 0 °C for 2 hours, then concentrated to dryness under reduced pressure. The crude residue was purified by column chromatography on silica gel eluting with dichloromethane/methanol (92:8 v/v) to give compound **120** (0.12 g, 94% yield) as a white powder.

^{1}H NMR (500 MHz, DMSO-d_6) δ 8.80 (s, 1H, H-2_{base}), 8.70 (s, 1H, H-8_{base}), 5.69 (t, $J_{2,1}$ = 7.3 Hz, 1H, H-2), 5.06 ($d_{1,2}$, *J* = 7.3 Hz, 2H, H-1), 4.87 (t, *J* = 5.5 Hz, 1H, 3-CH_2O*H*), 4.81 (t, *J* = 5.6 Hz, 1H, 3-CH_2O*H*), 4.18 (d, *J* = 5.4 Hz, 2H, 3-CH_2), 3.98 (d, *J* = 4.7 Hz, 2H, 3-CH_2).

^{13}C NMR (126 MHz, DMSO-d_6) δ 152.17 (C, Carom), 151.99 (CH, $C2_{base}$), 149.44 (C, Carom), 147.72 (CH, $C8_{base}$), 145.86 (C, C3), 131.31 (C, Carom), 118.35 (CH, C2), 62.76 (CH_2, 3-*C*H_2), 57.58 (CH_2, 3-*C*H_2), 41.34 (CH_2, C1).

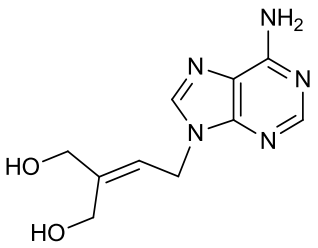

$C_{10}H_{13}N_5O_2$, MW 235.24

1-[3,3'-Bis-(hydroxymethyl)-prop-2-enyl]adenine (**27**).[20]

Procedure *a*:

Compound **120** (0.10 g, 0.38 mmol) was dissolved in a saturated (7M) solution of ammonia in methanol (5 mL). The reaction mixture was stirred in a screw-cap pressure glass tube at 75 °C for 48 hours, then cooled to room temperature and concentrated to dryness. The crude residue was purified by column chromatography on silica gel eluting with dichloromethane/methanol (90:10 v/v) to give compound **27** (0.051 g, 56% yield) as a white powder; mp: 176-177 °C.

Procedure *b*:

Compound **120** (0.60 g, 2.36 mmol) was suspended in a 28-30% aqueous ammonia solution (4 mL) and 1,4-dioxane (4 mL). The reaction mixture was stirred in a screw-cap pressure glass tube at 90 °C for 48 hours, then cooled to room temperature and concentrated to dryness by co-evaporation with ethanol. The crude residue was stirred in ethanol for 20 minutes and filtered under vacuo to give compound **27** (0.50 g, 90% yield) as a white powder.

^{1}H NMR (500 MHz, DMSO-d_6) δ 8.15 (s, 1H, H-2_{base}), 8.13 (s, 1H, H-8_{base}), 7.22 (br s, 2H, 6-NH_2), 5.63 (t, $J_{2,1}$ = 7.3 Hz, 1H, H-2), 4.98 (t, J = 5.6 Hz, 1H, 3-CH_2OH), 4.90 (d, $J_{1,2}$ = 7.3 Hz, 2H, H-1), 4.80 (t, J = 5.6 Hz, 1H, 3-CH_2OH), 4.16 (d, J = 5.5 Hz, 2H, 3-CH_2), 3.97 (d, J = 5.6 Hz, 2H, 3-CH_2).

^{13}C NMR (126 MHz, DMSO-d_6) δ 156.44 (C, Carom), 152.82 (CH, $C2_{base}$), 149.66 (C, Carom), 144.90 (C, C3), 141.01 (CH, $C8_{base}$), 119.45 (CH, C2), 119.22 (C, Carom), 62.82 (CH_2, 3-CH_2), 57.38 (CH_2, 3-CH_2), 40.39 (CH_2, C1).

HPLC (system 2) t_R = 13.61 min.

MS (ES+) *m/z* 258.1 [MNa^+].

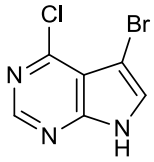

$C_6H_3BrClN_3$, MW 232.47

7-Bromo-6-chloro-7-deazapurine (**122**).[21]

N-bromosuccinimide (1.40 g, 7.81 mmol) was added slowly to a stirred suspension of 6-chloro-7-deazapurine **121** (1.00 g, 6.51 mmol) in anhydrous dichlomethane (20 mL) and the mixture was reacted at room temperature for 3 hours. The yellow suspension was concentrated under reduced pressure, added of water (50 mL) and filtered. The residue was washed with additional water and dichloromethane, dried under vacuo to obtain compound **122** as an off-white solid (1.09 g, 72% yield). The product was used in the next step without further purification.

^{1}H NMR (500 MHz, DMSO-d_6) δ 12.99 (br s, 1H, 9-N*H*), 8.64 (s, 1H, H-2), 7.97 (s, 1H, H-8).

^{13}C NMR (126 MHz, DMSO-d_6) δ 150.93 (C, C4), 150.88 (CH, C2), 150.16 (C, C6), 128.61 (CH, C8), 113.61 (C, C5), 85.76 (C, C7).

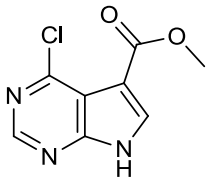

$C_8H_6ClN_3O_2$, MW 211.61

Methyl 6-chloro-7-deazapurine-7-carboxylate (**123**).[21]

To a stirred solution of **122** (1.00 g, 4.30 mmol) in anhydrous tetrahydrofuran cooled to -78 °C was added dropwise a solution of 1.6M *n*-butyllithium in hexane (5.65 mL, 9.03 mmol) under an argon atmosphere. The solution was reacted for 30 minutes at -78°C, before adding methyl chloroformate (0.30 mL, 3.87 mmol) dropwise at the same temperature. Then the reaction mixture was allowed to attain room temperature and stirred for 3 hours. The reaction was quenched by adding saturated aqueous NH_4Cl solution. The organic solvent was distilled off and the aqueous phase was extracted with ethyl acetate (3 x 150 mL). The combined organic layer was washed with water (300 mL), brine (300 mL), dried over anhydrous Na_2SO_4, filtered and evaporated to dryness. The residue was purified by column chromatography on silica gel eluting

with petroleum ether/ethyl acetate (50:50 v/v) to give compound **123** as a white solid (0.56 g, 61% yield); mp: 178-180 °C.

^{1}H NMR (500 MHz, DMSO-d_6) δ 13.28 (br s, 1H, 9-N*H*), 8.69 (s, 1H, H-2), 8.41 (s, 1H, H-8), 3.83 (s, 3H, OCH_3).

^{13}C NMR (126 MHz, DMSO-d_6) δ 162.20 (C, C=O), 153.24 (C, C4), 151.32 (C, C6), 151.23 (CH, C2), 135.52 (CH, C8), 113.67 (C, C5), 105.84 (C, C7), 51.31 (CH_3, OCH$_3$).

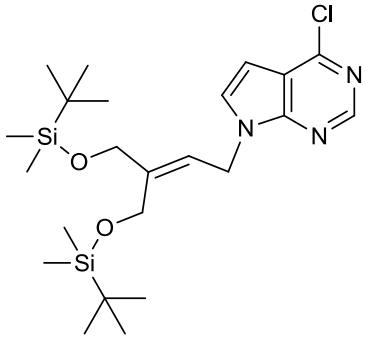

$C_{23}H_{40}ClN_3O_2Si_2$, MW 482.21

1-[3,3'-Bis-(*tert*-butyldimethylsilyloxymethyl)-prop-2-enyl]6-chloro-7-deazapurine (**124**).

Procedure *a*:

Compound **124** was prepared as described for **119** (procedure *a*) from **117** (0.16 g, 0.45 mmol) and 6-chloro-7-deazapurine **121** (0.16 g, 1.03 mmol). The crude residue was purified by flash column chromatography on silica gel (hexane to hexane/ethyl acetate 97:3 v/v) to give compound **124** (0.15 g, 69% yield) as a colourless oil.

Procedure *b*:

Compound **124** was prepared as described for **119** (procedure *b*) from **115** (0.46 g, 1.34 mmol) and 6-chloro-7-deazapurine **121** (0.47 g, 1.34 mmol). The crude residue was purified by flash column chromatography on silica gel (hexane/acetone 95:5 v/v to hexane/acetone 80:20 v/v) to give compound **124** (0.34 g, 52% yield) as a colourless oil.

^{1}H NMR (500 MHz, $CDCl_3$) δ 8.60 (s, 1H, H-2$_{base}$), 7.27 (d, $J_{8,7}$ = 3.6 Hz, 1H, H-8$_{base}$), 6.57 (d, $J_{7,8}$ = 3.6 Hz, 1H, H-7$_{base}$), 5.72 – 5.67 (m, 1H, H-2), 4.98 (d, $J_{1,2}$ = 7.4 Hz, 2H, H-1), 4.32 (s, 2H, 3-CH_2), 4.16 (d, $J_{3\text{-}CH2,H\text{-}2}$ = 0.8 Hz, 2H, 3-CH_2), 0.87 (s, 9H, *t*BuSi), 0.84 (s, 9H, *t*BuSi), 0.06 (s, 6H, 2 CH_3Si), -0.00 (s, 6H, 2 CH_3Si).

^{13}C NMR (126 MHz, $CDCl_3$) δ 152.00 (C, Carom), 150.87 (C, Carom), 150.57 (CH, C2$_{base}$), 143.44 (C, C3), 128.76 (CH, C8$_{base}$), 119.44 (CH, C2), 117.60 (C, Carom), 99.51 (CH, C7$_{base}$), 64.39 (CH_2, 3-CH$_2$),

59.24 (CH_2, 3-*C*H_2), 41.47 (CH_2, C1), 25.84 (CH_3, 6 *C*H_3-*t*BuSi), 18.33 (C, *C*-*t*BuSi), 18.26 (C, *C*-*t*BuSi), -5.41 (CH_3, 4 *C*H_3Si).

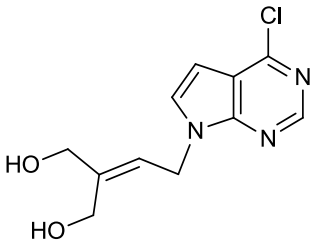

$C_{11}H_{12}ClN_3O_2$, MW 253.68

1-[3,3'-Bis-(hydroxymethyl)-prop-2-enyl]6-chloro-7-deazapurine (**126**).

Procedure *a*:

Compound **126** was prepared as described for **120** from **124** (0.13 g, 0.29 mmol). The crude residue was purified by flash column chromatography on silica gel (dichloromethane to dichloromethane/methanol 98:2 v/v) to give compound **126** (0.05 g, 76% yield) as a white powder.

Procedure *b*:

A 80% aqueous solution of acetic acid (25 mL) was added to a stirred solution of compound **124** (1.48 g, 3.07 mmol) in tetrahydrofuran (5 mL). The reaction mixture was stirred for 24 hour at room temperature, then concentrated to dryness by co-evaporation with ethanol to give compound **126** (0.78 g, 100% yield) as a white powder. The crude residue was used in the following step without purification.

^{1}H NMR (500 MHz, DMSO-d_6) δ 8.65 (s, 1H, H-2_{base}), 7.75 (d, $J_{8,7}$ = 3.6 Hz, 1H, H-8_{base}), 6.66 (d, $J_{7,8}$ = 3.6 Hz, 1H, H-7_{base}), 5.63 (t, $J_{2,1}$ = 7.2 Hz, 1H, H-2), 5.04 (d, $J_{1,2}$ = 7.3 Hz, 2H, H-1), 4.79 (t, *J* = 5.4 Hz, 1H, 3-CH_2O*H*), 4.72 (t, *J* = 5.6 Hz, 1H, 3-CH_2O*H*), 4.18 (d, $J_{CH2,OH}$ = 5.4 Hz, 2H, 3-CH_2), 3.98 (dd, $J_{CH2,OH}$ = 5.5 Hz, $J_{CH2,2}$ = 1.1 Hz, 2H, 3-CH_2).

^{13}C NMR (126 MHz, DMSO-d_6) δ 151.08 (C, Carom), 150.74 (C, Carom), 150.69 (CH, $C2_{base}$), 145.03 (C, C3), 131.52 (CH, $C8_{base}$), 119.46 (CH, C2), 117.27 (C, Carom), 98.97 (CH, $C7_{base}$), 62.89 (CH_2, 3-*C*H_2), 57.59 (CH_2, 3-*C*H_2), 41.99 (CH_2, C1).

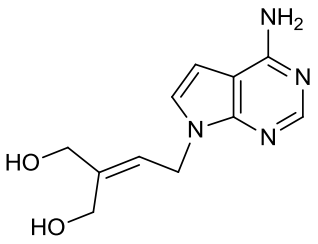

$C_{11}H_{14}N_4O_2$, MW 234.25

1-[3,3'-Bis-(hydroxymethyl)-prop-2-enyl]7-deaza-adenine (**128**).

Compound **126** (0.035 g, 0.14 mmol) was suspended in a 28-30% aqueous ammonia solution (1.5 mL) and 1,4-dioxane (1.5 mL). The reaction mixture was stirred in a screw-cap pressure glass tube at 90 °C for 48 hours, then cooled to room temperature and concentrated to dryness by co-evaporation with ethanol. The crude residue was purified by flash column chromatography on silica gel (dichloromethane to dichloromethane/methanol 90:10 v/v). The isolated product was further purified by flash column chromatography on silica gel (dichloromethane to dichloromethane/methanol 90:10 v/v) to give compound **128** (0.03 g, 85% yield) as a white powder; mp: 167-169 °C.

^{1}H NMR (500 MHz, DMSO-d_6) δ 8.05 (s, 1H, H-2_{base}), 7.14 (d, $J_{8,7}$ = 3.5 Hz, 1H, H-8_{base}), 6.95 (br s, 2H, 6-NH_2), 6.53 (d, $J_{7,8}$ = 3.5 Hz, 1H, H-7_{base}), 5.56 (t, $J_{2,1}$ = 7.3 Hz, 1H, H-2), 4.97 (t, J = 5.6 Hz, 1H, 3-CH_2OH), 4.85 (d, $J_{1,2}$ = 7.3 Hz, 2H, H-1), 4.76 (t, J = 5.6 Hz, 1H, 3-CH_2OH), 4.14 (d, J = 5.5 Hz, 2H, 3-CH_2), 3.97 – 3.95 (m, 2H, 3-CH_2).

^{13}C NMR (126 MHz, DMSO-d_6) δ 157.92 (C, Carom), 151.94 (CH, $C2_{base}$), 149.58 (C, Carom), 143.78 (C, C3), 124.26 (CH, $C8_{base}$), 120.68 (CH, C2), 102.89 (C, Carom), 98.98 (CH, $C7_{base}$), 62.90 (CH_2, 3-CH$_2$), 57.33 (CH_2, 3-CH$_2$), 41.18 (CH_2, C1).

HPLC (system 1) t_R = 10.05 min.

MS (ES+) *m/z* 257.1 [MNa^+], 235.1 [MH^+].

HRMS calculated for $C_{11}H_{15}N_4O_2$: 235.1195; found 235.1186.

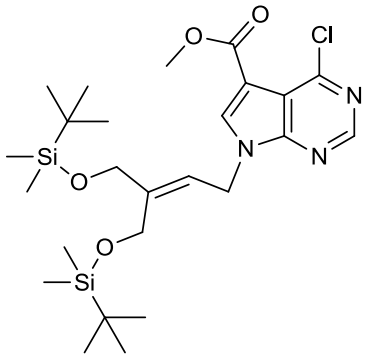

$C_{25}H_{42}ClN_3O_4Si_2$, MW 540.24

Methyl 1-[3,3'-bis-(*tert*-butyldimethylsilyloxymethyl)-prop-2-enyl]6-chloro-7-deazapurine 7-carboxylate (**125**).

Compound **125** was prepared as described for **119** (procedure *a*) from **117** (0.22 g, 0.60 mmol) and **123** (0.29 g, 1.38 mmol). The crude residue was purified by column chromatography on silica gel eluting with hexane/ethyl acetate (90:10 v/v) to give compound **125** (0.25 g, 78% yield) as a white powder.

^{1}H NMR (500 MHz, $CDCl_3$) δ 8.64 (s, 1H, H-2_{base}), 8.00 (s, 1H, H-8_{base}), 5.71 – 5.67 (m, 1H, H-2), 5.01 (d, $J_{1,2}$ = 7.5 Hz, 2H, H-1), 4.30 (s, 2H, 3-CH_2), 4.15 (br s, 2H, 3-CH_2), 3.85 (s, 3H, OCH_3), 0.86 (s, 9H, *t*BuSi), 0.83 (s, 9H, *t*BuSi), 0.05 (s, 6H, 2 CH_3Si), -0.00 (s, 6H, 2 CH_3Si).

^{13}C NMR (126 MHz, $CDCl_3$) δ 162.62 (C, C=O), 153.18 (C, Carom), 152.27 (C, Carom), 151.24 (CH, $C2_{base}$), 144.66 (C, C3), 135.78 (CH, $C8_{base}$), 118.40 (CH, C2), 114.90 (C, Carom), 106.95 (C, Carom), 64.45 (CH_2, 3-CH_2), 59.44 (CH_2, 3-CH_2), 51.49 (CH_3, OCH_3), 41.90 (CH_2, C1), 25.85 (CH_3, 3 CH_3-*t*BuSi), 25.83 (CH_3, 3 CH_3-*t*BuSi), 18.33 (C, *C*-*t*BuSi), 18.27 (C, *C*-*t*BuSi), -5.41 (CH_3, 2 CH_3Si), -5.46 (CH_3, 2 CH_3Si).

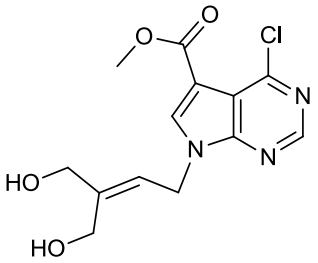

$C_{13}H_{14}ClN_3O_4$, MW 311.72

Methyl 1-[3,3'-bis-(hydroxymethyl)-prop-2-enyl]6-chloro-7-deazapurine 7-carboxylate (**127**).

Compound **127** was prepared as described for **120** from **125** (0.25 g, 0.46 mmol). The crude residue was purified by flash column chromatography on silica gel (dichloromethane to dichloromethane/methanol 97:3 v/v) to give compound **127** (0.14 g, 100% yield) as a yellow powder.

^{1}H NMR (500 MHz, DMSO-d_6) δ 8.78 (s, 1H, H-2_{base}), 8.50 (s, 1H, H-8_{base}), 5.68 (t, $J_{2,1}$ = 7.3 Hz, 1H, H-2), 5.12 (d, $J_{1,2}$ = 7.3 Hz, 2H, H-1), 4.85 (br s, 1H, 3-CH_2O*H*), 4.79 (br s, 1H, 3-CH_2O*H*), 4.21 (s, 2H, 3-CH_2), 4.01 (s, 2H, 3-CH_2), 3.87 (s, 3H, OCH_3).

^{13}C NMR (126 MHz, DMSO-d_6) δ 162.40 (C, C=O), 152.26 (C, Carom), 152.01 (C, Carom), 151.59 (CH, $C2_{base}$), 145.92 (C, C3), 138.12 (CH, $C8_{base}$), 118.61 (CH, C2), 114.51 (C, Carom), 105.74 (C, Carom), 62.89 (CH_2, 3-*C*H_2), 57.61 (CH_2, 3-*C*H_2), 51.86 (CH_3, O*C*H_3), 42.48 (CH_2, C1).

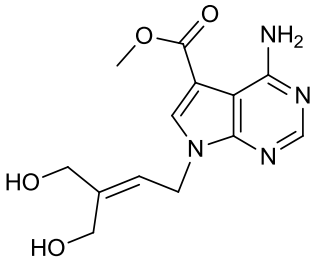

$C_{13}H_{16}N_4O_4$, MW 292.29

Methyl 1-[3,3'-bis-(hydroxymethyl)-prop-2-enyl]7-carboxylate-7-deaza-adenine (**129**).

Compound **127** (0.14 g, 0.46 mmol) was dissolved in a saturated (7M) solution of ammonia in methanol (5 mL). The reaction mixture was stirred in a screw-cap pressure glass tube at 75 °C for 72 hours, then cooled to room temperature and concentrated to dryness. The crude residue was purified by flash column chromatography on silica gel (dichloromethane to dichloromethane/methanol 90:10 v/v). The isolated product was further purified by column

chromatography on silica gel eluting with dichloromethane/methanol (95:5 v/v) to give compound **129** (0.04 g, 34% yield) as an off-white powder; mp: 182-184 °C.

^{1}H NMR (500 MHz, DMSO-d_6 δ 8.17 (s, 1H, H-2$_{base}$), 8.03 (s, 1H, H-8$_{base}$), 7.83 (br s, 1H, NH$_2$-*H*), 7.43 (br s, 1H, NH$_2$-*H*), 5.60 (t, $J_{2,1}$ = 7.4 Hz, 1H, H-2), 4.92 (m, 3H, H-1 and 3-CH$_2$O*H*), 4.80 (t, *J* = 5.6 Hz, 1H, 3-CH$_2$O*H*), 4.14 (d, *J* = 5.3 Hz, 2H, 3-CH_2), 3.97 (d, *J* = 5.6 Hz, 2H, 3-CH_2), 3.83 (s, 3H, OCH_3).

^{13}C NMR (126 MHz, DMSO-d_6) δ 165.79 (C, C=O), 158.12 (C, Carom), 153.64 (CH, C2$_{base}$), 151.08 (C, Carom), 145.07 (C, C3), 132.44 (CH, C8$_{base}$), 119.40 (CH, C2), 105.37 (C, Carom), 100.87 (C, Carom), 62.83 (CH$_2$, 3-*C*H$_2$), 57.39 (CH$_2$, 3-*C*H$_2$), 52.20 (CH$_3$, O*C*H$_3$), 41.72 (CH$_2$, C1).

MS (ES+) *m/z* 315.1 [MNa$^+$].

HRMS calculated for $C_{13}H_{17}N_4O_4$: 293.1250; found 293.1241.

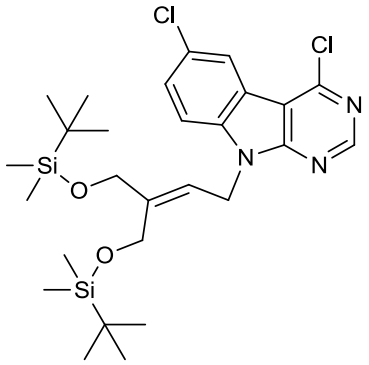

$C_{27}H_{41}Cl_2N_3O_2Si_2$, MW 566.71

1-[3,3'-Bis-(*tert*-butyldimethylsilyloxymethyl)-prop-2-enyl]4,6-dichloro-9*H*-pyrimido[4,5-*b*]indole (**130**).

Compound **130** was prepared as described for **119** (procedure *a*) from **117** (0.23 g, 0.63 mmol) and **97** (0.35 g, 1.46 mmol). The crude residue was purified by column chromatography on silica gel eluting with hexane/ethyl acetate (95:5 v/v) to give compound **130** (0.24 g, 65% yield) as an orange oil.

^{1}H NMR (500 MHz, $CDCl_3$) δ 8.63 (s, 1H, H-2$_{base}$), 8.20 (s, 1H, H-5$_{base}$), 7.42 – 7.36 (m, 2H, H-7$_{base}$ and H-8$_{base}$), 5.47 (t, $J_{2,1}$ = 6.2 Hz, 1H, H-2), 5.10 (d, $J_{1,2}$ = 6.5 Hz, 2H, H-1), 4.30 (s, 2H, 3-CH_2), 3.99 (s, 2H, 3-CH_2), 0.80 (s, 9H, *t*BuSi), 0.66 (s, 9H, *t*BuSi), -0.00 (s, 6H, 2 CH_3Si), -0.18 (s, 6H, 2 CH_3Si).

^{13}C NMR (126 MHz, $CDCl_3$) δ 155.71 (C, Carom), 154.24 (CH, C2$_{base}$), 152.85 (C, Carom), 142.66 (C, C3), 137.54 (C, Carom), 128.35 (CH, C$_{base}$), 127.80 (C, Carom), 122.84 (CH, C5), 119.70 (C, Carom), 119.41 (CH, C2), 111.74 (CH, C$_{base}$), 111.29 (C, Carom), 64.45 (CH$_2$, 3-*C*H$_2$), 59.48 (CH$_2$, 3-*C*H$_2$), 39.50

(CH_2, C1), 25.89 (CH_3, 3 *C*H_3-*t*BuSi), 25.79 (CH_3, 3 *C*H_3-*t*BuSi), 18.32 (C, *C*-*t*BuSi), 18.28 (C, *C*-*t*BuSi), -5.39 (CH_3, 2 *C*H_3Si), -5.44 (CH_3, 2 *C*H_3Si).

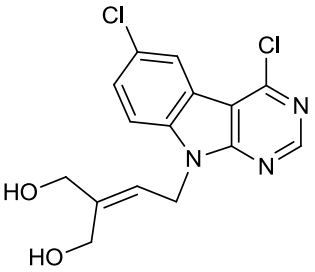

$C_{15}H_{13}Cl_2N_3O_2$, MW 338.19

1-[3,3'-Bis-(hydroxymethyl)-prop-2-enyl]4,6-dichloro-9*H*-pyrimido[4,5-*b*]indole (**131**).

Compound **131** was prepared as described for **120** from **130** (0.23 g, 0.40 mmol). The crude residue was purified by column chromatography on silica gel (from dichloromethane/methanol 98:2 v/v to dichloromethane/methanol 95:5 v/v) to give compound **131** (0.10 g, 71% yield) as an orange oil.

^{1}H NMR (500 MHz, DMSO-d_6) δ 8.89 (s, 1H, H-2$_{base}$), 8.27 (d, $J_{5,7}$ = 2.0 Hz, 1H, H-5$_{base}$), 7.86 (d, $J_{8,7}$ = 8.8 Hz, 1H, H-8$_{base}$), 7.73 (dd, $J_{7,8}$ = 8.8 Hz, $J_{7,5}$ = 2.1 Hz, 1H, H-7$_{base}$), 5.53 (t, $J_{2,1}$ = 6.8 Hz, 1H, H-2), 5.28 (d, $J_{1,2}$ = 6.9 Hz, 2H, H-1), 4.88 (t, *J* = 5.3 Hz, 1H, 3-CH_2O*H*), 4.67 (t, *J* = 5.5 Hz, 1H, 3-CH_2O*H*), 4.28 (d, *J* = 5.3 Hz, 2H, 3-C*H*$_2$), 3.95 (dd, $J_{CH2,OH}$ = 5.4 Hz, $J_{CH2,2}$ = 1.2 Hz, 2H, 3-C*H*$_2$).

^{13}C NMR (126 MHz, DMSO-d_6) δ 155.63 (C, Carom), 154.97 (CH, C2$_{base}$), 152.36 (C, Carom), 144.87 (C, C3), 137.85 (C, Carom), 128.87 (CH, C7$_{base}$), 127.02 (C, Carom), 122.05 (CH, C5$_{base}$), 119.20 (C, Carom), 118.60 (CH, C2), 113.48 (CH, C8$_{base}$), 110.77 (C, Carom), 62.83 (CH_2, 3-*C*H_2), 57.91 (CH_2, 3-*C*H_2), 39.75 (CH_2, C1).

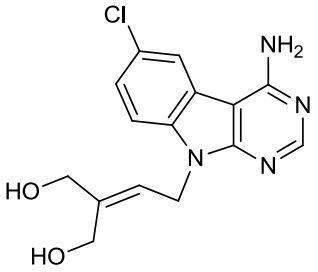

$C_{15}H_{15}ClN_4O_2$, MW 318.76

1-[3,3'-Bis-(hydroxymethyl)-prop-2-enyl]4-amino-6-chloro-9*H*-pyrimido[4,5-*b*]indole (**132**).

Compound **131** (0.10 g, 0.28 mmol) was dissolved in a saturated (7M) solution of ammonia in methanol (5 mL). The reaction mixture was stirred in a screw-cap pressure glass tube at 75 °C for 48 hours, then cooled to room temperature and concentrated to dryness. The crude residue was purified by flash column chromatography on silica gel (dichloromethane to dichloromethane/ methanol 92:8 v/v). The isolated product was further purified by flash column chromatography on silica gel (dichloromethane to dichloromethane/methanol 95:5 v/v) to give compound **132** (0.02 g, 26% yield) as an off-white powder; mp: > 230 °C.

^{1}H NMR (500 MHz, DMSO-d_6) δ 8.51 (d, $J_{5,7}$ = 2.0 Hz, 1H, H-5$_{base}$), 8.33 (s, 1H, H-2$_{base}$), 7.63 (d, $J_{8,7}$ = 8.7 Hz, 1H, H-8$_{base}$), 7.44 (dd, $J_{7,8}$ = 8.7 Hz, $J_{7,5}$ = 2.0 Hz, 1H, H-7$_{base}$), 7.38 (br s, 2H, 4-NH_2), 5.46 (t, $J_{2,1}$ = 6.8 Hz, 1H, H-2), 5.13 (d, $J_{1,2}$ = 6.8 Hz, 2H, H-1), 4.97 (t, *J* = 5.4 Hz, 1H, 3-CH$_2$O*H*), 4.72 (t, *J* = 5.6 Hz, 1H, 3-CH$_2$O*H*), 4.25 (d, *J* = 5.4 Hz, 2H, 3-CH_2), 3.93 (d, *J* = 5.6 Hz, 2H, 3-CH_2).

^{13}C NMR (126 MHz, DMSO-d_6) δ 158.11 (C, Carom), 155.86 (CH, C2$_{base}$), 155.57 (C, Carom), 143.89 (C, C3), 135.64 (C, Carom), 125.74 (C, Carom), 124.79 (CH, C7$_{base}$), 121.37 (C, Carom), 121.18 (CH, C5$_{base}$), 119.57 (CH, C2), 111.68 (CH, C8$_{base}$), 94.83 (C, Carom), 62.78 (CH$_2$, 3-*C*H$_2$), 57.68 (CH$_2$, 3-*C*H$_2$), 38.87 (CH$_2$, C1).

MS (ES+) *m/z* 341.1 [MNa$^+$], 319.1 [MH$^+$].

HRMS calculated for $C_{15}H_{16}ClN_4O_2$: 319.0962; found 319.0964.

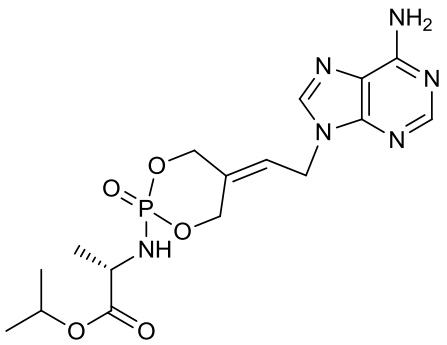

$C_{16}H_{23}N_6O_5P$, MW 410.36

1-[3,3'-Bis-(hydroxymethyl)-prop-2-enyl]adenine 3,3'-hydroxymethyl-(isopropoxy-L-alaninyl) phosphate (**133**).

Compound **27** (0.15 g, 0.64 mmol) was suspended in anhydrous dimethylformamide under a nitrogen atmosphere and *tert*-butylmagnesium chloride 1M in tetrahydrofuran (0.64 mL, 0.64 mmol) was added dropwise at room temperature. After stirring 10 minutes, a solution of compound **38** (0.26 g, 0.64 mmol) in anhydrous dimethylformamide was added slowly. The reaction mixture was stirred for 4 hours at room temperature, then quenched by adding water (1 mL) slowly. The mixture was concentrated under reduced pressure by coevaporation with toluene. The crude residue was purified by flash column chromatography on silica gel (dichloromethane to dichloromethane/methanol 90:10 v/v) to isolate the titled compound. Compound **133** was further purified by flash column chromatography on silica gel (dichloromethane to dichloromethane/methanol 92:8 v/v) and obtained as a white powder (0.10 g, 39% yield).

^{31}P NMR (202 MHz, $CDCl_3$) δ 5.04, 4.97.

^{1}H NMR (500 MHz, $CDCl_3$) δ 8.30 (s, 1H, H-2_{base}), 7.75, 7.75 (2 s, 1H, H-8_{base}), 5.70 – 5.67 (m, 1H, H-2), 5.52 (s, 2H, 6-NH_2), 5.11 – 5.02 (m, 2H, 3-CH_2OP), 5.01 – 4.95 (m, 1H, *H*-*i*Pr), 4.86 – 4.67 (m, 3H, 3-C*H*OP and H-1), 4.57 – 4.46 (m, 1H, 3-C*H*OP), 3.95 – 3.88 (m, 1H, C*H*CH_3), 3.59 – 3.50 (m, 1H, N*H*), 1.35, 1.33 (2 d, *J* = 1.9 Hz, 3H, CHCH_3), 1.21 – 1.17 (m, 6H, 2 CH_3-*i*Pr).

^{13}C NMR (126 MHz, $CDCl_3$) δ 153.37, 153.36 (CH, $C2_{base}$), 139.76 (CH, $C8_{base}$), 122.44, 122.34 (CH, C2), 70.16, 70.10, 70.05, 70.00 (3-*C*H_2OP), 69.37, 69.34 (CH, *C*H-*i*Pr), 64.79, 64.73 (3-*C*H_2OP), 50.29, 50.27, 50.23, 50.21 (CH, *C*HCH_3), 40.20, 40.15 (CH_2, C1), 21.72, 21.66 (CH_3, 2 *C*H_3-*i*Pr), 21.19, 21.17, 21.15 (CH_3, CH*C*H_3).

HPLC (system 1) t_R = 16.03, 16.57 min.

HPLC (system 2) t_R = 23.41, 23.82 min.

MS (ES+) *m/z* 433.1 [MNa^+], 411.1 [MH^+].

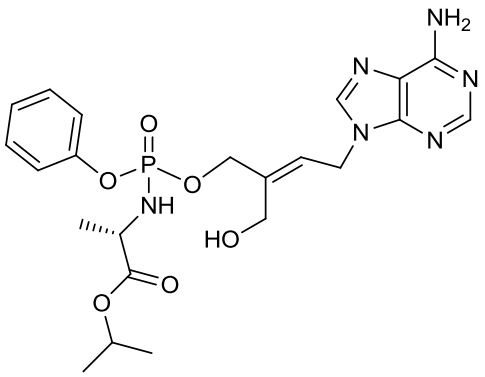

$C_{22}H_{29}N_6O_6P$, MW 504.48

1-[3,3'-Bis-(hydroxymethyl)-prop-2-enyl]adenine (*E*)-3-hydroxymethyl-[phenyl-(isopropoxy-L-alaninyl)] phosphate (**137**).

Conpound **27** (0.10 g, 0.42 mmol) was suspended in a mixture of anhydrous tetrahydrofuran/pyridine (1:4 v/v, 2 mL) in a 10 mL sealed microwave tube under a nitrogen atmosphere and 1-methylimidazole (0.21 mL, 2.68 mmol) was added dropwise at room temperature. After stirring 30 minutes, a solution of **36** (0.26 g, 0.85 mmol) in anhydrous tetrahydrofuran (1 mL) was added slowly and the reaction mixture was stirred for 5 minutes under MWI (100 W, 50 °C), then cooled to room temperature, diluted with dichloromethane/methanol and concentrated to dryness by co-evaporation with toluene. The crude residue was purified by flash column chromatography on silica gel (dichloromethane to dichloromethane/methanol 90:10 v/v) to isolate the titled compound. Compound **137** was further purified by flash column chromatography on silica gel (dichloromethane to dichloromethane/methanol 94:6 v/v) and obtained as a colourless wax (0.008 g, 3% yield).

^{31}P NMR (202 MHz, $CDCl_3$) δ 2.91, 2.79.

^{1}H NMR (500 MHz, $CDCl_3$) δ 8.21 (s, 1H, H-2_{base}), 7.74 (s, 1H, H-8_{base}), 7.23 – 7.17 (m, 2H, Harom), 7.11 – 7.03 (m, 3H, Harom), 5.93 (s, 2H, 6-NH_2), 5.64 – 5.57 (m, 1H, H-2), 4.95 – 4.83 (m, 3H, *H*-*i*Pr and H-1), 4.62 – 4.54 (m, 2H, 3-CH_2OP), 4.33 – 4.23 (m, 2H, 3-CH_2O*H*), 4.04 – 3.82 (m, 2H, C*H*CH_3 and N*H*), 1.28 – 1.23 (m, 3H, CHCH_3), 1.15 – 1.11 (m, 6H, 2 CH_3-*i*Pr).

^{13}C NMR (126 MHz, $CDCl_3$) δ 173.05, 173.00 (2 C, C=O), 155.67 (C, Carom), 152.62 (CH, $C2_{base}$), 150.70, 150.66, 150.65, 150.61, 149.37, 140.98, 140.94 (C, Carom and C3), 140.48 (CH, $C8_{base}$), 129.64, 129.62, 124.95 (CH, Carom), 122.80, 122.68 (CH, C2), 120.25, 120.21, 120.19, 120.16 (CH, Carom), 119.92 (C, Carom), 69.28 (CH, *C*H-*i*Pr), 68.31, 68.27, 68.23 (CH_2, 3-*C*H_2OP), 57.31, 57.28

(CH_2, 3-*C*H_2OH), 50.40, 50.35 (CH, *C*HCH$_3$), 40.93 (CH_2, C1), 21.67, 21.61 (CH_3, 2 *C*H$_3$-*i*Pr), 21.02, 20.98, 20.94 (CH_3, CH*C*H$_3$).

HPLC (system 1) t_R = 21.88, 22.32 min.

HPLC (system 2) t_R = 27.39, 27.63 min.

MS (ES+) *m/z* 527.2 [MNa$^+$], 505.2 [MH$^+$].

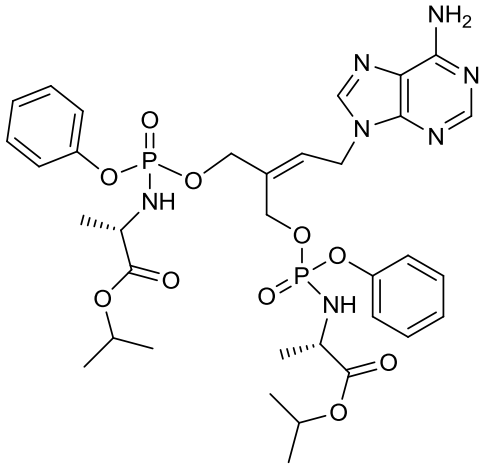

$C_{34}H_{45}N_7O_{10}P_2$, MW 773.71

1-[3,3'-Bis-(hydroxymethyl)-prop-2-enyl]adenine 3,3'-hydroxymethyl-*bis*-[phenyl-(isopropoxy-L-alaninyl)] phosphate (**140**).

Compound **140** was isolated as a side-product of the synthesis of compound **137**. After the first chromatographical purification, compound **140** was further purified by flash column chromatography on silica gel (dichloromethane to dichloromethane/methanol 95:5 v/v) and obtained as a colourless wax (0.02 g, 6% yield).

^{31}P NMR (202 MHz, $CDCl_3$) δ 3.79, 3.61, 3.27, 3.23, 2.93, 2.69, 2.55, 2.45.

^{1}H NMR (500 MHz, $CDCl_3$) δ 8.25, 8.24, 8.15, 8.12 (4 s, 1H, H-2$_{base}$), 7.77, 7.76 (2 s, 1H, H-8$_{base}$), 7.25 – 7.00 (m, 10H, Harom), 5.90 (s, 2H, 6-N*H*$_2$), 5.84 – 5.77 (m, 1H, H-2), 5.10 – 4.83 (m, 4H, 2 *H*-*i*Pr and H-1), 4.83 – 4.50, 4.35 – 4.30 (2 m, 5H, 2 3-C*H*$_2$OP and N*H*), 4.17 – 4.12, 4.04 – 3.84 (2 m, 3H, 2 C*H*CH$_3$ and N*H*), 1.32 – 1.20 (m, 6H, 2 CHC*H*$_3$), 1.16 – 1.10 (m, 12H, 4 C*H*$_3$-*i*Pr).

^{13}C NMR (126 MHz, $CDCl_3$) δ 173.71, 173.65, 173.52, 173.47, 173.37, 173.30, 173.12, 173.09, 173.05, 173.03, 173.02, 173.00, 172.98, 172.96, 172.92 (C, 4 C=O), 155.46, 155.42 (C, Carom), 152.89, 152.82, 152.76 (CH, C2$_{base}$), 150.70, 150.69, 150.65, 149.81, 149.77, 149.75 (C, Carom and C3), 140.51, 140.47, 140.41 (CH, C8$_{base}$), 134.70, 134.65, 134.59, 134.50, 134.45, 134.40 (C, Carom), 129.72, 129.67, 129.66, 129.63, 129.59, 127.78, 127.68, 125.01, 124.99, 124.91, 120.36,

120.32, 120.31, 120.28, 120.24, 120.23, 120.21, 120.19, 120.18, 120.17, 120.16, 120.14 (CH, Carom and C2), 119.48, 119.46, 119.43 (C, Carom), 69.27, 69.22, 69.20, 69.17, 69.16 (CH, 2 *C*H-*i*Pr), 67.38, 67.34, 67.32, 67.30 (CH_2, 3-*C*H_2OP), 61.19, 61.15, 61.12, 61.02, 60.98, 60.95, 60.91 (CH_2, 3-*C*H_2OP), 50.53, 50.51, 50.49, 50.45, 50.44, 50.40, 50.35, 50.34 (CH, 2 *C*HCH_3), 40.66, 40.63, 40.56, 40.52 (CH_2, C1), 21.69, 21.67, 21.63, 21.60 (CH_3, 4 *C*H_3-*i*Pr), 20.99, 20.98, 20.95, 20.91, 20.84, 20.81, 20.77 (CH_3, 2 CH*C*H_3).

HPLC (system 1) t_R = 27.70 min.

HPLC (system 2) t_R = 30.84 min.

MS (ES+) *m/z* 774.3 [MH^+], 796.3 [MNa^+].

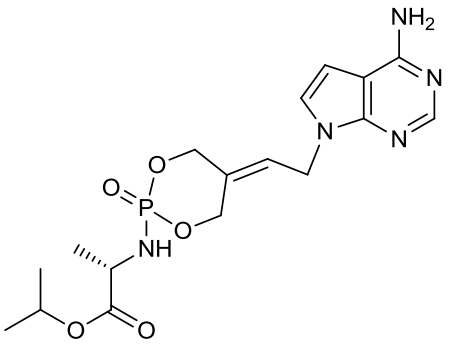

$C_{17}H_{24}N_5O_5P$, MW 409.38

1-[3,3'-Bis-(hydroxymethyl)-prop-2-enyl]7-deaza-adenine 3,3'-hydroxymethyl-(isopropoxy-L-alaninyl) phosphate (**134**).

Compound **128** (0.05 g, 0.22 mmol) was suspended in anhydrous dimethylformamide (1 mL) under a nitrogen atmosphere and *tert*-butylmagnesium chloride 1M in tetrahydrofuran (0.22 mL, 0.22 mmol) was added dropwise at room temperature. After stirring 10 minutes, a solution of compound **38** (0.09 g, 0.22 mmol) in anhydrous dimethylformamide (1 mL) was added slowly. The reaction mixture was stirred for 4 hours at room temperature, then quenched by adding water (0.5 mL) slowly. The mixture was concentrated under reduced pressure by coevaporation with toluene. The crude residue was purified by flash column chromatography on silica gel (dichloromethane to dichloromethane/methanol 90:10 v/v) to isolate the titled compound. Compound **134** was further purified by flash column chromatography on silica gel (dichloromethane to dichloromethane/methanol 92:8 v/v) and obtained as a white powder (0.02 g, 26% yield).

^{31}P NMR (202 MHz, $CDCl_3$) δ 5.04, 5.00.

^{1}H NMR (500 MHz, $CDCl_3$) δ 8.35 (s, 1H, H-2_{base}), 7.01 – 6.97 (m, 1H, H-8_{base}), 6.44 – 6.40 (m, 1H, H-7_{base}), 5.78 – 5.75 (m, 1H, H-2), 5.17 (s, 2H, 6-N*H*$_2$), 5.12 – 5.03 (m, 3H, 3-C*H*$_2$OP and *H*-*i*Pr), 4.92 – 4.84 (m, 2H, 3-C*H*$_2$OP), 4.81 – 4.75 (m, 1H, 3-C*H*OP), 4.65 – 4.55 (m, 1H, 3-C*H*OP), 4.04 – 3.95 (m, 1H, CHC*H*$_3$), 3.67 – 3.57 (m, 1H, N*H*), 1.44 – 1.41 (m, 3H, CHC*H*$_3$), 1.31 – 1.26 (m, 6H, 2 C*H*$_3$-*i*Pr).

^{13}C NMR (126 MHz, $CDCl_3$) δ 156.65 (C, Carom), 152.10 (CH, C2_{base}), 150.25, 132.15, 132.14, 132.09, 132.08 (C, Carom), 124.20, 124.15 (CH, C8_{base}), 124.03, 124.01 (CH, C2), 103.14 (C, Carom), 98.40, 98.37 (CH, C7_{base}), 70.39, 70.34, 70.31, 70.26 (3-*C*H$_2$OP), 69.31, 69.28 (CH, *C*H-*i*Pr), 64.98, 64.92, 64.86 (3-*C*H$_2$OP), 50.26, 50.24, 50.21 (CH, *C*HCH$_3$), 41.05, 41.00 (CH$_2$, C1), 21.72, 21.66 (CH$_3$, 2 *C*H$_3$-*i*Pr), 21.18, 21.15 (CH$_3$, CH*C*H$_3$).

HPLC (system 1) t_R = 17.24, 17.73 min.

HPLC (system 2) t_R = 24.34, 24.82 min.

MS (ES+) *m/z* 432.1 [MNa$^+$], 410.1 [MH$^+$].

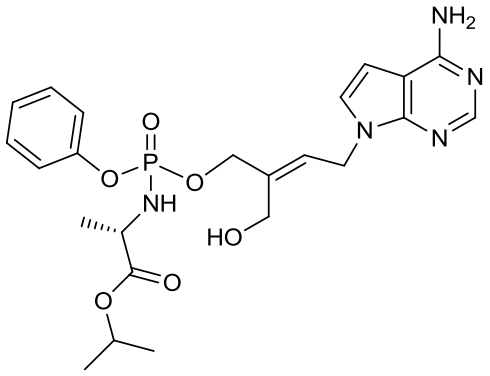

$C_{23}H_{30}N_5O_6P$, MW 551.53

1-[3,3'-Bis-(hydroxymethyl)-prop-2-enyl]7-deaza-adenine (*E*)-3-hydroxymethyl-[phenyl-(isopropoxy-L-alaninyl)] phosphate (**138**).

Compound **128** (0.07 g, 0.31 mmol) was suspended in a mixture of anhydrous tetrahydrofuran/pyridine (1:4 v/v, 2 mL) in a 10 mL sealed microwave tube under a nitrogen atmosphere and 1-methylimidazole (0.16 mL, 1.96 mmol) was added dropwise at room temperature. After stirring 30 minutes, a solution of **36** (0.19 g, 0.62 mmol) in anhydrous tetrahydrofuran (1 mL) was added slowly and the reaction mixture was stirred for 5 minutes under MWI (100 W, 50 °C), then cooled to room temperature, diluted with dichloromethane/methanol and concentrated to dryness by co-evaporation with toluene. The crude residue was purified by

flash column chromatography on silica gel (dichloromethane to dichloromethane/methanol 95:5 v/v) to give compound **138** (0.01 g, 6% yield) as a colourless wax.

^{31}P NMR (202 MHz, $CDCl_3$) δ 2.88, 2.76.

^{1}H NMR (500 MHz, $CDCl_3$) δ 8.14 (s, 1H, H-2_{base}), 7.22 – 7.19 (m, 2H, Harom), 7.10 – 7.04 (m, 3H, Harom), 6.88 (d, $J_{8,7}$ = 3.4 Hz, 1H, H-8_{base}), 6.30 (d, $J_{7,8}$ = 3.4 Hz, 1H, H-7_{base}), 5.63 – 5.56 (m, 1H, H-2), 5.49 (s, 2H, 6-NH_2), 4.94 – 4.86 (m, 1H, *H*-*i*Pr), 4.85 – 4.79 (m, 2H, H-1), 4.60 – 4.51 (m, 2H, 3-CH_2OP), 4.33 – 4.21 (m, 2H, 3-CH_2OH), 3.92 – 3.75 (m, 2H, C*H*CH_3 and N*H*), 1.27 – 1.22 (m, 3H, CHCH_3), 1.14, 1.13 (2 s, 6H, 2 CH_3-*i*Pr).

^{13}C NMR (126 MHz, $CDCl_3$) δ 173.04, 172.98 (2 C, C=O), 156.56 (C, Carom), 150.82 (CH, C2_{base}), 150.69, 150.64, 150.58, 149.17, 139.28, 139.23 (C, Carom and C3), 129.67, 129.64 (CH, Carom), 125.25, 125.24 (CH, C8_{base}), 124.95 (CH, Carom), 124.81, 124.73 (CH, C2), 120.29, 120.25, 120.22, 120.19 (CH, Carom), 98.00 (CH, C7_{base}), 69.30 (CH, *C*H-*i*Pr), 68.74, 68.70, 68.66 (CH_2, 3-*C*H_2OP), 57.20, 57.17 (CH_2, 3-*C*H_2OH), 50.37, 50.32 (CH, *C*HCH_3), 42.32 (CH_2, C1), 21.69, 21.62 (CH_3, 2 *C*H_3-*i*Pr), 21.03, 21.00, 20.96 (CH_3, CH*C*H_3).

HPLC (system 1) t_R = 22.92, 23.27 min.

HPLC (system 2) t_R = 28.09, 28.29 min.

MS (ES+) *m/z* 526.2 [MNa^+], 504.2 [MH^+].

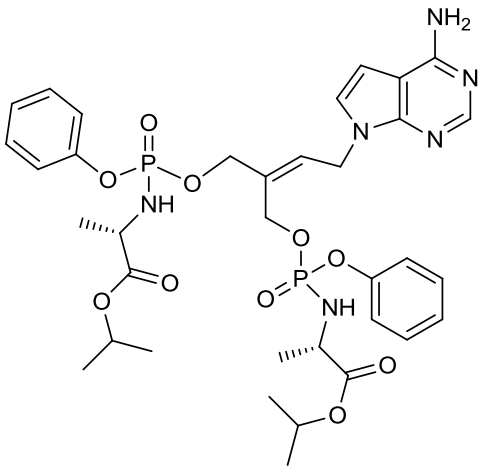

$C_{35}H_{46}N_6O_{10}P_2$, MW 772.72

1-[3,3'-Bis-(hydroxymethyl)-prop-2-enyl]7-deaza-adenine 3,3'-hydroxymethyl-*bis*-[phenyl-(isopropoxy-L-alaninyl)] phosphate (**141**).

Compound **141** was isolated as a side-product of the synthesis of compound **138**. After the first chromatographical purification, compound **141** was further purified by flash column

chromatography on silica gel (dichloromethane to dichloromethane/methanol 96:4 v/v) and obtained as a colourless wax (0.01 g, 4% yield).

^{31}P NMR (202 MHz, $CDCl_3$) δ 3.85, 3.61, 3.18, 3.11, 3.07, 2.76, 2.61, 2.48.

^{1}H NMR (500 MHz, $CDCl_3$) δ 8.16, 8.07, 8.03 (3 s, 1H, H-2_{base}), 7.24 – 7.03 (m, 10H, Harom), 6.85 – 6.83 (m, 1H, H-8_{base}), 6.30 (2 s, 1H, H-7_{base}), 5.83 – 5.75 (m, 1H, H-2), 5.69, 5.65 (2 s, 2H, 6-N*H*$_2$), 5.12 – 4.47, 4.40 – 4.30 (2 m, 9H, H-1, 2 *H*-*i*Pr, 2 3-C*H*$_2$OP and N*H*), 4.23 – 4.17, 4.02 – 3.86 (2 m, 3H, 2 C*H*CH_3 and N*H*), 1.33 – 1.20 (m, 6H, 2 CHC*H*$_3$), 1.16 – 1.09 (m, 12H, 4 C*H*$_3$-*i*Pr).

^{13}C NMR (126 MHz, $CDCl_3$) δ 173.82, 173.76, 173.59, 173.54, 173.48, 173.42, 173.18, 173.13, 173.11, 173.08, 173.06, 173.02, 173.00 (C, 4 C=O), 156.31, 156.22 (C, Carom), 150.74 (CH, C2_{base}), 150.65, 149.62, 149.56, 133.54, 133.48, 133.42, 133.32, 133.28, 133.22 (C, Carom and C3), 129.70, 129.64, 129.60, 124.94, 124.90 (CH, Carom and C2), 124.68, 124.59, 124.56 (CH, C8_{base}), 120.42, 120.38, 120.37, 120.35, 120.33, 120.32, 120.29, 120.25, 120.21, 120.17 (CH, Carom), 103.06, 103.02 (C, Carom), 98.55, 98.52 (CH, C7_{base}), 69.23, 69.19, 69.14, 69.12 (CH, 2 *C*H-*i*Pr), 67.64, 67.60, 67.56 (CH_2, 3-*C*H_2OP), 61.19, 61.15, 61.12, 61.01, 60.97, 60.90, 60.86 (CH_2, 3-*C*H_2OP), 50.55, 50.53, 50.51, 50.45, 50.44, 50.41, 50.34 (CH, 2 *C*HCH_3), 41.59, 41.48, 41.38, 41.35 (CH_2, C1), 21.71, 21.68, 21.64, 21.61 (CH_3, 4 *C*H_3-*i*Pr), 21.01, 20.97, 20.95, 20.91, 20.85, 20.81, 20.77 (CH_3, 2 CH*C*H_3).

HPLC (system 1) t_R = 27.88 min.

HPLC (system 2) t_R = 31.12 min.

MS (ES+) *m/z* 773.3 [MH^+], 795.3 [MNa^+].

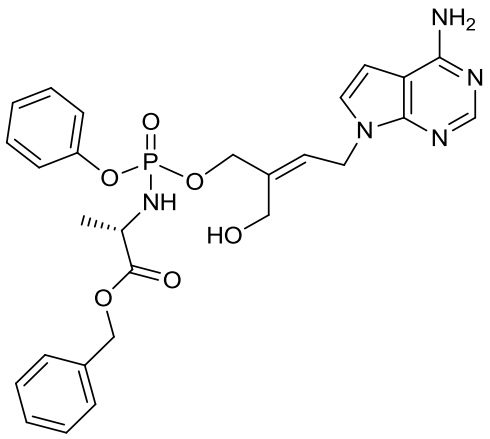

$C_{27}H_{30}N_5O_6P$, MW 551.53

1-[3,3'-Bis-(hydroxymethyl)-prop-2-enyl]7-deaza-adenine (*E*)-3-hydroxymethyl-[phenyl-(benzyloxy-L-alaninyl)] phosphate (**139**).

Compound **128** (0.06 g, 0.26 mmol) was suspended in a mixture of anhydrous tetrahydrofuran/pyridine (1:4 v/v, 2 mL) in a 10 mL sealed microwave tube under a nitrogen atmosphere and 1-methylimidazole (0.13 mL, 1.66 mmol) was added dropwise at room temperature. After stirring 30 minutes, a solution of **35** (0.10 g, 0.39 mmol) in anhydrous tetrahydrofuran (1 mL) was added slowly and the reaction mixture was stirred for 30 minutes under MWI (100 W, 50 °C), then diluted with dichloromethane/methanol and concentrated to dryness by co-evaporation with toluene. The crude residue was purified by flash column chromatography on silica gel (dichloromethane to dichloromethane/methanol 90:10 v/v) to isolate the titled compound. Compound **139** was further purified by flash column chromatography on silica gel (dichloromethane to dichloromethane/methanol 92:8 v/v) and obtained as a colourless wax (0.006 g, 4% yield).

^{31}P NMR (202 MHz, $CDCl_3$) δ 2.70, 2.56.

^{1}H NMR (500 MHz, $CDCl_3$) δ 8.16 (s, 1H, H-2_{base}), 7.29 – 7.16 (m, 7H, Harom), 7.09 – 7.03 (m, 3H, Harom), 6.88, 6.87 (2 d, $J_{8,7}$ = 2.1 Hz, 1H, H-8_{base}), 6.30 – 6.27 (m, 1H, H-7_{base}), 5.61 – 5.54 (m, 1H, H-2), 5.32 (s, 2H, 6-NH_2), 5.07 – 4.99 (m, 2H, CH_2(C_6H_5)), 4.88 – 4.75 (m, 2H, H-1), 4.57 – 4.43 (m, 2H, 3-CH_2OP), 4.31 – 4.21 (m, 2H, 3-CH_2OH), 4.03 – 3.91 (m, 1H, C*H*CH_3), 3.77 – 3.63 (m, 1H, N*H*), 1.29 – 1.24 (m, 3H, CHCH_3).

^{13}C NMR (126 MHz, $CDCl_3$) δ 173.53, 173.33 (2 C, C=O), 156.63, 156.50 (C, Carom), 151.41, 150.94 (CH, $C2_{base}$), 149.93, 149.29, 149.28, 149.24, 139.22, 135.29, 135.27, 131.94, 131.89 (C, Carom and C3), 129.65, 129.61, 128.65, 128.51, 128.30, 128.22 (CH, Carom), 125.25, 124.97 (CH, $C8_{base}$),

124.35, 124.19 (CH, C2), 120.24, 120.15, 115.49, 115.47 (CH, Carom), 98.74, 97.93 (CH, $C7_{base}$), 68.83, 68.79, 68.77 (CH_2, 3-*C*H_2OP), 67.31, 67.25 (CH_2, *C*H_2(C_6H_5)), 57.30, 57.25 (CH_2, 3-*C*H_2OH), 50.28, 50.21 (CH, *C*HCH_3), 41.06, 40.99 (CH_2, C1), 21.04, 20.92 (CH_3, CH*C*H_3).

HPLC (system 1) t_R = 24.44, 24.73 min.

HPLC (system 2) t_R = 29.13, 29.28 min.

MS (ES+) *m/z* 552.2 [MH^+], 574.2 [MNa^+].

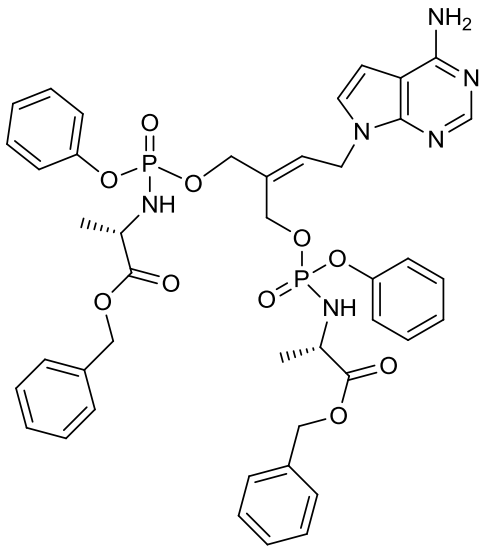

$C_{43}H_{46}N_6O_{10}P_2$, MW 868.81

1-[3,3'-Bis-(hydroxymethyl)-prop-2-enyl]7-deaza-adenine 3,3'-hydroxymethyl-*bis*-[phenyl-(benzyloxy-L-alaninyl)] phosphate (**142**).

Compound **142** was isolated as a side-product of the synthesis of compound **139**. After the first chromatographical purification, compound **142** was further purified by flash column chromatography on silica gel (dichloromethane to dichloromethane/methanol 92:8 v/v) and obtained as a colourless wax (0.01 g, 5% yield).

^{31}P NMR (202 MHz, $CDCl_3$) δ 3.73, 3.54, 2.96, 2.92, 2.88, 2.67, 2.40, 2.27.

^{1}H NMR (500 MHz, $CDCl_3$) δ 8.19, 8.09, 8.03 (3 s, 1H, H-2_{base}), 7.28 – 7.01 (m, 20H, Harom), 6.86 – 6.81 (m, 1H, H-8_{base}), 6.27 – 6.24 (m, 1H, H-7_{base}), 5.78 – 5.69 (m, 1H, H-2), 5.28, 5.26 (2 s, 2H, 6-NH_2), 5.11 – 4.43 (m, 10H, 2 CH_2(C_6H_5), 2 3-CH_2OP and H-1), 4.37 – 4.32, 4.19 – 3.83 (2 m, 4H, 2 C*H*CH_3 and 2 N*H*), 1.34 – 1.21 (m, 6H, 2 CHCH_3).

^{13}C NMR (126 MHz, $CDCl_3$) δ 173.43, 173.41, 173.38, 173.34, 173.32, 173.28 (C, 4 C=O), 156.23 (C, Carom), 150.93, 150.88 (CH, $C2_{base}$), 150.74, 150.69, 150.63, 135.34, 135.32, 135.28, 132.48 (C,

Carom and C3), 129.77, 129.75, 129.70, 129.65, 129.61, 128.82, 128.61, 128.46, 128.21, 128.19, 128.18, 128.16, 128.14 (CH, Carom and C2), 124.95, 124.91, 124.89, 124.63, 124.61 (CH, $C8_{base}$), 120.41, 120.37, 120.34, 120.31, 120.30, 120.29, 120.25, 120.23, 120.21, 120.20, 120.16 (CH, Carom), 103.09, 103.05 (C, Carom), 98.42, 98.39 (CH, $C7_{base}$), 67.68, 67.65 (CH_2, 3-*C*H_2OP), 67.20, 67.18, 67.15 (CH_2, 2 *C*$H_2(C_6H_5)$), 61.20, 61.16, 60.99, 60.95, 60.92, 60.88 (CH_2, 3-*C*H_2OP), 50.53, 50.52, 50.41, 50.39, 50.30 (CH, 2 *C*HCH_3), 41.56, 41.47, 41.36, 41.34 (CH_2, C1), 20.94, 20.90, 20.85, 20.85, 20.74, 20.69 (CH_3, 2 CH*C*H_3).

HPLC (system 1) t_R = 28.93 min.

HPLC (system 2) t_R = 31.60 min.

MS (ES+) *m/z* 869.3 [MH^+], 891.2.2 [MNa^+].

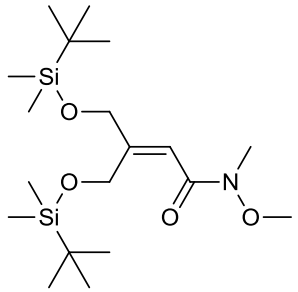

$C_{19}H_{41}NO_4Si_2$, MW 403.70

***N*-Methoxy-*N*-methyl-[3,3'-bis-(*tert*-butyldimethylsilyloxymethyl)]-prop-2-en-1-amide** (**143**).

Diethyl (*N*-methoxy-*N*-methyl-carbamoylmethyl)phosphonate (0.28 ml, 1.38 mmol) was added dropwise to a suspension of sodium hydride 60% dispersion in mineral oil (0.06 g, 1.63 mmol) in anhydrous tetrahydrofuran at 0 °C under a nitrogen atmosphere. The reaction mixture was stirred at room temperature for 30 minutes (a clear solution was formed), before cooling to 0 °C and adding slowly a solution of compound **113** (0.40 g, 1.26 mmol) in anhydrous tetrahydrofuran (2 mL). The reaction mixture was allowed to attain room temperature and stirred for 1 hours, then poured into water (20 mL) and extracted with ethyl acetate (3 x 20 mL), the combined organic layer was washed with water (50 mL) and brine (50 mL), dried over anhydrous $MgSO_4$, filtered and concentrated under reduced pressure. The residue was purified by column chromatography on silica gel eluting with hexane/ethyl acetate (95:5 v/v) to give compound **143** (0.44 g, 87% yield) as a colourless oil.

^{1}H NMR (500 MHz, $CDCl_3$) δ 6.44 (br s, 1H, H-2), 4.82 (s, 2H, 3-CH_2), 4.41 – 4.37 (m, 2H, 3-CH_2), 3.62 (s, 3H, OCH_3), 3.13 (s, 3H, NCH_3), 0.89 (s, 9H, *t*BuSi), 0.83 (s, 9H, *t*BuSi), 0.03 (s, 6H, 2 CH_3Si), -0.00 (s, 6H, 2 CH_3Si).

^{13}C NMR (126 MHz, $CDCl_3$) δ 167.61 (C, C=O), 158.73 (C, C3), 110.03 (CH, C2), 63.11 (CH_2, 3-*C*H_2), 61.65 (CH_2, 3-*C*H_2), 61.27 (CH_3, O*C*H_3), 32.03, 32.02, 31.95, 31.87 (CH_3, N*C*H_3), 25.73 (CH_3, 3 *C*H_3-*t*BuSi), 25.71 (CH_3, 3 *C*H_3-*t*BuSi), 18.16 (C, *C*-*t*BuSi), 18.04 (C, *C*-*t*BuSi), -5.60 (CH_3, 2 *C*H_3Si), -5.67 (CH_3, 2 *C*H_3Si).

MS (ES+) *m/z* 426.24 [MNa^+].

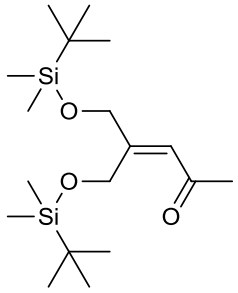

$C_{18}H_{38}O_3Si_2$, MW 358.66

4,4'-Bis-(*tert*-butyldimethylsilyloxymethyl)-but-3-en-2-one (**144**).

To a solution of 1.6M methyl lithium in diethyl ether (4.63 mL, 7.41 mmol) cooled to -78 °C, a solution of compound **143** (0.75 g, 1.85 mmol) in diethyl ether was added dropwise under a nitrogen atmosphere. The reaction mixture was allowed to warm to room temperature over 2 hours, then quenched with a 10% NH_4Cl aqueous solution (10 mL) and extracted with diethyl ether (3 x 20 mL). The combined organic layer was washed with water (50 mL) and brine (50 mL), dried over anhydrous $MgSO_4$, filtered and concentrated to dryness. The crude residue was purified by flash column chromatography on silica gel (from hexane/ethyl acetate 98:2 v/v to hexane/ethyl acetate 93:7 v/v) to give compound **144** (0.49 g, 73% yield) as a colourless oil.

^{1}H NMR (500 MHz, $CDCl_3$) δ 6.31 – 6.28 (m, 1H, H-3), 4.71 (s, 2H, 4-CH_2), 4.38 – 4.34 (m, 2H, 4-CH_2), 2.12 (s, 3H, H-1), 0.85 (s, 9H, *t*BuSi), 0.79 (s, 9H, *t*BuSi), -0.00 (s, 6H, 2 CH_3Si), -0.05 (s, 6H, 2 CH_3Si).

^{13}C NMR (126 MHz, $CDCl_3$) δ 198.72 (C, C=O), 161.10 (C, C4), 118.85 (CH, C3), 62.91 (CH_2, 4-*C*H_2), 62.60 (CH_2, 4-*C*H_2), 31.55 (CH_3, C1), 25.89 (CH_3, 3 *C*H_3-*t*BuSi), 25.77 (CH_3, 3 *C*H_3-*t*BuSi), 18.40 (C, *C*-*t*BuSi), 18.15 (C, *C*-*t*BuSi), -5.47 (CH_3, 2 *C*H_3Si), -5.62 (CH_3, 2 *C*H_3Si).

MS (ES+) *m/z* 381.22 [MNa^+].

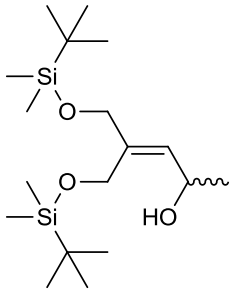

$C_{18}H_{40}O_3Si_2$, MW 360.68

(*R*,*S*)-4,4'-Bis-(*tert*-butyldimethylsilyloxymethyl)-but-3-en-2-ol (**145**).

To a solution of compound **144** (0.36 g, 0.99 mmol) in anhydrous dichloromethane, a solution of 1M DIBALH in cyclohexane (2.1 mL, 2.08 mmol) was added slowly at -20 °C and the reaction mixture was stirred for 1 hour in the dry ice-acetone bath at the temperature of -20 °C to 0 °C. Then, methanol (2.5 mL) was added and the mixture poured into 10% Rochelle salt aqueous solution (20 mL) and ethyl acetate (20 mL). The two-phase solution was stirred vigorously for 1 hour at room temperature, until the two phases were clearly separated. The organic layer was separated, washed with brine/water (1:1 v/v, 2 x 10 mL), dried over $MgSO_4$, filtered and concentrated under reduced pressure. The residue was purified by column chromatography on silica gel eluting with hexane/ethyl acetate (96:4 v/v) to give compound **145** (0.21 g, 60% yield) as a colourless syrup.

^{1}H NMR (500 MHz, $CDCl_3$) δ 5.54 (d, $J_{3,2}$ = 8.0 Hz, 1H, H-3), 4.62 – 4.56 (m, 1H, H-2), 4.21 (d, J_{gem} = 12.3 Hz, 1H, 4-C*H*), 4.10 (d, J_{gem} = 12.1 Hz, 1H, 4-C*H*), 4.06 (s, 2H, 4-CH_2), 2.45 (br s, 1H, 2-O*H*), 1.19 (d, $J_{1,2}$ = 6.3 Hz, 3H, H-1), 0.84 (s, 9H, *t*BuSi), 0.83 (s, 9H, *t*BuSi), 0.02 (s, 6H, 2 CH_3Si), -0.00 (s, 6H, 2 CH_3Si).

^{13}C NMR (126 MHz, $CDCl_3$) δ 139.35 (C, C4), 131.27 (CH, C3), 64.87 (CH_2, 4-*C*H_2), 63.65 (CH, C2), 59.27 (CH_2, 4-*C*H_2), 25.92 (CH_3, 3 *C*H_3-*t*BuSi), 25.84 (CH_3, 3 *C*H_3-*t*BuSi), 23.30 (CH_3, C1), 18.36 (C, *C*-*t*BuSi), 18.20 (C, *C*-*t*BuSi), -5.31 (CH_3, 2 *C*H_3Si), -5.43 (CH_3, 2 *C*H_3Si).

MS (ES+) *m/z* 383.2 [MNa^+].

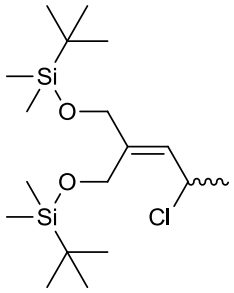

$C_{18}H_{39}ClO_2Si_2$, MW 379.13

(*R*,*S*)-4,4'-Bis-(*tert*-butyldimethylsilyloxymethyl)-but-3-en-2-yl chloride (**146**).

A solution of **145** (0.16 g, 0.44 mmol) in anhydrous pyridine was cooled to 0 °C under a nitrogen atmosphere before adding methanesulfonyl chloride (0.07 mL, 0.89 mmol) dropwise. The reaction mixture was allowed to attain room temperature and stirred for 2 hours, then the solvent was evaporated under reduced pressure and the crude residue was purified by column chromatography on silica gel eluting with hexane/ethyl acetate (95:5 v/v) to give compound **146** (0.06 g,33% yield) as a colourless oil.

^{1}H NMR (500 MHz, $CDCl_3$) δ 5.57 (d, $J_{3,2}$ = 9.4 Hz, 1H, H-3), 4.97 – 4.89 (m, 1H, H-2), 4.21 (d, J_{gem} = 12.6 Hz, 1H, 4-C*H*), 4.14 – 4.07 (m, 3H, 4-C*H* and 4-CH_2), 1.51 (d, $J_{1,2}$ = 6.5 Hz, 3H, H-1), 0.84 (s, 9H, 3 CH_3-*t*BuSi), 0.82 (s, 9H, 3 CH_3-*t*BuSi), -0.00 (s, 6H, 2 CH_3Si), -0.00 (s, 6H, 2 CH_3Si).

^{13}C NMR (126 MHz, $CDCl_3$) δ 140.02 (C, C4), 127.53 (CH, C3), 64.07 (CH_2, 4-*C*H_2), 59.12 (CH_2, 4-*C*H_2), 52.97 (CH, C2), 26.18 (CH_3, C1), 25.93 (CH_3, 3 *C*H_3-*t*BuSi), 25.83 (CH_3, 3 *C*H_3-*t*BuSi), 18.41 (C, *C*-*t*BuSi), 18.23 (C, *C*-*t*BuSi), -5.31 (CH_3, *C*H_3Si), -5.33 (CH_3, *C*H_3Si), -5.40 (CH_3, *C*H_3Si), -5.45 (CH_3, *C*H_3Si).

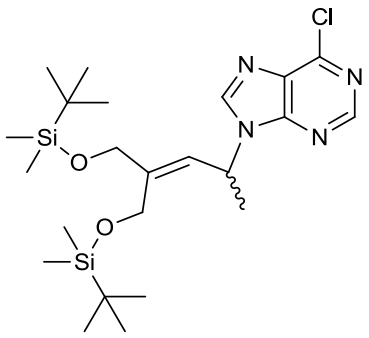

$C_{23}H_{41}ClN_4O_2Si_2$, MW 497.22

2-(*R*,*S*)-[4,4'-Bis-(*tert*-butyldimethylsilyloxymethyl)-but-3-enyl]6-chloropurine (**149**).

To a stirred solution of 0.1M **145** (0.19 g, 0.53 mmol) in anhydrous tetrahydrofuran was added triphenylphosphine (0.14 g, 0.53 mmol) at room temperature under a nitrogen atmosphere. The solution was cooled to 0 °C before adding di-isopropyl azodicarboxylate (0.1 mL, 0.53 mmol) dropwise. After 5 minutes, the solution was allowed to attain room temperature. 6-chloropurine **118** (0.05 g, 0.35 mmol) was added and the reaction mixture was heated at reflux for 20 hours, then cooled to room temperature and concentrated to dryness under reduced pressure. The crude residue was purified by flash column chromatography on silica gel (hexane to hexane/ethyl acetate 75:25 v/v) to give compound **149** (0.06 g, 21% yield) as a colourless oil.

^{1}H NMR (500 MHz, $CDCl_3$) δ 8.69 (s, 1H, H-2_{base}), 8.13 (s, 1H, H-8_{base}), 5.87 (d, $J_{3,2}$ = 9.5 Hz, 1H, H-3), 5.78 – 5.71 (m, 1H, H-2), 4.30 (d, J_{gem} = 12.7 Hz, 1H, 4-C*H*), 4.19 – 4.07 (m, 3H, 4-C*H* and 4-CH_2), 1.68 (d, $J_{1,2}$ = 6.8 Hz, 3H, H-1), 0.85 (s, 9H, 3 CH_3-*t*BuSi), 0.81 (s, 9H, 3 CH_3-*t*BuSi), 0.01 (s, 6H, 2 CH_3Si), -0.00 (s, 6H, 2 CH_3Si).

^{13}C NMR (126 MHz, $CDCl_3$) δ 151.63 (CH, C2_{base}), 151.34 (C, Carom), 150.88 (C, Carom), 143.36 (C, C4), 143.33 (CH, C8_{base}), 131.77 (C, Carom), 122.94 (CH, C3), 63.92 (CH_2, 4-*C*H_2), 59.46 (CH_2, 4-*C*H_2), 48.85 (CH, C2), 25.87 (CH_3, 3 *C*H_3-*t*BuSi), 25.76 (CH_3, 3 *C*H_3-*t*BuSi), 22.02 (CH_3, C1), 18.37 (C, *C*-*t*BuSi), 18.20 (C, *C*-*t*BuSi), -5.37 (CH_3, *C*H_3Si), -5.38 (CH_3, *C*H_3Si), -5.50 (CH_3, *C*H_3Si), -5.53 (CH_3, *C*H_3Si).

MS (ES+) *m/z* 519.2 [MNa^+].

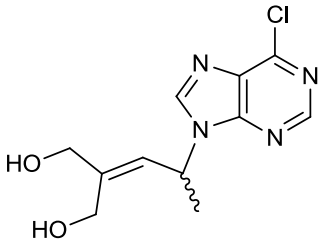

$C_{11}H_{13}ClN_4O_2$, MW 268.70

2-(*R*,*S*)-[4,4'-Bis-(hydroxymethyl)-but-3-enyl]6-chloropurine (**150**).

A 80% aqueous solution of acetic acid (0.85 mL) was added to a stirred solution of compound **149** (0.05 g, 0.10 mmol) in tetrahydrofuran (0.15 mL). The reaction mixture was stirred for 24 hour at room temperature, then concentrated to dryness by co-evaporation with ethanol. The crude residue was purified by flash column chromatography on silica gel (dichloromethane to dichloromethane/methanol 96:4 v/v) to give compound **150** (0.04 g, 74% yield) as a colourless wax.

^{1}H NMR (500 MHz, CD_3OD) δ 8.75 (s, 1H, H-2_{base}), 8.70 (s, 1H, H-8_{base}), 6.04 (d, $J_{3,2}$ = 9.7 Hz, 1H, H-3), 5.91 (dq, $J_{2,3}$ = 9.7 Hz, $J_{2,1}$ = 6.8 Hz, 1H, H-2), 4.36 (d, J_{gem} = 12.8 Hz, 1H, 4-C*H*), 4.27 (d, J_{gem} = 12.8 Hz, 1H, 4-C*H*), 4.18 – 4.10 (m, 2H, 4-CH_2), 1.80 (d, $J_{1,2}$ = 6.8 Hz, 3H, H-1).

^{13}C NMR (126 MHz, CD_3OD) δ 151.31 (C, Carom), 151.28 (CH, C2_{base}), 149.76 (C, Carom), 145.18 (CH, C8_{base}), 143.22 (C, C4), 131.10 (C, Carom), 124.84 (CH, C3), 62.97 (CH_2, 4-*C*H_2), 57.34 (CH_2, 4-*C*H_2), 49.38 (CH, C2), 20.15 (CH_3, C1).

MS (ES+) *m/z* 291.1 [MNa^+], 269.1 [MH^+].

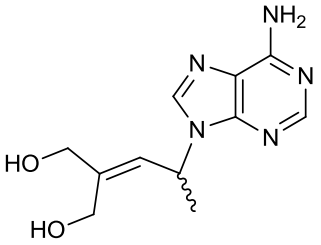

$C_{11}H_{15}N_5O_2$, MW 249.27

2-(*R*,*S*)-[4,4'-Bis-(hydroxymethyl)-but-3-enyl]adenine (**28**).

Compound **150** (0.05 g, 0.19 mmol) was dissolved in a 28-30% aqueous ammonia solution (0.5 mL) and 1,4-dioxane (0.5 mL). The reaction mixture was stirred in a screw-cap pressure glass tube at 90 °C for 48 hours, then cooled to room temperature and concentrated to dryness by co-evaporation with ethanol. The crude residue was purified by flash column chromatography on silica gel (dichloromethane to dichloromethane/methanol 87:13 v/v) to give **28** (0.03 g, 64% yield) as a white powder.

^{1}H NMR (500 MHz, DMSO-d_6) δ 8.26 (s, 1H, H-2_{base}), 8.14 (s, 1H, H-8_{base}), 7.19 (s, 2H, 6-NH_2), 5.84 (d, $J_{3,2}$ = 9.7 Hz, 1H, H-3), 5.62 (m, 1H, H-2), 4.87 (t, J = 5.5 Hz, 1H, O*H*), 4.80 (t, J = 5.5 Hz, 1H, O*H*), 4.16 (dd, J_{gem} = 12.6 Hz, $J_{CH,OH}$ = 5.5 Hz, 1H, 4-C*H*), 4.02 (dd, J_{gem} = 12.6 Hz, $J_{CH,OH}$ = 5.5 Hz, 1H, 4-C*H*), 4.00 – 3.90 (m, 2H, 4-CH_2), 1.63 (d, $J_{1,2}$ = 6.8 Hz, 3H, H-1).

^{13}C NMR (126 MHz, DMSO-d_6) δ 156.47 (C, Carom), 152.61 (CH, $C2_{base}$), 149.28 (C, Carom), 143.06 (C, C4), 139.44 (CH, $C8_{base}$), 124.82 (CH, C3), 119.45 (C, Carom), 62.69 (CH_2, 4-*C*H_2), 57.41 (CH_2, 4-*C*H_2), 47.97 (CH, C2), 21.90 (CH_3, C1).

HPLC (system 1) t_R = 10.09 min.

HPLC (system 2) t_R = 16.49 min.

MS (ES+) *m/z* 250.1 [MH^+], 272.1 [MNa^+].

4.2.6 PROCEDURES AND SPECTRAL DATA – SECTION 2.2.5

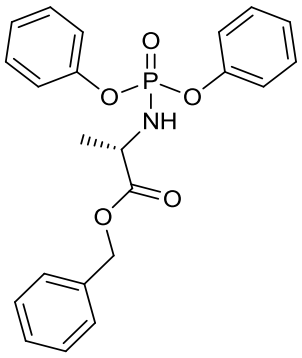

$C_{22}H_{22}NO_5P$, MW 411.39

***N*-(diphenoxyphosphinyl)-L-alanine benzyl ester** (**152**).

L-alanine benzyl ester *p*-tosylate salt **32** (0.50 g, 1.42 mmol) was dissolved in anhydrous dichloromethane under a nitrogen atmosphere and diphenylchlorophosphate **151** (0.30 mL, 1.42 mmol) was added at room temperature. The mixture was cooled to -78 °C before adding triethylamine (0.40 mL, 2.85 mmol) dropwise. The reaction mixture was stirred at -78 °C for 1 hour, then allowed to attain room temperature and stirred for additional 2 hours. The solvent was removed under reduced pressure. The crude residue was suspended in ethylacetate and stirred for 15 minutes, then filtered under vacuo. The filtrate was evaporated under reduced pressure and the crude residue was purified by flash column chromatography on silica gel (hexane to hexane/acetone 70:30 v/v) to obtain compound **152** (0.56 g, 96% yield) as a colourless oil.

^{31}P NMR (202 MHz, $CDCl_3$) δ -2.79.

^{1}H NMR (500 MHz, $CDCl_3$) δ 7.39 – 7.22 (m, 13H, Harom), 7.21 – 7.15 (m, 2H, Harom), 5.14 (s, 2H, C*H*$_2$(C_6H_5)), 4.27 – 4.12 (m, 2H, C*H*CH_3 and N*H*), 1.41 (d, *J* = 7.0 Hz, 3H, CHC*H*$_3$).

^{13}C NMR (126 MHz, $CDCl_3$) δ 173.13 (d, $J_{C\text{-}C\text{-}N\text{-}P}$ = 7.5 Hz, C, C=O), 150.72 (m, C, Carom), 135.29 (C, Carom), 129.72 (d, $J_{C\text{-}C\text{-}O\text{-}P}$ = 4.4 Hz, CH, Carom), 128.66 (CH, Carom), 128.50 (CH, Carom), 128.23 (CH, Carom), 125.07 (CH, Carom), 120.30 (m, CH, Carom), 67.23 (CH_2, *C*H_2(C_6H_5)), 50.56 (d, $J_{C\text{-}N\text{-}P}$ = 1.0 Hz, *C*HCH_3), 20.95 (d, $J_{C\text{-}C\text{-}N\text{-}P}$ = 4.9 Hz, CH_3, CH*C*H$_3$).

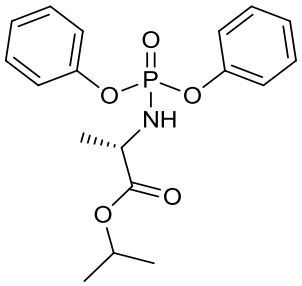

$C_{18}H_{22}NO_5P$, MW 363.34

***N*-(diphenoxyphosphinyl)-L-alanine isopropyl ester** (**153**).

L-alanine isopropyl ester hydrochloride **33** (0.50 g, 2.98 mmol) was dissolved in anhydrous dichloromethane under a nitrogen atmosphere and diphenylchlorophosphate **151** (0.62 mL, 2.98 mmol) was added at room temperature. The mixture was cooled to -78 °C before adding triethylamine (0.83 mL, 5.97 mmol) dropwise. The reaction mixture was stirred at -78 °C for 1 hour, then allowed to attain room temperature and stirred for additional 2 hours. The solvent was removed under reduced pressure. The crude residue was suspended in ethylacetate and stirred for 15 minutes, then filtered under vacuo. The filtrate was evaporated under reduced pressure and the crude residue was purified by flash column chromatography on silica gel (hexane to hexane/acetone 70:30 v/v) to obtain compound **153** (0.90 g, 83% yield) as a colourless oil.

^{31}P NMR (202 MHz, $CDCl_3$) δ -2.81.

^{1}H NMR (500 MHz, $CDCl_3$) δ 7.38 – 7.32 (m, 4H, Harom), 7.29 – 7.24 (m, 4H, Harom), 7.21 – 7.17 (m, 2H, Harom), 5.07 – 4.98 (m, 1H, *H*-*i*Pr), 4.16 – 4.06 (m, 1H, C*H*CH_3), 3.79 (m, 1H, N*H*), 1.39 (d, *J* = 7.0 Hz, 3H, CHC*H*$_3$), 1.24 (d, *J* = 4.2 Hz, 6H, 2 C*H*$_3$-*i*Pr).

^{13}C NMR (126 MHz, $CDCl_3$) δ 173.72 (d, $J_{C\text{-}C\text{-}N\text{-}P}$ = 7.4 Hz, C, C=O), 150.69 (m, C, Carom), 129.71 (d, $J_{C\text{-}C\text{-}O\text{-}P}$ = 2.0 Hz, CH, Carom), 125.06 (CH, Carom), 120.26 (m, CH, Carom), 69.34 (CH, *C*H-*i*Pr), 50.56 (CH, *C*HCH_3), 21.61 (CH_3, 2 *C*H_3-*i*Pr), 21.10 (d, $J_{C\text{-}C\text{-}N\text{-}P}$ = 3.1 Hz, CH_3, CH*C*H_3).

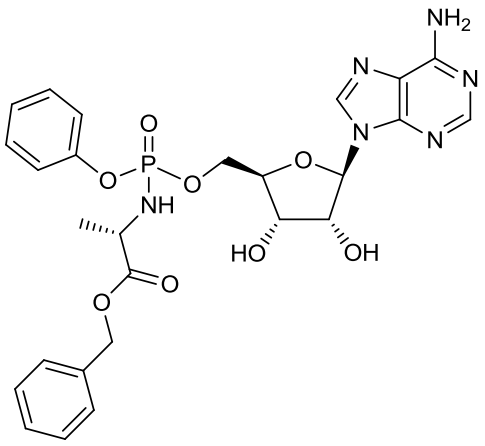

$C_{26}H_{29}N_6O_8P$, MW 584.52

Adenosine 5'-*O*-[phenyl-(benzyloxy-L-alaninyl)] phosphate (**155**).

General procedure under MWI condition:

Compound **154** (0.08 g, 0.28 mmol) was dissolved in anhydrous tetrahydrofuran (1.6 mL) and *N*-methyl-2-pyrrolidone (0.55 mL) in a 10 mL sealed microwave tube under a nitrogen atmosphere and *tert*-butylmagnesium chloride 1M in tetrahydrofuran (0.84 mL, 0.84 mmol) was added dropwise at room temperature. After stirring 10 minutes, a solution of *p*-nitrophenolate **37** (0.26 g, 0.56 mmol) in anhydrous tetrahydrofuran (1 mL) was added slowly. The reaction mixture was stirred under MWI (100 W, 65 °C) for 5 minutes, then cooled to room temperature, poured into a 10% aqueous solution of NH_4Cl (10 mL) and extracted with dichloromethane (3 x 10 mL), the combined organic layer was washed with water (20 mL) and brine (20 mL), dried over anhydrous $MgSO_4$, filtered and concentrated under reduced pressure. The residue was purified by flash column chromatography on silica gel (dichloromethane to dichloromethane/methanol 92:8 v/v) to give compound **155** (0.06 g, 40% yield) as a colourless wax.

General procedure by conventional heating:

Compound **154** (0.08 g, 0.24 mmol) was dissolved in anhydrous tetrahydrofuran (1.6 mL) and *N*-methyl-2-pyrrolidone (0.55 mL) under a nitrogen atmosphere and *tert*-butylmagnesium chloride 1M in tetrahydrofuran (0.84 mL, 0.84 mmol) was added dropwise at room temperature. After stirring 10 minutes, a solution of *p*-nitrophenolate **37** (0.26 g, 0.56 mmol) in anhydrous tetrahydrofuran (1 mL) was added slowly. The reaction mixture was heated to 55 °C and stirred for 1 hour, then cooled to room temperature, poured into a 10% aqueous solution of NH_4Cl (10 mL) and extracted with dichloromethane (3 x 10 mL), the combined organic layer was washed with water (20 mL) and brine (20 mL), dried over anhydrous $MgSO_4$, filtered and concentrated under

reduced pressure. The residue was purified by flash column chromatography on silica gel (dichloromethane to dichloromethane/methanol 92:8 v/v) to give compound **155** (0.07 g, 42% yield) as a colourless wax.

Procedure for the deprotection of **157**:

Compound **157** (0.06 g, 0.09 mmol) was dissolved in a 60% aqueous solution of acetic acid (5 mL). The reaction mixture was stirred at room temperature for 16 hours, then evaporated by co-evaporation with ethanol. The residue was purified by flash column chromatography on silica gel (dichloromethane to dichloromethane/methanol 92:8 v/v) to give compound **155** (0.02 g, 40% yield) as a colourless wax.

^{31}P NMR (202 MHz, CD_3OD) δ 3.90, 3.66.

^{1}H NMR (500 MHz, CD_3OD) δ 8.28 – 8.19 (m, 2H, H-2 and H-8), 7.35 – 7.26 (m, 7H, Harom), 7.22 – 7.14 (m, 3H, Harom), 6.07 – 6.03 (m, 1H, H-1'), 5.15 – 5.05 (m, 2H, CH_2(C_6H_5)), 4.67, 4.64 (2t, *J* = 5.1 Hz, 1H, H-2'), 4.44 – 4.37 (m, 2H, H-3' and H-5'a), 4.36 – 4.28 (m, 1H, H-5'b), 4.28 – 4.24 (m, 1H, H-4'), 4.04 – 3.91 (m, 1H, C*H*CH_3), 1.33, 1.28 (2d, *J* = 7.2 Hz, 1H, CHCH_3).

^{13}C NMR (126 MHz, CD_3OD) δ 173.43 (d, $J_{C\text{-}C\text{-}N\text{-}P}$ = 3.5 Hz, C, C=O), 173.22 (d, $J_{C\text{-}C\text{-}N\text{-}P}$ = 4.1 Hz, C, C=O), 155.90, 155.88 (C, Carom), 152.54, 152.50 (CH, C2), 150.70, 150.65, 149.28, 149.25, 135.83, 135.76 (C, Carom), 129.37, 128.15, 127.90, 127.86, 124.78, 120.05, 120.01, 119.99, 119.95, 119.09 (CH, Carom and C8), 88.56 (CH, C1'), 82.97 (d, $J_{C\text{-}C\text{-}0\text{-}P}$ = 4.0 Hz, CH, C4'), 82.91 (d, $J_{C\text{-}C\text{-}0\text{-}P}$ = 3.8 Hz, CH, C4'), 73.99 (CH, C2'), 70.18, 70.06 (CH, C3'), 66.56, 66.55 (CH_2, *C*H_2(C_6H_5)), 66.14 (d, $J_{C\text{-}O\text{-}P}$ = 4.2 Hz, CH_2, C5'), 65.73 (d, $J_{C\text{-}O\text{-}P}$ = 4.1 Hz, CH_2, C5'), 50.29 (d, $J_{C\text{-}N\text{-}P}$ = 0.4 Hz, CH, *C*HCH_3), 50.18 (d, $J_{C\text{-}N\text{-}P}$ = 0.4 Hz, CH, *C*HCH_3), 19.01 (d, $J_{C\text{-}C\text{-}N\text{-}P}$ = 5.2 Hz, CH_3, CH*C*H_3), 18.84 (d, $J_{C\text{-}C\text{-}N\text{-}P}$ = 5.8 Hz, CH_3, CH*C*H_3).

MS (ES+) *m/z* 607.2 [MNa^+], 585.2 [MH^+].

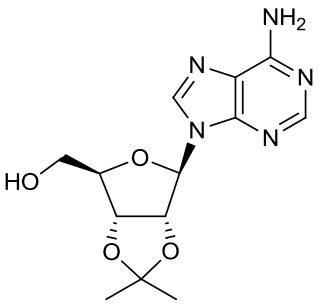

$C_{13}H_{17}N_5O_4$, MW 307.31

2',3'-*O*,*O*-isopropylidene-adenosine (**156**).[22]

A 70% aqueous solution of perchloric acid (0.56 mL, 6.55 mmol) was added dropwise to a stirred suspension of compound **154** (1.0 g, 3.74 mmol) in acetone at room temperature. The resulting solution was stirred for 30 minutes, then added of saturated aqueous $NaHCO_3$ solution and concentrated to dryness by co-evaporation with ethanol. The crude residue was purified by flash column chromatography on silica gel (dichloromethane to dichloromethane/methanol 90:10 v/v) to give compound **156** (1.09 g, 95% yield) as a white powder; mp: 216-218 °C (lit: 220 °C).

^{1}H NMR (500 MHz, DMSO-d_6) δ 8.35 (s, 1H, H-2), 8.16 (s, 1H, H-8), 7.35 (s, 2H, 6-NH_2), 6.13 (d, $J_{1',2'}$ = 3.1 Hz, 1H, H-1'), 5.35 (dd, $J_{2',3'}$ = 6.1 Hz, $J_{2',1'}$ = 3.1 Hz, 1H, H-2'), 5.24 (t, $J_{5'\text{-}OH,\ 5'}$ = 5.6 Hz, 1H, 5'-O*H*), 4.97 (dd, $J_{3',2'}$ = 6.1 Hz, $J_{3',4'}$ = 2.5 Hz, 1H, H-3'), 4.22 (td, $J_{4',5'}$ = 4.8 Hz, $J_{4',3'}$ = 2.5 Hz, 1H, H-4'), 3.55 (m, 2H, H-5'a and H-5'b), 1.56 (s, 3H, *i*Pr-CH_3), 1.34 (s, 3H, *i*Pr-CH_3).

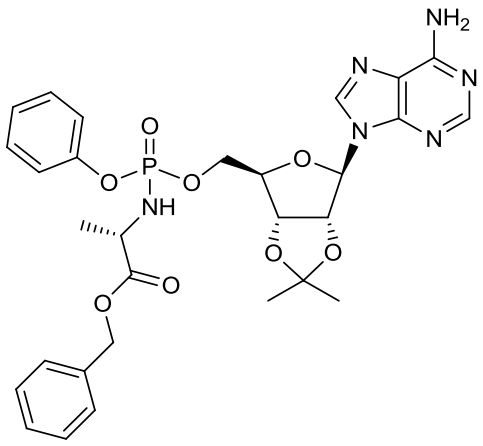

$C_{29}H_{33}N_6O_8P$, MW 624.58

2',3'-*O*,*O*-isopropylidene-adenosine 5'-*O*-[phenyl-(benzyloxy-L-alaninyl)] phosphate (**157**).

General procedure under MWI conditions:

Compound **156** (0.08 g, 0.24 mmol) was dissolved in anhydrous tetrahydrofuran (1.6 mL) and *N*-methyl-2-pyrrolidone (0.55 mL) in a 10 mL sealed microwave tube under a nitrogen atmosphere and *tert*-butylmagnesium chloride 1M in tetrahydrofuran (0.49 mL, 0.49 mmol) was added dropwise at room temperature. After stirring 10 minutes, a solution of the phosphoramidating reagent (2 equivalents) in anhydrous tetrahydrofuran (1 mL) was added slowly. The reaction mixture was stirred under MWI (100 W, 65 °C) for 2 to 60 minutes, then cooled to room temperature, poured into a 10% aqueous solution of NH_4Cl (10 mL) and extracted with dichloromethane (3 x 10 mL), the combined organic layer was washed with water (20 mL) and brine (20 mL), dried over anhydrous $MgSO_4$, filtered and concentrated under reduced pressure. The residue was purified by flash column chromatography on silica gel (dichloromethane to dichloromethane/methanol 97:3 v/v) to give compound **157** as a colourless wax.

Selected conditions:

Compound **156** was treated with *p*-nitrophenolate **37** (0.22 g, 0.49 mmol) over 2 minutes to give compound **157** (0.06 g, 41% yield) after chromatographical purification.

General procedure by conventional heating:

Compound **156** (0.08 g, 0.24 mmol) was dissolved in anhydrous tetrahydrofuran (1.6 mL) and *N*-methyl-2-pyrrolidone (0.55 mL) under a nitrogen atmosphere and *tert*-butylmagnesium chloride 1M in tetrahydrofuran (0.49 mL, 0.49 mmol) was added dropwise at room temperature. After stirring 10 minutes, a solution of the phosphoramidating reagent (2 equivalents) in anhydrous tetrahydrofuran (1 mL) was added slowly. The reaction mixture was heated to 55 °C and stirred for

2 to 8 hours, then cooled to room temperature, poured into a 10% aqueous solution of NH_4Cl (10 mL) and extracted with dichloromethane (3 x 10 mL), the combined organic layer was washed with water (20 mL) and brine (20 mL), dried over anhydrous $MgSO_4$, filtered and concentrated under reduced pressure. The residue was purified by flash column chromatography on silica gel (dichloromethane to dichloromethane/methanol 97:3 v/v) to give compound **157** as a colourless wax.

Selected conditions:

Compound **156** was treated with *p*-nitrophenolate **37** (0.22 g, 0.49 mmol) over 30 minutes to give compound **157** (0.07 g, 46% yield) after chromatographical purification.

^{31}P NMR (202 MHz, CD_3OD) δ 3.72, 3.40.

^{1}H NMR (500 MHz, CD_3OD) δ 8.24 – 8.21 (m, 2H, H-2 and H-8), 7.34 – 7.26 (m, 7H, Harom), 7.17 – 7.08 (m, 3H, Harom), 6.21, 6.20 (2d, $J_{1',2'}$ = 2.5 Hz, 1H, H-1'), 5.37, 5.27 (2dd, $J_{2',3'}$ = 6.3 Hz, $J_{2',1'}$ = 2.5 Hz, 1H, H-2'), 5.12 – 5.05 (m, 3H, CH_2(C_6H_5) and H-3'), 4.49 – 4.46, 4.45 – 4.41 (2m, 1H, H-4'), 4.34 – 4.18 (m, 2H, H-5'a and H-5'b), 3.99 – 3.91 (m, 1H, C$H$$CH_3$), 1.60 (s, 3H, *i*Pr-C$H_3$), 1.38 (s, 3H, *i*Pr-C$H_3$), 1.31 – 1.26 (m, 3H, CHCH_3).

^{13}C NMR (126 MHz, CD_3OD) δ 173.42 (d, $J_{C-C-N-P}$ = 4.3 Hz, C, C=O), 173.20 (d, $J_{C-C-N-P}$ = 4.9 Hz, C, C=O), 155.96 (C, Carom), 152.67 (CH, C2), 150.64, 150.62, 150.59, 150.57, 148.88, 148.83 (C, Carom), 140.13, 139.99 (CH, C8), 135.82, 135.77 (C, Carom), 129.35, 128.18, 127.96, 127.93, 127.92, 127.90, 127.86, 124.79, 124.75, 119.98, 119.97, 119.94, 119.93 (CH, Carom), 119.18, 114.23, 114.11 (C, Carom), 90.66, 90.36 (CH, C1'), 85.09 (d, $J_{C-C-0-P}$ = 8.5 Hz, CH, C4'), 85.03 (d, $J_{C-C-0-P}$ = 6.6 Hz, CH, C4'), 84.01, 83.99 (CH, C2'), 81.31, 81.29 (CH, C3'), 66.56 (CH_2, $C$$H_2$($C_6H_5$)), 66.21 (d, J_{C-O-P} = 4.3 Hz, CH_2, C5'), 66.20 (d, J_{C-O-P} = 3.9 Hz, CH_2, C5'), 50.28, 50.13 (CH, $C$$HCH_3$), 26.09, 26.06 ($CH_3$, $C$$H_3$-*i*Pr), 24.20, 24.15 ($CH_3$, $C$$H_3$-*i*Pr), 18.98 (d, $J_{C-C-N-P}$ = 6.7 Hz, CH_3, CH$C$$H_3$), 18.87 (d, $J_{C-C-N-P}$ = 7.2 Hz, CH_3, CH$C$$H_3$).

MS (ES+) *m/z* 647.3 [MNa^+], 625.3 [MH^+].

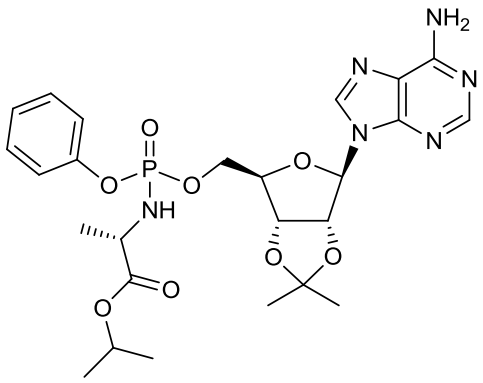

$C_{25}H_{33}N_6O_8P$, MW 576.54

2',3'-*O*,*O*-isopropylidene-adenosine 5'-*O*-[phenyl-(isopropoxy-L-alaninyl)] phosphate (**158**).[7]

General procedure under MWI conditions:

Compound **156** (0.08 g, 0.24 mmol) was dissolved in anhydrous tetrahydrofuran (1.6 mL) and *N*-methyl-2-pyrrolidone (0.55 mL) in a 10 mL sealed microwave tube under a nitrogen atmosphere and *tert*-butylmagnesium chloride 1M in tetrahydrofuran (0.49 mL, 0.49 mmol) was added dropwise at room temperature. After stirring 10 minutes, a solution of the phosphoramidating reagent (2 equivalents) in anhydrous tetrahydrofuran (1 mL) was added slowly. The reaction mixture was stirred under MWI (100 W, 65 °C) for 2 to 60 minutes, then cooled to room temperature, poured into a 10% aqueous solution of NH_4Cl (10 mL) and extracted with dichloromethane (3 x 10 mL), the combined organic layer was washed with water (20 mL) and brine (20 mL), dried over anhydrous $MgSO_4$, filtered and concentrated under reduced pressure. The residue was purified by flash column chromatography on silica gel (dichloromethane to dichloromethane/methanol 97:3 v/v) to give compound **158** as a colourless wax.

Selected conditions:

Compound **156** was treated with *p*-nitrophenolate **38** (0.20 g, 0.49 mmol) over 2 minutes to give compound **158** (0.10 g, 67% yield) after chromatographical purification.

General procedure by conventional heating:

Compound **156** (0.08 g, 0.24 mmol) was dissolved in anhydrous tetrahydrofuran (1.6 mL) and *N*-methyl-2-pyrrolidone (0.55 mL) under a nitrogen atmosphere and *tert*-butylmagnesium chloride 1M in tetrahydrofuran (0.49 mL, 0.49 mmol) was added dropwise at room temperature. After stirring 10 minutes, a solution of the phosphoramidating reagent (2 equivalents) in anhydrous tetrahydrofuran (1 mL) was added slowly. The reaction mixture was heated to 55 °C and stirred for 2 to 8 hours, then cooled to room temperature, poured into a 10% aqueous solution of NH_4Cl (10

mL) and extracted with dichloromethane (3 x 10 mL), the combined organic layer was washed with water (20 mL) and brine (20 mL), dried over anhydrous $MgSO_4$, filtered and concentrated under reduced pressure. The residue was purified by flash column chromatography on silica gel (dichloromethane to dichloromethane/methanol 97:3 v/v) to give compound **158** as a colourless wax.

Selected conditions:

Compound **156** was treated with *p*-nitrophenolate **38** (0.20 g, 0.49 mmol) over 30 minutes to give compound **158** (0.11 g, 77% yield) after chromatographical purification.

^{1}H NMR (500 MHz, CD_3OD) δ 8.16, 8.15 (2s, 1H, H-2), 8.12, 8.11 (2s, 1H, H-8), 7.24 – 7.17 (m, 2H, Harom), 7.09 – 7.00 (m, 3H, Harom), 6.12, 6.11 (2d, $J_{1',2'}$ = 2.5 Hz, 1H, H-1'), 5.30, 5.20 (2dd, $J_{2',3'}$ = 6.3 Hz, $J_{2',1'}$ = 2.5 Hz, 1H, H-2'), 5.03, 5.00 (2dd, $J_{3',2'}$ = 6.3 Hz, $J_{3',4'}$ = 3.1 Hz, 1H, H-3'), 4.85 – 4.80 (m, 1H, C*H*-*i*Pr), 4.43 – 4.39, 4.37 – 4.33 (2m, 1H, H-4'), 4.25 – 4.11 (m, 2H, H-5'a and H-5'b), 3.76 – 3.68 (m, 1H, C*H*CH_3), 1.50 (s, 3H, *i*Pr-CH_3), 1.29, 1.28 (2s, 3H, *i*Pr-CH_3), 1.18 – 1.14 (m, 3H, CHCH_3), 1.12 – 1.07 (m, 6H, 2 CH_3-*i*Pr).

4.3 REFERENCES

[1] C. G. Noble, S. P. Lim, y.-L- Chen, C. W. Liew, L. Yap, J. Lescar, P.-Y. Shi. Conformational flexibility of the dengue virus RNA-dependent RNA polymerase revealed by a complex with an inhibitor. *J. Virol.*, 87(9): 5291-5295, 2013.

[2] R. T. Mosley, T. E. Edwards, E. Murakami, A. M. Lam, R. L. Grice, J. Du, M. J. Sofia, P. A. Furman, M. J. Otto. Structure of Hepatitis C virus polymerase in complex with primer-template RNA. *J. Virol.,* 86: 6503-6511, 2012.

[3] T. L. Yap, T. Xu, Y.-L. Chen, H. Malet, M.-P. Egloff, B. Canard, S. G. Vasudevan, J. Lescar. Crystal structure of the dengue virus RNA-dependent RNA polymerase catalytic domain at 1.85-angstrom resolution. *J. Virol.*, 81(9): 4753-4765, 2007.

[4] M. Serpi, K. Madela, F. Pertusati, M. Slusarczyk. Synthesis of phosphoramidate prodrugs: ProTide approach. *Curr. Protoc. Nucleic Acid Chem.*, supplement 53, 15.5.1-15.5.15, June 2013.

[5] M. Derudas, D. Carta, A. Brancale, C. Vanpouille, A. Lisco, L. Margolis, J. Balzarini, C. McGuigan. The application of phosphoramidate ProTide technology to acyclovir confers anti-HIV inhibition. *J. Med. Chem.*, 52: 5520-5530, 2009.

[6] A. Eneroth, B. Klasson, M. Nilsson, P. Pinho, B. Samuelsson, C. Sund. Preparation of antiviral nucleotides and their use as HCV polymerase inhibitors. Medivir AB. US 20130143835 A1. June 6, 2013.

[7] B. S. Ross, P. Ganapadi Reddy, H.-R. Zhang, S. Rachakonda, M. J. Sofia. Synthesis of diastereomerically pure nucleotide phosphoramidates. *J. Org. Chem.*, 76: 8311-8319, 2011.

[8] G. Parmentier, G. Schmitt, F. Dolle, B. Luu. A convergent synthesis of 2'-*O*-methyl uridine. *Tetrahedron*, 50(18): 5361-5368, 1994.

[9] A. B. Eldrup, M. Prhavc, J. Brooks, B. Bhat, T. P. Prakash, Q. Sing, S. Bera, N. Bhat, P. Dande, P. D. Cook, C. F. Bennett, S. S. Carroll, R. G. Ball, M. Bosserman, C. Burlein, L. F. Colwell, J. F. Fay, O. A. Flores, K. Getty, R. L. LaFemina, J. Leone, M. MacCoss, D. R. McMasters, J. E. Tommassini, D. Von Langen, B. Wolanski, D. B. Olsen. Structure-activity relationship of heterobase-modified 2'-*C*-methyl ribonucleosides as inhibitors of hepatitis C virus RNA replication. *J. Med. Chem.*, 47: 5284-5297, 2004.

[10] S.-Y. Han, M. M. Joullié. Investigations of the formation of cyclic acetal and ketal derivatives of D-ribono-1,4-lactone and 2-deoxy-D-ribono-1,4-lactone. *Tetrahedron*, 49(2): 349-362, 1993.

[11] L. Cappellacci, G. Barboni, M. Palmieri, M. Pasqualini, M. Grifantini, B. Costa, C. Martini, P. Franchetti. Ribose-modified nucleosides as ligands for adenosine receptors: synthesis, conformational analysis, and biological evaluation of 1'-*C*-methyl adenosine analogues. *J. Med. Chem.*, 45 (6): 1196-1202, 2002.

[12] M. S. Valle, A. Tarrade-Matha, P. Dauban, R. H. Dodd. Regioselective electrophilic substitution of 2,3-aziridino-γ-lactones: preliminary studies aimed at the synthesis of α,α-disubstituted α- or β-amino acids. *Tetrahedron*, 64: 419-432, 2008.

[13] M. Tichý, R. Pohl, H. Y. Xu, Y.-L. Chen, F. Yokokawa, P.-Y. Shi, M. Hocek. Synthesis and antiviral activity of 4,6-disubstituted pyrimido[4,5-*b*]indole ribonucleosides. *Bioorg. Med. Chem.*, 20: 6123-6133, 2012.

[14] F. Stazi, W. Maton, D. Castoldi, P. Westerduin, O. Curcuruto, S. Bacchi. Efficient methods for the synthesis of arylacetonitriles. *Synthesis*, 19: 3332-3338, 2010.

[15] K. Kobayashi, T. Komatsu, Y. Yokoi, H. Konishi. Synthesis of 2-aminoindole-3-carboxylic acid derivatives by the copper(I) iodide catalyzed reaction of *N*-2-iodophenyl)formamides with malononitrile or cyanoacetates. *Synthesis*, 5: 764-768, 2011.

[16] M. Tichý, R. Pohl, E. Tloust'ová, J. Weber, G. Bahador, Y.-J. Lee, M. Hocek. Synthesis and biological activity of benzo-fused 7-deazaadenosine analogues. 5- and 6-substituted 4-amino- or 4-alkylpyrimido[4,5-*b*]indole ribonucleosides. *Bioorg. Med. Chem.*, 21: 5362-5372, 2013.

[17] R. Storer, A. Moussa, N. Chaudhuri, F. Waligora. Process for the production of 2'-branched nucleosides. Idenix Cayman Limited. WO 2004052899 A2. Jun 24, 2004.

[18] J. H. Hong, H. O. Kim, H. R. Moon, L. S. Jeong. Synthesis and antiviral activity of fluoro-substituted apio dideoxynucleosides. *Arch. Pharm. Res.*, 24(2): 95-99, 2001.

[19] J. H. Hong, O. H. Ko. Synthesis and antiviral evaluation of novel acyclic nucleosides. *Bull. Korean Chem. Soc.*, 24(9): 1284-1288, 2003.

[20] J. H. Hong, S.-Y. Kim, C.-H. Oh, K. H. Yoo, J.-H. Cho. Synthesis and antiviral evaluation of novel open-chain analogues of neplanocin A. *Nucleosides Nucleotides Nucleic Acids*, 25: 341-350, 2006.

[21] Y.-L. Chen, Z. Yin, J. Duraiswamy, W. Shul, C. C. Lim, H. Y. Xu, M. Qing, A. Yip, G. Wang, W. L. Chan, H. P. Tan, M. Lo, S. Liung, R. R. Kondreddi, R. Rao, H. Gu, H. He, T. H. Keller, P.-Y. Shi. Inhibition of dengue virus RNA synthesis by an adenosine nucleoside. *Antimicrob. Agents Chemother.*, 54(7): 2932-2939, 2010.

[22] J.-H. Cho, S. J. Coats, R. F. Schinazi. Efficient synthesis of exo-N-carbamoyl nucleosides: application to the synthesis of phosphoramidate prodrugs. *Org. Lett.*, 14(10): 2488-2491, 2012.

APPENDIX

Table 20. List of adenosine analogues known to be inhibitors of DENV RdRp, of which the phosphorylated derivatives were docked using the model of the DENV RdRp *de novo* initiation complex (see paragraph 2.1.1.2 for details), and their anti-DENV activity.

DENV RdRp inhibitors	**Anti-DENV activity**	**Reference**
2'-*C*-methyl-7-deazaadenosine	EC_{50} 15 µM[a]	[1]
2'-*C*-acetylene-7-deazaadenosine (NITD008)	EC_{50} 0.64 µM[b]	[2]
2'-*C*-acetylene-7-deaza-7-fluoroadenosine	EC_{50} 0.42 µM[c]	[3]
2'-*C*-acetylene-7-deaza-7-cyanoadenosine	EC_{50} 3.1 µM[c]	[3]
2'-*C*-acetylene-7-deaza-7-carbamoyladenosine (NITD449)	EC_{50} 2 µM[c]	[3]
2-amino-2'-*C*-methyladenosine	EC_{50} 9.5 µM[c]	[4]
4-amino-9-β-D-ribofuranosyl-pyrimido[4,5-*b*]indole	EC_{50} 39.6 µM[a]	[5]
4-amino-5-chloro-9-β-D-ribofuranosyl-pyrimido[4,5-*b*]indole	EC_{50} 0.85 µM[a]	[5]
4-amino-5-butyl-9-β-D-ribofuranosyl-pyrimido[4,5-*b*]indole	EC_{50} 14.8 µM[a]	[5]
4-amino-6-thiophen-3-yl-9-β-D-ribofuranosyl-pyrimido[4,5-*b*]indole	EC_{50} 18.8 µM[a]	[5]
4-amino-6-benzofuran-2-yl-9-β-D-ribofuranosyl-pyrimido[4,5-*b*]indole	EC_{50} 15.4 µM[a]	[5]
6-chloro-4-(furan-2-yl)-9-β-D-ribofuranosyl-pyrimido[4,5-*b*]indole	IC_{50} 0.238 µM[d]	[6]
6-chloro-4-(thiophen-2-yl)-9-β-D-ribofuranosyl-pyrimido[4,5-*b*]indole	IC_{50} 0.335 µM[d]	[6]
4-(benzofuran-2-yl)- 6-chloro-9-β-D-ribofuranosyl-pyrimido[4,5-*b*]indole	IC_{50} 0.976 µM[d]	[6]

Antiviral assays were performed in the following cell lines: [a]African green monkey kidney cells (Vero cells); [b]primary human peripheral blood mononuclear cells (PBMCs); [c]baby hamster kidney cells (BHK-21); [d]human hepatoma cells (Huh7). DENV RdRp: Dengue virus RNA-dependent RNA polymerase.

REFERENCES

[1] D. B. Olsen, A. B. Eldrup, L. Bartholomew, B. Bhat, M. R. Bosserman, A. Ceccacci, L. F. Colwell, J. F. Fay, O. A. Flores, K. L. Getty, J. A. Grobler, R. L. LaFemina, E. J. Markel, G. Migliaccio, M. Prhavc, M. W. Stahlhut, J. E. Tomassini, M. MacCoss, D. J. Hazuda, S. S. Carroll. A 7-deaza-adenosine analog is a potent and selective inhibitor of hepatitis C virus replication with excellent pharmacokinetic properties. *Antimicr. Agents Chemother.*, 48(10): 3944-3953, 2004.

[2] Z. Yin, Y.-L. Chen, W. Schul, Q.-Y. wang, F. Gu, J. Duraiswamy, R.R. Kondreddi, P. Niyomrattanakit, S. B. Lakshminarayana, A. Goh, H. Y. Xu, W. Liu, B. Liu, J. Y. H. Lim, C. Y. Ng, M. Qing, C. C. Lim, A. Yip, G. Wang, W. L. Chan, H. P. Tan, K. Lin, B. Zhang, G. Zou, K. A. Bernard, C. Garrett, K. Beltz, M. Dong, M. Weaver, H. He, A. Pichota, V. Dartois, T. H. Keller, P.-Y. Shi. An adenosine nucleoside inhibitor of dengue virus. *Proc. Natl. Acad. Sci.*, 106(48): 20435-20439, 2009.

[3] Y.-L. Chen, Z. Yin, J. Duraiswamy, W. Schul, C. C. Lim, H. Y. Xu, M. Qing, A. Yip, G. Wang, W. L. Chan, H. P. Tan, M. Lo, S. Liung, R. R. Kondreddi, R. Rao, H. Gu, H. He, T. H. Keller, P.-Y. Shi. Inhibition of dengue virus RNA synthesis by an adenosine nucleoside. *Antimicrob. Agents Chemother.*, 54(7): 2932-2939, 2010.

[4] L. Bassit, P. Chatterjee, B. Kim, S. J. Coats, R. F. Schinazi. 2,6-Diaminopurine nucleosides are a novel class of anti-DENV inhibitors. *First International Symposium of Human Vector-Borne Diseases HVBD DART*. December 12-13, 2013.

[5] M. Tichý, R. Pohl, E. Tloustʼová, J. Weber, G. Bahador, Y.-J. Lee, M. Hocek. Synthesis and biological activity of benzo-fused 7-deazaadenosine analogues. 5- and 6-substituted 4-amino- or 4-alkylpyrimido[4,5-*b*]indole ribonucleosides. *Bioorg. Med. Chem.*, 21: 5362-5372, 2013.

[6] M. Tichý, R. Pohl, H. Y. Xu, Y.-L. Chen, F. Yokokawa, P.-Y. Shi, M. Hocek. Synthesis and antiviral activity of 4,6-disubstituted pyrimido[4,5-*b*]indole ribonucleosides. *Bioorg. Med. Chem.*, 20: 6123-6133, 2012.